The Role of NF-κB in the Response to Reoxygenation-Induced Oxidative Stress

Catherine Vida Park

Thesis Submitted for the Degree of Doctor of Philosophy

Institute for Cell and Molecular Bioscience
Faculty of Medical Sciences
Newcastle University
October 2018

Contents

List of Figures

List of Tables

List of Abbreviations

9-1-1	RAD9-RAD1-Hus1
Apaf1	apoptotic protease activating factor 1
ARNT	aryl hydrocarbon receptor nuclear translocator
ATM	ataxia telangiectasia-mutated
ATR	ATM and rad3-related
ATRIP	ATR interacting protein
BCL	B-cell lymphoma
Bcl2	B-cell lymphoma 2
BER	base excision repair
BIR	baculovirus IAP repeat
BSA	bovine serum albumin
CA9	carbonic anhydrase 9
CaMK2	calcium/calmodulin-dependent kinase 2
CDK	cycin-dependent kinase
Chk1	checkpoint kinase 1
Chk2	checkpoint kinase 2
cIAP	cellular inhibitor of apoptosis
CK2	casein kinase 2
COX	cyclooxygenase-2

CRC	chromatin remodelling complex
DAPI	4',6-diamidino-2-phenylindole
DBD	DNA binding domain
DDB	DNA-damage binding
DISC	death-inducing signalling complex
DMEM	Dulbecco's modified Eagle's medium
DMOG	dimethyloxaloylglycine
DNA	deoxyribonucleic acid
DNA-PK	DNA-Dependent protein kinase
DSB	double strand break
DSBR	double strand break repair
ECL	enhanced chemiluminescence
EMSA	electrophoretic mobility shift assay
ERK	extracellular signal-regulated kinase
FACS	fluorescence-activated cell sorting
FATC	FRAP, ATM and TRRAP C-terminal
FBS	foetal bovine serum
FLIP	FLICE-like inhibitory protein
FOXA2	Forkhead box protein A2
GG-NER	global genomic-NER

H2AX	H2A histone family member, X
HAT	histone acetyl transferase
HFF-1	human foreskin fibroblast-1
HIF	hypoxia inducible factor
HIF1α	hypoxia inducible factor-1α
HR	homologous recombination
IκB	inhibitor of κB
IAP	inhibitor of apoptosis
IKK	IκB kinase
IL-8	Interleukin-8
iNOS	inducible nitric oxide synthase
JNK	c-Jun N-terminal kinase
Kap1	KRAB associated protein 1
LC8	8-kDa dyenin light chain
LDL	low density lipoprotein
LOX	lipoxygenase
LPS	lipopolysaccharide
MAPK	mitogen-activated protein kinase
Mdm2	mouse double minute 2 homolog
MEK	mitogen-activated protein kinase kinase

MKK	mitogen-activated protein kinase kinase
MLH1	MutL homolog 1
MMEJ	microhomology-mediated end joining
MRN	Mre11, RAD50 and Nbs1
mRNA	messenger RNA
Msh2	MutS protein homolog 2
Msh6	MutS protein homolog 6
mTOR	mammalian target of rapamycin
NAC	N-acetyl cysteine
NADPH	nicotinamide adenine dinucleotide phosphate
NEMO	NF-κB essential modulator
NER	nucleotide excision repair
NF-κB	nuclear factor kappa-light-chain-enhancer of activated B cells
NHEJ	non-homologous end joining
NIK	NF-κB-inducing kinase
NLR	NOD-like receptor
NLS	nuclear localisation sequence
NQO1	NAD(P)H dehydrogenase (quinone) 1
p38	p38 mitogen-activated protein kinase

p53	tumour protein p53
PAGE	polyacrylamide gel electrophoresis
PARP	poly (ADP-ribose) polymerase
PBS	phosphate buffered saline
PCNA	proliferating cell nuclear antigen
PCR	polymerase chain reaction
PDK1	phosphoinositide-dependent protein kinase-1
PHD	proline hydroxylase
PI3K	phosphoinositide-3-kinase
PIC	pre-initiation complex
PIKK	phosphatidylinositol 3-kinase-related kinases
PIP2	phosphatidylinositol biphosphate
PIP3	phosphatidylinositol triphosphate
PKB	protein kinase B
PKD	protein kinase D
PRDX-3	peroxiredoxin-3
PTEN	phosphatase and tensin homolog
PVDF	polyvinylidene difluoride
RHD	rel homology domain
RIP	receptor interacting protein

RNA	ribonucleic acid
ROS	reactive oxygen species
RPA	replication protein A
SDS	sodium dodecyl sulphate
SDSA	synthesis-dependent strand annealing
SHIP-1	SH-2 containing inositol 5' polyphosphatase 1
SMAC	second mitochondria-derived activator of kinases
SMG1	serine/threonine protein kinase
SOD-2	superoxide dismutase 2
SOD-1	superoxide dismutase 1
STAT3	signal transducer and activator of transcription 3
TAB	TAK1-binding protein
TAB2/3	TAK1-binding protein 2/3
TAD	transactivation domain
TAE	tris-acetate-EDTA
TAF	TBP-associated factors
TAK1	transforming growth factor-β activated kinase-1
TBE	tris-borate-EDTA
TBP	TATA-binding protein

TCA	trichloroacetic acid
TC-NER	transcription coupled-NER
TDP1	tyrosyl-DNA phosphodiesterase 1
TGF	transforming growth factor beta
TLR	Toll-like receptor
TNF	tumour necrosis factor
TopBP1	Topoisomerase II binding protein 1
TPCA	3-Thiophenecarboxamide
TRAF	TNF receptor associated factor
TRRAP	transformation/transcription domain associated protein
VEGF	vascular endothelial growth factor
VHL	von Hippel-Lindau
XOR	xanthine oxidoreductase
XPA	xeroderma pigmentosum group A-complementing protein
XPG	xeroderma pigmentosum group G-complementing protein

Acknowledgements

I would like to thank my supervisor Niall Kenneth for the opportunity to carry out the research presented in this thesis, as well as for the advice and guidance that he has given me throughout. I would also like to thank my second supervisor Neil Perkins for providing many inhibitors, primers and other essential reagents, without which this research would not have been possible. I would also like to extend my gratitude to my progression panel; Janet Quinn and Viktor Korolchuk for pushing me and for their valuable advice and comments. I would like to further thank Janet Quinn for her much appreciated guidance, help and feedback on my writing and corrections; I am extremely grateful for all of her support.

In particular I would like to thank all members of the Perkins laboratory, past and present including Hélène Sellier, Adam Moore, Ling-I Su, Iglika Ivanova, Jill Hunter, George Schlossmacher, Nicky Hannaway and Adrian Yemm for their continued support, reassurance and advice, as well as for their positive comments regarding my cheese scones. I would also like to extend my gratitude to other colleagues who have provided support both scientifically and socially including Faye Curtis, Zoe Underwood, Hannah Swinburne, Sara Luzzi, Cameron Robertson and Vicky Torrence, as well as to Keith Roberts for his assistance with nitrogen cylinders. I would like to give a special thank you to Ben Wetherall for his microscopy assistance and extensive mechanical keyboard usage, as well as for his continued patience and support throughout the last few months. It would have been a difficult journey without you.

Finally I would like to thank my friends and family for their continued support and confidence in me, as well as their patience and understanding throughout some hard times. This thesis would not be possible without any of the people mentioned here, I therefore extend my warmest thanks and appreciation to you all. Believe it or not, I still think science is fun!

Abstract

Hypoxia followed by rapid reoxygenation within the body can lead to cell and tissue damage through the production of reactive oxygen species (ROS) and the resulting oxidative stress. This ischemia and reperfusion is associated with a number of common human diseases such as cancer, stroke and cardiovascular conditions. The cellular response to oxidative stress is characterised by post-translational modification and changes in gene expression. This project focusses on how oxidative stress induced by hypoxia and rapid reoxygenation affects the activation of NF-κB; a rapidly-acting transcription factor that plays a key role in the eukaryotic cell response to infection, radiation and oxidative stress. NF-κB is perpetually activated in a variety of common human diseases such as heart disease, chronic inflammation and cancer; conditions that are also associated with oxidative stress.

Investigations presented in this thesis demonstrate the profound effects that hypoxia and reoxygenation have on cell biology, as well as highlighting how these opposite stimuli are so closely connected. The effects of hypoxia and reoxygenation on the cell cycle, DNA damage, cell proliferation and cell survival are all explored in this project, giving great insight into the possible mechanisms at work in response to these stresses.

It has been demonstrated previously that certain members of the phosphatidylinositol 3-kinase-related kinase (PIKK) family such as Ataxia Telangiectasia-Mutated (ATM) are able to coordinate the activation of NF-κB pathways in response to specific stimuli such as following DNA damage or oxidative stress. This project has identified a novel role of another member of this family, Ataxia Telangiectasia and Rad-3-related protein (ATR) in the NF-κB response to reoxygenation-induced oxidative stress.

Introduction

Hypoxia and reoxygenation, or ischemia and reperfusion, describe a drop in oxygen levels in cells or tissues to a level lower than normal followed by a return of oxygen. Fluctuations in oxygen levels are a common occurrence in the body and can occur in healthy tissues, even coordinating physiological processes such as stem cell differentiation and digestion. As such, the control of oxygen gradient and reactive oxygen species (ROS) is critical for the health of a cell, a loss of ROS homeostasis can lead to protein, lipid and DNA damage; a state known as oxidative stress. Oxidative stress as a result of hypoxia and reoxygenation occurs in many disease states, such as chronic inflammation, stroke, heart disease and cancer. Understanding the effects of this stress on cells and tissues, and the mechanisms involved in the cellular response to these stimuli, is therefore critical in the treatment of these conditions.

Previous work on hypoxia and reoxygenation has implicated the NF-κB family of rapidly-acting transcription factors in the response to these stresses. The NF-κB transcription factors are activated in response to a wide range of stresses such as infection, inflammation and DNA damage, in addition they regulate the expression of many target genes either directly or through cross-talk with other signalling pathways. Coordinated activation of upstream signalling pathways to control NF-κB activity is therefore critical so that the cell responds to a stress appropriately; each stimulus activates a unique pathway encompassing different proteins, post-translational modifications and timings. Aberrant activation of the NF-κB pathway is associated with many diseases, including all of those mentioned above, therefore understanding the mechanism involved in the response to individual stresses is critical in understanding disease pathogenesis and developing potential novel therapies.

Some progress has been made on elucidating the molecular mechanisms responsible for the activation of this pathway in hypoxia, however literature describing the kinetics of this activation in response to reoxygenation is scarce. In addition due to the variations in oxygen level, cell line, timings and gas exchange protocols used in previous work, many publications present conflicting findings. Here an improved method of gas exchange was used to determine the effects of hypoxia and reoxygenation on NF-κB pathway activation. This thesis describes how hypoxia and reoxygenation induces canonical NF-κB signalling, with particular focus on the key proteins and post-translational modifications involved in this activation. In addition investigations into cell proliferation, gene transcription and cell cycle dynamics were performed to determine the cellular effects of this activation.

Together data presented in this thesis as uncovered some of the mechanisms of NF-κB activation in response to hypoxia and reoxygenation, as well as determining the effects that these stresses have on the health of the cell. More work needs to be done to characterise these mechanisms further, however this project provides a good starting point to develop from and highlights some key areas of future work.

1.1 Cell Biology Background

1.1.1 The Central Dogma

Virtually every cell in the human body contains the human genome; around 6 billion bases of nucleic acid sequence in most somatic (diploid) cells. This deoxyribonucleic acid (DNA) code comprises just 4 different nitrogen-containing nuclear bases; cytosine (C), guanine (G), adenine (A) and thymine (T). The specific order, position and combination of these 4 seemingly simple bases within the genome encodes all of the information required to build a whole organism, in this case a human. Each human has its own unique, yet predominantly similar code, which in an individual can dictate eye colour or predisposition to disease. The human genome encodes an estimated 20,000 different protein coding genes as well as non-coding DNA such as pseudogenes, introns and untranslated areas of DNA as well as regulatory sequences. The organisation and regulation of these is critical to build a living organism.

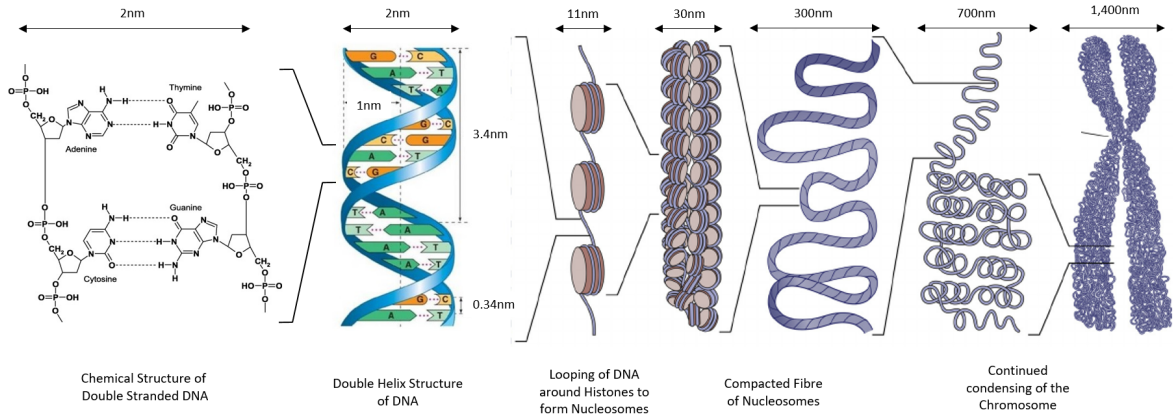

Figure 1. The Structure and Organisation of DNA within a Chromosome. The chemical structure of a DNA nucleotide comprises a phosphate group, a sugar group and a base group. The sugar and phosphate groups form phosphodiester bonds to create a sugar-phosphate backbone, while the bases; cytosine (C), guanine (G), adenine (A) and thymine (T) protrude inwards, pairing to complementary bases on the other strand by hydrogen bonding. This structure forms a double strand DNA helix, which is compacted into the nucleus through wrapping around proteins called histones to form nucleosomes on a 'thread'. Protein interactions between the nucleosomes allows further complex coiling to occur, culminating in the formation of a compacted chromosome structure. Adapted from Nielson, Kumar and Jansen's papers [1][2][3].

In spite of being so large, the human genome is organised in such a specific and controlled manner that it fits into the nucleus of the cell, with the exception of a small circle of mitochondrial DNA that is located within the mitochondria. DNA is commonly present in a double stranded helix, with sequences running in opposite 5' to 3' direction (Fig. 1).

Hydrogen bonds between A and T, and C and G hold the helix in place, ensuring that the strands are complimentary to one another. These complementary double stranded DNA helices fit into tiny spaces such as the nucleus in structures known as chromosomes. The human genome contains 23 pairs of chromosomes, that exist in the cell as the highly structurally regulated form of chromatin. Chromatin is comprised of DNA and histone proteins, which allows DNA to become tightly packed and folded in a specific, highly conserved and tightly regulated manner. This chromatin must be loosened by epigenetic and histone modifications to allow transcription to occur as specific genes need to be accessed by the the transcription machinery [4]. Chromatin therefore plays an important role in many aspects of cell biology including DNA repair, replication and transcription.

The central dogma describes how this DNA code is transcribed to produce ribonucleic acid (RNA), which is then translated into proteins (Fig. 2). This process requires regulation every step of the way, from control of gene expression by transcription factors and other regulatory proteins, to correct processing of the pre-mRNA (messenger RNA) to mRNA, then the transport and localisation of this mRNA to the cytoplasm where it is either degraded or translated into proteins by the ribosome. The cell contains a plethora of proteins that control and coordinate each step of this process, to allow cells to carry out normal functions involving metabolism and development, as well as responding to a given stimuli.

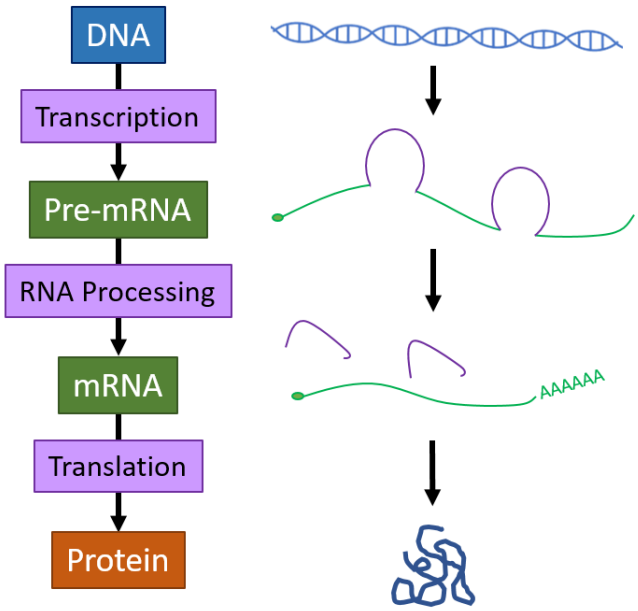

Figure 2. The Central Dogma of Molecular Genetics. This figure summarises the central dogma of molecular genetics, showing the transfer of information from DNA to protein.

1.1.2 Transcription by RNA Polymerase II

RNA polymerase II is one of 3 eukaryotic DNA-dependent RNA polymerases and is responsible for the synthesis of pre-messenger RNA (mRNA), the RNA required for protein production [5]. The initiation of transcription by RNA polymerase II at the promoters of genes requires the coordinated recruitment of a series of general transcription factors alongside an RNA polymerase enzyme, which is responsible for RNA transcription (Fig. 3) [6].

The transcription machinery is systematically recruited to the promoter region of the gene beginning with the TFIID transcription factor (Fig. 3). This contains the TATA-binding protein (TBP) and TBP-associated factors (TAF)s that facilitate this binding [7]. TFIIB then locates the start of the gene, and together with TFIID undergoes a large conformational change, bending the DNA helix and initiating the melting or breaking of the hydrogen bonds by the general transcription factors [8]. This forms an 18 base unwound section of DNA helix is known as an RNA-polymerase-promoter open complex. Following this, TFIIF is recruited alongside RNA polymerase II to form the pre-initiation complex (PIC) [5][9][10]. Finally TFIIE and TF11H are recruited to complete formation of the transcription initiation complex [11].

Transcription is initiated when the C-terminal domain (CTD) of RNA polymerase II is phosphorylated, the majority of the general transcription factors then dissociate from the complex and RNA pol II moves along the the length of the gene producing RNA (Fig. 4). This occurs in a 3' to 5' direction along the template strand of the DNA [12][13][14]. During transcription complementary RNA nucleotides are hydrogen bonded to the exposed template strand of the DNA, with the sugar-phosphate backbone being constructed in parallel by the RNA polymerase II subunit RPB1 to form an mRNA strand [15].

As transcription continues beyond the promoter region, elongation factors and chromatin remodelling complexes are recruited to regulate the elongation stage of transcription [16]. When RNA pol II reaches the end of the gene, termination of transcription commences (Fig. 4). Adenines are added to the new 3' end in a process called polyadenylation and a 5' cap is added to the start of the mRNA to prevent degradation when the pre-mRNA is released. The newly synthesised mRNA, the RNA polymerase and associated factors dissociate from the DNA strand, allowing the helix to close back up into its normal double stranded form [17][18].

1.1.3 Transcription Factors and Co-regulators

The general transcription factors are sufficient for basal transcription, however they work alongside other more specialised transcription factors and co-regulators in order to control responses to certain stimuli or in a cell-specific manner [19]. Recruitment of the PIC and transcription machinery to a gene's promotor was initally thought to be controlled by

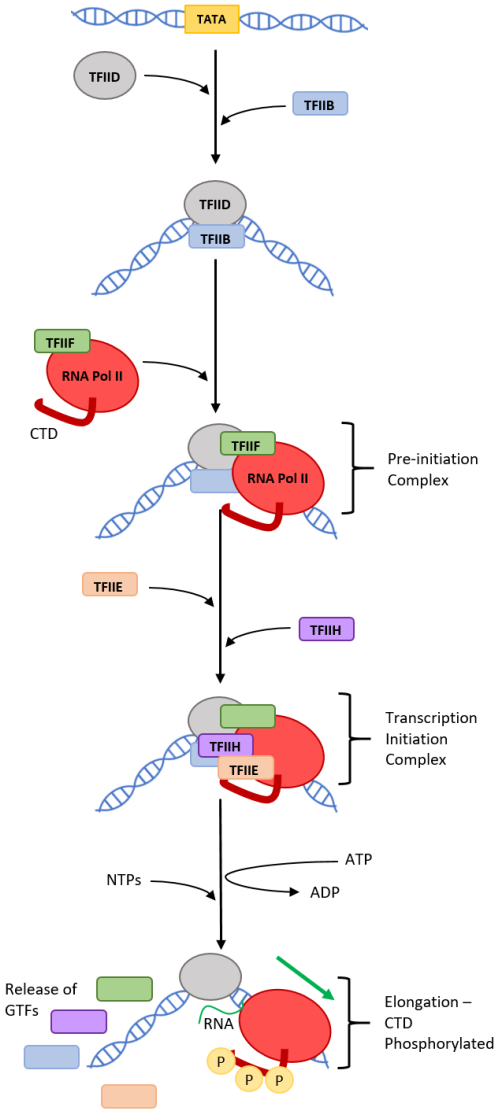

Figure 3. RNA Polymerase II Recruitment and Transcription Initiation. RNA polymerase II is recruited to the TATA site of a gene systematically by a series of general transcription factors. The first of these, TFIID, senses the promoter of the gene, binds to the DNA and leads to a conformational change in the DNA. This leads to the recruitment of TFIIB, then TFIIF, which mediates the recruitment of RNA polymerase II to the DNA. This complex is referred to as the pre-initiation complex. Recruitment of further general transcription factors, TFIIE and TFIIH follows to form the transcription complex. Elongation is initiated by phosphorylation of the C-terminal domain (CTD) of RNA polymerase II, general transcription factors are released and transcription commences.

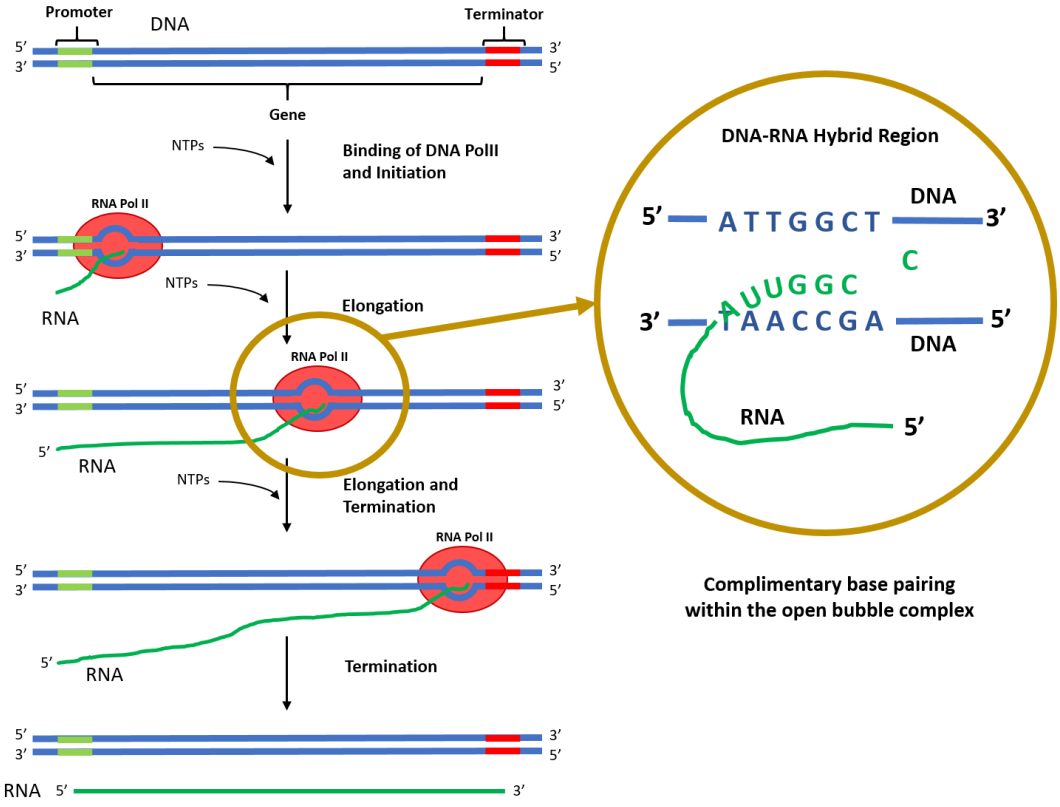

Figure 4. RNA Polymerase II Transcription Elongation and Termination. Once RNA polymerase II is recruited to the site of the gene and is phosphorylated it begins transcription. Double stranded DNA is 'melted' and hydrogen bonds are broken to form an 'open bubble complex', which moves in a 3' to 5' direction down the gene with the RNA polymerase. In this site the RNA polymerase recruits RNA NTPs and pairs them to complementary bases on the DNA forming a DNA-RNA hybrid. The sugar-phosphate backbone is built and the RNA is slowly released as the DNA-RNA bonds are broken. The open complex closes up as the RNA polymerase continues down the gene until it reaches the termination sequence. Here the open complex is closed up, the RNA polymerase dissociates from the DNA and the new RNA is cleaved and released for further processing.

transcription factors alone [20][21], however this is now believed to be regulated by a wide range of general transcription factors as well as other co-regulators [6][22]. These specialised transcription factors control the rate of gene transcription through promoting or repressing RNA polymerase activity directly, through binding to nearby promoters or through more distal elements on the DNA [23]. This allows specific and controlled coordination of this critical first step in the initiation of transcription [6].

Transcription factors contain sequence specific DNA-binding domains and bind DNA through helix-loop-helix, helix-turn-helix, leucine zipper or zinc finger domains. Many of these proteins contain a transcriptional activation domain as well as this DNA binding domain, suggesting that they have roles as transcription factors independently of the general transcription machinery [24][25]. When specialised transcription factors do not bind directly with the general transcription machinery co-factors are required to control activation; these do not bind to the DNA. Transcription factors can either activate or repress transcription of specific genes through their interaction with co-factors; co-activators or co-repressors [5][23][26][27].

1.1.4 Post-translational Regulation of Proteins

Following biosynthesis of the protein by the ribosome post-translational modifications are carried out (Fig. 5). These modifications ensure that the protein is present in the cell in its mature form, as well as controlling many aspects of molecular biology and cell signalling through promoting or inhibiting activity, targeting the protein for degradation or promoting stability. These encompass both reversible and irreversible events to regulate levels of active protein in the cell. As there are so many varieties of post-translational modifications in mammalian cells, only a select few will be covered in this thesis [28].

Post-translational modifications can occur anywhere along the length of a protein at specific sites that usually act as the nucleophile in the chemical reaction that occurs during the modification process. These reactions often involve the modification of an existing functional group or the addition of a new functional group to the existing protein by a specific enzyme. An example of modification of an existing functional group includes deamidation where glutamine or asparagine residues are converted to glutamic acid or aspartic acid residues respectively. Whereas addition of a functional group to the protein includes a plethora of reactions including phosphorylation, hydroxylation and methylation.

In other cases post-translational modifications can include structural modifications through proteolytic cleavage of the protein at specific peptide bonds and/or the formation of new disulphide bonds by covalent linkage between two cysteine amino acids. These modifications can also control localisation of the protein within the cell, for example covalent addition of a C_{14} saturated acid to a glycine residue in a process called myristolation leads to lipid membrane localisation of the targeted protein. In other instances proteins

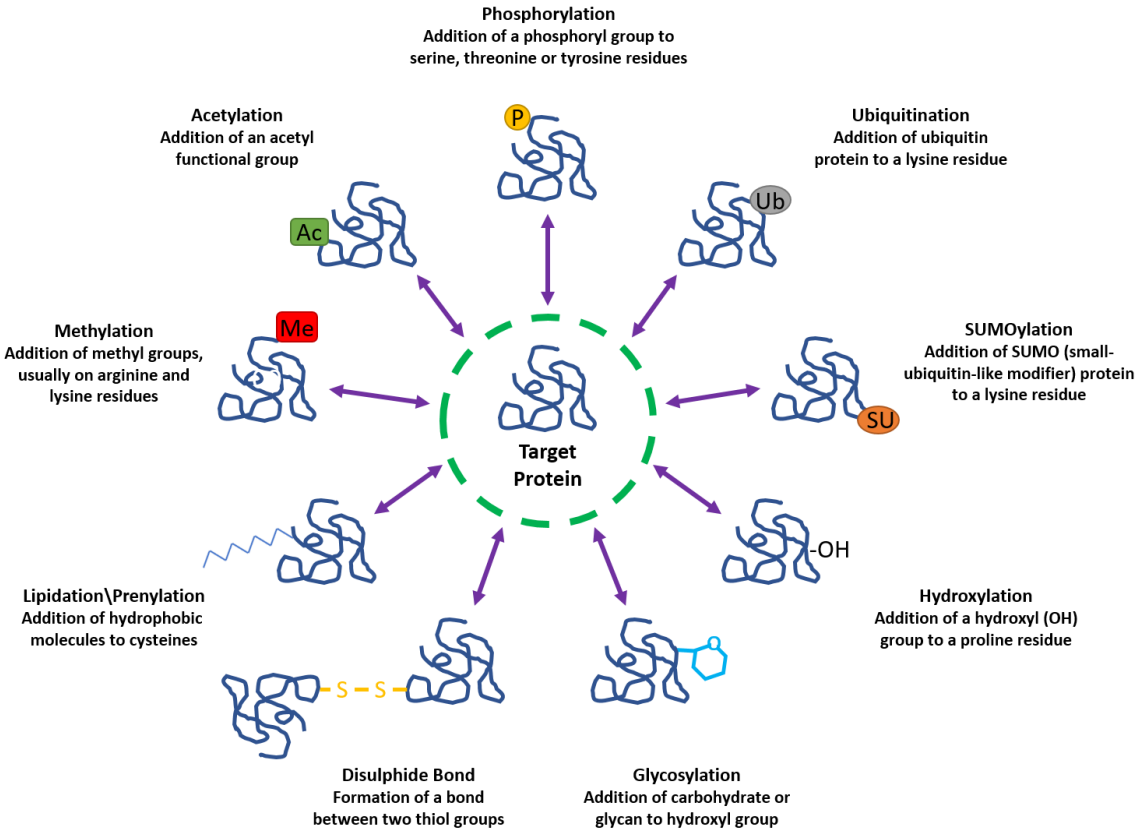

Figure 5. Post-Translational Modifications. Overview of some of the reversible post-translational modifications that occur in eukaryotic cells. These control many aspects of molecular cell biology including, protein stability, protein activation, protein inhibition and signalling pathway activation.

are modified in a manner that targets them for degradation by the proteosome, such as addition of the protein ubiquitin in a process called ubiquitination. Many of these post-translational modifications can have different effects on a protein, for example although ubiquitination can lead to degradation, it can also control nuclear-cytoplasmic location of the protein as well as promoting and repressing interactions with other proteins in a signalling pathway.

The most common post-translational modification is phosphorylation (Fig. 6), with 58383 different phosphorylation events reported experimentally [29]. Phosphorylation describes the process by which a phosphate group is covalently bound to an amino acid residue; usually serine, threonine or tyrosine in eukaryotes. This can lead to a change in the structural conformation of the protein leading to its activation, deactivation or modifying its function. Phosphorylation is carried out by kinase enzyme proteins, while the reverse reaction, dephosphorylation, is carried out by phosphatase enzymes. This process is readily reversible, rapid and energy efficient, making it an excellent mechanism in rapidly-acting signalling pathway responses. The conformational change incurred due to phosphorylation is due to the charged, hydrophilic group that is added during this reaction. This

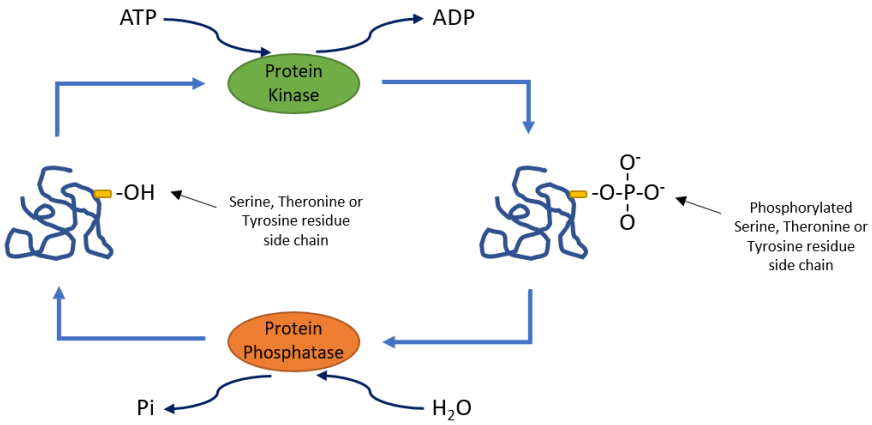

Figure 6. Phosphorylation of Target Proteins. Phosphorylation is one of the most commonly occurring post-translational modifications in eukaryotic cells and controls many aspects of protein function including signal transduction. Phosphorylation occurs through transfer of a phosphoryl group to serine, threonine or tyrosine residues from an ATP to produce ADP. The reverse reaction, dephosphorylation, is carried out by the phosphatase enzyme and requires H_2O.

alters how this amino acid interacts with amino acids physically close due to the primary, secondary, tertiary and quarternary structure of the protein. The function of the protein is therefore altered as these modifications affect how the modified protein interacts with other proteins, blocking and creating binding sites. As a result phosphorylation may lead to a variety of responses depending on the context and location of the modification. As well as activating or inhibiting protein activation, phosphorylation has been linked to protein degradation and protein-protein interactions. In a laboratory setting, specific phosphorylation events can be detected using primary antibodies raised against them. This can be used to monitor activation of key signalling pathways and responses to stress and is an important tool used in this thesis.

Another post-translational modification of note is ubiquitination (Fig. 7). Unlike phosphorylation this process involves the covalent bonding of a 76 amino acid polypeptide [30][31][32]. Ubiquitination can modify substrate proteins in a variety of different ways, making them one of the most versatile mechanisms of post-translational modification. The most simple form of this, monoubiquitination, involves the binding of one ubiquitin protein to the target, this occurs in three steps; activation, conjugation and ligation by the E1, E2 and E3 ubiquitin ligases respectively in a cascade. Further conjugation of ubiquitin to this first ubiquitin can occur through successive isopeptide bonds at the start methionine or at specific lysines at positions 6, 11, 27, 29, 33, 48 and 63. Polyubiquitination usually occurs at lysines 48 or 63, generally resulting in targeting proteins for degradation by the proteosome or functioning in the control of signal transduction, DNA damage response and DNA repair respectively [33][34][35][36].

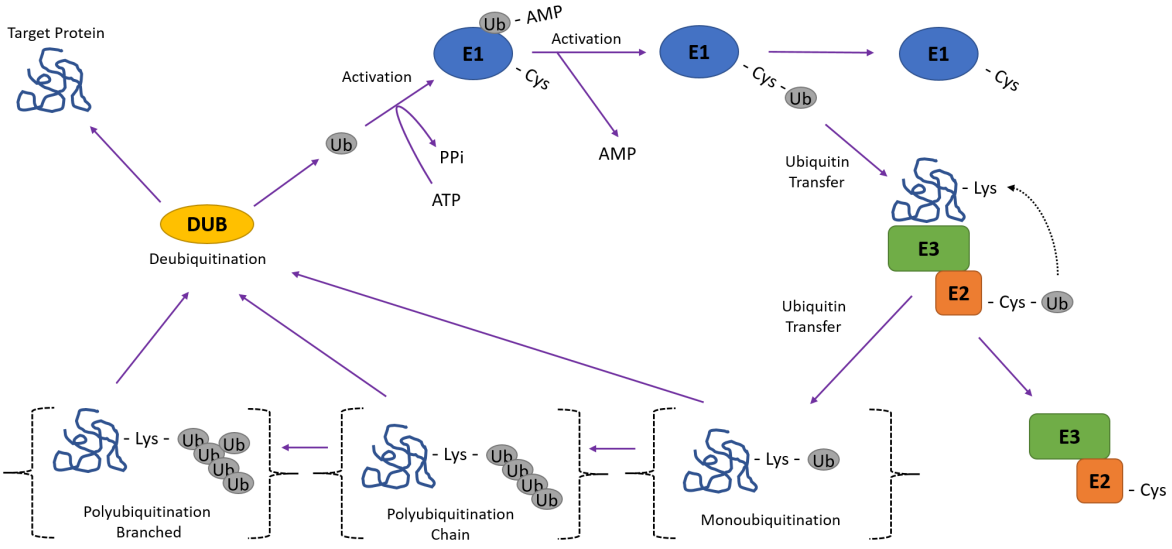

Figure 7. Ubiquitination of Target Proteins. Ubiquitination describes the addition of one or several ubiquitin proteins to lysine residues. This requires a two-stage activation process involving the E1 ubiquitin-activating enzyme that produces a ubiquitin-adenylate intermediate then binding of an E1 cysteine to ubiquitin by a thioester bond, causing the release of AMP. The E2 ubiquitin-conjugating enzyme then transfers the ubiquitin from the E1 enzyme to a cysteine on the E2 enzyme. The E3 ubiquitin ligases then recognise and bind a target protein and transfer the active ubiquitin to a lysine residue. Further additions of ubiquitin can occur in linear or branched forms, these can occur on the same lysine residues of ubiquitin up the chain or on a mixure of different lysine residues. Multiple mono-ubiquitination can also occur along the protein. In this activation cascade, E1 proteins can bind many E2s that can in turn bind many E3s to precisely coordinate the appropriate form of activation.

As a result of this diverse polyubiquitination, ubiquitination is one of the most versatile post-translational modifications that occurs in the cell. Ubiquitination therefore creates a range of changes in protein conformation to control activation, repression, degradation and stability of the protein [37][38][39]. Reversal of ubiquitination occurs readily by a group of deubiquitination enzymes, or DUBs, allowing rapid removal of ubiquitination events on proteins.

One final post-translational modification of note for this thesis is hydroxylation. This chemical reaction involves the covalent binding of a hydroxyl group an amino acid; mostly commonly proline, lysine or asparagine. The latter is critical in the response of cells to hypoxia, this will be covered in more detail in a later section, but generally the loss of oxygen prevents hydroxylation from occurring leading to changes in signalling pathway activation and protein stability.

1.2 The NF-κB Family of Transcription Factors

This project focusses predominantly on the activation of the NF-κB family of transcription factors and the mechanism behind this activation (Fig. 8). Originally identified in B lymphocytes in 1986, NF-κB was discovered to bind to the κ light chain enhancer sequence of immunoglobulins and the SV40 enhancers to control gene expression in response to a given stimulus [40][41].

There are 5 members of the NF-κB family; RelA, RelB, c-Rel, NF-κB1 and NF-κB2 that are characterised by a 300 amino acid long rel homology domain (RHD) present towards the N-terminal of the proteins (Fig. 8). This region shares homology with the v-Rel oncogene and has 3 main functions; DNA binding through the DNA binding domain (DBD), dimerisation or inhibitor binding and a domain that promotes nuclear translocation through a nuclear localisation sequence (NLS) [42]. Despite being highly conserved, variations in the RHD enables different NF-κB subunits to form different combinations of hetero- and homo-dimers to respond to different stimuli. These different combinations of hetero- and homo-dimers to recognise distinct κB sites of 9-10 base pairs of an almost palindromic DNA sequence; 5'-GGGRNWYYCC-3' (N, any base; R, purine; W, adenine or thymine; Y, pyrimidine). This κB sequence is located in the promoters or enhancers of hundreds of genes [42][43].

There are 2 main classes of NF-κB proteins, characterised by the protein sequence to the C-terminus of the RHD, which determines the method by which the protein is sequestered in the cytoplasm and the resulting method of activation. Class I describes subunits NF-κB1 and NF-κB2 [42], which are present in the cytoplasm as the inactive precursors p105 and p100. These inactive precursors contain multiple inhibitory ankyrin repeats at the C-terminal end of the protein. Ankyrin repeats are 33-residue motifs that mediate protein-protein interactions and protein folding, however in the context of precursor class I NF-κB subunits they act as transrepressors; negative regulators of activation. Following activation from upstream signalling pathways, these ankyrin repeats are proteolytically cleaved and processed from their inactive precursor forms to their mature forms; p50 and p52 respectively. These cleaved forms of NF-κB1 and NF-κB2 are no longer sequestered in the cytoplasm and are free to move in the the nucleus as directed by their nuclear localisation signal. Class 1 NF-κB subunits also contain a glycine rich region directly to the C-terminus of the RHD that acts as a processing signal to aid this activation.

Although class I NF-κB subunits play a key role in transcriptional control, to directly activate gene expression rather than repressing transcription they must dimerise with the second class of subunits; RelA(p65), RelB and c-Rel [42]. In addition to their DBDs these class II subunits contain transactivation domain (TAD)s on their C-terminus and are therefore potent activators of gene expression. Sequestration of class II subunits in the cytoplasm requires blocking of a nuclear localisation signal on the NF-κB subunit by a family of inhibitors known as the inhibitor of κB (IκB)s. The IκB protein holds NF-κB in

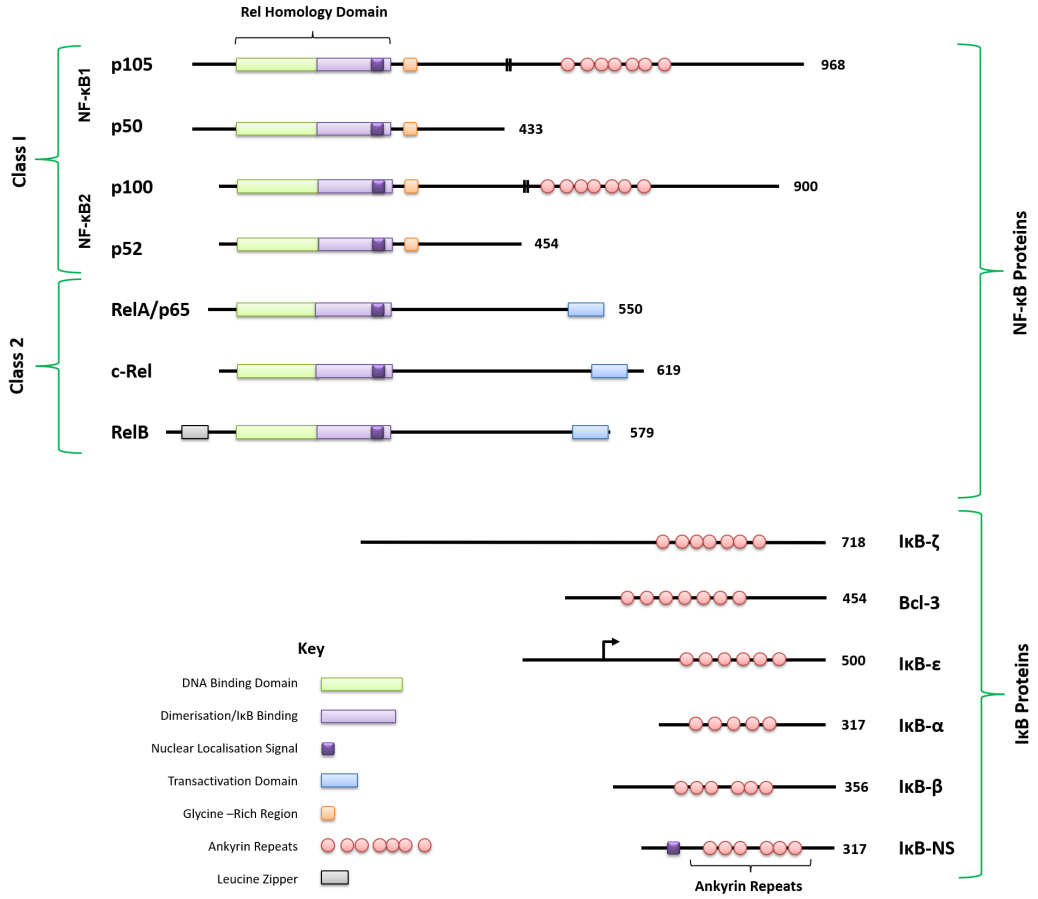

Figure 8. The NF-κB Family and Inhibitors. The NF-κB family of rapidly acting transcription factors comprises 5 different subunits that form a range of homo- and heterodimers that recognise distinct 9-10 base pair sequences on DNA to moderate transcription. They are activated through post-translational modification either through the cleavage of ankyrin repeat transrepressors (p105/p50 and p100/p52) or through the phosphorylation, ubiquitination and degradation of ankyrin-containing inhibitors (RelA, c-Rel and RelB).

the cytoplasm in an inactive form until upstream signalling leads to IκB phosphorylation and inactivation. IκB then releases its class II NF-κB subunit, which is able to translocate into the nucleus to control gene expression.

The inhibitors of class II NF-κB subunits (IκBα, IκBβ, IκBϵ, BCL-3, IκBζ and IκBNS) and the precursors to p50 and p52 (p105/IκBγ and p100/IκBδ) contain ankyrin repeat sequences (Fig. 8). The former subset work by binding to NF-κB and covering the NLS, the latter must be proteolytically cleaved to allow activation. Cleavage of p105 to p50 occurs in relatively constant amounts regardless of external stimulus, however cleavage of p100 to p52 requires external stimuli and signalling from upstream kinases to be initiated. The function of these IκB proteins and motifs allows control of NF-κB activation and allows for almost instant activation of these rapidly-acting transcription factors [44].

1.2.1 The NF-κB Family in Health and Disease

NF-κB has been implicated in a wide range of diseases and conditions that comprise both general diseases as well as multiple forms of cancer [45][46][47] (Fig. 9). The large number of diseases that NF-κB is linked to is most likely due to the large number of inducers of NF-κB activation as well as the sheer number of NF-κB target genes. The cross-talk between other critical cell signalling pathways again highlights the complexity of NF-κB signalling and the need for precise control of its activation through elaborate pathways and mechanisms. Loss of control of signalling could occur in many stages of NF-κB activation and could have a knock-on effect in many aspects of cell biology. It is for these reasons that aberrant NF-κB activation is linked with so many diseases.

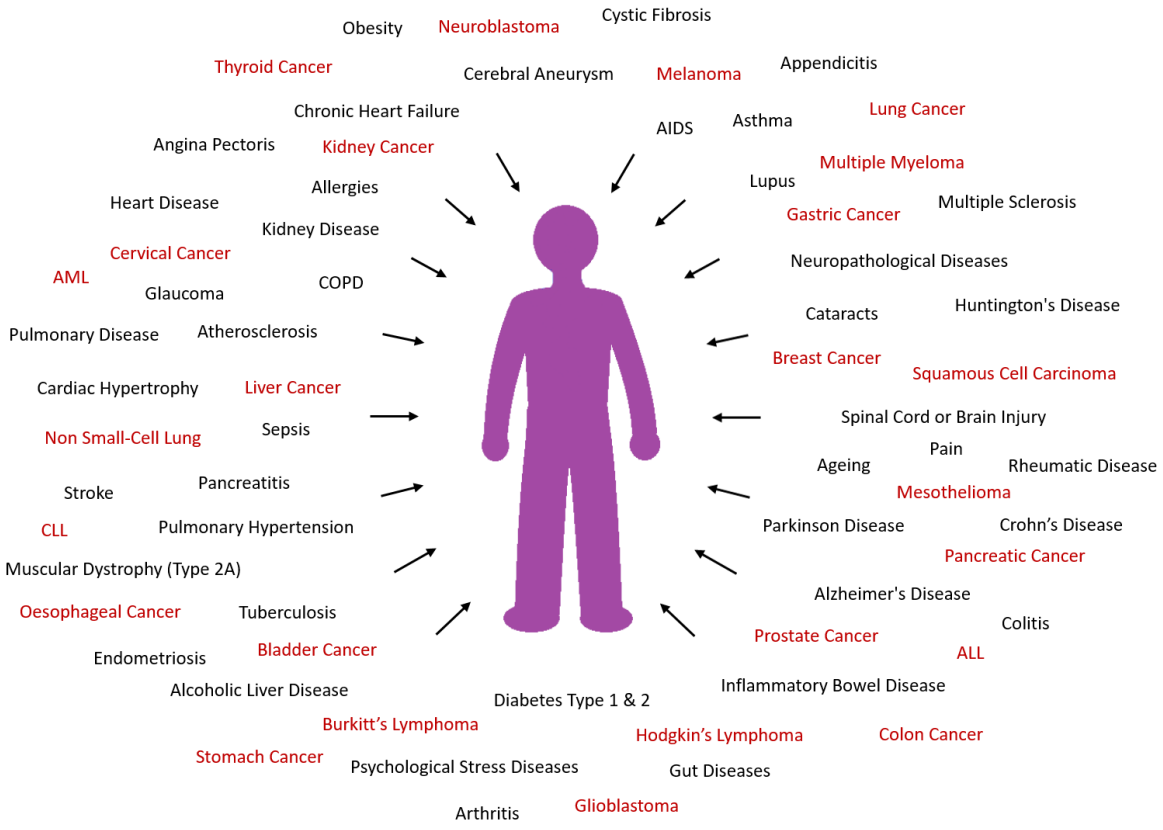

Figure 9. General Diseases and Cancers Linked with NF-κB Activation. A wide-range of general diseases (black) and cancers (red) have been previously linked with NF-κB [43].

The range of general diseases that NF-κB has been linked to is broad and affects many organs and biological mechanisms across the body (Fig. 9). Ageing related diseases such as Alzheimers disease, Parkinsons disease, cataracts, hearing loss and arthritis have all been linked to NF-κB and its role in inflammation and response to stress [48][49][50][51][52][53]. Diseases affecting other organs such as the lung are also commonly linked to NF-κBs role in inflammation either following injury [54][55] or as secondary effect of another condition such as asthma through inflammatory reactions, chronic obstructive pulmonary disease through the onset of oxidative stress [56][57], or cystic fibrosis, the latter of which

has been shown to affect the NF-κBs crosstalk with the apoptotic response to stress [58].

Diseases affecting the cardiovascular system have also been linked with aberrant NF-κB activation. Transcription of genes associated with the development of pulmonary hypertension is controlled by NF-κB activation, the temporal and spatial expression of these can lead to tissue-remodelling involved in the development of this often fatal condition [59][60]. NF-κB has also been implicated in chronic heart failure through its role in immune and inflammatory responses [61] as well as in the development of hypercholesterolemia and atheroschlerosis. These closely linked conditions of the vascular wall have been linked to aberrant NF-κB activation through its role in the response to oxidative stress as well as inflammation [62][63]. This role of NF-κB in the response to cycling oxygen levels and ischemia and reperfusion stresses will be discussed in more detail in a later section, however it is important to note this critical link between NF-κB, oxidative stress and the inflammatory response.

Conditions affecting the liver, pancreas, kidneys and digestive tract have also been demonstrated as having a strong link to NF-κB activation [64][65][66][67][68][69][70]. In the case of alcoholic liver disease, regularly increased levels of ethanol exacerbates oxidative stress in tissues and the mechanisms that control for this stress for example through the activation of NF-κB [65]. Liver disease is closely linked to pancreatic disease; the activation of NF-κB in a diseased liver due to inflammatory responses leads to increased production of chemokines and cytokines by NF-κB. Aside from promoting hepatic necrosis, this has been linked to an increased risk of pancreatitis through increased production of inflammatory cytokines and chemokines [66]. Inflammatory bowel disease and other autoimmune conditions have also been associated with aberrant regulation of NF-κB activation. NF-κB is an essential responder in the intestinal immune system, however unsolicited activation and the resulting production of inflammatory and immune factors occurring against the self can lead to the development of Crohns disease or colitis symptoms [68][69][70].

In many of these conditions, disease pathogenesis occurs due to complex responses of the cell to oxidative stress and inflammation (Fig. 10) [71]. Within the body each tissue has its own physiological niche, each with its own 'normal' level of oxygen and its own immunological activity. Indeed many of these tissues commonly undergo hypoxic stress due to high levels of cell proliferation and increased metabolic demand, here the hypoxic gradient is controlled, regulating pathways associated with physiological processes such as haematopoietic stem cell differentiation and homeostasis. Within pathological sites, such as in inflamed tissues, loss of control of the oxygen gradient may occur [71]. Erratic blood supply within a tumour enviroment or uncontrolled metabolic processes associated with inflammation can lead to changes in oxygen levels. This onset of hypoxia contributes to the loss of control of processes such as immune cell differentiation and cell signalling, promoting inflammation and disease further (Fig. 10). Cross-talk between hypoxic and non-hypoxic signalling pathways can lead to the production of pro-inflammatory cytokines

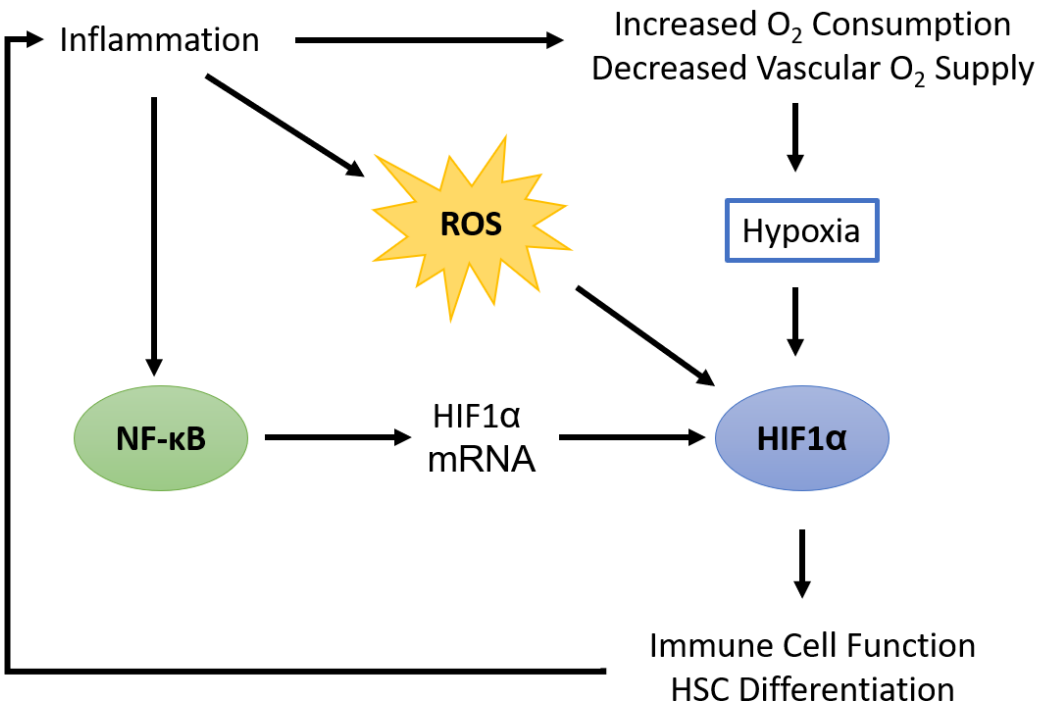

Figure 10. Oxidative Stress and Inflammation. The link between oxidative stress, the immune response and inflammation is a tightly regulated process. Loss of regulatory control across this dynamic pathway can lead to increased inflammation, immune response and oxidative stress. As these are all so closely linked, aberrant activation of one part of this mechanism can have knock-on effects elsewhere in a cycle of inflammation, immune response and oxidative stress. Figure adapted from Taylor et al., 2017 [71].

such as tumour necrosis factor (TNF), which further amplify inflammatory responses [72][73]. As such hypoxia inducible factor (HIF) plays a key role in the control of oxidative stress-induced inflammation. HIF controls gene expression in immune cells exposed to hypoxia, coordinating their downstream effects and controlling their metabolism, thereby controlling inflammation and the immune response [71][72].

In addition to its role in the development of these inflammatory, immune and stress disorders, aberrant NF-κB activation can lead to the promotion of cancer development. This constitutive activation of NF-κB can occur following mutations in NF-κB subunits and upstream pathway components such as IKK subunits that could affect the regulation of NF-κB activation, affecting key cellular responses and processes such as through promotion of proliferation and survival, angiogenesis, metastasis and inflammation [74][75][76]. The promotion of these processes occurs mostly through aberrant regulation of NF-κB activation, for example upregulation in the expression of cyclin D1 leads to increase movement through the cell cycle and results in increased proliferation; causing the cell to bypass essential cell cycle checkpoints [77].

A second example of tumour promotion directed by NF-κB is through aberrant expression of genes involved in apoptosis. Up-regulation in the expression of inhibitor of apoptosis (IAP)s such as cIAP-2 and other proteins involved in regulation of apoptosis can lead to an increased survival of cancer cells and can lead to cancer progression. Both of these processes can contribute to the progression of cancer as cells containing DNA damage will not be repaired and will avoid apoptosis, allowing mutations to be passed to daughter cells [78][79]. NF-κB also plays an important role in the development of cancer in new sites in the body. Its role as a transcriptional regulator of pro-angiogenesis genes such as VEGF and the transcription factor HIF, promotes the growth of new vasculature, allowing cancer cells to move into the blood stream to other sites in the body [80]. NF-κB's role in cancer development and progression also promotes metastasis through the increased production of cell adhesion molecules, allowing cancer cells to adhere to a new secondary site in the body through matrix metalloproteinases [81]. These factors combined highlight NF-κB as an important promoter in the progression of cancer. Studies have also implicated NF-κB as a negative regulator of cancer development, this is particularly important in the early stages of the disease due to NF-κB's role in the immune and inflammatory response where it assists in the targeting and controlled destruction of tumour cells [82].

1.2.2 Activation of The NF-κB Pathway

The NF-κB response was originally thought of as a fairly simple activation process that responded to inflammation following stimulation from TNF or lipopolysaccharides, however over the years the diversity of NF-κB stimulating factors has become apparent (Fig. 11) [42][83][44]. Studies carried out in the late 1980s mostly identified viral products such as Tax1 (HIV-1), E1A (Adenovirus 5) and iel (CMV) [84] [85][86], as well as the inflammatory cytokine TNF and the eukaryotic parasite *Theileria parva* [87][88][89].

Throughout the 1990s a whole range of other inducers were identified, including bacteria (*Staphyllococcus aureus*) [90], bacterial products such as membrane lipoproteins [91], therapeutic drugs such as camptothecin, cisplatin and etoposide [92][93][94], receptor ligands such as CD-40[95], growth factors (TNFα) [96] and chemical agents such as thapsigargin that causes ER stress [56]. Around this time it was discovered that physical and environmental stresses could also initiate NF-κB activation. These include but are not limited to; shear stress [97], UV irradiation [98], cigarette smoke [99] and heavy metals such as lead and nickel [100][101]. Oxidative stress also induces NF-κB activation through chemical induction after treatment with hydrogen peroxide [102], while more physical methods of oxidative stress induction such as hyperoxia [103], ischemia/hypoxia [104] and reoxygenation [105] can also activate NF-κB. Further investigations have since identified hundreds of other inducers of NF-κB pathway activation (Fig. 11) [43]. Based on these findings it is likely that other inducers of NF-κB pathway activation will be discovered in the years to come.

Figure 11. NF-κB is Activated by a Variety of Inducers. NF-κB pathway activation is induced by a plethora of diverse stimuli. This schematic does not show all inducers, rather giving an idea of the sheer number of inducers of the NF-κB pathways. Inducers of the NF-κB pathways include responses to inflammation and infection via cytokines, viruses, bacteria and proteins, through exposure to stresses from the environment, through physical and physiological stresses and following oxidative stress. It can also be activated following exposure to chemicals and after treatment with certain drugs. Apoptotic mediators, modified and over-expressed proteins, receptor ligands, mitogens, hormones and growth factors can also activate NF-κB. This broad range of inducers highlights both the importance of the NF-κB proteins and the need to control activation and downstream effects through elaborate activation pathways [43].

Each inducer of NF-κB leads to the activation of its own specific version of the pathway, involving different protein interactions and different post-translational modification events. Regardless of the upstream or downstream signalling pathway specificities, the majority of signals converge on the IKK complex. Chemokines and cytokines for example can activate the NF-κB pathway through interactions with cell surface receptors, which in turn interact with proteins in the cytosol to transduce the signal downstream to the IKK complex [87][88]. The pattern recognition receptors (PRR)s such as Toll-like receptor (TLR)s and NOD-like receptor (NLR)s are expressed in cells involved in the innate immune response. Damage-associated molecular patterns (DAMP)s and pathogen-associated molecular patterns (PAMP)s initiate noninfectious and infectious inflammatory responses respectively through interaction with these PRRs, which can lead to the activation of the NF-κB pathway after upstream signals converge on the IKK complex [106].

In addition to these responses to inflammation and infection, other stresses such as genotoxic and oxidative stress activate the NF-κB pathway, again through the convergence of upstream signalling to the IKK complex. An example of genotoxic stress leading to the activation of the NF-κB pathway is that of camptothecin treatment. Camptothecin [92] is a DNA damaging agent that causes doubles strand breaks. Following detection of this damage, ATM is activated and in turn activates the NF-κB pathway. In this instance activation of NF-κB occurs as a result of independent sensing of damage rather than simple upstream interaction of a receptor ligand with a cytokine such as TNFα [87][88]. Reports on the effects of oxidative stress on NF-κB activation have been conflicting [107]; studies suggest that reactive oxygen species (ROS) can affect signalling across many aspects of the pathway including direct interactions with the IKK complex itself [108][109][110][111]. The cellular responses to genotoxic stress and oxidative stress will be covered in more detail in a later section.

1.2.3 NF-κB Signalling

NF-κB pathways requires a wide range of post-translational modifications such as phosphorylation and ubiquitination. Different post-translational modifications occur on different proteins and residues depending on the specific inducer and the strength of the stimulus. These proteins act as intermediates between the stress or sensor of stress and the activation of the IKK complex, and subsequently NF-κB subunits. Often two upstream pathways will act in parallel upstream of the IKK complex following exposure to different inducers. In some cases there will be overlaps in the proteins and post-translational modifications involved but each pathway will have distinct inducers and downstream effects [42][112].

NF-κB signalling comprises two main pathways; the canonical (classical) and non-canonical (alternative) pathways (Fig. 12). RelA, c-Rel and p105/p50 dimers are associated with canoncial pathway activation, while RelB and p100/p52 dimers are present as part of the

non-canonial pathway[113]. There are several key differences between these two signalling pathways, one of which is the mechanism behind activation. The former is dependent on the phosphorylation and degradation of the IκB protein that inhibits activation, while the latter is activated following phosphorylation and subsequent ubiquitin-mediated proteasomal cleavage to process p100 to p52. This activation of either pathway cannot take place without the post-translational modification of the IκB protein. The protein complex responsible for this, the IKK complex, is therefore pivotal in the activation of NF-κB.

The sub-units of the IKK complex differ between the canonical and non-canonical NF-κB pathways. A trimeric form of the IKK complex is present in the canonical pathway, comprising of 1 regulatory subunit, the NF-κB essential modulator (NEMO)/IKKγ, and 2 kinase subunits IKKα and IKKβ [113][114]. In the canonical pathway IKKβ is widely considered to be kinase responsible for downstream signal transduction and NF-κB activation. In the non-canonical pathway the IKK complex comprises an IKKα homodimer, therefore IKKα is responsible for signal transduction as opposed to IKKβ [42]. In both the canonical and non-canonical pathways, regardless of stimulus or the upstream proteins and post-translational modifications involved, signalling mostly converges on the IKK complex. This again highlights the importance of the IKK complex and its role as a central regulator of the activation of NF-κB.

The upstream mechanism of canonical IKK complex activation varies greatly from stimulus to stimulus, but usually requires the activation and coordination of upstream targets such as TAK1-binding protein 2/3 (TAB2/3), TAK1, receptor interacting protein (RIP) and TNF receptor associated factor (TRAF) (canonical pathway) or NIK (non-canonical pathway). It has been reported that TRAF is involved in activation of both canonical and non-canonical NF-κB activation, while RIP is only involved in canonical pathway signalling through interactions with NEMO[42]. Ubiquitination is essential for the transduction of signal to the IKK complex. Here TRAF6 acts as an E3 ubiquitin ligase to induce activation of the IKK complex alongside an E2 conjugating enzyme complex comprising Ubc13 and Uev1A. This activation occurs through K63-linked polyubiquitination of NEMO to activate the IKK complex. This leads to the activation of the IKKβ subunit, through phosphorylation events on serine residues [115][42].

As part of the canonical pathway, activation of IKKβ then leads to the phosphorylation of IκBα at serines 32 and 36, leading to dissociation of IκBα from RelA [116]. RelA is no longer being sequestered in the nucleus by the ankyrin repeats of IκBα and its nuclear localisation signal is no longer blocked, RelA is therefore able to form dimers with other NF-κB family members, translocate into the nucleus and control gene expression [117]. This process was characterised by Hunag et al in 2000 [117]. The phosphorylation and subsequent release of IκBα leads to its polyubiquitination and degradation by the 26S proteasome. This degradation and removal of IκBα is observed following induction of the NF-κB pathway by inducers such as TNFα, however following exposure to other stimuli such as hypoxia degradation is not observed [118].

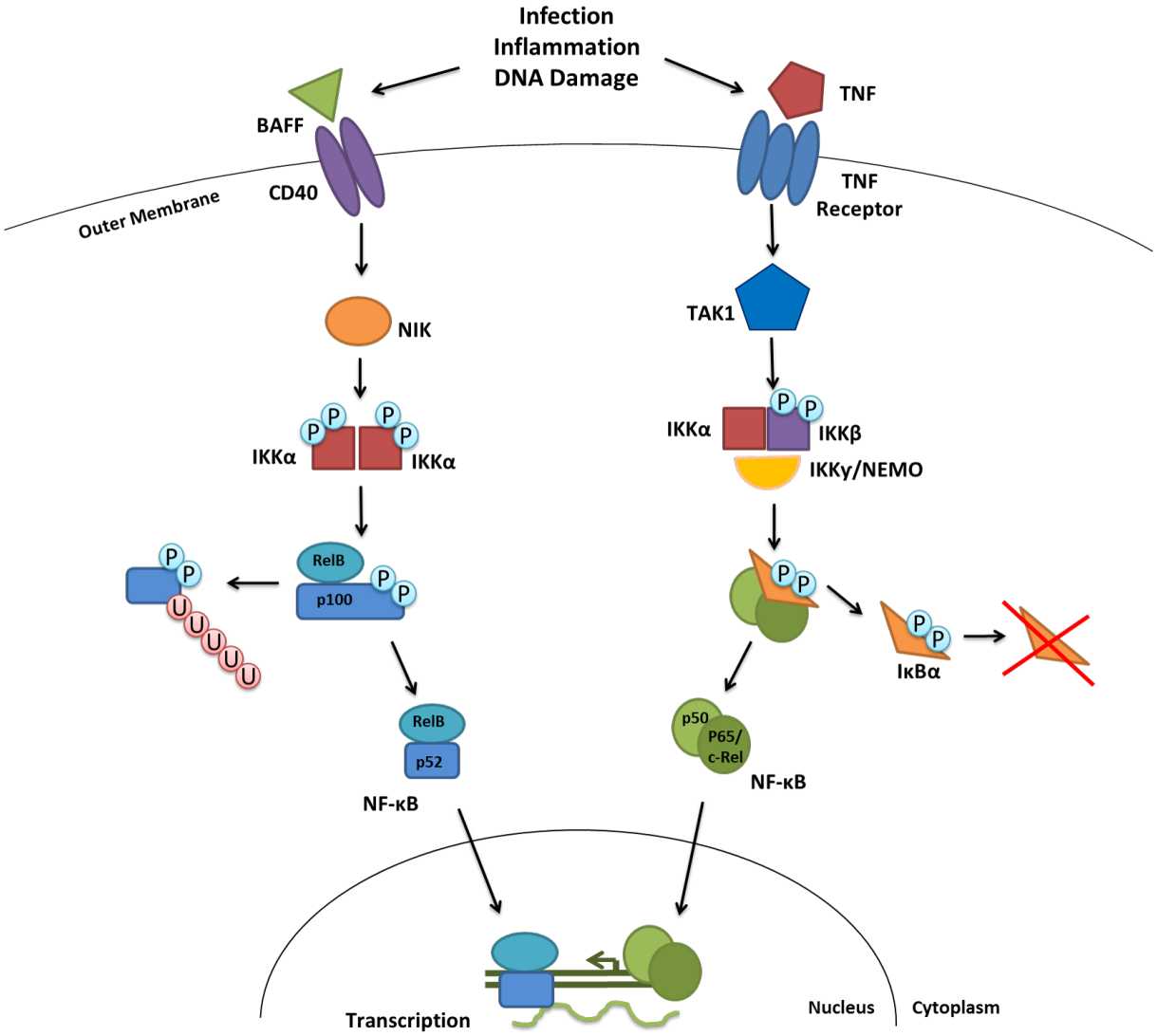

Figure 12. Canonical and Non-Canonical NF-κB Signalling. NF-κB is activated in response to a wide range of stimuli. Non-Canonical signalling typically occurs through NF-κB-inducing kinase (NIK) and involves transduction through a IKKα homodimer to activate RelB and p100 dimers. Ubiquitination of p100 leads to its processing and subsequent release of RelB and p52 heterodimers into the nucleus to coordinate gene expression. In the canonical signalling pathway, upstream signals converge on a trimeric form of the IKK complex from upstream kinases such as transforming growth factor-β activated kinase-1 (TAK1). Phosphorylation of the beta subunit of the IKK complex allows signal transduction to IκBα. The subsequent phosphorylation of IκBα causes its dissociation from RelA, p50 and c-Rel dimers and degradation. Since IκBα can no longer sequester NF-κB in the cytoplasm, NF-κB is free to move into the nucleus and coordinate transcription.

The activation of the NF-κB pathway described above is broadly considered to be the 'typical' route of canonical signalling. The activation through the IKK complex that leads to the the serine 32/36 phosphorylation, ubiquitination and degradation of IκBα and the subsequent release of RelA, has been extensively studied. This rapid, almost immediate, activation of the canonical NF-κB pathway is associated with the 'traditional' activators such as inflammatory cytokines and bacterial products. Due to the vast range of different stimuli and downstream targets NF-κB signalling is extremely complex, as such this 'typical' mechanism of activation is not always upheld [42][119].

As discussed earlier, other activators of the canonical NF-κB pathway include DNA damage inducers such as chemotherapeutic drugs and UV-C radiation. As one would imagine the cellular response to DNA damage is very different to the response to inflammation and infection, as such the response of the canonical NF-κB to this stress is different [42][117]. Earlier studies have described a mechanism for NF-κB that occurs independently of the IKK complex following UV stress, and involves alternative post-translational modifications of IκBα to control its degradation [120][121][122]. In this slower actvation of NF-κB, downstream transduction of signal to IκBα occurs in a p38 and casein kinase 2 (CK2)-dependent manner rather than through the IKK complex, although other reports indicate that NEMO is still required for this signalling [123].

In the late 1990s and early 2000s it was reported that IκBα degradation can occur in the absence of serine 32/36 phosphorylation in the response to DNA damage induced by chemotherapeutic agents [120][122]. Other studies have implicated tyrosine 42 phosphorylation of IκBα as an alternative means of releasing and activating NF-κB, and contributing to the subsequent ubiquitin-mediated degradation of IκBα [124][125]. In addition, activation of NF-κB in the absence of IκBα has been reported alongside tyrosine 42 phosphorylation [118]. Until more recently, phosphorylation of IκBα at serines 32/36 has been linked to its degradation, following K-48-linked ubiquitination [78][126][127][128]. However these studies have highlighted some of the alternative means of inducing NF-κB activation through regulation of IκBα, as well as indicating that serine 32/36 phosphorylation was not as critical for IκBα degradation as previously believed. Indeed, more recent reports suggest that IκBα can be sumoylated at this ubiquitination site, which prevents ubiquitination and degradation, stabilising IκBα, yet allowing for the release and activation of NF-κB [129][130].

As described above, this activation of NF-κB subunits is complex both in terms of upstream signalling, and the transduction of signal through the IKK complex to either the IκB proteins or the class I NF-κB subunits. Following the activation and release of NF-κB subunits and the formation of homo- and hetero-dimers, further modifications can occur on the NF-κB subunits themselves to allow them coordinate gene expression appropriately in the nucleus. The best characterised subunit, RelA, contains many residues that are known to be phosphorylated in response to different stimuli to elicit the correct transcriptional response.

Inactivation of the NF-κB pathways occurs once the activation signal has stopped; at this stage the level of nuclear export of NF-κB subunits is greater than import [131][132]. In addition to this the inhibitory IκB proteins are direct transcriptional targets of NF-κB leading to the inhibition of NF-κB through a negative feedback loop [133].

1.2.4 Regulation of Transcription by The NF-κB Family of Transcription Factors

As discussed earlier, the NF-κB pathways are activated by a plethora of different inducers, in response to inflammation, infection and other stresses. It therefore makes sense that NF-κB equally regulates the transcription of a large number of different genes, with perhaps as large a range of diversity as the inducers have.

In addition to coordinating the transcription of the gene encoding IκBα in a negative feedback loop [126], NF-κB controls the transcription of class 1 NF-κB family members. Full length inactive p105 and p100 precursors are transcribed to replace the activated cleaved forms of these proteins so that the pathway is able to be activated again in future rounds of signal pathway activation [134][135]. Studies have highlighted the complexity of this process as expression of the p50 precursor p105 is controlled by both RelA and p50 itself [134]. p100 expression is also promoted by RelA interactions but suppressed following p52 binding in a negative feedback loop [135]. In addition to this, the expression of NF-κB subunits c-Rel and RelB are controlled by NF-κB pathway activation. The former, c-Rel is autoregulated through a negative feedback loop [136], while RelB expression is controlled by both RelA and RelB [137].

Several studies have demonstrated that NF-κB itself is able to coordinate the expression of activators of the NF-κB pathways [138][139][140][141]. Transcription of genes encoding Interleukin-8 (IL-8) and TNF chemokines can lead to prolongation of NF-κB activation or the activation of other NF-κB dimers to coordinate the expression of different genes. Both IL-8 and TNF activate NF-κB through interaction with cell surface receptors, allowing signalling to continue through a positive feedback loop [138][139][140][141].

NF-κB also coordinates the transcription of genes whose products are required in critical cellular responses and pathways. Cellular inhibitor of apoptosis (cIAP)-2 is critical in the control of apoptosis. The role of NF-κB in apoptosis is complex and has been described as both pro- and anti-apoptotic. The transcription of Bcl-2 and Bcl-XL suggests that activation could be pro-apoptotic as these proteins are required for the initiation of apoptosis. In contrast to this, transcription of IAPs such as cIAP-2 in response to NF-κB stimulation following inflammatory cytokine production leads to inhibition of apoptosis. This prevents the initiation of apoptosis in response to inflammation to allow for resolution of the problem rather than initiating programmed cell death [142][143].

NF-κB also controls the expression of genes that encode products involved in the cell cycle through coordination with other key transcriptional regulators such as JunD and

Figure 13. NF-κB Controls the Transcription of a Plethora of Genes. NF-κB pathway activation culminates in the control of expression of a wide range of different genes. This schematic does not show all target genes, and is designed to give an idea of the range and number of genes that NF-κB has been linked to. Genes linked to activation of the NF-κB pathways include those involved in the response to inflammation and infection such as cytokines and chemokines as well as antigens and immunoreceptors. Other target genes are linked with response to stress and apopotosis as well as growth factors, ligands and enzymes. NF-κB also controls the expression of other transcription factors, highlighting its importance in the activation of other pathways and the indirect control of expression of other sets of genes [43].

signalling transducers such as phosphoinositide-3-kinase (PI3K) family members [144]. Here NF-κB functions as a promoter of cell cycle progression in the early phase of the cell from G1-phase to S-phase through direct control of cyclin D1 transcription. This regulates cell growth and differentiation through encouraging proliferation and preventing G0-phase [77][145].

In many cases NF-κB target genes encode proteins that act as part of a feedback loop to control NF-κB pathway activation. In PI3K-Akt pathway activation PI3K phosphorylates phosphatidylinositol biphosphate (PIP2), this then phosphorylates phosphoinositide-dependent protein kinase-1 (PDK1), which in turn phosphorylates Akt (Fig. 14). This leads to activation of NF-κB. NF-κB controls the expression of PTEN, which acts as an inhibitor of this activation through dephosphorylating phosphatidylinositol triphosphate (PIP3), therefore preventing activation of PDK1 and Akt. PTEN expression therefore blocks the activation of NF-κB in a negative feedback loop through the PI3K-Akt signalling cascade [144][146].

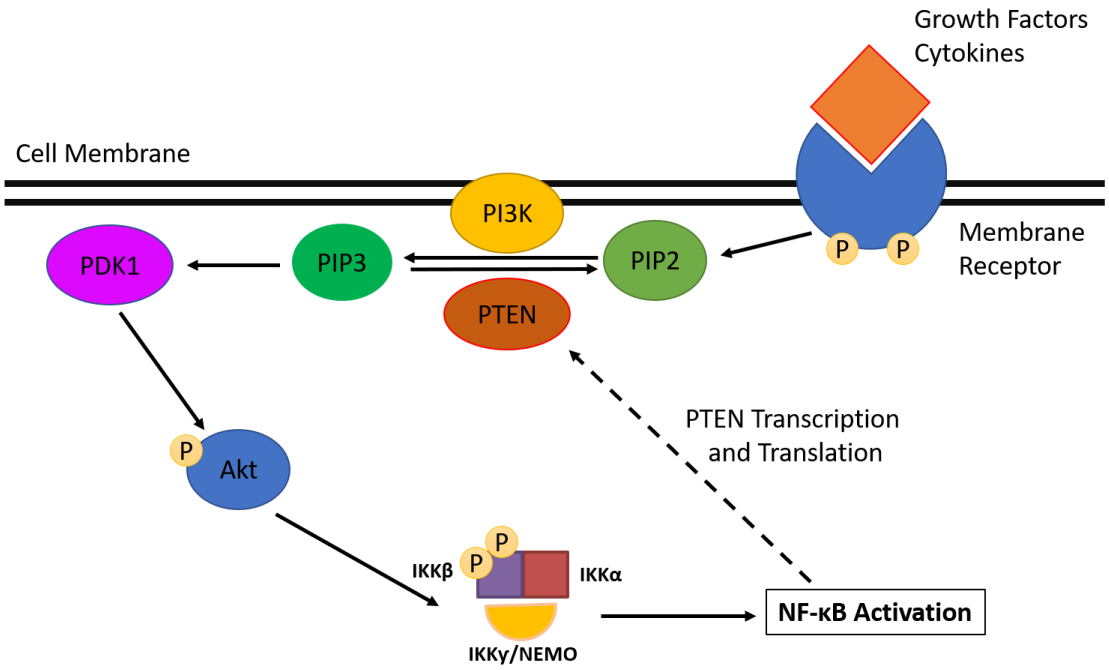

Figure 14. Crosstalk Between PI3K Signalling and the Canonical NF-κB Pathway. Following exposure to external stimuli such as cytokines and growth factors, the PI3K-Akt signalling pathway is activated. This is in turn able to activate the canonical NF-κB pathway through phosphorylation of key members of the IKK complex. In turn, NF-κB regulates the expression of phosphatase and tensin homolog (PTEN), adding a further level of feedback and control to the activation of these pathways. Figure adapted from Kucuksayan et al., 2016 [146].

NF-κB is also a regulator of other key signalling pathways. This cross-talk does not

only occur through coordinating the transcription of cell cycle regulatory proteins and apoptosis, but through interactions with a plethora of other signalling pathways. NF-κB is also directly involved in the expression of HIF-1α in the presence of hypoxic stress [147]. This transcription factor in turn controls the expression of other sets of genes associated with the response to hypoxia [148].

Crosstalk between the canonical NF-κB pathway and other signalling pathways can occur through many different mechanisms. This can occur through protein-protein interactions upstream, following gene expression where NF-κB targets such as PTEN are involved in independent pathways or where gene products of other transcription factors activate NF-κB. One example of this that is relevant to this thesis is that of TAK1. As discussed previously TAK1 is an upstream kinase of IKKβ, however it also acts as an upstream kinase of the c-Jun N-terminal kinase (JNK) signalling pathway. This is one of three mitogen-activated protein kinase (MAPK) signalling pathways that function as a cascades through a series of kinases; MAP kinase kinase kinase (MAPKKK or MAP3K) such as mitogen-activated protein kinase kinase (MKK)2/3, a MAP kinase kinase (MAPKK or MAP2K) such as mitogen-activated protein kinase kinase (MEK)5, and a MAP kinase (MAPK). The MAPK signalling cascades are named after the MAPK proteins; extracellular signal-regulated kinase (ERK), JNK and p38. The ERK pathway is more commonly associated with proliferation and differentiation, while the JNK and p38 pathways are activated in response to cell stresses.

As well as coordinating the response to oxidative stress through promotion of HIF1α expression, NF-κB is able to directly coordinate the expression of a wide range of genes involved in the response to loss of ROS homeostasis. Expression of antioxidant enzymes such as the Cu/Zn-superoxide dismutase superoxide dismutase 1 (SOD-1), the manganese superoxide dismutase superoxide dismutase 2 (SOD-2) and the quinone oxidoreductase nicotinamide adenine dinucleotide phosphate (NADPH) oxidase are all controlled by NF-κB subunits in the response to oxidative stress [149][150][151].

1.3 NF-κB, The PIKK Family and Critical Cellular Responses

As discussed previously, genotoxic stress, or DNA damage, is a known activator the NF-κB pathway [92]. Coordination between the DNA damage response, the cell cycle and the apoptotic pathways is required to ensure that the cell is able to respond to genotoxic stress in the correct way. This complex network of signalling pathways is controlled by PIKK family members, through the activation of ATM, ATR and DNA-Dependent protein kinase (DNA-PK) in the response to DNA damage. Once active ATM and ATR phosphorylate downstream targets to arrest the cell cycle while DNA is repaired, as well as interacting with the NF-κB pathway. This ensures that the cells respond correctly to DNA damage; pausing the cell cycle to carry out repairs and preventing or promoting apoptosis through interactions with the NF-κB pathway as required.

1.3.1 DNA Damage and Repair

DNA damage can occur as a result of exposure to endogenous sources such as following an increase in cellular ROS levels or from exogenous or external sources following exposure to different frequencies of radiation, exposure to chemical agents such as chemotherapeutic drugs or through viral transposition. Some examples of endogenous damage include oxidation, alkylation, hydroylsis (deamination and depurination), bulky adduct formation, mono- or di-adduct damage or base mismatch. Exogenous damage can include formation of pyrimidine dimers, strand breaks, depurination and cross-linking. The ability of the cell to detect and determine the form of damage is critical for DNA repair to occur. A range of different repair mechanisms are used by the cell to repair each specific type of DNA damage (Table 2).

DNA damage occurs at a high frequency, with thousands of lesions occurring in a given cell every day, most of which cause changes in the tertiary structure of the DNA double strand helix. It is critical that DNA damage is detected and repaired rapidly and appropriately to prevent passing on the damage to daughter cells, accumulation of further damage and loss of function. The accumulation of unrepaired DNA damage can lead to the initiation of a plethora of cellular process such as senescence and apoptosis, and in extreme cases can lead to unregulated cell division, uncontrollable proliferation and the development of cancer. This loss of function occurs when damage occurs in parts of the genome that are essential for key cellular mechanisms, however cells are often able to function almost normally when mutations occur in non-essential genes.

Double-strand DNA damage or breaks can be repaired by three different mechanisms; non-homologous end joining (NHEJ) (Fig. 15), microhomology-mediated end joining (MMEJ) and homologous recombination (HR)(Fig. 16). Often the mechanism of repair is dictacted by the position of the cell in the cell cycle, with HR acting exclusively in S- and G2- phase as it requires templates in the form of sister chromatids, while NHEJ can be performed in post-mitotic and G1-phase cells. The repair pathway initiated following double strand breaks is dependent on whether homologous DNA is present on another chromosome or DNA strand to act as a template [152][153][154]. The PIKK family members ATM, ATR and DNA-PK play important roles in the response to double-strand and single strand breaks, as their activity is crucial for interactions with other pathways to coordinate cell cycle arrest, NF-κB activation and histone modification.

Like HR, single-strand DNA damage utilises complementary base pairing as a tool in repair. Single-strand breaks often have a far smaller aberrations, usually consisting of one or two damaged or incorrect bases on one strand of DNA rather than double stranded breaks. There are 3 main types of single-strand break repair that often work to excise and replace the offending lesions, these include; base excision repair (BER) (Fig. 17), nucleotide excision repair (NER) (Fig. 18) and mismatch repair (Fig. 19).

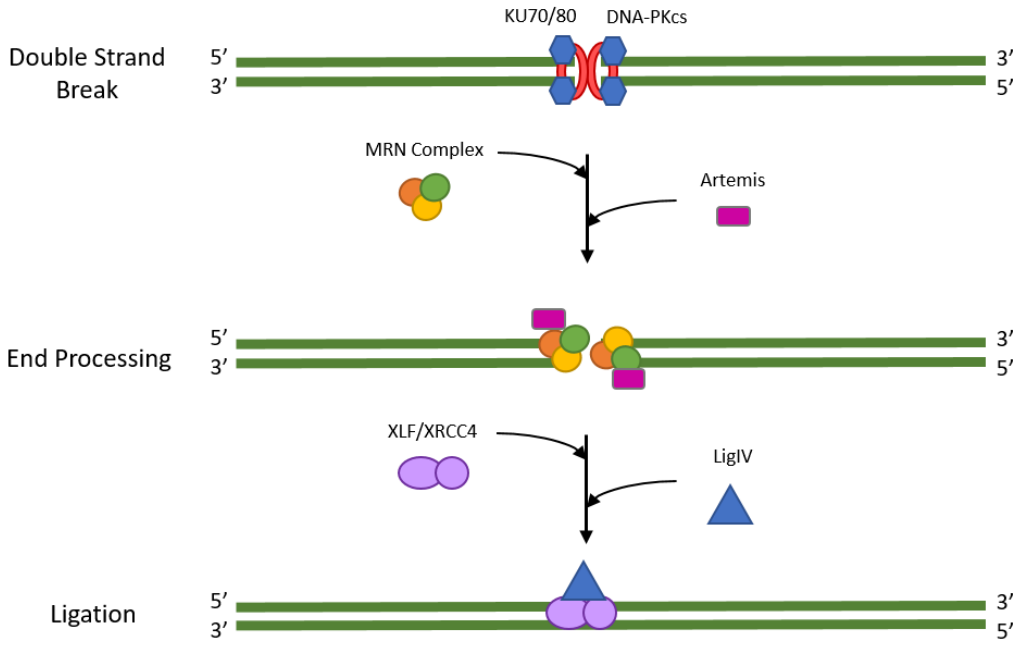

Figure 15. Non-Homologous End Joining. NHEJ occurs in the absence of sister chromatids, therefore the broken ends of the DNA are simply ligated together. Often overhangs of the broken DNA can be used as guides as small homologous sections, or microhomologies, can be present here. The initial stage of NHEJ involves the recognition and binding of a Ku heterodimer (Ku70/Ku80) to the site of the lesion. Recruitment and binding of the Mre11, RAD50 and Nbs1 (MRN) complex and DNA-PKs to the exposed ends of the DNA follows, forming a complex with the Ku dimer and activating DNA-PK. At this stage the exposed ends of the DNA are processed, this involves the removal of any damaged bases by nucleases and the synthesis of new bases by DNA polymerases. The DNA ligase IV complex (DNA ligase IV and XRCC4) is recruited and bound by the Ku heterodimer to ligate the broken fragments of DNA together[155][156][157].

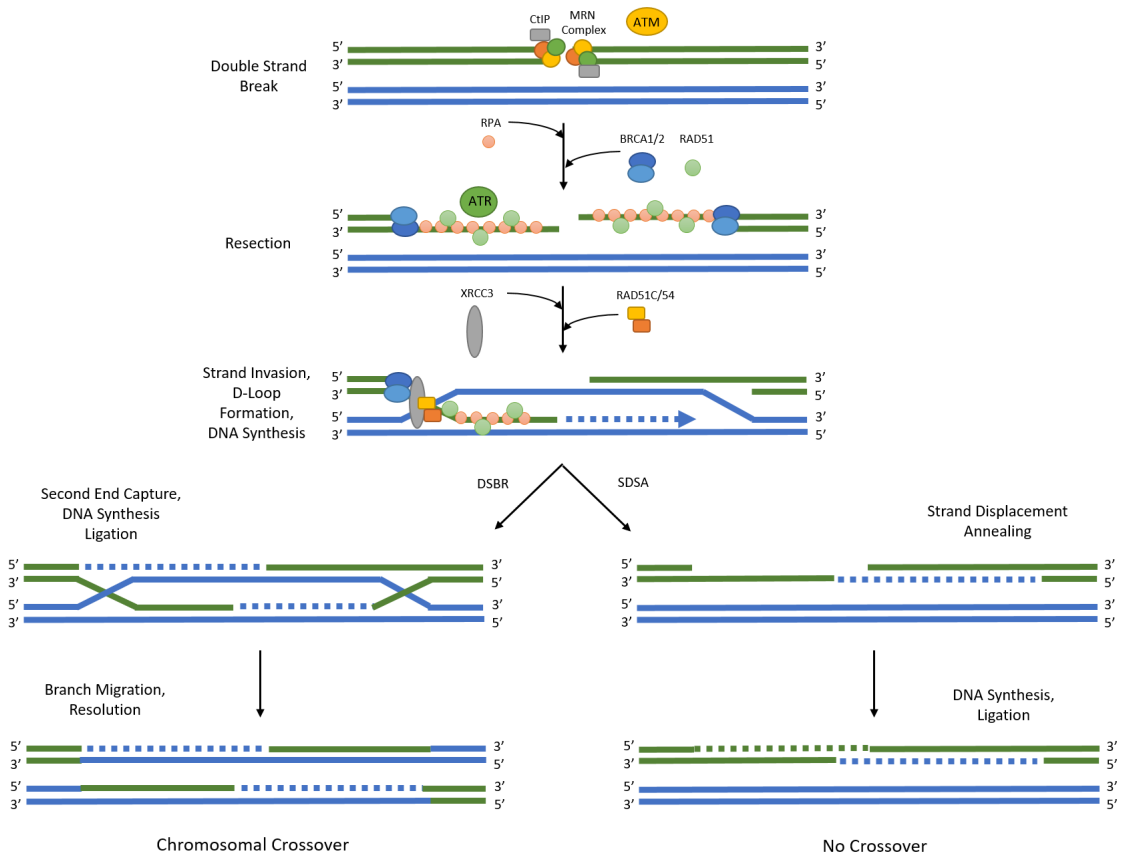

Figure 16. Homologous Recombination. HR occurs when a template sequence such as a sister chromatid is available. HR occurs during meiosis in the absence of DNA damage to introduce variation between gamete cells. There are two main methods by which HR occurs in human cells; the double strand break repair (DSBR) pathway and the synthesis-dependent strand annealing (SDSA) pathway. The initial steps are the same; the MRN complex is recruited to the site of damage [158], ATM is activated by the MRN complex, leading to the phosphorylation of downstream targets such as checkpoint kinase 2 (Chk2) to block cell cycle progression and H2A histone family member, X (H2AX) to control chromatin structure [159][160][161]. 5' ends of the broken section of DNA are then resected to form 3' overhangs [162][163][164]. Replication protein A (RPA) then binds the single stranded DNA and Rad51 forms a nucleoprotein filament, coordinating strand invasion from one 3' overhang. D-loop (displacement-loop) formation and new DNA synthesis occurs [165]. This invading 3' strand forms a cross-over with the template DNA strand following synthesis, this is known as a Holliday junction. In the case of the DSBR pathway, the second 3' overhand also forms a Holliday junction; these are cut by endonucleases and repaired. DSBR commonly results in chromosomal crossover. In contrast in SDSA the invading 3' strand is extended along the template by DNA polymerase in a process known as branch migration. Any remaining overhands are degraded and the phosphodiester backbone is repaired by ligation. This mechanism of HR does not result in any chromosomal crossover [166].

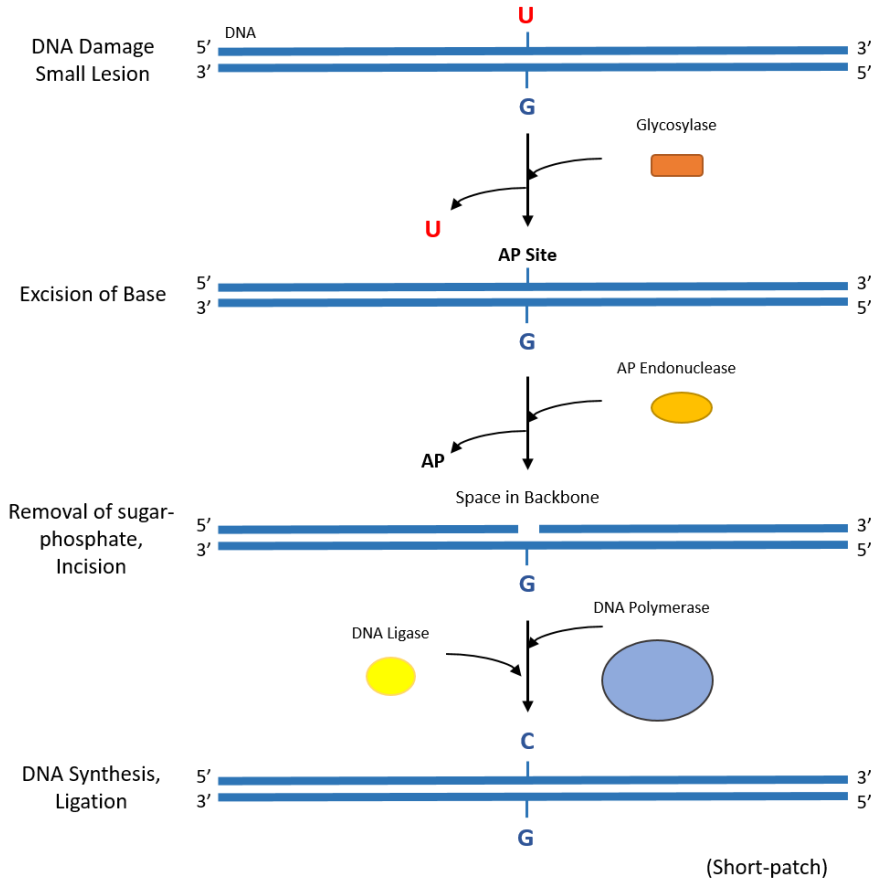

Figure 17. Base Excision Repair. BER is responsible for the removal and replacement of relatively small DNA adducts that do not alter the physical tertiary helical structure of double stranded DNA [167][168] . Although small, it is important that this DNA damage is resolved as it could lead to mispairing, mutations and even double strand breaks following replication. Oxidised, alkylated or deaminated bases are sensed by legion-specific DNA glycosylases, which then cleave out the damage base portion of the nucleotide leaving an abasic (AP) site behind. This DNA backbone is then incised by an AP endonuclease leaving a 3' hydroxyl and a 5' deoxyribosephosphate at the site of damage, the latter of which is converted into a ligatable 5' phosphate by tyrosyl-DNA phosphodiesterase 1 (TDP1) [169]. DNA polymerase then completes the repair process through DNA synthesis followed by ligation of the phosphodiester backbone by the XXRCC1/Ligase III complex, which is recruited to the site of damage by the nuclear protein poly (ADP-ribose) polymerase (PARP). This can be carried out by two mechanisms; short-patch repair or long-patch repair, which depends on the length of DNA excised and replaced [170].

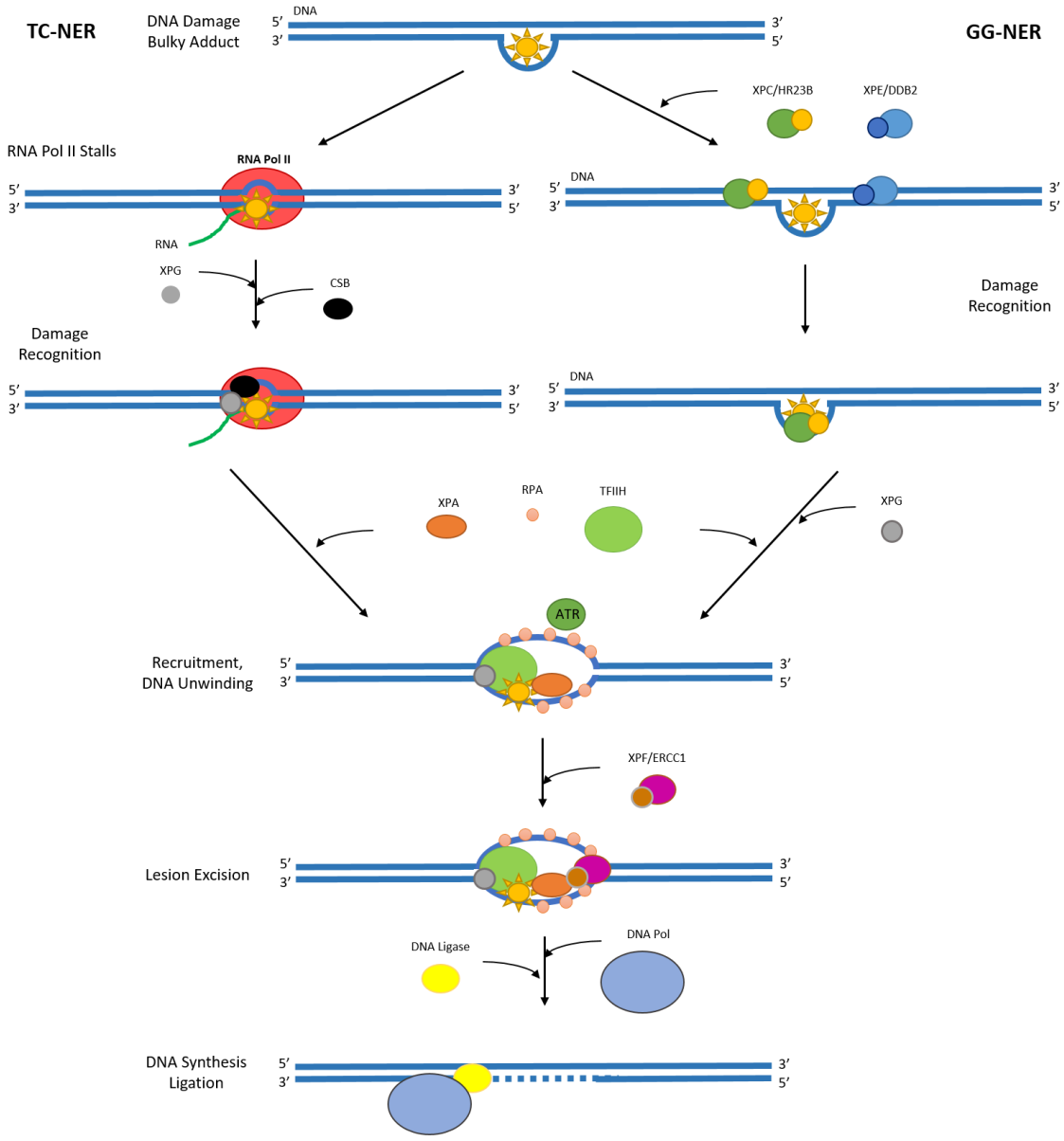

Figure 18. Nucleotide Excision Repair. NER is used to repair bulkier, helix-distorting DNA adducts [171][172]. There are two eukaryotic NER pathways; global genomic-NER (GG-NER) and transcription coupled-NER (TC-NER) [173][174]. In the GG-NER pathway, the bulky adducts are sensed by DNA-damage binding (DDB) and XPC-Rad23B complexes due to helix distortion [175][176][177]. TC-NER is activated when RNA polymerase stalls at the site of a DNA damage lesion. At this stage the two pathways converge as TFIIH is localised to the site of damage [178][179]. Other proteins are then recruited sequentially to coordinate DNA unwinding. TFIIH is responsible for the dual excision of the unwound damaged DNA [176]. The xeroderma pigmentosum group A-complementing protein (XPA) and RPAs stabilise the single stranded DNA and recruit the xeroderma pigmentosum group G-complementing protein (XPG) endonuclease and the ERCC1-XPF to incise the damaged strand [180][181]. DNA is then synthesised using the complementary strand as a template. Sealing of the phospho-diester backbone is carried out by DNA ligases to complete the process [182][183].

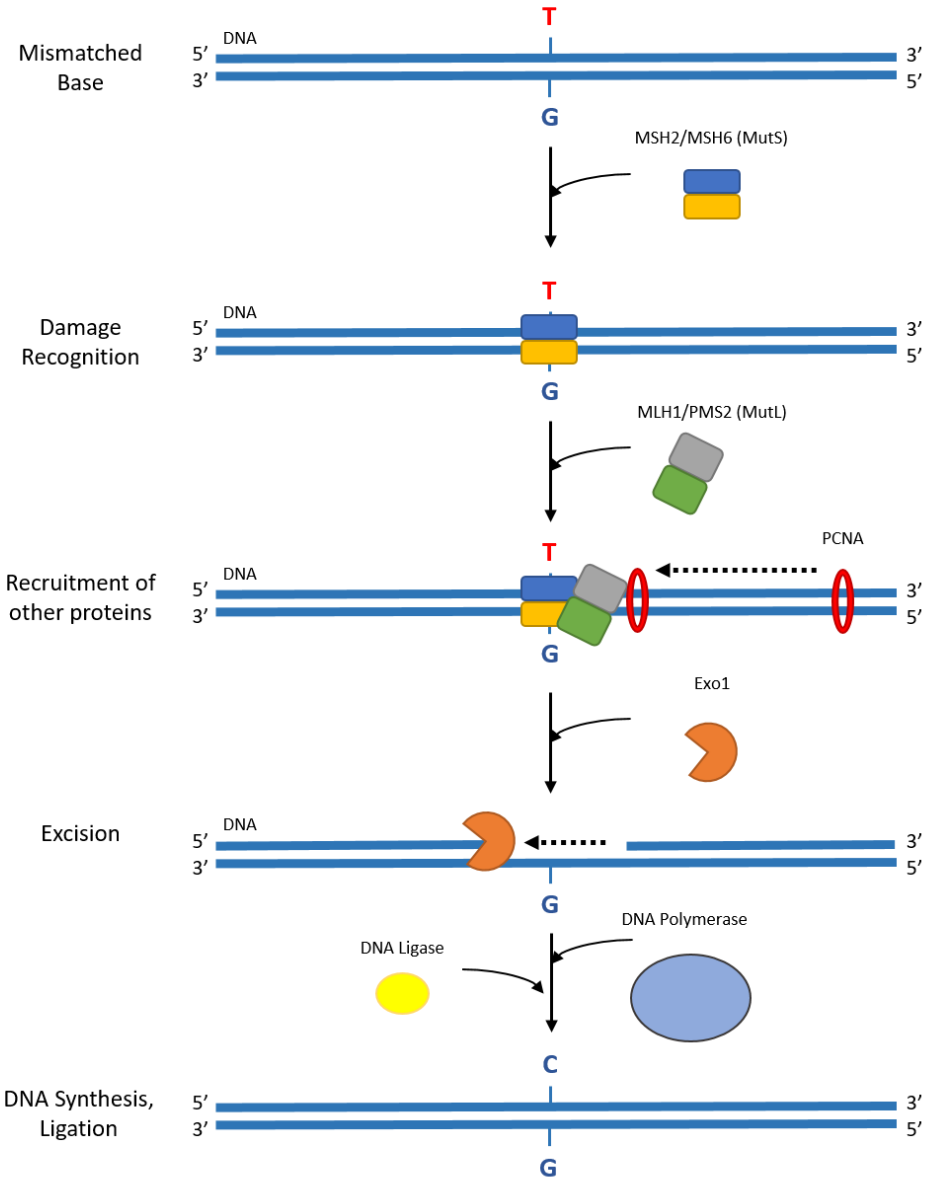

Figure 19. Mismatch Repair. This process recognises and repairs mismatched bases as well as small insertions and deletions. In eukaryotes the site of damage is recognised on the newly synthesised strand of the DNA by the a MutS protein homolog 2 (Msh2)/MutS protein homolog 6 (Msh6) protein dimer, the hydrolysis of ATP activates this complex and leads to the recruitment and subsequent activation of PMS2/MutL homolog 1 (MLH1). This dimer is able to move along the DNA in a 5' or 3' direction to scan for errors in the DNA. Following this the DNA clamp proliferating cell nuclear antigen (PCNA) translocates along the daughter strand of the DNA, this leads to the recruitment of the exonuclease Exo1, starting from a nick in the DNA, this degrades the damages DNA strand in a 3' to 5' direction. Following excision of 100s of nucleotides PCNA then binds to DNA polymerase, which moves to the damaged site to synthesise new DNA using the parent strand as a template. Ligation then occurs to seal the phosphodiester backbone [184].

DNA Damage and Repair		
Source of Damage	Damage Induced	Repair Pathway
Alkylating Agents, UV Radiation, Nitrosourease, Streptoztocin, Methylation	Alkylated Bases, Pyrimidine Dimers, O-6-methyl-guanine, N-7-methyl-guanine	Direct Reversal
ROS, Ionising Radiation, X-rays, Alkylating Agents, Spontaneous Hydrolysis	Single Strand Breaks, Oxidised Bases, 8-oxo-guanine, Alkylated Bases, abasic/apurinic/apyrimidinic sites, Uracil	BER
ROS, Cigarette Smoke, UV(C) Light	Cross Links (intra/inter-strand, DNA-protein), Bulky Lesions, 6-4 Photoproduct, Cyclobutane	NER
Oxidation, Alkylation, Replication Errors	Small Insertion Loops, A-G or T-C Mismatched Bases, Deletions	MMR
Ionising Radiation, Replication Errors, Anti-Tumour Agents, X-Rays, ROS	Double-strand Breaks, Intra-strand Crosslinks	HR or NHEJ

Table 2. Table of DNA Damage Inducers, Effects and Repair Mechanism. There are many different types of DNA damage that come from a wide range of different sources. This are each resolved through activation of distinct and mechanistically complex repair pathways.

1.3.2 The PIKK Family

The PIKK family of kinases encompasses several proteins including ATM, ATR, DNA-PK, mammalian target of rapamycin (mTOR), transformation/transcription domain associated protein (TRRAP) and serine/threonine protein kinase (SMG1). They are closely related to the PI3K family of protein kinases (Fig. 20). With the exception of TRRAP function as protein kinases to activate downstream signalling pathways through phosphorylation of key serine and threonine residues [185][186][187][188]. Members of the PIKK family are large proteins that are characterised by the presence of the catalytic domain FRAP, ATM and TRRAP C-terminal (FATC) and N-terminal α-helices that enable protein-protein interactions and recruitment to targets [186].

ATM, ATR and DNA-PK are key responders to DNA damage events, and activate downstream targets to control DNA damage responses through coordination of cell cycle arrest and initiating DNA repair. ATM, ATR and DNA-PK respond to different types of damage, coordinating downstream targets to induce the most appropriate DNA repair pathway. Both ATM and DNA-PK are essential for the cellular response to DNA double strand break (DSB)s (Fig. 15, Fig. 16); ATM is involved in homologous recombination repair and controls cell cycle progression through phosphorylation of its substrate Chk2

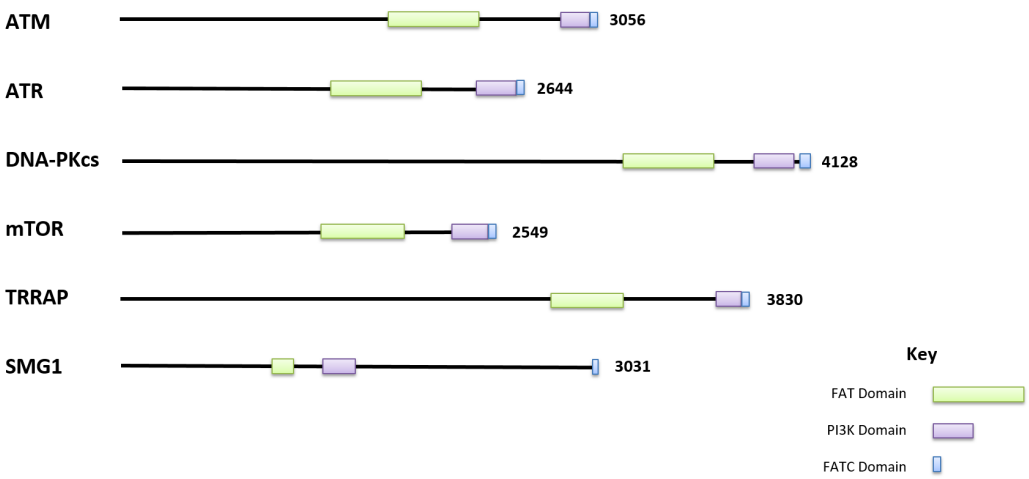

Figure 20. The PIKK Family. The PIKK family of serine/threonine kinases are characterised by the presence of a FAT and FATC domains. They are close relatives of the PI3K family of kinases and work in a wide range of cell signalling pathways including the DNA damage response as well as transcription and translation. They are large proteins and as such their crystal structure has not yet been successfully characterised.

[189], while DNA-PK is involved in NHEJ [190]. ATR, on the other hand is involved in cellular response to single-stranded DNA, such as errors encountered during DNA replication (Fig. 16, Fig. 18). Activation of ATR leads to cell cycle arrest through phosphorylation of proteins such as checkpoint kinase 1 (Chk1) [191].

Inactive ATM is present in the nucleus as an inactive homodimer; in response to DNA DSBs ATM is activated though autophosphorylation of serine 1981. It then splits into 2 active monomers and phosphorylates the histone H2AX, which signals the site of DNA damage to the cells and leads to the recruitment of MRN complex to the site of damage to coordinate DNA repair [189]. Following full activation of ATM through aurophosphorylation on serines 367, 189 and 1981 [192] on recruitment to the MRN complex ATM is able to phosphorylate a number of substrates directly or indirectly, both inside and outside of the nucleus. These subsrates include Chk2, tumour protein p53 (p53) and mouse double minute 2 homolog (Mdm2) to coordinate cell cycle arrest, allowing for this DNA repair to take place. In addition, ATM activation leads to transcriptional changes through the activation of transcription factors such as NF-κB [191].

Although ATM is considered to be the main kinase of H2AX, some publications have demonstrated that both ATR and DNA-PK are able to phosphorylate H2AX at serine 139. Following hydrogen peroxide treatment and the resulting formation of single stranded breaks, ATR is able to induce γH2AX independently of ATM [193]. Following exposure to ionising radiation, DNA-PK carries out this phosphorylation of H2AX in an overlapping manner with ATM [194], while another study described that this was stimulated by prior

acetylation of histones [195].

As the name suggests, ATR is very similar to ATM, however rather than responding to double strand breaks in DNA, ATR is activated during S-phase in the presence of a stalled replication fork due to the presence of exposed single stranded DNA structures. These can occur following the formation of base-crosslinks, following exposure to certain DNA damaging agents and as an intermediate in DNA repair pathways in response to double strand breaks [196][197]. This highlights the close connection and overlap in function that exists between ATM and ATR [198].

ATR and the RAD9-RAD1-Hus1 (9-1-1) complex are recruited to the site of DNA damage by RPA and through interactions with ATR interacting protein (ATRIP). This 9-1-1 complex in turn recruits the ATR activator Topoisomerase II binding protein 1 (TopBP1) which induces ATR activation through phosphorylating ATR at threonine 1989 [199][200]. Autophosphorylation on serine 428 following exposure to other stresses such as UV radiation or oxidative stress also leads to ATR activation [201]. Following activation ATR phosphorylates a plethora of downstream targets such as Chk1 to control cell cycle progression and coordinate DNA repair[186].

1.3.3 The Cell Cycle

The cell cycle describes the process by which cells duplicate their DNA and divide. There are several stages of the eukaryotic cell cycle; G1-phase (gap 1), S-phase (synthesis), G2-phase (gap 2) and Mitosis (chromatid separation). The cell then splits into two daughter cells through a process called cytokinesis. Proliferating cells then enter G1-phase again, while differentiated cells leave the cell cycle and enter G0 phase. This process is highly conserved in eukaryotic cells and is a tightly regulated process; loss of control of the cell cycle can lead to increased proliferation, accumulation of DNA or cell death. Cell replication is critical in multicellular organisms for the controlled development of specific tissues and in the response to external stresses and is controlled by a complex series of upstream activation pathways that respond to extracellular and intracellular signals to coordinate replication in a timely and correct manner (Fig. 21).

Control of the cell cycle is tightly regulated through four main checkpoint controls; the intra-S phase checkpoint, the spindle-assembly checkpoint, the spindle position checkpoint and the DNA-damage checkpoint [205][206] (Fig. 21). The upstream kinases ATM and ATR are essential in both the intra-S phase and DNA damage checkpoints. Here ATR detects single stranded DNA on replication forks to determine whether DNA synthesis has been completed [207]. ATM detects DNA damage events throughout the cell cycle [208][209]. ATR and ATM are responsible for signalling between the DNA damage response proteins and the downstream kinases Chk1 and Chk2 to arrest the cell cycle until DNA damage has been resolved [210][211] (Fig. 21). If left undetected DNA damage may be propagated forward to future generations, leading to accumulation of further mu-

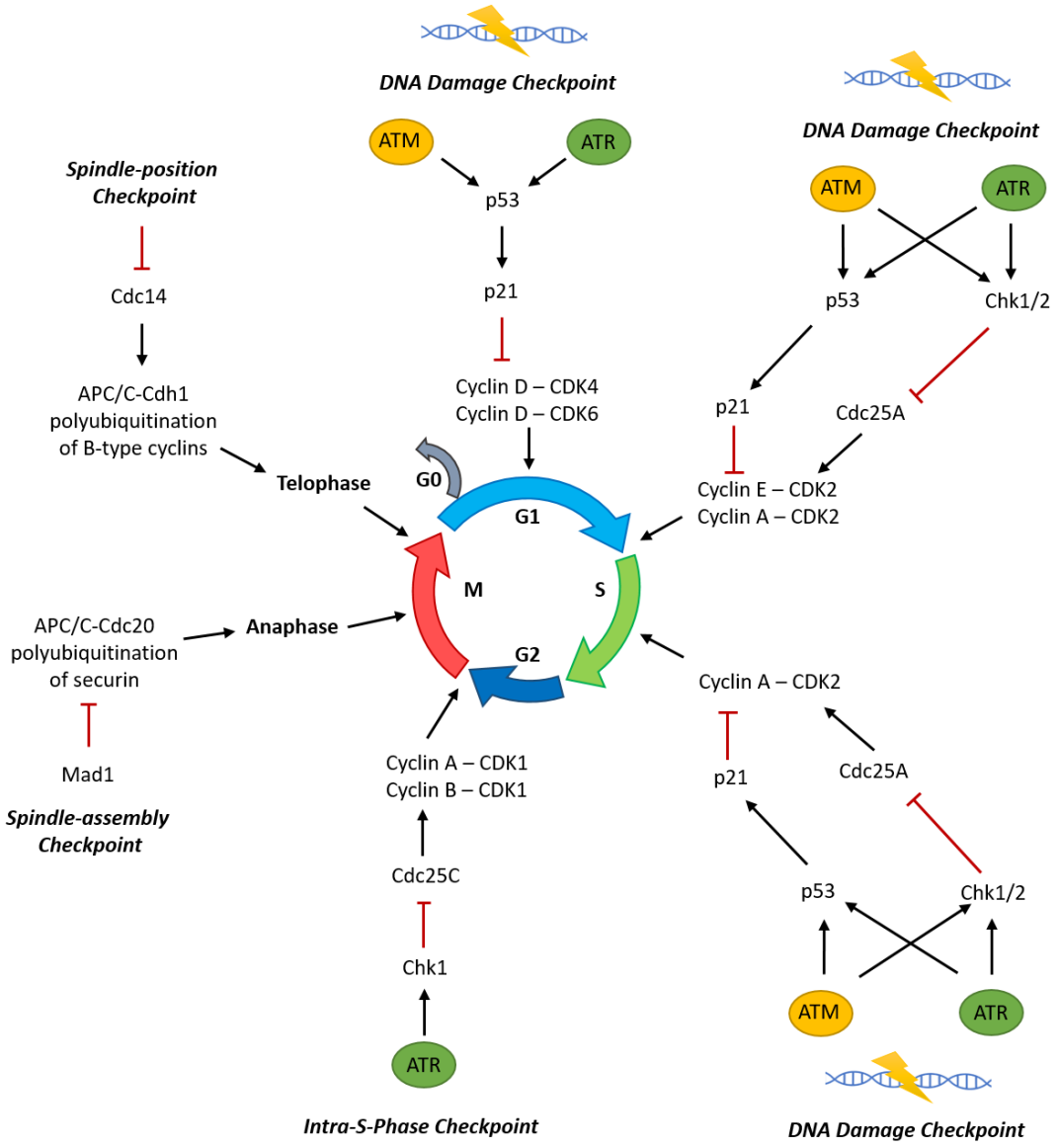

Figure 21. Regulation of the Cell Cycle. Progression through the cell cycle is controlled by fluctuations in levels of cyclin proteins and cycin-dependent kinase (CDK)s [202][203][204]. Different combinations of these proteins function as heterodimers in different stages of the cell cycle to coordinate the phosphorylation of downstream targets. Activation and inhibition of cyclin-CDKs is therefore critical in the control of the cell cycle. Further control occurs through checkpoint mechanisms at points in the cycle where changes in expression or activity of these heterodimers changes. Sensing of DNA damage is essential throughout the whole process and relies heavily on the upstream kinases ATM and ATR.

tations, uncontrolled proliferation and diseases such as cancers. In the event the DNA damage cannot be repaired apoptosis is initiated to prevent mutations from being passed to future generations.

1.3.4 Apoptosis

There are two main forms of cell death; programmed cell death (apoptosis) and non-physiological cell death (necrosis) [212]. The latter occurs as a result of massive injury or damage to the cell from external sources, this results in autolysis and uncontrolled death that causes an inflammatory response [213][214]. In contrast to this, programmed cell death such as apoptosis occurs in a controlled and physiological way through initiation of cell signalling pathways in response to internal factors. Apoptotic cells are easily identifiable under a microscope as they go through distinct morphological changes; cell shrinking, cytoskeleton collapse, nucleus and chromatin condensing, fragmenting, blebbing and formation of apoptotic bodies. Unlike necrosis, this allows the neighbouring macrophages to engulf and degrade any by-products, rather than spilling their contents and causing harm to neighbouring cells [215].

Apoptosis is intimately linked with other cellular processes such as autophagy. Autophagy describes a predominantly cytoplasmic response as lysosomes degrade substrates in order to obtain metabolic building blocks and obtain energy in circumstances where energy is depleted. During amino acid starvation autophagy is able to prevent initiation of apoptosis by degrading non-essential proteins to supply the cell with the amino acids that it needs to survive. In addition it is responsible for maintaining organelle integrity, responding to infection and clearance of aggregated proteins; functions essential for the health of the cell and preventing apoptosis [216]. Apoptosis and autophagy are also closely linked through the B-cell lymphoma (BCL) family of proteins, these control the permeabilisation of the mitochondrial membrane to regulate the balance of pro-apoptotic and anti-apoptotic signals, as well as regulating the initiation of autophagy. As such autophagy has a great influence over whether a cell undergoes apoptosis or survives [216].

Apoptosis is critical in many aspects of cell biology and plays an important role in development, removal of damaged cells and in the immune system to prevent autoimmune responses [217]. Apoptosis is generally initiated either through the loss of a sensing of trophic factors, which the cell receives to encourage it to survive, or through the detection of a signal that initiates apoptosis. This section will predominantly focus on the latter method of induction and will describe two forms of the signalling pathway used to initiate apoptosis; the extrinsic and intrinsic pathways (Fig. 22).

Both the extrinsic and intrinsic apoptosis pathways involve the activation and signalling of caspase proteins [218]. Caspase proteins are a family of proteases that are synthesised as inactive precursers known as procaspases. There are several different caspases; 2, 8, 9 and 10 are initiator caspases, 3, 6 and 7 are executioner caspases, and 1 and 11 are not involved

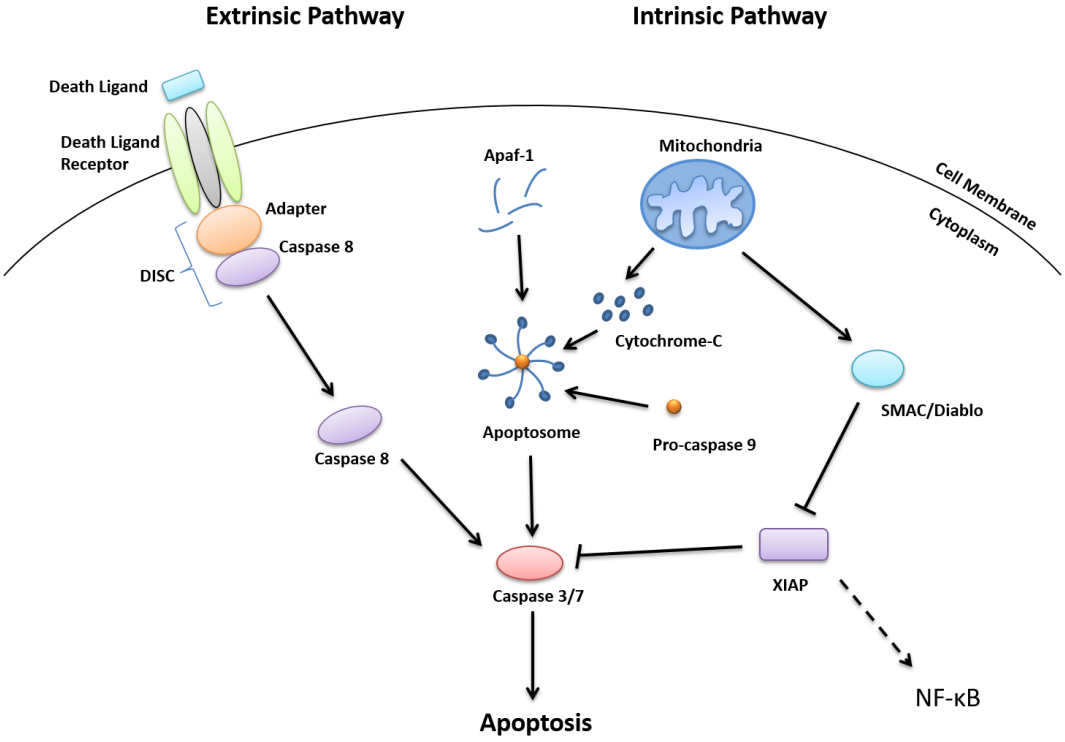

Figure 22. Extrinsic and Intrinsic Apoptosis Pathways. The extrinsic apoptosis pathway is initiated following the binding of extracellular death ligands binding to a cell membrane receptor [214]. The death domains of the receptor become activated and recruit adaptor proteins that recruit an initiator procaspase such as caspase 8 or 10 [218]. This complex is referred to as a death-inducing signalling complex (DISC) and leads to the cleavage and activation of this initiator caspase. Control of apoptosis in this pathway occurs upstream of the caspase proteins through binding of the adapter with the protein FLICE-like inhibitory protein (FLIP), which acts like a procaspase but does not contain proteolytic activity, competing with procaspases in DISC formation. The intrinsic pathway is initiated when the mitochondria releases the cytochrome C electron transport chain protein into the cytoplasm [219][220]. In some instances the intrinsic pathway is activated or repressed in response to the activation of the extrinsic pathway, to amplify or repress apotosis induction. This involves the B-cell lymphoma 2 (Bcl2) family of intracellular regulator proteins, which either promote or inhibit the release of cytochrome C from the mitochondria in a pro- or anti-apoptotic manner respectively [221]. When cytochrome C is released into the nucleus it forms a complex with apoptotic protease activating factor 1 (Apaf1), a pro-caspase activating adaptor protein. Seven Apaf1/cytochrome C dimers form a heptamer complex in a ring shape; this is known as the apoptosome. The apoptosome acts in a similar way to the DISC complex in the extrinsic pathway, cleaving and activating initiator procaspase 9 to begin the caspase cascade downstream and inducing apoptosis.

in apoptosis and work instead in the control of the inflammatory response, for example NF-κB-dependent caspase-11 expression is up-regulated following lipopolysaccharide (LPS) exposure in response to bacterial infection [222][223]. Caspases become activated following cleavage at a specific aspartic acid site and form heterodimers comprising of a large and small subunit. Two of these subunits assemble into an active tetramer; this active caspase is able to cleave downstream procaspases to form other active caspases. The caspase activation pathway is commonly described as a caspase cascade as an initiator caspase activates executioner caspases to cleave and degrade a variety of other target proteins such as nuclear lamin or endonucleases in an amplifying proteolytic cascade. The culmination of the activation of these caspases is the degradation of multiple cellular components and the onset of apoptosis [217].

A family of proteins known as the IAPs, have been shown to bind and inhibit activated caspases due to the presence of baculovirus IAP repeat (BIR) domains. In some cases IAPs are able to inhibit apoptosis through polyubiquitinating caspases, leading to their subsequent targeting and degradation by the proteosome. The presence of these proteins at certain levels prevents apoptosis from occurring as the caspase cascade cannot be effectively activated. In mammalian cells this is overcome by the inhibitors of IAPs; the anti-IAP proteins. The anti-IAP proteins such as second mitochondria-derived activator of kinases (SMAC)/DIABLO are released from the mitochondria as the intrinsic pathway is activated to ensure that apoptosis is carried out. SMAC is able to bind IAPs, releasing caspases to activate apoptosis. The presence of IAPs and anti-IAPs is critical for the control of apoptosis and adds another level of regulation to this import cellular response [219][217].

NF-κB plays a role in the regulation of apoptosis, for example TNF binding activates the extrinsic apoptosis pathway as well as the canonical NF-κB pathway. The exact effect that NF-κB has on cell survival is dependent on a number of factors such as the cell type, stimulus and temporal pattern of activation [116]. Although generally thought of as being anti-apoptotic, NF-κB has been described has being both a promoter and antagonist of cell death. Kaltschmidt et al. showed through colony formation assays that after inhibition of NF-κB HeLa cells had increased survival after TNFα treatment compared to untreated and no apoptosis after hydrogen peroxide treatment [224]. Fan et al. showed that variation in cell death in response to different stimuli was in part mediated by alternate post-translational modifications on serine or tyrosine residues of IκBα [116].

1.3.5 The PIKK Family, NF-κB and Oxidative Stress

Previous research has implicated members of the PIKK family in the cellular response to oxidative stress. In 2010, Guo et al. studied ATM activation and phosphorylation of downstream targets in response to bleomycin induced genotoxic stress and hydrogen

peroxide induced oxidative stress. Non-chromatin associated substrates of ATM, Chk2 and p53, were activated in response to both oxidative and genotoxic stress. In contrast chromatin associated substrates of ATM such as KRAB associated protein 1 (Kap1) and H2AX were only observed following genotoxic stress indicating that following hydrogen peroxide treatment ATM is activated in the absence of DNA damage. In response to hydrogen peroxide treatment, oxidised ATM is present as an activated disulphide cross-linked dimer rather than an autophosphorylated active monomer. Activation of ATM through oxidation was blocked through the mutations of cysteine residues in the ATM FATC domain; residues critical for the formation of the disulphide bonds. This study highlighted an alternative role of ATM in response to these two cell stresses [225]. In unpublished work in the Kenneth laboratory we have observed that this form of ATM is activated in response to chemical oxidants and is necessary for the activation of hydrogen peroxide-induced NF-κB.

It has been demonstrated previously in tumours that ATR is activated in response to hypoxia while ATM is activated in response to reoxygenation. In extreme hypoxia (0.2% O_2) ATR substrates p53 and Chk1 are phosphorylated indicating that ATR is phosphorylated and activated in response to this stress. In this extreme hypoxia, ATM was not activated. This ATR activation is maintained throughout reoxygenation however ATM is autophosphorylated and activated in response to reoxygenation in the presence of DNA damage. The reoxygenation-induced ATM dependent phosphorylation of p53 was inhibited after the treatment with the anti-oxidant N-acetyl cysteine (NAC) indicating that ROS production was leading to this DNA damage [226]. These proteins could therefore be critical in the response of NF-κB to oxidative stress, as sensors of stress or DNA damage, as inducers of downstream pathways and potentially as activators of the NF-κB pathways. This link between PIKK family members and NF-κB activation is not new, genotoxic stress induced by chemotherapy or irradiation activates NF-κB in a manner dependent on the protein kinase ATM [92].

1.4 Reactive Oxygen Species and Oxidative Stress

ROS such as free radicals are produced in the mitochondria as a by-product of aerobic respiration; the oxygen-dependent process by which cells produce energy in the form of ATP from organic compounds such as carbohydrates, fats and proteins [227]. These ROS include species such as superoxide, peroxides, singlet oxygen and hydroxyl radicals. Although initially considered as damaging to the cell due to the discovery of the SOD-1 and SOD-2 enzymes [228], it has since become clear that ROS play an important role in many aspects of biology such as the immune response [229][230][231], vasodilation [232][233] and metabolic pathways [234]. Homeostasis of ROS is therefore vital for normal cell function; an imbalance can lead to a state known as oxidative stress [235], where high levels of ROS cause cell damage through chemical and structural aberrations of proteins,

DNA and lipids [236][237].

Excessive ROS production and the resulting oxidative stress can occur after exposure to a range of chemical, physiological and environmental stresses, examples of which include chemotherapeutic drugs, irradiation and pollutants such as those found in cigarette smoke [235]. Oxidative stress can also be induced as a result of ischemia and reperfusion; a deficiency of oxygen in cells (hypoxia) followed by rapid reoxygenation, causing cell stress and tissue damage [238]. This can occur as a result of physical trauma, stroke and is seen in solid tumours due to poorly structured vasculature. Exposure of DNA, proteins and lipids to high levels of ROS can lead to cell damage through the formation of chemical aberrations and structural interference [237][236]. The initial cellular response is to reduce the extent of the damage through the reduction of oxygen consumption and damage repair, alongside removal of excess ROS through a series of enzyme catalysed chemical reactions. When this damage is too severe it may not be resolved causing physiological dysfuntion, cell cycle arrest, quiescence, apoptosis or necrosis. Oxidative stress through ischemia and reperfusion causes and propagates a number of human diseases such as atherosclerosis, cancers and neurodegenerative conditions; conditions also associated with NF-κB dysfunction.

There are many forms of ROS that can cause oxidative stress, with each species having alternate effects on the cell [239][240][241]. In order to remove these ROS enzymes in the cell catalyse specific redox reactions, commonly resulting in the eventual production of oxygen and water. In the process of removing a particular ROS, these enzymes produce intermediate ROS. This occurs in a rapid and dynamic manner, as such the levels of a particular species in an environment is constantly changing (Fig. 23) [242].

SOD-1, SOD-2, NADPH oxidase and ferritin are just some of the enzymes and cofactors involved in the catalysis of these redox reactions. SOD-1 and SOD-2 catalyse the reaction that converts excess superoxide free radicals to hydrogen peroxide and oxygen in the response to ischemia and reperfusion [149][150]. SOD-1 is present in the intermembrane space between the mitochondria and cytoplasm and binds copper and zinc ions, whereas SOD-2 is present in the mitochondrial matrix and binds iron and manganese. In contrast, NADPH oxidase functions in the removal of excess ROS through the production of reducing agents such as glutathione and functions throughout the cell [149][150][151]. FTMT or ferritin is a mitochondrial ferroxidase enzyme that catalyzes the oxidation of iron, which prevents hydrogen peroxide from reacting with iron and producing the harmful hydroxyl radical [243] (Fig. 23). NF-κB has been implicated as a transcriptional regulator of all of these oxidative stress linked genes, highlighting its role as an essential responder to loss of ROS homeostasis.

The expression of these proteins allows the cell to remove excess ROS and restore ROS homoeostasis. Failure to do so will not only affect ROS-dependent cell mechanisms such as the immune response, vasodilation and metabolic pathways, but could lead to protein, lipid and DNA damage. Damage caused by ROS could lead to the subsequent activation of

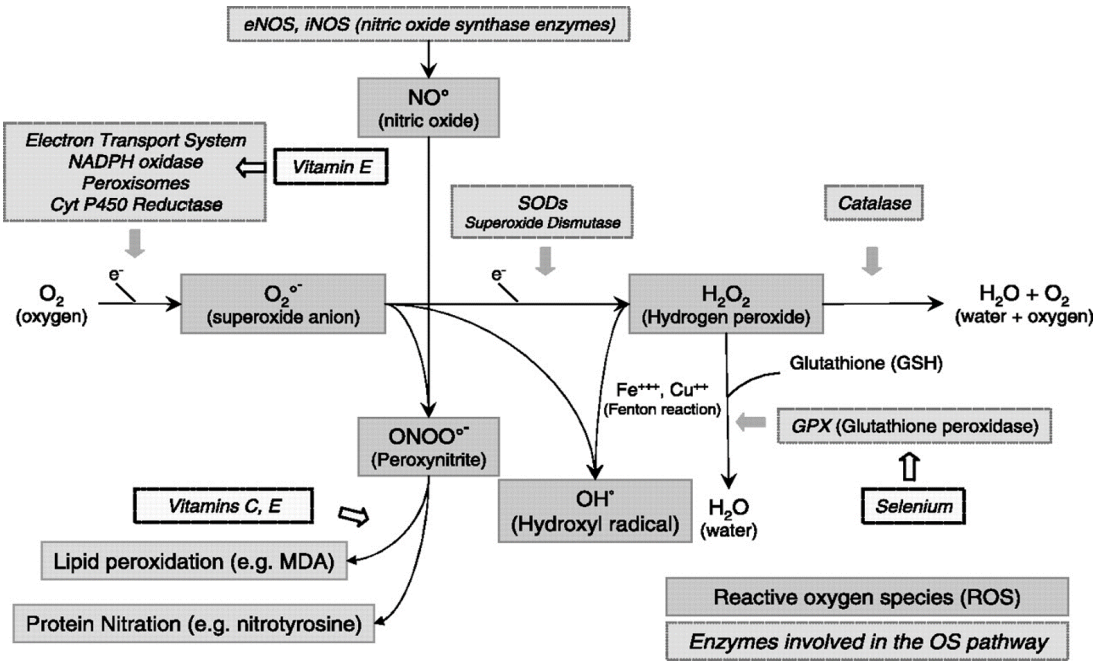

Figure 23. Production and Removal of Reactive Oxygen Species through Enzyme Coordinated Redox Reactions. Figure taken from Djamali and Arjang, 2007 [242].

multiple stress-activated signalling pathways, such as the NF-κB pathways, DNA damage response pathways, apoptosis and the cell cycle. Restoration of ROS homoeostasis is therefore critical to ensure the health of the cell and greater organism [244].

1.4.1 The NF-κB Pathway and Oxidative stress

Oxidative stress and NF-κB signalling are closely linked, however this interaction is complex. Many NF-κB pathway activators trigger the production of ROS, and many antioxidants such as NAC inhibit NF-κB pathway activation. For example TNF exposure leads to the production of ROS through increased inflammatory responses initiated by the NF-κB pathway, the resulting increased metabolism causes oxidative stress [245]. In some situations activation of the NF-κB pathway can be protective resulting in the restoration of ROS homeostasis. One example of this is following oxidative stress-induced ER-stress, where NF-κB activation triggers autophagy to reduce ROS levels [246][245].

Global studies of oxidative stress induced gene expression have been carried out previously, these have predominantly focussed on the role of oxidative stress in certain human diseases or conditions. In 2010 a study on the effects of oxidative and UV stress on human dermal fibroblasts highlighted changes in inflammatory and DNA damage response genes between younger and older patients. The genes selected for analysis were limited in this study and therefore did not cover many NF-κB target genes [247]. Another study focussed on changes in gene expression of 1,152 genes in cardiac cells from atrial fibrillation patients. Results highlighted decreases in gene expression of superoxide dismutase and NADPH oxidase, two NF-κB dependent genes [248]. In addition, Murray et al. carried out a

cDNA microarray on HeLa cells and primary human fibroblasts that are cultured as normal in the laboratory. Here, they studied changes in gene expression following a range of different stresses including heat shock, ER stress and oxidative stress. This study failed to highlight any oxidative stress specific regulated genes, however the authors comment that many of the genes associated with heat shock and ER stress have pro- or anti-oxidant roles [249]. As a result many of the oxidative stress-associated NF-κB target genes have been identified through a more targeted approach rather than through a global gene expression study.

Many NF-κB target genes are pro-oxidants, for example NADPH oxidase and the NOX2 subunit, gp91phox, both lead to the production of ROS [245]. Other pro-oxidants associaed with NF-κB include xanthine oxidoreductase (XOR) [250], cyclooxygenase-2 (COX) [251], inducible nitric oxide synthase (iNOS) [252] and lipoxygenase (LOX) [253]. In contrast to this, the activation of NF-κB can lead to the expression of anti-oxidant genes such as SOD-1, SOD-2, thiredoxins, NAD(P)H dehydrogenase (quinone) 1 (NQO1) [254], NADPH oxidase and ferritin, reducing ROS accumulation and decreasing lipid peroxidation and protein oxidation [246][255]. As such, expression of these sets of genes are critical for the removal of excess ROS and the restoration of ROS homeostasis (Fig. 24).

As discussed earlier, hydrogen peroxide is a known activator of NF-κB [102]. Schreck et al. demonstrated that in Jurkat cells this activation occurs independently of the IKK complex, results in the Y42 phosphorylation of IκBα and does not involve the degradation of IκBα [102]. More recent findings have determined that this is not necessarily the case in all cell lines, indeed later studies have shown that classical NF-κB activation occurs in other T-cells and some epithelial cells (HeLa) following exposure to hydrogen peroxide [256][257]. The difference in response is believed to be due to the presence or absence of SH-2 containing inositol 5' polyphosphatase 1 (SHIP-1). Without SHIP-1 the cell is unable to activate the IKK complex in response to hydrogen peroxide exposure [257].

T-cells have very specific responses to oxidative stress as they are regularly exposed to increased levels of hydrogen peroxide produced by macrophages and neutrophils in inflammatory tissues. Activation of T-cells occurs in response to ROS with this exposure having anti-apoptotic effects on the cell [256]. Thus it follows that in this environment hydrogen peroxide activates the NF-κB pathway in order to promote survival and increase the number of T-cells present to react to the inflammation or infection appropriately.

In HeLa epithelial cells, a classical activation of the NF-κB pathway occurs in a manner very similar to the T-cell response following exposure to hydrogen peroxide. However rather than this activation being coordinated by SHIP-1, protein kinase D (PKD) is responsible for the transduction of signal to the IKK complex [256]. In contrast in lung epithelial cells, hydrogen peroxide exposure leads to the inhibition of NF-κB signalling when combined with pro-inflammatory cytokine (TNF) treatment [256]. In this situation hydrogen peroxide treatment leads to the oxidation of critical cysteine residues in the IKK complex, preventing its activation.

Other forms of ROS also have contrasting effects on the activation of the canonical NF-κB pathway. Like hydrogen peroxide, singlet oxygen exposure has been reported to activate the canonical NF-κB pathway [239]. Hypochlorus acid and peroxynitrite have both been shown to inhibit pathway activation [240][241]. Like hydrogen peroxide, peroxynitrite is produced under inflammatory conditions such as following myocardial infarction and heart failure. Peroxynitrite treatment blocks IKKβ phosphoryation and induces Y66 and Y152 nitration on RelA. This reduces the DNA binding affinity of RelA, thereby increasing the proportion of inhibitor p50 homodimers that are bound to the promoters of target genes [241]. Hypochlorus acid is a strong oxidant that can react with amines to produce chloramines. In turn these are able to oxidise IκBα at methionine 45, which has an inhibitory effect on NF-κB activation in response to lipopolysaccharide exposure [240].

In addition to the oxidiation of methionine 45 on IκBα, other members of the NF-κB signal transduction pathway can be oxidised. p50 can be oxidised on cysteine 62, reducing its DNA binding affinity [258], while IKKβ can be oxidised on cysteine 179 following hydrogen peroxide treatment, preventing TNF-induced activation of the NF-κB pathway [259]. Oxidation of proteins that are not part of the main canonical NF-κB pathway may also influence NF-κB activation. Oxidation of 8-kDa dyenin light chain (LC8), a component of the dyenin motor complex, occurs following TNF exposure [260]. LC8 binds IκBα in a redox-dependent manner, preventing IκBα phosphorylation by IKKβ. Following oxidation of LC8, it dissociates from IκBα allowing for the activation of NF-κB [260].

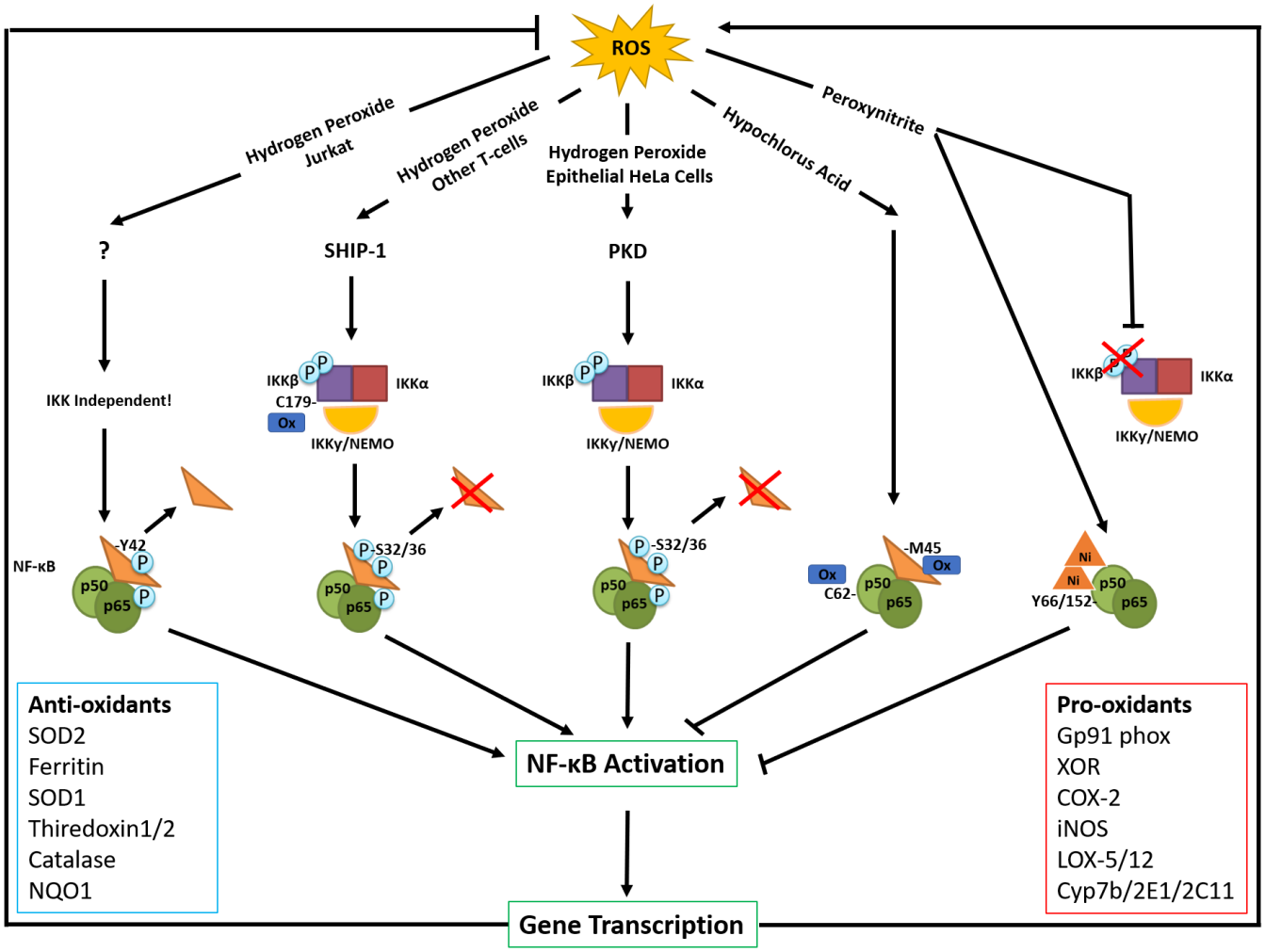

Figure 24. Oxidative Stress and the NF-κB pathway. A number of different ROS are able to promote or inhibit the activation of the canonical NF-κB through diverse methods. The response is both cell line dependent and ROS dependent, and may consist of a 'classic' activation pathway or one that is more atypical. This activation or inhibition leads to the control of a range of anti- or pro-oxidant genes, the transcription of which controls the levels of ROS in the cell.

1.4.2 Cellular Responses to Hypoxia and Rapid Reoxygenation

Hypoxia and reoxygenation, or ischemia and reperfusion, is defined as a drop in oxygen levels below those normally seen in that particular environment (hypoxia), followed by a rapid return to basal oxygen levels (reoxygenation) [238]. This can occur as a result of a drop in oxygen level of blood that is reaching the tissue, or could be by physical blocking of vessels that pass blood to tissues. In addition hypoxia can occur in inflamed tissues, where the inflammatory response leads to an increase in metabolism, thus leading to a decrease in oxygen levels.

Indeed, in many tissues hypoxia and reoxygenation play a fundamental role in normal, healthy cell processes. An example of this is in the regulation of haemopoetic stem cell differentiation and function. T lymphocytes are often exposed to fluctuations in oxygen levels as they often change environment; the bone marrow is far more hypoxic than the blood stream. As these cells encounter changes in oxygen in their environment, a range of hypoxia sensing and signalling pathways are activated, altering the differentiation and downstream effector mechanisms of the cell to respond to infection and inflammation as appropriate [261]. In addition, epithelial cells of the intestine are usually hypoxic as they are present on the luminal membrane of the highly anoxic intestinal lumen. These cells are located at the lower end of a steep oxygen gradient, as they are positioned adjacent to the highly vascularised lamina propria. Cells must be able to respond rapidly to changes in oxygen demands, increasing blood flow and 'reoxygenating' cells during digestion as cell metabolism increases [262] (Fig. 25).

Hypoxia and reoxygenation, or ischemia and reperfusion, is also linked to a wide range of different diseases or conditions. As well as its role in inflammation as discussed earlier, these include but are not limited to stroke, heart disease and physical injuries, it is often seen in solid tumours due to inefficient and poorly structured vasculature [263]. This rapid reoxygenation also contributes to the pathogenesis and development of several prevalent diseases such as atherosclerosis [264][265], cancers and neurodegenerative conditions.

Atherosclerosis has strong links to oxidative stress through transient ischemia and reperfusion and the resulting production of ROS. Plaques are formed on the vascular endothelium as a result of a chronic inflammatory response where low density lipoprotein (LDL) interacts with ROS to become oxidised. In response to this lipid oxidation NF-κB is activated, leading to the transcription of genes to regulate this inflammatory response and LDL-ROS interaction [264][265]. The repeated cycling of oxygen levels leads to the development of atherosclerosis, tissue damage, stroke or myocardial infarction. The development of atherosclerosis in turn leads to further tissue damage through ischemia and reperfusion injury and eventual fibrosis with NF-κB continuing to play an integral role in this through transcriptional regulation. The myocardial endothelium is sensitive to reperfusion injury caused by ischemia followed by reoxygenation of tissues [266]. Like all cells, endothelial cells produce ROS, however ROS play an integral role in the sensitivity of

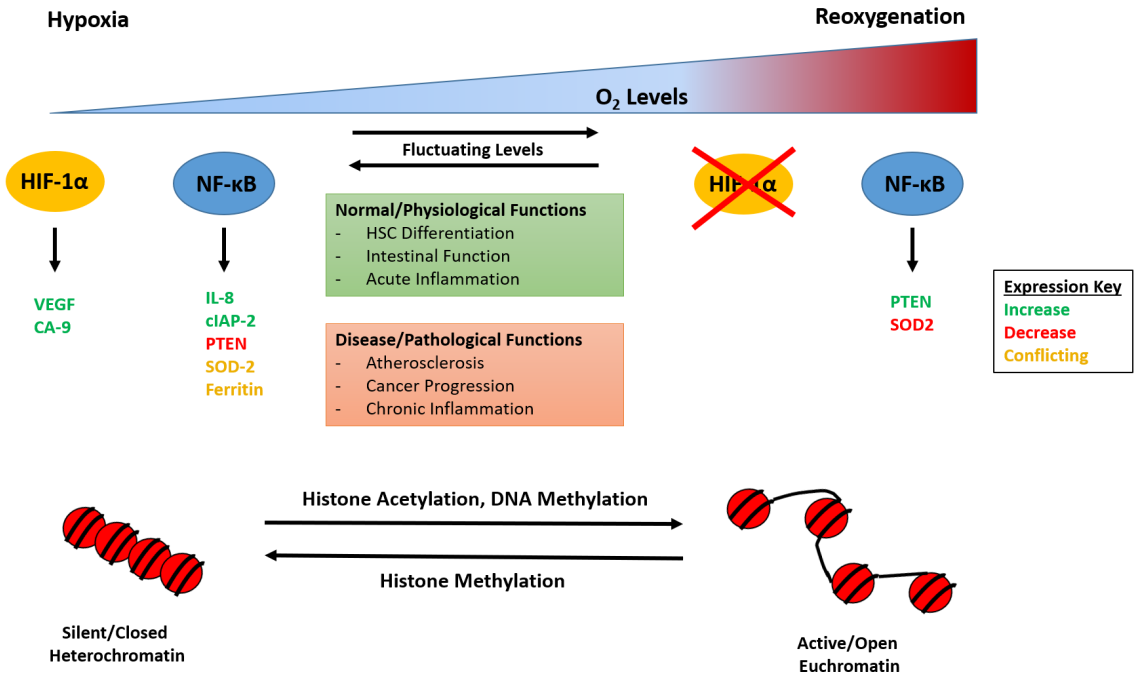

Figure 25. Hypoxia and Reoxygenation Overview. Although closely related, hypoxia and reoxygenation have differing effects on cell signalling, gene transcription and chromatin structure. In addition cycling hypoxia has been associated with a number of physiological processes in normal healthy cells as well as several disease conditions. Although this figure shows that reoxygenation leads to chromatin remodelling, this can also occur during hypoxia. This figure depicts that changes in oxygen level affects chromatin structure, the silencing of chromatin following hypoxia is a generalisation and this compaction not necessarily the case across the whole genome.

endothelial cells to ischemia and reperfusion; endothelial preconditioning [267]. Changes in ROS levels leads to cell damage, necrosis or apoptosis.

Tumours are also exposed to variations in oxygen levels due to abnormal vasculature that can constrict or dilate causing transient cycles of hypoxia and reoxygenation within the tumour microenvironment [263]. This reoxygenation and the associated formation of reactive oxygen species can cause DNA damage in already cancerous, mutated cells. In a cell that has lost the ability to repair DNA correctly, or has lost functional cell cycle checkpoint response genes this can cause further problems [268]. Mutations will become permanent as they are passed on to daughter cells allowing mutations to accumulate over the generations through cell division. In a cell where mutations have contributed to defects in apoptosis, positive selection of mutated cells will occur over those able to undergo apoptosis leading to increased proliferation and metastasis [269]. It is important to note that NF-κB plays a critical role in the progression of cancer due to its interaction with multiple signalling molecules and pathways and the resulting initiation of a diverse range of transcription factors.

The link between hypoxia and reoxygenation and cancer can also be attributed directly to the effects of these cycling oxygen levels, particularly in the context of DNA damage and proliferation. Both hypoxia and reoxygenation have been previously linked to the DNA damage response and cell cycle arrest. Frieberg et al. demonstrated that although no DNA damage occurs during hypoxia, cells undergo a Chk2-mediated G2-phase cell cycle arrest, and following reoxygenation this arrest is maintained in the presence of DNA damage [270]. In contrast Pires et al. showed that hypoxia does induce DNA damage as well as an S-phase arrest. These differences in findings could be due to variations in protocol used, namely differences in oxygen levels [271].

In addition to DNA damage, hypoxia and reoxygenation have been shown to reduce and promote cell proliferation respectively, due to variations in metabolic activity as hypoxic cells are starved of the oxygen required to carry out aerobic respiration [272][273][274]. Somewhat alarmingly, in certain cell lines hypoxia exposure leads to an increase in proliferation due to mutations in proteins involved in the response to replication stress, DNA damage and the control of cell cycle progression [275][276]. Together these reports indicate that hypoxia and reoxygenation can contribute to cancer progression through the introduction of further mutations, the bypassing of critical cellular responses to damage and the promotion of proliferation, migration and metastasis.

One of the main protein families involved in the cellular response to hypoxia is the HIF family of transcription factors [277][278]. As discussed previously the most studied and well-characterised form of HIF, hypoxia inducible factor-1α (HIF1α), is transcribed by the NF-κB pathway in response to hypoxic stress and cytokines such as TNFα [148][147]. HIF is then able to coordinate the expression of over 100 genes required in the response to oxidative or inflammatory stres, through restoration of ROS homeostasis, growth, metabolism and survival [4].

The HIF1 heterodimer complex comprises a HIF1α subunit and a HIF1β subunit. The stability and activity of this complex is dependent on HIF1α, which is rapidly degraded in normal oxygen conditions through a series of post-translational modifications. In the presence of oxygen, HIF1α is readily hydroxylated by proline hydroxylase (PHD)s. This targets HIF1α for ubiquitination by the E3 ubiquitin ligase von Hippel-Lindau (VHL), leading to the subsequent degradation of HIF1α [279][280]. In the absence of oxygen, such as in a hypoxic environment, hydroxylation of HIF1α cannot be carried out by the PHDs. This prevents ubiquitination and degradation, leading to the stabilisation of the HIF1 complex and the initiation of transcription [281].

The control of gene transcription by transcription factors such as HIF1α and NF-κB is tightly linked with chromatin modifications [4]. Chromatin is highly dynamic, and modifications to its structure can occur through post-translational modifications on histones or epigenetic modifications on the DNA itself. The addition or removal of these groups can lead to the compacting/silencing of chromatin, thereby preventing transcription, or the opening/activation of transcription and the promotion of transcription. Some of the

most commonly studied chromatin modifications are acetylation of the histone octamer and histone methylation. These modifications provide binding sites for bromodomain-containing chromatin remodelling complex (CRC)s, which in turn are able to modify the structure of the chromatin [4]. The exact role for individual CRCs in the response to hypoxia has not been extensively studied, the majority of detail in the literature is based on speculation and untested hypotheses [4][282]. It has been established however that the SWI/SNF family is required for full activation of HIF to occur [283], again the exact mechanism for this is unknown at this stage.

Hypoxia and reoxygenation can lead to changes in chromatin structre through changes in histone methylation, histone acetylation and DNA methylation [284][285]. These chromatin modifications can lead to the compaction or opening of the chromatin depending on the context and the gene. The Jumonji family of histone demethylases are critical regulators of chromatin structure in the response to hypoxia [286]. Not only are they transcribed by HIF, they are also dioxygenase enzymes and therefore require oxygen to work. The Jumonji family are therefore sensors of oxygen level, an decrease in oxygen reduces their activity therefore leading to an increase in methylated histones in the response to hypoxia [4]. This increase in methylation levels can both promote or repress transcription depending on the context; it can provide binding sites for transcription factors, but can also recruit CRCs and lead to chromatin compaction [285][4].

Histone acetylation by histone acetyl transferase (HAT)s is associated with an increase in transcription as charges on the acetyl groups opens up the chromatin structure [282]. Following hypoxia an increase in acetylation of HIF target genes such as vascular endothelial growth factor (VEGF) and carbonic anhydrase 9 (CA9) is observed, contributing to their increased transcription [287]. It is important to consider the complexity of chromatin modifications, this acetylation does not occur across the whole genome and as such will only lead to transcriptional changes in particular genes. In contrast to histone acetylation, DNA hypermethylation on the promoter of target genes prevents HIF binding [282]. Globally DNA methylation decreases following exposure to hypoxia, indicating that a decrease in gene transcription is occurring across some regions of the genome. It should be noted however that although it is commonly associated with repression of transcription, hypomethylation at critical CpGs can promote gene expression. These examples highlight the contrasting effects of the different modifications across the genome, and demonstrate the complexity of chromatin modifications in the regulation of transcription.

Reports on the effects of hypoxia and rapid reoxygenation on ROS production in cells is conflicting. Advances in the techniques used to determine the presence of ROS over recent years have failed to provide clear evidence of the exact changes in ROS levels following hypoxia and rapid reoxygenation. Guzy et al. utilised a redox-sensitive FRET protein sensor to determine the changes in protein oxidation during hypoxia; they concluded that following exposure to hypoxia the mitochondria rapidly produces hydrogen peroxide and not superoxide [288]. A FRET-based assay was again used by Bernandi et al. to deter-

mine the effects of hypoxia exposure on ex vivo carotid body tissues and mitochondrial suspensions [289]. Following hypoxia they found a rapid decrease in ROS production in one population of samples and a rapid increase in ROS production in a second population of samples. Another study published in 2012 demonstrates that the method of ROS detection can have profound effects on experimental conclusions. They report that use of lucigenin to detect ROS shows a decrease in ROS levels during hypoxia and an increase following reoxygenation. The use of DHE oxidation shows the opposite result [290].

Studies that have shown a decrease in ROS production have predominately focussed on NADPH and therefore ROS levels in the endoplasmic reticulum or mitochondria [291][292][293]. These studies have shown a decrease in the removal of hydrogen peroxide through the Fenton reaction in hypoxia [291] or a decrease in hydrogen peroxide release during hypoxia by the plasma membrane [292][293]. Collectively these experiments have highlighted the complexity of oxidative stress through the species and location of ROS production. This complexity is again increased when the complex network of ROS removing redox reactions are taken into account (Fig. 23). As such there are still many unknowns regarding the cellular responses to hypoxia and reoxygenation and the link to ROS production.

1.4.3 The NF-κB Pathway Response to Hypoxia and Reoxygenation

It is well established that NF-κB is activated after hydrogen peroxide treatment due to the formation of ROS [164]. Some studies have also demonstrated that both hypoxia and reoxygenation lead to activation of the canonical NF-κB pathway, however the majority of these studies have focussed on hypoxia. Publications on the effects of reoxygenation on NF-κB pathway activation have failed to establish any precise mechanisms behind this activation, they have however implicated the canonical NF-κB pathway in this response [105][125]. The exact mechanism of NF-κB pathway activation following hypoxia and reoxygenation is therefore not fully understood.

The mechanism behind hypoxia-induced NF-κB activation has been widely debated. Early work demonstrated that the kinetics of NF-κB activation following hypoxia was similar to that following hydrogen peroxide exposure. Here, activation occurs independently of the IKK complex relying on tyrosine 42 phosphorylation of IκBα rather than serine 32/36 phosphorylation to activate NF-κB [125]. More recent work has contradicted this, Cummins et al. argue that IKKβ is involved in the response to hypoxia, as the hydroxylation on the proline residue 191 in normoxic conditions decreases as this hydroxylation is lost after a drop in oxygen levels, thus leading to IKKβ activation. This work however utilised dimethyloxaloylglycine (DMOG), a cell permeable prolyl-4-hydroxylase inhibitor, to simulate hypoxia, rather than hypoxia itself. As such whether this finding is accurate following actual exposure to hypoxia is currently unknown [294]. Another paper demonstrated that both IKKα and IKKβ are required for the response to hypoxia,

however in this study rather than looking at kinetics of pathway activation, they studied HIF1α levels as a readout of NF-κB pathway activation. Here knockout of one subunit had no significant effect on HIF1α expression by NF-κB however knockout of both IKKα and IKKβ completely blocked HIF1α expression [147]. Further investigations by Culver et al. established a potential mechanism of NF-κB pathway activation following exposure to hypoxia. They posit that under hypoxic conditions the IKK complex is activated in a calcium/calmodulin-dependent kinase 2 (CaMK2)-dependent manner that requires TAK1 and Ubc13. In this context phosphorylation of IκBα occurs on serines 32 and 36, as well as tyrosine 42, and sumoylation on critical lysine residues prevents IκBα degradation but still allows NF-κB activation to occur [118].

Many studies that have focussed on hypoxia have used NF-κB target genes as a readout of NF-κB pathway activation. Multiple studies have demonstrated that an increase in transcription of IL-8 occurs following exposure to hypoxia. This has been shown in a variety of cell backgrounds and contexts [295][296][297][298][299]. In one of these papers Culver et al. demonstrated that an increase in IL-8 expression occurs after 16 hours of hypoxia [118]. Two other genes regulated by NF-κB, PTEN and cIAP-2 [300][142][301], have been previously linked with hypoxia. Both Culver et al. and Walsh et al. observed a significant decrease in mRNA levels of the tumour suppressor PTEN following exposure to hypoxia [118][302], while an increase in expression of cIAP-2 has been observed following hypoxia [303].

In addition to these commonly studied NF-κB target genes, work has been carried out focussing on expression of some of the antioxidant target genes that NF-κB controls the expression of. No genome wide transcript profiling of mammalian cellular responses to hypoxia have been performed previously, therefore many of the oxidative stress linked target genes have been established through more targeted experimentation. Previous work has shown changes in SOD-2 expression following exposure to hypoxia, however the direction of change differs between studies probably due to differences in the cell lines used and experimental design [304][305]. In addition Goralska et al. reported a decrease in ferritin expression following exposure to hypoxia [306]. These changes indicate that the cell is responding to an increase in ROS in a NF-κB-dependent manner to reduce oxidative stress and to reinstate ROS homeostasis.

Reoxygenation has not been as widely studied as hypoxia, as such there are fewer reports on the kinetics behind its activation. In 1995 Rupec et al. demonstrated that following reoxygenation RelA/p50 NF-κB heterodimers were rapidly activated in HeLa cells as measured by electrophoretic mobility shift assay (EMSA) and expression of a luciferase reporter [105]. A year later Imbert et al. showed that this activation occurred through the phosphorylation of IκBα at tyrosine 42 and did not result in IκBα degradation [125]. They did not identify the tyrosine kinase responsible for this phosphorylation event.

Aside from these two studies not much is known about the kinetics of NF-κB activation in response to reoxygenation. More recent studies have shown that reoxygenation leads to

changes in expression of NF-κB target genes, however the focus of these studies was not NF-κB activation. Sun et al. reported that reoxygenation lead to an increase in PTEN expression [307], while Lanoix et al. reported a decrease in levels of SOD-2 mRNA following reoxygenation [308]. The expression of other genes of interest following reoxygenation is unknown.

Aims

The principle aim of this project was to identify the mechanisms of canonical NF-κB activation following exposure to hypoxia and reoxygenation. Although the former stimulus has been investigated previously, there have been some differences in findings regarding gene expression, proliferation, DNA damage and kinetics of activation. These differences are possibly due to variations in the hypoxia protocol, such as the timings and oxygen levels used, as well as the cell lines selected for the study. Reoxygenation has not been extensively studied, particularly in the context of NF-κB signalling. As such, this project aimed to uncover the molecular mechanism of NF-κB activation following reoxygenation, the upstream kinases involved and the resulting changes in gene expression. To investigate this the effects of hypoxia and reoxygenation on many aspects of cellular biology were carried out, including cell cycle dynamics, DNA damage and cell proliferation. All of which have been linked to hypoxia, reoxygenation and the NF-κB pathway previously.
Specific aims include:

1. Assess the effects of hypoxia and reoxygenation on the general health of the cell, including investigating cell cycle dynamics, DNA damage and cell proliferation.

2. Determine the mechanism of NF-κB pathway activation following hypoxia and rapid reoxygenation, and evaluate how this differs from the response to other stimuli.

3. Uncover potential upstream kinases or sensors of hypoxia and reoxygenation that contribute to the activation of NF-κB in response to these stresses.

Together this information will further our understanding of the NF-κB response to hypoxia and reoxygenation-induced stress, including the upstream signalling dynamics, the effects on transcription and the overall cellular response to the stress. Understanding of these critical mechanisms of cell biology is vital in our understanding of progression of ischemia and reperfusion associated conditions, and may in time lead the way in the development of novel treatments for stroke, cancer, atherosclerosis and other prevalent conditions.

Materials and Methods

3.1 Mammalian Cell Culture

3.1.1 Cell Lines

U-2 OS cells were selected for use as they have responsive p53 and have wild type versions of all proteins of interest investigated throughout this project according to the Sanger COSMIC Database [309]. The majority of experiments were therefore performed using U-2 OS cells, a highly used immortalised cell line originally derived from a tibia osteosarcoma of a 15 year old female. They have an epithelial adherant cell morphology and are moderately differentiated.

The primary cell line human foreskin fibroblast-1 (HFF-1) was also used in key experiments to confirm finding seen in U-2 OS cells. These are normal fibroblasts pooled from two newborn individuals in 2003, as such these cell do not have mutations associated with disease or affecting any of the pathways of interest discussed in this thesis.

3.1.2 Cell Culture Conditions

U-2 OS cells were cultured in Dulbecco's modified Eagle's medium (DMEM) (LONZA; #3235) supplemented with 10% sterile-filtered foetal bovine serum (FBS) (Gibco; #10270), penicillin and streptomycin and l-glutamine (LONZA;#7779). Cells were kept in a humidified incubator at 37°C with 5% CO_2/21% O_2. For passage, cells were washed once with room temperature phosphate buffered saline (PBS) (LONZA; #3053) and dissociated from their surface using 1x trypsin (LONZA; #1366) at 37°C for no more than 10 minutes. Trypsin was inactivated through addition of fresh DMEM and cells were resuspended into a single cell suspension before either counting and seeding or splitting by a dilution factor of 1:4-1:6. Cells were predominantly grown in 10cm plates, however 15cm plates or T75 flasks were used in some circumstances. Cells were not grown beyond 80% confluence and were split at 70-80% confluence.

The primary cell line HFF-1 was cultured in PromoCell Fibroblast Growth Medium (PromoCell; #C-23010) but otherwise grown in the same conditions as U-2 OS cells. For passage, cells were washed once with room temperature HEPES-BSS solution (PromoCell; #C-40000) and dissociated from the plate through incubation with Trypsin/EDTA solution (PromoCell; #C-41000) at room temperature for no longer than 10 minutes. The same volume of Trypsin Neutralising Solution (PromoCell; #C-41100) was then added, cells were agitated and aspirated into cell suspension and transferred into a 15cm falcon tube. Cells were centrifuged at 220rcf for 3 minutes to pellet cells, the supernatent was discarded and the cells were resuspended in growth medium. Cells were then counted and seeded as required. Cells were passaged at 70% confluence and were not split at levels harsher than 1:3-1:4.

3.1.3 Frozen Cell Storage

Cells were washed once in room temperature PBS (LONZA; #3053) and dissociated from their surface using 1x trypsin (LONZA; #1366) at 37°C for no more than 10 minutes. Trypsin was inactivated through addition of fresh DMEM (LONZA; #3235) and cells were resuspended into a single cell suspension before being centrifuged at 400r x g for 5 minutes to pellet out the cells. Supernatent was then carefully removed and the cells were resuspended in 10% DMSO (Sigma-Aldrich; #D2650) in normal FBS-supplemented growth media. 1ml of this cell suspension was then aliquoted into cryovials. Cells were frozen slowly using Mr. Frosty^{TM} (Sigma-Aldrich;#C1562) and stored at -80°C or in liquid nitrogen (long-term).

To thaw cells, cryovials were removed from storage and kept on dry ice until the last possible moment. Cryovials were placed in a 37°C water bath to quickly thaw the cells. The contents of the cryovial was then immediately transferred into a pre-prepared flask or plate of the correct size containing the appropriate growth media. Plates were stored in the incubator overnight. After 24h of incubation media was replaced with fresh growth media to remove any DMSO. Cells were then checked regularly to ensure healthy growth before passage was carried out. Early passages were split at a lower ratio of 1:2-1:4 depending on the observed health of the cell.

3.1.4 Mycoplasma Contamination

Cells were tested for mycoplasma using the MycoAlert^{TM} mycoplasma detection kit (LONZA; #LT07) following the manufacturers protocol.

3.2 Treatment of Mammalian Cells for Experiments

3.2.1 Hypoxia and Rapid Reoxygenation

A humidified anaerobic chamber (RUSKINN INVIVO$_2$400) was set to 5% CO_2 and 1% O_2 at 37°C for hypoxic conditions. Gas levels were checked regularly throughout each experiment. Where necessary PBS (LONZA; #3053) or growth media was pre-equilibrated to a hypoxic state before the start of the experiment. Media was changed as cells were moved into the anaerobic chamber from a standard normoxic incubator to allow for immediate exposure of cells to hypoxia. Media was either spent or fresh as described for individual experiments, meaning that it either had or had not been used on cells previously.

For reoxygenation, cells were exposed to hypoxic conditions for 24 hours to allow cells to acclimatise to the conditions. Cells were removed from the anaerobic chamber and media was changed to allow for immediate reoxygenation. Again, this media was either spent or fresh as described for individual experiments. After the media change cells were incubated in normoxic conditions in a humidified incubator; 37°C with 5% CO_2/21% O_2 until harvesting.

As indicated above, media changes were used to immediately expose cells to hypoxic or normoxic conditions. Fresh media was stored in the anaerobic chamber for hypoxic conditions, and either on the bench or in the standard incubator for normoxic conditions as indicated for each experiment. Spent media was produced by plating out extra identical plates of clones for each experiment and moving media from that plate to the plate requiring treatment. These plates were either kept in the anaerobic chamber for hypoxic conditions or in the standard incubator for normoxic conditions. Unless stated otherwise media used to expose cells to certain gas states contained the standard volume of FBS (Gibco; #10270).

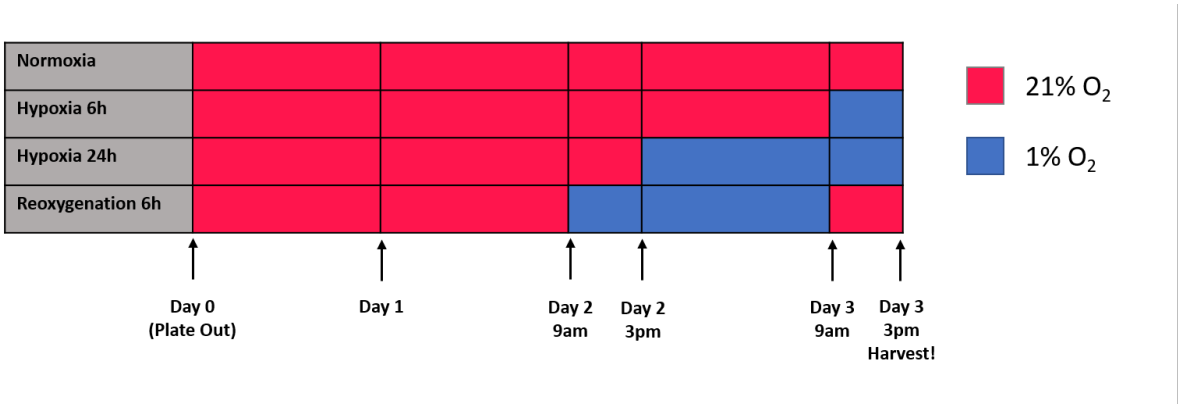

Figure 26. Schematic of a Hypoxia and Rapid Reoxygenation Time Course. U-2 OS cells were plated out on day zero and incubated in normoxic conditions for at least 48 hours. Plates were then moved to and from the anaerobic chamber over the course of 3 days. For example the 6 hour reoxygenation plates were moved into 1% O_2 on day 2 at 9am, 48 hours after plating out, and returned to 21% O_2 after 24 hours for a further 6 hours prior to harvesting.

3.2.2 Chemically Inducing NF-κB Activation

Standard methods to activate the canonical NF-κB pathway or cause DNA damage were used as controls in many experiments. The topoisomerase inhibitor etoposide was used at 25μM and TNF treatments were performed at 10ng/ml unless stated otherwise for the desired times. Hydrogen peroxide treatments were carried out as described in individual experiments.

3.2.3 Treatment with Small Molecule Inhibitors of Proteins of Interest

Small molecule inhibitors targeting proteins of interest were used at standard concentrations as described in figure 3. All inhibitors were added directly to the plates 30 minutes prior to hypoxia, reoxygenation, hydrogen peroxide or etoposide. Inhibitors were also added to any media that was used in the hypoxia or reoxygenation process.

Other treatments used in this manner include the anti-oxidant scavenger NAC (Sigma-Aldrich;#138061).

Small Molecule Inhibitors			
Target Protein	Inhibitor	Concentration	Source
ATM	KU-55933	5μM	Sigma; #SML1109
ATR	VE-821	10μM	Sigma; #SML1415
Chk-1	CCT245737	5μM	SelleckChem #CCT245737
IKKα	IKKα	3μM	Strathclyde
IKKβ	TPCA	10μM	Sigma; #T1452
IKKβ	BMS-345541	5μM	Sigma; #B9935
TAK-1	5Z-7-oxozeaenol	10μM	Sigma; #O9890

Table 3. Table of Small Molecule Inhibitors. The IKKα inhibitor was kindly provided by Prof. Simon Mackay of Strathclyde University.

The anti-oxidant NAC (Sigma; #A7250) was used at 10mM in the same manner. NAC is an acetylated cysteine residue that acts as a potent anti-oxidant through the scavenging of free radicals. The presence of this in cells is critical for the response of cells to oxidative stress and the removal of ROS [310].

3.3 Detection of ROS after Induction of Oxidative Stress

ROS detection assays were carried out using the ROS-ID Total ROS/Superoxide Detection Kit (ENZO; ENZ-51010) following the manufacturer's instructions where possible. Some deviations from the protocol provided where necessary and are described below. The protocol was carried out using 96-well plates (NUNC; #165305) and analysed on a micro-plate reader (BMG LabTech; POLARstar Omega).

3.3.1 Treatments and Conditions

Cells were plated at 2,500 cells/well on experimental day 1 into black polystyrene, optical bottom 96-well plates (NUNC; #165305). Additional plates were plated at this time in to standard 96-well plates to harvest spent media for treatments. Phenol-red-free media (LONZA; #BE12-917F) was used to minimise interference with the fluorescence signal.

On day 3, plates designated for 24 hour hypoxia or reoxygenation treatments were put in the humidified anaerobic chamber (RUSKINN INVIVO$_2$400) (5% CO_2, 1% O_2 at 37^{o}C). Additional plates for spent media extraction were also placed in hypoxic conditions.

On day 4 reagents and treatments were prepared following the manufacturers protocol. The fluorescence dye-containing reagents were made up in either fresh or spent phenol-red-free media harvested from the extra 96-well plates; this was carried out in the anaerobic

chamber where necessary. Both reagents were made up into the same solution however control wells containing either oxidative stress or superoxide sensing probes only were carried out in parallel as a control for fluoresence overlap. Any drug treatments such as hydrogen peroxide or NAC, were made up in this dye-containing media as described. For cells undergoing hypoxia or reoxygenation, gas-equilibrated dye-containing media was sufficient.

3.3.2 Procedure

All initial experiments had treatment times of 1 hour as the manufacturers protocol stated that addition of the dye needed to occur 1 hour prior to reading and that this should occur in parallel with any treatments. 24 hour hypoxia samples were exposed to hypoxia for 23 hours, and the dye-containing media was added for the last hour before reading fluorescence on the micro-plate reader.

The micro-plate reader was set to measure fluorescence from the bottom optic with 3mm orbital averaging to mininise edge effect. Two filter settings were used, one for the 'oxidative stress' detection (Ex;485-12, Em;520) and one for the 'superoxide' detection (Ex;544, Em;620-10). Gain was automatically set using the highest fluorescing well on a positive control plate.

3.3.3 Analysis

Fluorescence was normalised to readings taken from cell-free wells with dye-containing phenol-red-free media on the same plate. Data was then plotted and analysed using GraphPad PRISM, performing statistical analyses as described per experiment.

3.4 Protein Extracts

3.4.1 Whole Protein Extract by Urea Lysis

Media was aspirated and plates were washed once with room temperature, equilibrated PBS. An 8M urea lysis buffer stock (8M urea, 300mM NaCl, 20mM Tris pH8, 20mM Na_2HPO_4, 1% NP-40) was prepared in advance and stored at 4°C until required. Into 10ml of this stock 1.25μM Na_3VO_4, 1μM DTT, 5mM NaF and 1 protease inhibitor tablet was added (Roche; #04693159001). The phosphatase inhibitor Na_3VO_4 inhibits Serine/Threonine and acidic phosphatases, while NaF inhibits Tyrosine and alkaline phosphatases respectively. Protease inhibitors such as DTT and those present in the inhibitor tablet prevent degradation of the whole protein through processes such as preventing oxidation. Depending on cell confluence 400-600μl of lysis buffer was added to cover the surface of a 10cm plate. This stage was carried out in the anaerobic chamber where necessary however after addition of the lysis buffer, cells could be removed from the anaerobic chamber.

Plates were scraped and the lysates stored in Eppendorf tubes. Lysates were flash frozen and stored at -20°C before sonication. After thawing lysates were sonicated at 4°C for 30 seconds using Soniprep (MSE; Soniprep 150) or on high for 2 cycles of 30 seconds using the Bioruptor (Bioruptor Next Gen; Diagenode).

3.4.2 Whole Protein Extract by RIPA Lysis

For cells lysed using RIPA lysis buffer (1% v/v NP-40, 50mM Tris-HCL pH 7.4, 50 mM NaCl, 2mM EDTA, 0.1% SDS). 1.25μM Na_3VO_4, 1μM DTT, 5mM NaF and 1 protease inhibitor tablet) was added to 10ml of this stock, 400-500μl of lysis buffer was added to the plate depending on cell confluence and left for 10 minutes at 4°C ensuring complete coverage of the plate. Plates were scraped and the lysates stored in Eppendorf tubes for 10 minutes on ice. Lysates were centrifuged at 4°C at 13,200 rpm for 10 minutes. The supernatant was removed and stored in a fresh Eppendorf at -20°C.

3.4.3 Cytoplasmic and Nuclear Extraction

Cytoplasmic and nuclear extraction procedures were adapted from Dignam et al. 1983 [311]. Media was aspirated and plates were washed once with temperature/gas-equilibrated PBS, followed by a fast wash with 1ml of cold buffer A (10 mM HEPES, pH 7.9, 1.5 mM $MgCl_2$, 10 mM KCl, 0.1 mM PMSF, and 0.5 mM DTT). 500μl of cold buffer A+ (buffer A supplemented with a protease inhibitor tablet) was added to each plate. Cells were scraped into Eppendorf tubes and put on ice for 15 minutes. At this stage cells harvested inside the anaerobic chamber were removed from the chamber.

Cells were manually homogenised on ice and centrifuged at 16,100 x g for 15 minutes at 4°C. The supernatant containing the cytoplasmic components was carefully removed, transferred into fresh Eppendorf tubes and flash frozen for storage at -80°C. The pellet was then resuspended in 500μl buffer A+ and centrifuged at 16,100 x g for 15 minutes at 4°C. The supernatent was removed and discarded and the pellet containing nuclear components was resuspended in 100μl buffer C (20 mM HEPES, pH 7.9, 0.42 M NaCl, 1.5 mM $MgCl_2$, 0.2 mM EDTA, 0.1 mM PMSF, 0.6 mM DTT, and 25% glycerol). Extracts were incubated at 4°C for 20 minutes prior to centrifugation at 16,100 x g for 15 minutes. The supernatent containing the nuclear components was removed, transferred into fresh Eppendorf tubes and flash frozen for storage at -80°C for use in western blots. These extracts were used immediately for EMSA.

3.5 Protein Analysis

3.5.1 Bradford Assay

Protein concentrations of lysates were determined by a Bradford assay (Bio-Rad Protein Assay Dye Reagent Concentrate; #500-0006) and read using POLARstar Omega (BMG

LABTECH). BSA was used to produce a standard curve alongside the protein samples.

3.5.2 SDS-PAGE

Sodium dodecyl sulphate (SDS)-polyacrylamide gel electrophoresis (PAGE) gels were cast to appropriate concentrations for resolving proteins of interest (Table 4). These were poured in two layers; the separating gel at 6-12% acrylamide (Tris pH8.8) and the stacking gel at 5% acrylamide (Tris pH6.8) with 10 or 15 wells as required. Equal amounts of protein (10-40μg) were mixed with SDS loading buffer and heated to 95°C for 2-3 minutes. Gels were assembled in the running cassette, combs were removed and the tank was filled with running buffer. Samples were loaded into the wells and 5μl of PageRuler Protein Ladder (ThermoFisher;#26616) was loaded into lane 1. Gels were run at 100V for 10 minutes (Bio-Rad; Mini-PROTEAN 3 Cell) and then 150-200V until the dye front reached the bottom of the gel.

Buffers for SDS-PAGE	
Buffer	Ingredients
Tris pH6.8	1.5M Tris (Sigma; #TRIS-RO) in MQ H_2O, pH6.8 using HCl
Tris pH8.8	1.5M Tris (Sigma; #TRIS-RO) in MQ H_2O, pH8.8 using HCl
Stacking Gel	5% Acrylamide (Flowgen; #EC-852), 187.5μM Tris pH6.8, 1% (w/v) SDS (Sigma; #L3771), 1% (w/v) Ammonium Persulfate (Sigma, #A3678), TEMED (Sigma; #T9281) to set
Separating Gel	6-15% Acrylamide (Flowgen; #EC-852), 187.5μM Tris pH6.8, 1% (w/v) SDS (Sigma; #L3771), 1% (w/v) Ammonium Persulfate (Sigma, #A3678), TEMED (Sigma; #T9281) to set
10x Running Buffer	0.25M Tris (Sigma; #TRIS-RO), 1.92M Glycine (Sigma; #G8898), 1% (w/v) SDS (Sigma; #L3771)
4x Loading Buffer	0.25 M Tris (Sigma; #TRIS-RO), pH 8.1 using HCL, 10 % (w/v) SDS, 30% (w/v) Glycerol, 0.02% Bromophenol Blue, 10% (w/v) β-mercapthoethanol in MQ H_2O

Table 4. Buffer Recipes for SDS-PAGE

3.5.3 Western Blot

Proteins were transferred onto nitrocellulose (ThermoFisher; #88018) or polyvinylidene difluoride (PVDF) membrane (Immobilon-P; #IPVH00010). Membranes were activated following the manufacturers instructions. Proteins were transferred AT 15-20V by semi-dry transfer (Bio-Rad; Trans-Blot SD) for 1 hour and 30 minutes with two layers of blotting paper to protect the gels and membranes 5. Membranes were blocked in 4% Marvel/TBS-T for 1 hour at room temperature, washed 3 times in TBST for 5 minutes, then incubated with primary antibodies (Table 6) overnight at 4°C or for 1 hour at

Buffers for Western Blot	
Buffer	Ingredients
10x Transfer Buffer (Semi-Dry)	0.48M Tris (Sigma; #TRIS-RO), 0.39M Glycine (Sigma; #G8898), 0.1% (w/v) SDS (Sigma; #L3771)
1x Transfer Buffer (Semi-Dry)	80% MQ H_2O, 10% 10x Transfer Buffer and 10% Methanol
TBS-Tween20 (TBS-T)	20mM Tris-HCL ph 7.6, 120mM NaCl and 0.02% Tween20 (Sigma; #P1379)
Blocking Buffer	4% Marvel Milk Powder in TBS-T
Primary Antibody Mix	2% bovine serum albumin (BSA) (Sigma; #A9647) in TBS-T
Secondary Antibody Mix	4% Marvel Milk Powder in TBS-T

Table 5. Buffer Recipes for Western Blot

room temperature. After primary antibody incubation, membranes were removed and antibody solutions were stored at 4°C. Membranes were washed 3 times in TBS-T for 5 minutes prior to incubation for 1 hour at room temperature in appropriate HRP-tagged secondary antibody (5μl antibody in 10ml 4% Marvel/TBS-T). Cells were washed 3x in TBS-T for 5 minutes before being treated with Pierce^{TM} Enhanced chemiluminescence (ECL) western Blotting Substrate (ThermoFisher; #32106) following the manufacturers protocol. Membranes were developed on x-ray film using an automatic x-ray film processor (Xograph Compact X4), exposure times varied depending on the strength of the signal. The antibody for PRDX-3 was kindly provided by Dr. Elizabeth Veal.

Densitometry was carried out using ImageJ following the protocol described [312][313]. Significance was determined using GraphPad PRISM using analysis of variance (ANOVA) tests to test for differences in the mean band density across different groups, as three or more groups were present in all experiments. Multiple comparisons were accounted for using Sidak's or Tukey's test depending on the comparisons being made within an individual experiment [314][315].

3.5.4 EMSA

This was performed by Adam Moore (Perkins Lab) as radiation training is required. A 4% 0.25x tris-borate-EDTA (TBE) gel was poured in the lab and pre-run in 0.25x TBE buffer for 1 hour at 7.5V. 2μM of nuclear extract (obtained as described above) was incubated at room temperature with 1 μg of poly(dI-dC) in modified buffer D (20 mM HEPES, pH 7.9, 50 mM KCl, 0.2 mM EDTA, 0.1 mM PMSF, 0.5 mM DTT) up to 20μl. 0.1μl of the 32P-radiolabelled probes κB-EMSA-oligo-1 (GAT CCA GGG ACT TTC CGC TGG GGA CTT TCC A) and κB-EMSA-oligo-2 (GAT CTG GAA AGT CCC CAG CGG AAA GTC CCT G), were added and run on pre-run 4% 0.25x TBE gel [316]. Autoradiography was performed overnight at -80°C.

Primary Antibodies				
Target Protein	Concentration	Secondary	Source	Catalogue No.
Total Actin	1:10000	M	Sigma-Aldrich	A5441
Phospho ATM (S1981)	1:1000	M	Cell Signaling	4526
Total ATM	1:1000	Rb	Cell Signaling	2873S
p-ATR (S428)	1:1000	Rb	Cell Signaling	2853
Total ATR	1:1000	Rb	Cell Signaling	13934
p-Chk1 (S298)	1:1000	Rb	Cell Signaling	2349
Total Chk1	1:1000	M	Cell Signaling	2360
p-Chk2 (T68)	1:1000	Rb	AbCam	ab32148
Total Chk2	1:1000	Rb	OncoGene	PC483T
p-Erk1/2 (T202/Y204)	1:1000	Rb	Cell Signaling	9101
Total Erk1/2	1:1000	Rb	Cell Signaling	9102
Total HIF-1α	1:1000	M	BD Bioscience	610958
p-IκBα (S32/36)	1:1000	M	Cell Signaling	9246
Total IκBα	1:1000	Rb	Cell Signaling	9242
p-IKKα/β (S176/177)	1:1000	Rb	Cell Signaling	2078S
Total IKKα	1:1000	Rb	Cell Signaling	2682
Total IKKβ	1:1000	Rb	Cell Signaling	8943
Total IKKγ/Nemo	1:1000	Rb	Cell Signaling	8330
p-Kap1 (S824)	1:1000	Rb	AbCam	ab133440
K48-linked Ub	1:1000	Rb	Cell Signaling	4289
K63-linked Ub	1:1000	Rb	Cell Signaling	5621
p-SAPK/JNK (T183/Y185)	1:1000	Rb	Cell Signaling	9251S
Total Jnk	1:1000	Rb	Cell Signaling	9252
p-p38 (T180/Y182)	1:1000	Rb	Cell Signaling	4631
Total p38	1:1000	Rb	Cell Signaling	9212
Total p52	1:1000	M	Santa-Cruz	sc-7386
Total PARP	1:2000	Rb	Cell Signaling	9542
Total PRDX-3	1:1000	Rb	Abcam	ab73349
p-RelA (S536)	1:1000	Rb	Cell Signaling	3033
Total RelA	1:1000	M	Santa-Cruz	sc-8008
p-Stat3 (Y705)	1:1000	Rb	Cell Signaling	9131
Total Stat3	1:1000	M	Cell Signaling	9139
Total β-Tubulin	1:5000	Rb	Cell Signaling	2146

Table 6. Table of Primary Antibodies and Concentrations Used.

3.6 mRNA Analysis

3.6.1 Harvesting Cells for mRNA Extraction

Media was aspirated from plates and RNA was extracted following the manufacturer's protocol (PeqLab peqGOLD Total RNA; #123014). Where necessary lysis buffer was added to hypoxia treated plates in the anaerobic chamber, plates were removed once they had been fully lysed. mRNA from a 10cm plate was eluted into 50μl of nuclease-free water, this was flash frozen and stored at -80^{o}C.

3.6.2 Analysis of mRNA Concentration and Quality

RNA concentration and purity was analysed using a spectrophotometer (Thermo Scientific; NanoDrop 2000c) blanked to nuclease-free H_2O. Measurements were read at 260nm, 280nm and 230nm to determine the quantities of nucleic acids, aromatic amino acids and other contaminants respectively. The 260/280 ratio was calculated to determine nucleic acid purity value compared with aromatic amino acids (acceptable ratios were 1.8-2.2) and the 260/230 ratio was calculated to determine the purity compared to other contaminants (accepted at 1.7<) [317].

3.6.3 Reverse Transcription

Reverse transcription was performed using 1μg of RNA following the manufacturer's protocol (Qiagen QuantiTect Reverse Transcription Kit; #205310 or Quanta Biosciences qScript^{TM} cDNA Synthesis Kit; #95047). DNA removal steps were carried out as described in the protocol for the Qiagen kit, however an additional DNase kit (Quanta Biosciences PerfeCTa DNase I; #95150) was used in conjunction with the Quanta reverse transcription kit. cDNA was diluted 1 in 20 in nuclease-free water before further use.

3.6.4 Primer Design and Validation

A literature search was performed to establish appropriate NF-κB or HIF transcribed genes. Establised primers found in the literature or well-characterised primers already present in the laboratory were used (Table 7). Primers for real-time quantitative polymerase chain reaction (PCR) were designed using Ensembl and Primer Blast and checked alongside the UCSC Genome browser. Primers were ordered from IDT DNA and tested before use using temperature gradient checks and standard curves. The reference gene RPL13A was selected as this has been shown not to be affected by exposure to hypoxic conditions.

Primers		
Target Gene	Forward Primer	Reverse Primer
RPL13A	CCT GGA GGA GAA GAG GAA AGA GA	TTG AGG ACC TCT GTG TAT TTG TCA A
IL-8	CCA GGA AGA AAC CAC CGG A	GAA ATC AGG AAG GCT GCC AAG
PTEN	CGG TGT CAT AAT GTC TTT CAG C	TGA AGG CGT ATA CAG GAA CAA T
IκBα	CTG AGC TCC GAG ACT TTC GAG G	CGT CCT CTG TGA ACT CCG TG
p100	AGC CTG GTA GAC ACG TAC CG	CCG TAC GCA CTG TCT TCC TT
cIAP-2	GTC AAA TGT TGA AAA AGT GCC A	GGG AAG AGG AGA GAG AAA GAG C
Ferritin	CCA GAA CTA CCA CCA GGA CTC	ACA GGT AAA CGT AGG AGG CG
SOD-2	TGG AAA AAT GGG GTA ACT TAG CAG	CGC TTT GGT ACT CTT GTC TCT AAT
CA9	CTT TGC CAG AGT TGA CGA GG	CAG CAA CTG CTC ATA GGC AC
VEGF	CCT GGT GGA CAT CTT CCA GGA GTA CC	GAA GCT CAT CTC TCC TAT GTG CTG GC

Table 7. Table of Primers.

3.6.5 Agarose Gel Electrophoresis

Agarose gel electrophoresis was used for temperature gradient analysis of primer sets and troubleshooting real-time quantitative PCRs. Depending on the size of the product to be resolved, 1% or 2% agarose gels (Helena; #8201) were made up in 1x tris-acetate-EDTA (TAE) buffer (40mM Tris, 1:1000 Glacial Acetic Acid, 1mM EDTA pH8). The solution was heated until boiling in the microwave, after a brief period of cooling 2.5μl of SYBR safe (ThermoFisher;#S33102) was added to 100μl. Gels were then poured and left to set. DNA samples were mixed 1:1 with 5x Green Go-Taq Flexi Buffer (Promega;#M8911) and 10-20μl was loaded per well. 100bp or 1Kb ladders (Invitrogen; #10488) were used depending on the size of the product to be resolved. Gels were then run at 150V (HU13 System) until the dye front almost reached the edge of the gel. Bands were visualised using Fujifilm LAS-4000.

3.6.6 Real-Time Quantitative PCR

For each reaction 5μl of the diluted cDNA was added to 15μl of master mix (4μl H_2O, 4μl 5x GoTaq Colourless Reaction Buffer, 3μl 2mM dNTPs, 3.2μl $MgCl_2$, 0.8μl 10mM

Primer Mix, 0.2μl 1:200 Syber Green/DMSO, 0.2μl GoTaq G2 DNA Polymerase; Promega #M7845). Real-time quantitative PCR was carried out using using the SYBR green method using Qiagen Rotor-Gene Q with the following settings: 95°C for 30 seconds, 60°C for 30 seconds and 72°C for 30 seconds for 40 cycles. Readings were taken after the annealing step of each cycle. A final 10 minute gradual increase in temperature from 60°C to 95°C was used to produce a melt curve. DNA-free controls were used for each primer per run. Each reaction was carried out in triplicate with the reference gene RPL13A used in each reaction.

Following completion, threshold values were set at 0.1 across all runs, ensuring that this crossed the exponential increase phase of the reaction. At this point outliers were excluded and the melt curve analysed for double products or unusual curves. Ct values were then exported for further analysis.

3.6.7 Data analysis

Data was normalised using the Δ Δ CT method using the reference gene RPL13A [318]. Hypoxia treatments were normalised to normoxia values and reoxygenation treatments were normalised to 24 hour hypoxia values. Graphs were plotted using GraphPad Prism and statistically analysed as described per figure.

Raw Ct values were also plotted using GraphPad Prism to ensure that the reference gene was not moving (data not shown) and that this method of analysis was not skewing the data presented in its final form.

3.7 Flow Cytometry

All cells used for flow cytometry analysis were grown on 15cm plates to ensure that enough cells were present for analysis.

3.7.1 Fixing Cells for FACS Analysis

Media was aspirated and plates were washed once in PBS. 1x Trypsin/PBS was added to cover the surface, plates were left in the humidified incubator for up to 10 minutes to allow cells to unadhere from the surface. At this stage cells could be removed from the anerobic chamber where necessary. Cells were then resuspended in PBS and centrifuged for 5 minutes at 400 x g to pellet out the cells. Supernatent was removed and cells were resuspended in 1ml PBS and fixed in 3.7% formaldehyde (Sigma; #F8775) in PBS for 10 minutes at room temperature. Cells were centrifuged at 400 x g for 5 minutes and were washed in PBS. After a final centrifugation step pellets were resuspended in 100μl PBS and 1ml of 70% ethanol was added and mixed in. Cells were then stored at -20°C until staining.

3.7.2 BrDU Incorporation

BrDU (0.1mM) was added 1:1000 to plates 1 hour before harvesting to allow for incorporation into the DNA. On the day of staining, samples were removed from the -20°C freezer and allowed to acclimatise for 10 minutes. Samples were then centrifuged at 400 x g for 5 minutes to pellet out the cells. Supernatent was removed and the pellet was washed 2x in 1ml PBS, after centrifugation the pellet was resuspended on 100μl of PBS. 1ml of HCl-Triton x100 (2mM HCl, 0.5% Triton x100) was added to samples for 30 minutes in the dark at room temperature. Cells were centrifuged for 5 minutes at 400 x g and supernatent was removed. Pellets were resuspended in 200μl of 0.1M Sodium Tetraborate, samples were incubated for 5 minutes in the dark at room temperature. Cells were centrifuged for 5 minutes at 400 x g and supernatent was removed. Pellets were then washed and pelleted twice before staining.

FITC-conjugated anti-BrDU antibody (BD Biosciences; 347583) was diluted 1:100 in PBS - 1% BSA and 50-100μl was added to each pellet. A negative control of PBS-1%BSA only was carried out in parallel. Samples were left to incubate for 1 hour in the dark at room temperature. 400μl of 1:5000 DAPI stain was added to each tube (200μl if 50μl of antibody was used). Samples were incubated for 1 hour in the dark at room temperature before being analysed by fluorescence-activated cell sorting (FACS).

3.7.3 γH2AX Staining for DNA Damage Analysis

On the day of staining, samples were removed from the -20°C freezer and centrifuged at 400 x g to pellet out the cells. Cells were washed once in 1ml of PBS and centrifuged at 400 x g for 5 minutes. Supernatent was removed and PBS-1% Triton was added for 15 minutes at room temperature. Samples were centrifuged at 400 x g for 5 minutes and the supernatent removed. After resuspending in 1ml of PBS each sample was split into 2 tubes before the centrifugation step was repeated and supernatent was removed. Pellets were resuspended in either 50μl of 1:100 FITC-conjugated γH2AX antibody (BD Biosciences; #560445) in PBS-1% BSA or 50μl of 1:100 FITC-conjugated IgG antibody (BD Biosciences; #557782) in PBS-1% BSA (negative control for each sample). Samples were incubated in the dark for one hour at room temperature. 450μl of 4',6-diamidino-2-phenylindole (DAPI) was then added and samples were incubated in the dark for one hour at room temperature before being analysed by FACS.

3.7.4 Data Analysis

Data was collected using FACS Canto II at 10,000 events per sample measuring Log SSC-A and Lin FSC-A. In all experiments FITC was measureed at 488nm and DAPI controls were measured at 405nm. Data was analysed using BD FACSDIVA software. Graphs were plotted using GraphPad Prism and appropriate statistical analyses were carried out as described.

3.8 Microscopy

3.8.1 Fixing Cells for Immunofluorescence Microscopy

8000 cells per well were plated out on 8-well slides (Nunc Lab-Tek II Chamber Slide^{TM} System; #154543) on experimental day 1. 24 hour hypoxia and reoxygenation slides were exposed to the humidified anaerobic chamber on day 3. Shorter hypoxia and reoxygenation time points were carried out on day 4 before immediate fixing.

To fix cells, media was removed and cells were washed 3x in PBS. 3.7% formadehyde-PBS (Sigma; #F8775) was added to wells and slides were incubated at room temperature for 20 minutes. Formadehyde-PBS was removed from the wells and cells were washed 3x in PBS. PBS was added to each well one final time and slides were stored at 4°C until staining. Slides were stored for no longer than 2 weeks.

3.8.2 Fixing and Staining Cells for Immunofluorescence

Slides were removed from 4°C and left to acclimatise for 10 minutes before PBS was removed. PBS-1% Triton-0.05% Tween 20 was added to each well and slides were incubated at room temperature for 15 minutes. Slides were then blocked in 5% BSA-PBS-Tween 20 for 1 hour at room temperature. This was then aspirated and primary antibodies were added. IKKβ (Santa-Cruz; #7330) antibody was added in a 1:150 dilution in 5% BSA-PBS-Tween 20 and IKKγ (Cell Signaling; #8330) antibody was added in a 1:200 dilution in 5% BSA-PBS-Tween 20. Negative control slides without primary antibodie were carried out in parallel using 5% BSA-PBS-Tween 20 only. Slides were then incubated in a dark wet chamber at room temperature for 1 hour and 30 minutes. Slides were then washed 3x with PBS-Tween 20. Secondary antibodies were made up 1:200 in 5% BSA-PBS-Tween 20 (if not conjugated to the primary antibody) and slides were incubated in a dark wet chamber at room temperature for 1 hour. Negative control slides containing no secondary antibody were performed in parallel with 5% BSA-PBS-Tween 20 only. Slides were washed 3x in PBS-Tween 20 before removal of wells and mounting in DAPI-containing mounting solution. Slides were left to cure in the dark overnight before sealing and storing at -20°C before analysis.

3.8.3 Microscopy

Fluorescence microscopy was carried out using a Zeiss Axiolmager without apotome, using Zeiss' Zen software. Images were processed using ImageJ using plug-ins to automate the relative nuclear and cytoplasmic signal.

3.9 Cell Survival

3.9.1 Clonogenic Assay

After an accurate cell count was performed, 4 x 10^5 U-2 OS cells were seeded in 6-well plates and incubated in normoxic conditions overnight. Cells were exposed to hypoxia for 24 hours, treated with the IKK inhibitor 3-Thiophenecarboxamide (TPCA) or NAC at concentrations of 10μM prior to a 3 hour reoxygenation. Untreated controls for both normoxic and reoxygenated cells were performed in parallel and each condition was performed in triplicate. Following the 3 hour reoxygenation media was aspirated, plates were washed once with PBS and the cells were trypsinsed and resuspended in DMEM. Cells were counted and seeded in 10cm plates at 100, 500, 1000 or 2000 cells per plate. Plates were incubated in normoxic conditions for 2 weeks to allow for colony formation. After 2 weeks media was aspirated and cells were fixed with acetic acid for 20 minutes then stained with crystal violet for a further 20 minutes. Colonies were counted using OpenCFU [319] and checked manually. Raw data was plotted using GraphPad PRISM and appropriate statistical analyses were carried out as described.

3.9.2 Presto-Blue Assay

Cells were plated out in 96-well plates at 2,500 cells/well with 200μl of media. Plates were exposed to hypoxia and reoxygenation and the required time points however with PrestoBlue readings observed after 4 days in all cases, regardless of treatment times so that cells had been proliferting for the same time. PrestoBlue assays were performed following the manufacturers protocol. Absorbance was recorded at 570nm after a 60 minute incubation of cells with the PrestoBlue reagent using an automatically set gain. Cell viability was expressed as a percentage relative to untreated controls. Graphs and statistical analyses were carried out using GraphPad Prism as described.

3.10 Statistical Analyses

Statistical analyses were carried out where at least 3 experimental replicates were available, the exact number of repeats is described in the corresponding figure legend. All statistical tests and graphs were produced using GraphPad PRISM and all error bars show standard deviation. Significance was determined using GraphPad PRISM using the Student's t-test where comparisons were being made between two groups, while analysis of variance (ANOVA) tests were carried out to determine statirtical differences across multiple groups and parameters. Where three or more groups were being compared, multiple comparisons were accounted for using Sidak's or Tukey's test depending on the comparisons being made within an individual experiment [314][315]. Statistics were reported as an adjusted p-value (* - $p < 0.05$, ** - $p < 0.01$, *** - $p < 0.001$, **** $p < 0.0001$). All tests carried out are described in the corresponding figure legend.

Chapter 4: Characterising the Cellular Response to Hypoxia and Rapid Reoxygenation

Hypoxia and rapid reoxygenation is linked to a plethora of clinical conditions such as stroke, cancer and atherosclerosis [263][264][265]. Improving our understanding of the molecular mechanisms and cellular responses to these stresses would contribute to a greater ability to treat patients that have undergone ischemic injury. Many of the diseases associated with ischemia and reperfusion have been previously linked to the NF-κB family of rapidly acting transcription factors, although there have been conflicting reports regarding the mechanism behind this activation [105][125][320]. As discussed in section 1.4 there have also been variations in findings concerning the effects of this activation on gene expression, which appear to be due to the use of different cell lines and variations in experimental design.

The first part of this project therefore aimed to confirm the effects of hypoxia and rapid reoxygenation on NF-κB activation using the experimental design presented in section 3.2, as well identifying the upstream signalling mechanisms that lead to this activation. The data presented in this chapter uncovers that the previously established method of inducing hypoxia and reoxygenation activates the canonical NF-κB pathway, independently of other stimuli. Thus the data presented in the second part of this chapter is entirely novel, because an alternative, improved protocol was followed to induce hypoxia and rapid reoxygenation than has been used in previous studies.

Using this novel method for inducing hypoxia and rapid reoxygenation, experiments were designed to determine the precise mechanism behind the activation of the canonical NF-κB pathway, as well as the effects of this activation on transcription of target genes. These experiments were carried out through the use of western blots, EMSA, real-time qPCR and immunofluorescence microscopy.

As discussed in section 1.4 reports describing the effects of hypoxia and rapid reoxygenation on ROS production have conflicting findings. This appears to be mostly dependent on the technique used to analyse ROS production [290], as well as the sample being studied [289]. A second aim of this chapter was therefore to determine the nature of the ROS produced following hypoxia and rapid reoxygenation. Understanding this is key to understanding the physiological mechanisms occurring within the cell, and would give insight into the fundamental effects of hypoxia and rapid reoxygenation on the cell. These investigations were carried out through western blots, ROS detection assays and real-time qPCR.

The final aim of this chapter was to understand the downstream effects of hypoxia and rapid reoxygenation on the cell, again using the novel method for inducing hypoxia and rapid reoxygenation. Uncovering how hypoxia and rapid reoxygenation affects the proliferation, survival and cell cycle progression of a cell is critical for understanding which

upstream pathways are implicated and why. Previous work has indicated that across most cell lines hypoxia leads to a reduction in proliferation due to a reduction in metabolic activity as the cell is starved of oxygen [272], however the opposite is true in some cancer cell lines [272][275][276]. Following reoxygenation, proliferation has been reported to increase [273][274]. The effects of hypoxia and reoxygenation on proliferation on U 2-OS cells has not previously been assessed. This final aim is key to the design of future experiments presented later in this thesis and was investigated using western blot, colony formation assays, PrestoBlue assays, flow cytometry and microscopy.

4.1 Hydrogen Peroxide Treatment Activates The Canonical NF-κB Pathway in U-2 OS cells

The NF-κB pathways are activated in response to a wide range of cell stresses including, inflammation, infection, DNA damage and oxidative stress. Previous work in the Kenneth laboratory has demonstrated that hydrogen peroxide treatment leads to the activation of the canonical NF-κB pathway in HEK-293 cells. To confirm these results in U-2 OS cells, cells were treated with 20μM of hydrogen peroxide for the times indicated (Fig. 27), whole cell lysates were extracted and analysed by western blotting for proteins associated with canonical NF-κB activation. Results presented here confirm that the oxidative stress caused by hydrogen peroxide treatment activates the canonical NF-κB pathway.

Phosphorylation of IKKα/β and RelA are well-established markers of canonical NF-κB activation [321]. The former is an upstream signalling factor responsible for downstream transduction of the signal, while the latter is a canonical NF-κB subunit. Phosphorylation of IKKα/β and RelA was observed following treatment with hydrogen peroxide, indicating that hydrogen peroxide treatment leads to the activation of the canonical NF-κB pathway (Fig. 27). Quantification of these blots showed that effects observed across 3 independent experiments were significant with regard to phosphorylation of IKKα/β but not phosphorylation of RelA at this particular residue.

The data presented in this section verifies previous data from the Kenneth laboratory that sees activation of the canonical NF-κB pathway following hydrogen peroxide treatment. This information is useful knowledge to have for future experiments focussing on the more physiologically representative and more technically complex stimuli of hypoxia and rapid reoxygenation. It will allow for comparisons to be made between the three methods of inducing oxidative stress as well as its role as a useful positive control in several experiments.

4.2 ROS Production Following Exposure to Hydrogen Peroxide, Hypoxia and Rapid Reoxygenation

As described in Chapter 1 Section 1.4, there are conflicting reports regarding whether hypoxia and rapid reoxygenation produce ROS [288][289][290]. This appears to be dependent on the method used to detect ROS and the tissue, cell type or organelle being studied.

To try to elucidate whether hypoxia and rapid reoxygenation leads to the production of ROS an ENZO total ROS/superoxide detection kit was used (ENZO; #51010). Using a microplate reader the cell permeable probe named 'oxidative stress' provided fluoresced in the presence of ROS (hydrogen peroxide (H_2O_2), peroxynitrite ($ONOO^-$), hydroxyl radicals (HO), nitric oxide (NO) and peroxy radical (ROO)). The second probe provided reacts specifically with superoxide (O_2^-). Probes were made up in combination in phenol

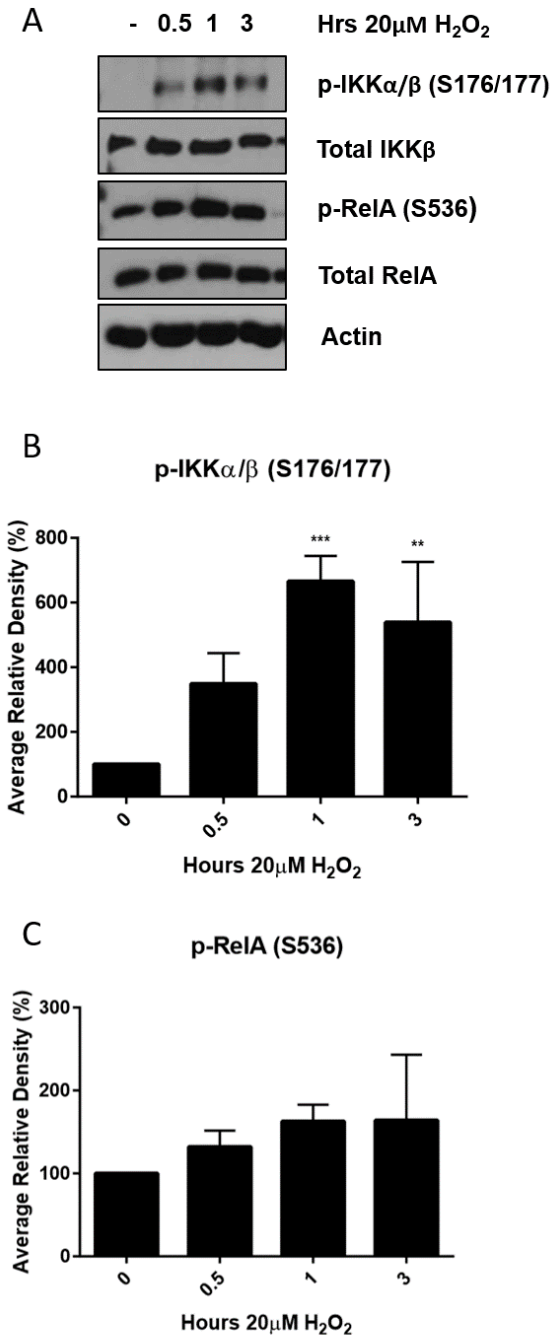

Figure 27. Hydrogen Peroxide Treatment leads to Canonical NF-κB Activation in U-2 OS Cells. Cells were treated with 20μM of H_2O_2 for between 30 minutes and 3 hours. Whole cell lysates were extracted using 8M urea lysis buffer and western blots were performed for phosphorylation events associated with canonical NF-κB activation. Quantitative analysis of western blots (n=3) demonstrates that this activation is significant with regard to IκBα phosphorylation (one-way ANOVA analyses using Tukey's test for multiple comparisons). A - Representative western blot from 3 independent experiments. B - Relative density of p-IKKα/β(S176/177) normalised to actin and total IKKβ. C - Relative density of p-RelA normalised to actin and total RelA.

red-free pre-equilibrated media alongside any additional treatments and were added for 1 hour before detection on the microplate reader as described in the manufacturer's protocol (ENZO; ENZ-51010).

The initial phase of this experiment aimed to establish whether the kit was working as planned. Cells were treated with 20μM of hydrogen peroxide for 1 hour in combination with the probes. The ROS scavenger NAC was used in parallel as a negative control to confirm that hydrogen peroxide treatment was causing the production of ROS and superoxide. Data shows that treatment with hydrogen peroxide causes an increase in the amount of ROS detected by the oxidative stress probe ($p = 0.0002$) and an increase in the amount of superoxide ($p < 0.0001$)(Fig. 28). NAC treatment alongside hydrogen peroxide exposure significantly reduced the levels of ROS and superoxide detected by the kit. These results indicate that the kit can successfully detect changes in ROS and superoxide levels in U-2 OS cells.

After confirmation that the ROS/superoxide detection assay was working focus turned to analysing ROS/superoxide production after hypoxia and rapid reoxygenation (Fig. 29). Once again the probes were made up in combination with pre-equilibrated media and treatments were carried out in parallel with addition of the probes for 1 hour before reading fluorescence on the microplate reader. Normoxia only and 24 hour hypoxia samples were treated with the probe for one hour before analysis, for the last hour of the time course (eg: 23 hours hypoxia + 1 hour hypoxia with new probe-containing media).

After 1 hour of hypoxia a decrease in ROS detected by the 'oxidative stress' probe was observed ($p = 0.0023$) (Fig. 29A). ROS levels returned to basal levels following 24 hours of hypoxia and remained unchanged after 1 hour of rapid reoxygenation. Addition of the free-radical scavenger NAC leads to a significant decrease in ROS levels following hypoxia ($p = 0.0039$) and an increase following rapid reoxygenation ($p = 0.0145$). An increase in in ROS levels following treatment with a free-radical scavenger is unexpected and the precise reasons for this are unknown, clearly the NAC treatment is having the anticipated effect following hypoxia, therefore it must be some characteristic of reoxygenation that is leading to this effect. Perhaps the response of cells to reoxygenation is faster than that to hypoxia, thus we may have missed a critical early time point where the scavenger does have an effect. In this hypothesis the complex network of redox reactions presented earlier (Fig. 23) allows the cells to compensate for this decrease in ROS, leading to the increase observed here. Undoubtedly this would have to be investigated further in future experiments.

An increase in superoxide production was observed after 1 hour of hypoxia ($p < 0.0001$), indicating that superoxide is the main contributor to oxidative stress in hypoxia (Fig. 29B). This is the opposite observation from changes in ROS species detected by the 'oxidative stress' probe. Perhaps it is these polarised differences in superoxide and global ROS levels following hypoxia that has contributed to some of the opposing findings presented in the literature [289][290].

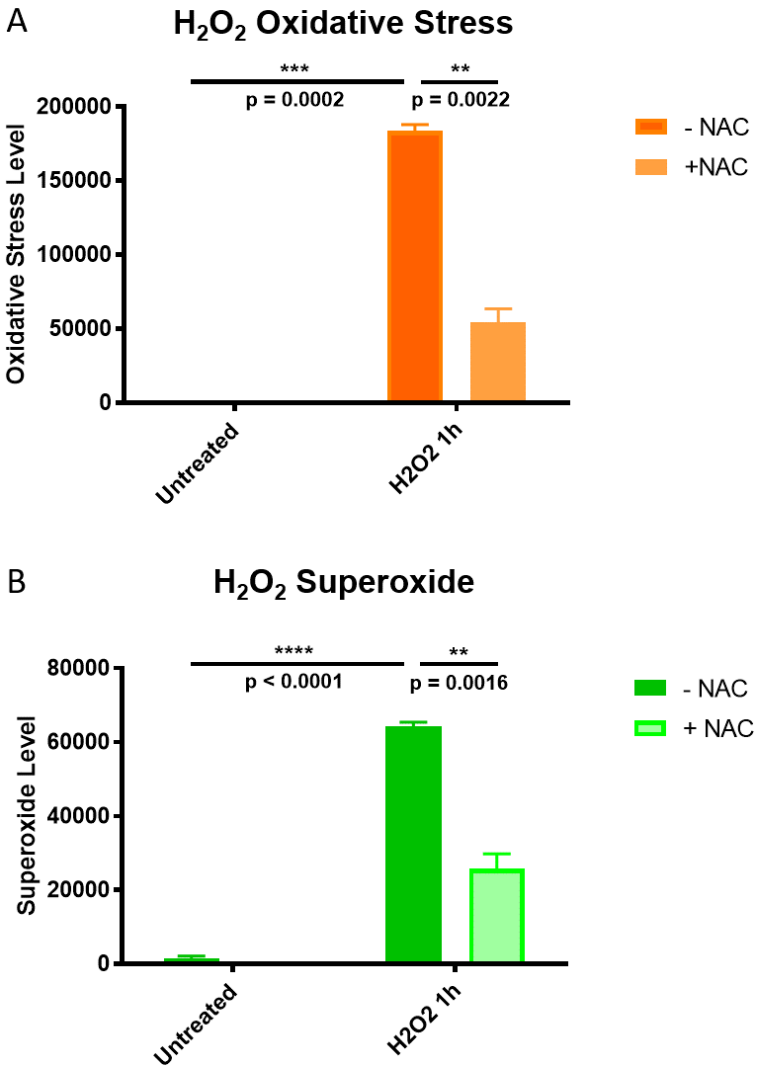

Figure 28. Hydrogen Peroxide Treatment causes Oxidative Stress and Superoxide Production in U-2 OS Cells. Cells were treated with 20μM of hydrogen peroxide for 1 hour with or without the presence of the ROS scavenger NAC, and oxidative stress and superoxide levels were detected using the ENZO ROS kit. Hydrogen peroxide treatment causes production of oxidative stress species ($p = 0.0002$) and superoxide species ($p < 0.0001$) and NAC treatment is able to partially rescue the cells from this stress ($p = 0.0022$, $p = 0.0061$). Data was analysed using two-way ANOVA with Tukey's multiple comparison test on the means of 3 independent experiments.

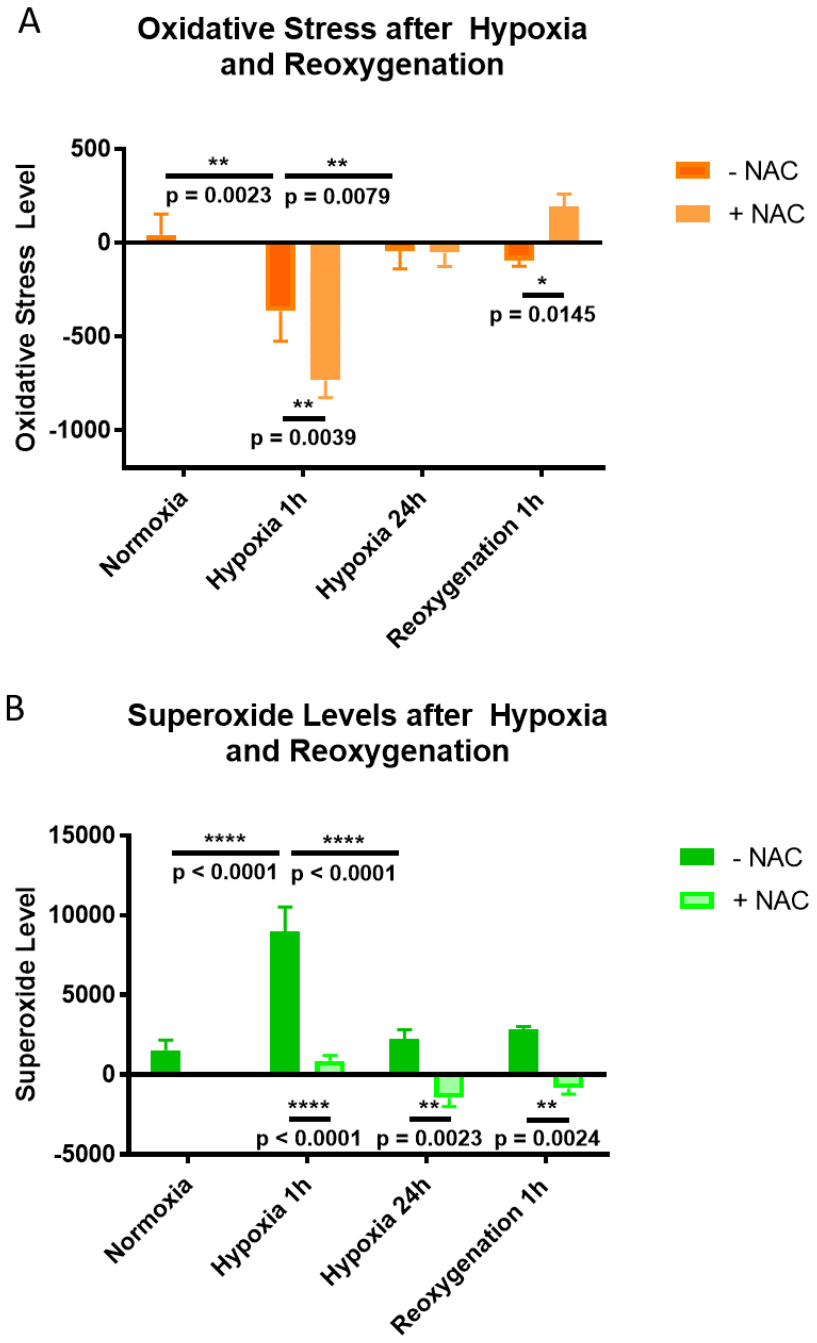

Figure 29. Hypoxia and Rapid Reoxygenation Treatment Causes Changes in Oxidative Stress and Superoxide Production in U-2 OS Cells. Cells were exposed to hypoxia for 1 hour, hypoxia for 24 hours, or hypoxia for 24 hours followed by rapid reoxygenation for 1 hour with or without the presence of the ROS scavenger NAC. Oxidative stress species (A) and superoxide levels (B) were detected using the ENZO ROS kit after 1 hour of treatment and exposure to the probes. Hypoxia and rapid reoxygenation have significant effects on ROS and superoxide levels as determined by two-way ANOVA using Tukey's multiple comparison test on the means of 3 independent experiments.

After 24 hours of hypoxia, oxidative stress and superoxide levels return to those seen in normoxia, indicating that after 24 hours in 1% O_2 cells become accustomed to the conditions and no longer produce ROS. Superoxide levels do not change following 1 hour of reoxygenation. As predicted treatment of all samples with NAC leads to a significant reduction in oxidative stress and superoxide species.

An explanation for the lack of ROS and superoxide production following reoxygenation could be due to the use of a single 1 hour time point; an earlier spike in oxidative stress could have been missed. Previous work has demonstrated that changes in superoxide production are almost immediate, and levels decrease rapidly in the first 10 minutes of reoxygenation [290]. As demonstrated in figure 23 of the introduction, an increase in production of different ROS leads to a series of complex chemical reactions to remove the species. Superoxide for example is readily converted to peroxynitrate, hydroxyl radicals or hydrogen peroxide. It is therefore possible that at the time point used here, species that has been originally produced following hypoxia have already been converted or scavenged and are therefore no longer detectable by the probes. To test this hypothesis, and to gain a greater understanding of the mechanics of ROS production following hypoxia and rapid reoxygenation, this experiment could be performed again across a series of shorter time points.

The change in levels of oxidative stress and superoxide species after 1 hour of hypoxia was startling, especially in comparison to other treatments. It was therefore important to take a closer look at the raw data to confirm whether this could be having some effect on the results presented in figure 29. Raw data from the blank wells on each plate were plotted for both the oxidative stress detecting probe and the superoxide detecting probe (Fig. 29). The plotted raw data (not normalised) shows that there is definite variation in background fluorescence levels in the absence of cells both between treatment times and within the same treatments. These blank wells contained no cells, only the phenol red-free media containing the different probes, therefore any changes observed could only be due to the oxygen content of the surrounding air. The largest observable change seems to be in the hypoxia samples where fluorescence from both the oxidative stress detection probe and the superoxide detection probe goes up in all hypoxia samples (both 1 hour and 24 hour). This suggests that exposure to 1% O_2 has an effect on the probes in some way. Although these background readings are subtracted from the sample readings, the fact that oxygen levels impact on the probes used means that the data obtained using this ROS detection kit must be treated with caution.

To assess whether hypoxia and rapid reoxygenation causes oxidative stress through other methods western blots were carried out probing for changes in total peroxiredoxin-3 (PRDX-3) levels (Fig. 31). Peroxiredoxin-3 is a mitochondrial protein with antioxidant function that is responsible for metabolising hydrogen peroxide [322]. Oxidation of PRDX-3 during reduction of hydrogen peroxide leads to dimerisation of PRDX-3, observable as a higher band on a western blot. However since total protein extracts of U-2 OS

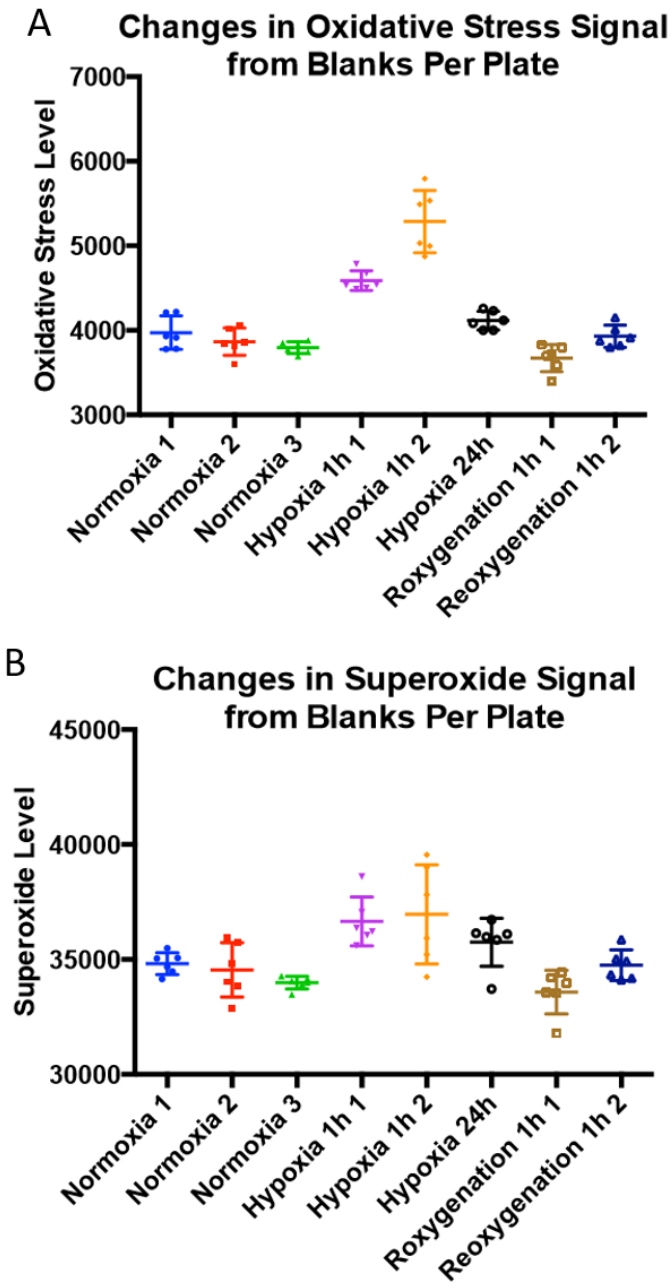

Figure 30. Hypoxia Exposure causes changes in Background Fluorescence of Oxidative Stress and Superoxide Probes. Raw data from blank wells (wells containing phenol red-free media with the different fluorescence probes) was taken from the data presented in figure 29 was plotted. Large amounts of variation in background fluorescence from both oxidative stress and superoxide probes is observed between different treatment types, in particular plates exposed to hypoxia directly before reading on the microplate reader. Smaller variations can been observed between plates of the same treatment.

cells were obtained here using RIPA buffer, both dimer and monomer bands are visible on the blot even in the absence of oxidative stress. An improved method of extraction would be to use trichloroacetic acid (TCA); this would allow for the analysis of the oxidative state of protein as it prevents the spurious oxidation events (such as disulphide bond formation) that occur during protein extraction under native non-acidic conditions. Future work should be carried out to determine whether PRDX-3 is oxidised following exposure to both hypoxia and reoxygenation.

Results presented in figure 31 show an increase in PRDX-3 levels following both hypoxia and rapid reoxygenation, with an initial decrease in signal occurring immediately after reoxygenation. The results observed here indicate that total protein levels are changing across the time course. There is evidence of sequence homology for several transcription factors and enhancers at the promoter of the PRDX-3 gene [323], some of which have links to stress responses. Binding sites for transcription factors of note include: aryl hydrocarbon receptor nuclear translocator (ARNT) , otherwise known as HIF1β, the second subunit of the HIF1 heterodimer, Forkhead box protein A2 (FOXA2), a protein involved in glucose homeostasis [324] and SMAD family members that are transducers for the transforming growth factor beta (TGF)β superfamily [325]. Due to the role of PRDX-3 in the removal of hydrogen peroxide, the change in total PRDX-3 levels across the time course presented in figure 31 indicates that hydrogen peroxide is produced during hypoxia and rapid reoxygenation, either directly or as a by-product during the removal of different ROS (Fig. 23).

4.3 Hypoxia and Rapid Reoxygenation Activates The Canonical NF-κB Pathway in U2-OS cells

As discussed earlier, hydrogen peroxide is a known activator of NF-κB. Although previous studies have shown a link between hypoxia and rapid reoxygenation and NF-κB activation [124][105], it was important to validate these findings as part of the project in U-2 OS cells. This section demonstrates that both hypoxia and rapid reoxygenation lead to activation of the canonical NF-κB pathway through western blot analysis and EMSA.

U-2 OS cells were exposed to 1% O_2 for the times indicated to observe the effects of hypoxia (Fig. 32), while rapid reoxygenation was carried out by incubating cells in 1% O_2 for 24 hours then returning plates to 21% O_2 for the times indicated. Membranes were probed for specific phosphorylation events associated with canonical NF-κB activation alongside the total protein levels. In addition to the use of actin as a loading control, membranes were probed for HIF1α as a control for hypoxia as it is stabilised in low oxygen conditions. A 30 minutes 25μM etoposide treatment was run as well as a positive control of canonical NF-κB activation [94].

The increase in HIF1α observed throughout all hypoxia time points demonstrates that HIF1α has become stabilised in response to the low oxygen conditions (Fig. 32B). This

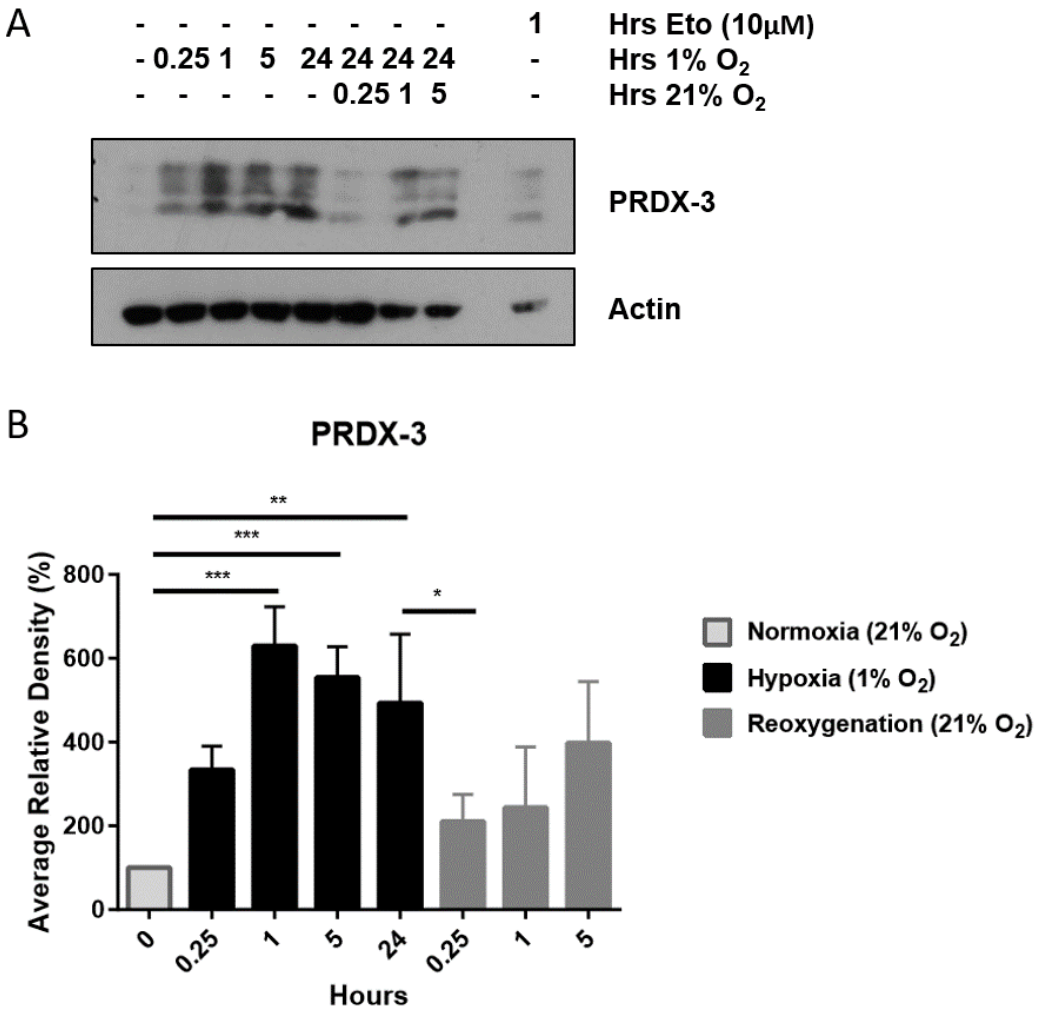

Figure 31. Hypoxia and Rapid Reoxygenation leads to Oxidative Stress as Measured by Peroxyredoxin Signal. U-2 OS cells were exposed to 1% O_2 for the indicated times. Reoxygenated samples were exposed to 1% O_2 for 24 hours prior to rapid reoxygenation. Proteins were extracted using RIPA lysis buffer with added protease inhibitors and western blots were performed probing for PRDX-3. A - Both hypoxia and rapid reoxygenation lead to changes in band intensity of peroxyredoxin-3, indicating that both hypoxia and rapid reoxygenation lead to oxidative stress. B - Quantification of western blots was carried out normalising to the loading control, actin. Relative density of 3 independent experiments shows that these findings are significant based on two-way ANOVA analysis using Tukey's test for multiple analyses. P-values presented show the statistical significance compared to the normoxia control.

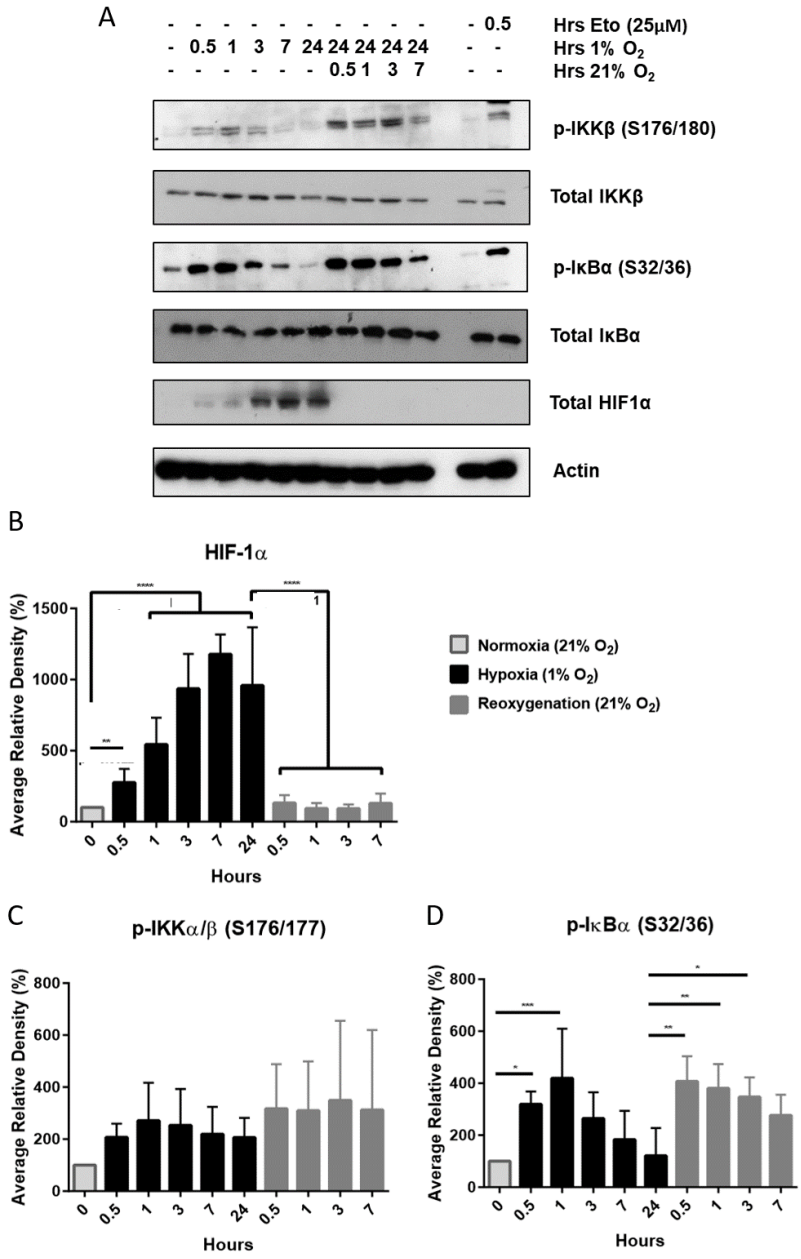

Figure 32. Both Hypoxia and Rapid Reoxygenation lead to Canonical NF-κB Activation in U-2 OS Cells. A - Representative blot of canonical NF-κB pathway activation following hypoxia and rapid reoxygenation. Cells were exposed to hypoxia (1% O_2) or reoxygenated (21% O_2) for the times indicated prior to lysis with 8M urea lysis buffer. A positive control of 25μM of etoposide treatment for 30 minutes was run alongside the experimental samples to confirm that antibodies were working as expected. B-D - Relative density of bands was determined across 4 independent experiments, normalising to actin and total protein.

Two-way ANOVA analyses were carried out to assess statistical significance.

demonstrates that the hypoxic incubator was working as expected as in the absence of oxygen HIF1α does not become hydroxylated by the PHDs, is not targeted for degradation, and is stabilised [279][280]. Following rapid reoxygenation the opposite is true. The PHDs are able to hydroxylate HIF1α leading to its subsequent ubiquitination and degradation as observed due to the sudden loss of HIF1α signal following reoxygenation. The second control of actin demonstrates that wells have been loaded evenly and the results presented are not due to changes in total overall protein level.

The western blot shown in figure 32 demonstrates that both hypoxia and rapid reoxygenation activate the canonical NF-κB pathway. Phosphorylation of IKKα/β and IκBα is observed following both hypoxia and rapid reoxygenation. Phosphorylation of both IKKα (lower band) and IKKβ (higher band) is observed indicating that both kinases of the canonical IKK complex are involved in the response to these stimuli. This is unexpected as IKKα is predominantly associated with the activation of the non-canonical NF-κB pathway. Quantification of relative band density from 4 independent experiments shows that this phosphorylation of IKKα/β is not significant, however changes in phosphorylation of IκBα are. The fact that changes in IKKα/β phosphorylation are not significant in spite of clear changes observed on the western blot presented is most likely due to variability in the signal strength of the antibody across multiple repeats.

Another notable observation is the decrease in IκBα phosphorylation following 24 hours of hypoxia exposure (Fig. 32). This indicates that the cells have adapted the low oxygen conditions and have adjusted their signalling accordingly. This demonstrates that IκBα is phosphorylated following both hypoxia and reoxygenation. For these reasons it was important to expose cells to hypoxia for 24 hours before rapid reoxygenation as if phosphorylation events and signal pathway activation had not subsided it would be impossible to tell whether an increase in phosphorylation was due to reoxygenation or a prolonged response to hypoxia. In all reoxygenation experiments presented in this thesis, cells were therefore exposed to 24 hours before rapid reoxygenation would take place.

In addition, it is clear that total IκBα levels remain constant throughout hypoxia and rapid reoxygenation even though the protein itself is phosphorylated. Culver et al. have observed this effect after hypoxia exposure previously, although their observations were focussed on tyrosine rather than serine phosphorylation events [118]. Phosphorylation at serines 32/36 is commonly associated with the subsequent K48-linked ubiquitination and degradation of IκBα by the proteosome [78][126][127][128]. Following hypoxia and rapid reoxygenation we observe stabilisation of IκBα; previous studies have shown that sumoylation of this ubiquitination site prevents degradation of IκBα as ubiquitination is blocked [129][130]. Additional experiments should be carried out to explore this hypothesis further. In addition, alternative methods of protein extraction could be carried out to observe some of the finer details of protein degradation; the urea lysis buffer used here is a rigorous method of whole cell extraction, which in some cases can mask small effects. Nuclear and cytoplasmic extracts could be carried out to confirm whether any degradation

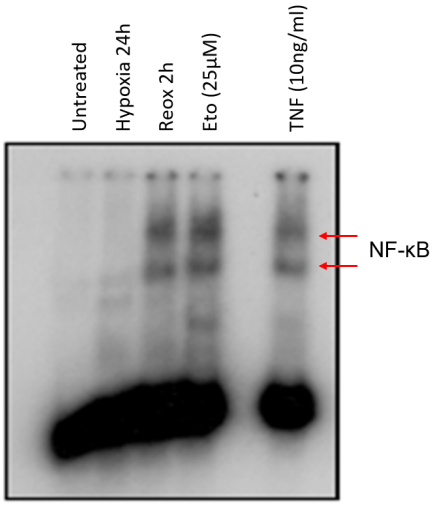

Figure 33. Rapid Reoxygenation leads to p65/p65 homodimer and p65/p50 heterodimer-DNA binding in U-2 OS Cells. U-2 OS cells were exposed to hypoxia for 24 hours, were reoxygenated for 2 hours or were treated with 25μM etoposide or 10ng/ml TNF for 1 hour and 30 minutes respectively. Nuclear extracts were probed for RelA/p65 as part of an EMSA. 24 hour hypoxia samples showed no p65 DNA binding however reoxygenation, etoposide and TNF treated samples showed DNA association of NF-κB.

is occurring.

The blot presented in figure 32 demonstrates that the IκBα, the final protein involved in activation of the canonical NF-κB pathway and the protein responsible for the release and translocation of RelA, is phosphorylated in the response to both hypoxia and rapid reoxygenation. To confirm that this activation leads to binding of RelA to κB sites on DNA an EMSA was carried out on nuclear U-2 OS cell extracts (Fig. 33). U-2 OS cells were exposed to hypoxia, reoxygenation, 25μM etoposide or 10ng/ml TNFα for the times indicated. This allowed comparison of binding of RelA across multiple activators of the canonical NF-κB pathway.

No DNA binding of RelA/p65 is observed in the normoxia and 24 hour hypoxia samples, while RelA/p65 DNA binding occurs following 2 hours of rapid reoxygenation (Fig. 33). As expected etoposide and TNF treatments lead to DNA binging of RelA/p65, these are potent activators of the canonical NF-κB pathway and lead to the binding of NF-κB subunit homodimers and heterodimers as observed by two distinct bands on the gel [94][87][88]. Without performing supershifts it is not possible to be certain which dimers have formed in response to these stimuli. Data presented in Kenneth et al. 2014 using the same probes and methods showed similar patterns of binding and confirmed by that they were p65/p50 and p50/p50 dimers [316]. Although it is not possible to be certain without further analysis the same dimer pairs could be binding here.

This section has shown that the upstream canonical pathway is activated following hypoxia and reoxygenation (as indicated by phosphorylation events on proteins of interest) (Fig. 32) and the EMSA has shown that NF-κB homodimers and hetrodimers are present on the DNA following these stimuli. Interestingly the signal from the reoxygenated sample is just as strong as those seen in the positive control samples of etoposide and TNFα treatments. This demonstrates that rapid reoxygenation is also a potent activator of the canonical NF-κB pathway and confirms findings shown in figure 32. The positive controls of etoposide and TNF used here are representative of two of the most well-established activators of the NF-κB pathway; DNA damage and cytokine detection through extracellular receptors respectively. This led the project towards evaluating the potential roles of extracellular and autocrine signalling as a potential activator of, or response to, hypoxia and rapid reoxygenation. The effects of DNA damage on canonical NF-κB activation will be explored in a later section.

4.4 Investigating the Potential Role of an Autocrine Feedback Loop in the NF-κB Response to Rapid Reoxygenation

One of the main mechanisms behind canonical NF-κB pathway activation is through extracellular receptor signalling, for example detection of members of the TNF receptor family or other chemokines and cytokines via a range of cell surface receptors [43]. Indeed many of the classical inducers of the NF-κB signalling pathway act through cell surface receptor interactions. Figure 33 demonstrated that similar levels of RelA-DNA binding occurs following both reoxygenation and TNF stimulation. To investigate whether an autocrine feedback mechanism similar to TNF signalling was responsible for the signalling pathway activation observed after rapid reoxygenation, experiments were carried out that involved swapping media between normoxic and reoxygenated plates. The initial hypothesis behind these experiments was that reoxygenation causes cells to produce chemokines or cytokines that could be exported from the cell into the surrounding media. Once in the media these cellular products would be sensed by extracellular membrane receptors, which would in turn activate signalling pathways downstream, leading to the NF-κB response described in section 1.2.

To investigate this autocrine feedback hypothesis U-2 OS cells were reoxygenated for 1 hour as described in previous sections. Again, media was changed to fresh gas-equilibrated media when plates were reoxygenated to induce immediate changes in oxygen level. To establish whether this new media on reoxygenated plates was able to activate the canonical NF-κB pathway, this media was taken off the reoxygenated plate after 1 hour of reoxygenation and added to an otherwise untreated normoxic plate (Fig. 34). The resulting plate was therefore never exposed to changes in oxygen levels, only the media from a reoxygenated plate that would contain any chemokines or cytokines secreted from the reoxygenated cells. An additional etoposide only treatment was again used as a positive

control of NF-κB activation, as well as a plate that had simply undergone a change of media (completely in normoxic conditions). Whole cell lysates were obtained using urea lysis buffer and western blots were carried out probing for phosphorylation events associated with canonical NF-κB pathway activation.

As seen in previous sections, activation of the canonical NF-κB pathway was not observed following normoxia and 24 hour hypoxia samples (Fig. 34). Results from 1 hour of reoxygenation were also consistent with earlier experiments, showing an increase in phosphorylation events associated with canonical NF-κB activation (Fig. 34B). Quantitative analysis shows that again, phosphorylation of RelA at serine 536 is not significant following reoxygenation or indeed following etoposide treatment. The latter is most likely due to experimental variation as indicated to by the large error bars (Fig. 34C).

Interestingly, exposure to media taken from the reoxygenation plate (lane 4) induces phosphorylation of both IκBα and RelA (Fig. 34). This data suggests that the addition of media taken from a plate of U-2 OS cells to an otherwise untreated plate of cells is enough to activate the canonical NF-κB pathway. However, the use of the final control presented in lane 7 (Fig. 34A) demonstrates clearly that this increase in canonical NF-κB activation is due to the sudden presence of fresh media rather than as a result of cells being exposed to reoxygenation plate media. Quantitative analysis demonstrates that these changes in phosphorylation of IκBα and RelA are significant and indicates that an unknown factor in the fresh media is able to activate the canonical NF-κB pathway. This unconsidered variable may be contributing to the effect observed in previous work carried out using fresh media to ensure rapid transition between oxygen environments. It is impossible to know whether the activation seen in previous figures is due to changes in gas levels and the resulting oxidative stress or due to this fresh media phenomenon.

It was therefore of importance to explore how the addition of fresh media was leading to the activation of the canonical NF-κB pathway. A new and improved hypoxia and reoxygenation protocol was needed for use in future experiments. There were multiple possible reasons for this fresh media induced activation, one of which was the CO_2 levels of the media. Media that was pre-equilibrated in the hypoxia chamber was exposed to 5% CO_2 and plates that were incubated in the normal incubator were also kept at 5% CO_2, however fresh media was warmed in the bottle at normal atmospheric CO_2 levels (0.04%). This change in CO_2 levels could be responsible for NF-κB activation in the experiments presented here, similar experiments have been carried out previously investigating the role of CO_2 in NF-κB activation [294]. The change in CO_2 levels can also lead to a change in the pH of media, which could also explain the changes in signalling levels. Further experiments therefore used CO_2 equilibrated media.

The presence of fresh serum in the media could also be leading to this NF-κB activation. To investigate whether this is the case, experiments were performed to investigate the role of serum in this phenomenon (Fig. 35). U-2 OS cells were kept in normoxic conditions and were exposed to fresh equilibrated media (5% CO_2-equilibrated), serum-free media or

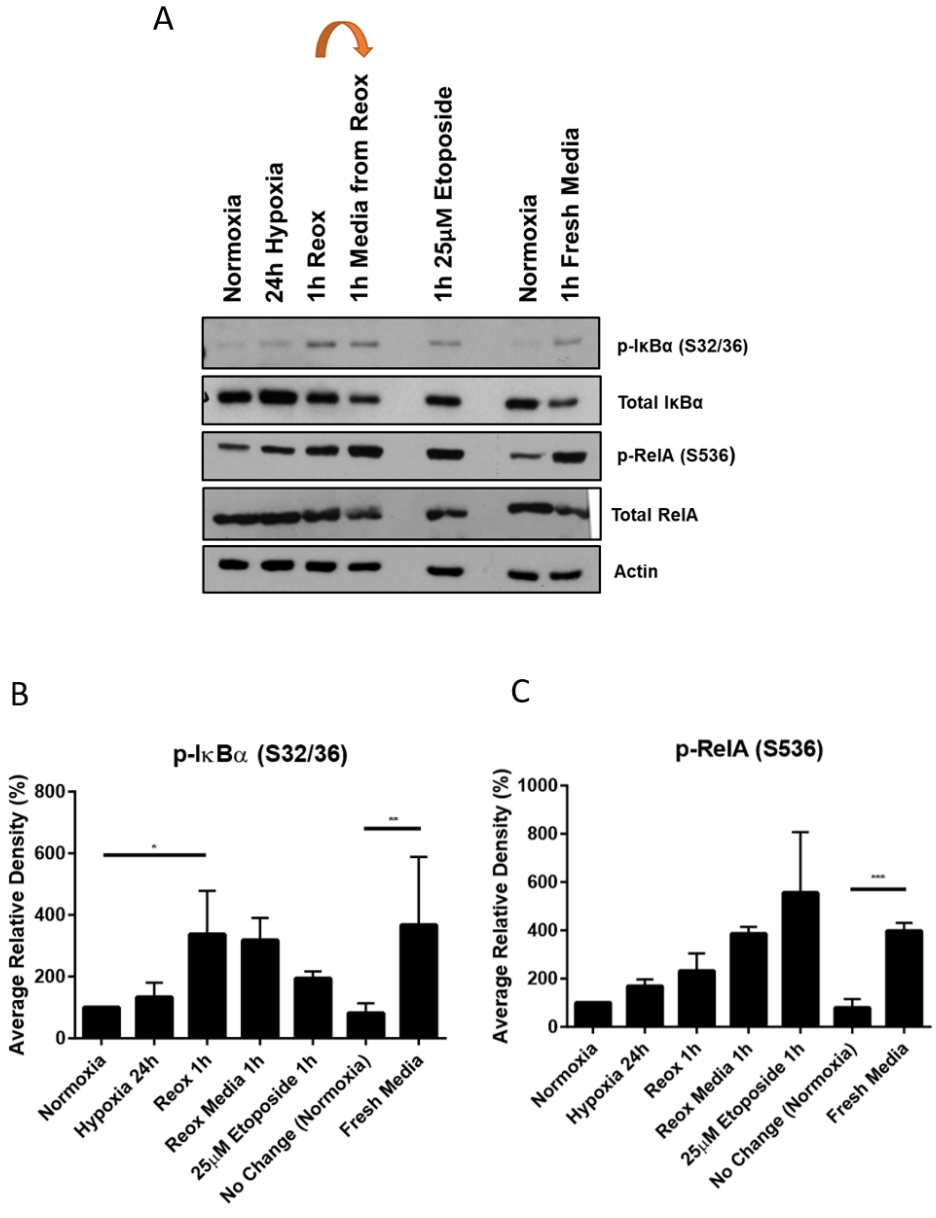

Figure 34. Exposure of Untreated U-2 OS Cells to Fresh Media leads to Canonical NF-κB Activation. U-2 OS cells were exposed to different stimuli and media changes to determine whether reoxygenated cells produce cytokines or chemokines that can activate the canonical NF-κB pathway in cells that have not been exposed to any other stimuli. To control for the media change involved in this an otherwise untreated plate was exposed to fresh media for 1 hour. A - Extracts were analysed by western blots probing for proteins associated with canonical NF-κB activation. B and C - Quantification of 3 independent experiments and statistical analyses by two-way ANOVA confirms that these findings are significant according to Tukey's test.

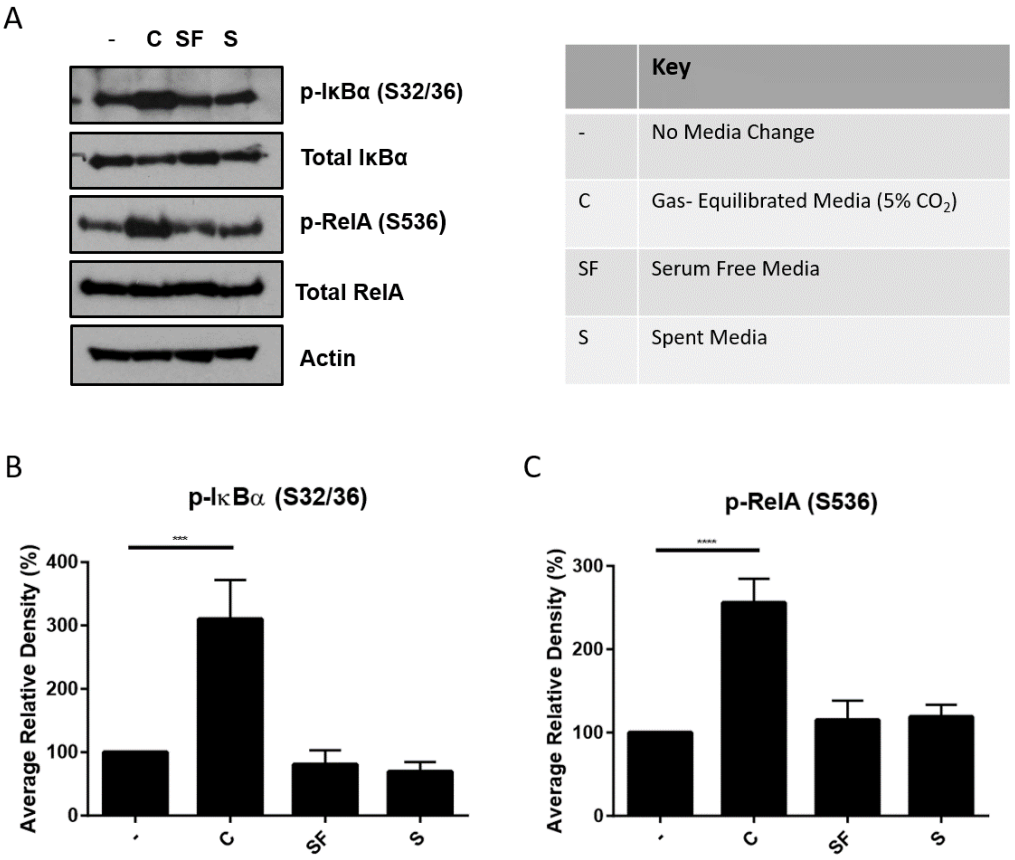

Figure 35. Fresh Serum in Media is able to Activate the Canonical NF-κB Pathway in U-2 OS Cells. U-2 OS cells were exposed to normoxia only and treated with fresh equilibrated media (5% CO_2), serum-free media or spent media for one hour. A control plate that underwent no media changes was harvested alongside. A - Extracts were analysed by western blots probing for proteins associated with canonical NF-κB activation. B and C - Quantification of relative band density was carried out across 3 independent experiments (one-way ANOVA, Tukey's test).

spent media (media previously used on identical cell populations) for one hour alongside a control plate that underwent no media changes. Protein was extracted using urea lysis buffer and samples were again analysed for phosphorylation of proteins associated with canonical NF-κB activation.

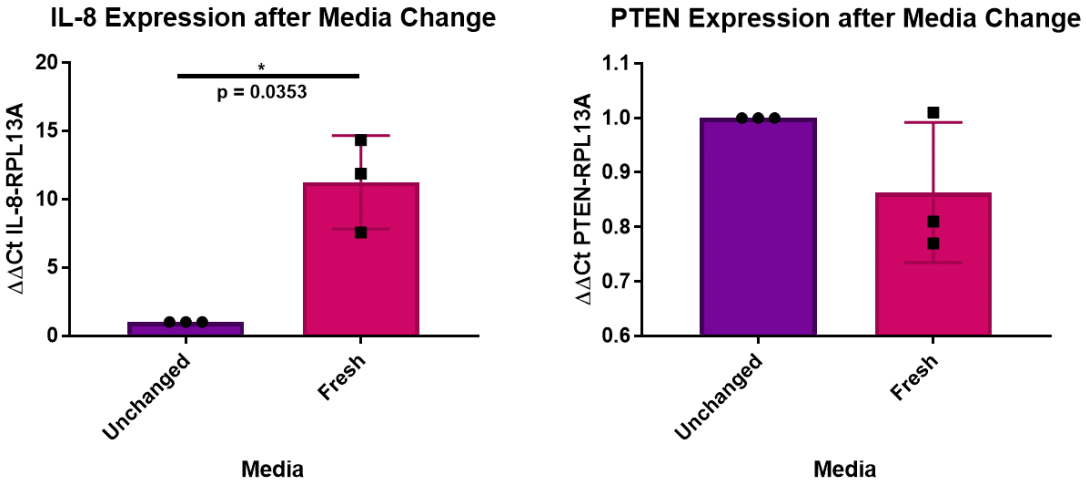

Figure 36. Fresh Media Leads to Changes in NF-κB Target Gene Expression. U-2 OS cells were exposed to normoxia only for 4 days after seeding and treated with fresh equilibrated media (5% CO_2) for 6 hours on day 4 before being harvested for total RNA. A control plate that underwent no media changes was harvested alongside the fresh media plates. Reverse transcription was carried out followed by real-time qPCR to assess the relative abundance of the NF-κB target genes IL-8 and PTEN, using RPL13A as a housekeeping gene. Results show a significant increase in IL-8 expression following the media change ($p = 0.0353$) as confirmed by two-tailed paired t-test.

An increase in canonical NF-κB activation is observed after one hour exposure to fresh media compared with untreated plates (Fig. 35). No change in phosphorylation is observed in both the serum-free and spent media samples. This clearly demonstrates that fresh serum in media is able to activate the canonical NF-κB pathway independently of other treatments. It follows that after seeding, cells use up nutrients and growth factors present in the media and in turn secrete waste products. After 3-4 days of this the media in a plate will be very different from fresh media containing fresh serum.

To determine whether the state of the media affects the control of gene expression by NF-κB real-time qPCR experiments were carried out. Two plates containing U-2 OS cells were seeded on day 0 and left to grow for 4 days at 37°C in a normal incubator. On day 4 the media on one plate was changed for fresh media while the other remained unchanged. Cells were lysed for total RNA 6 hours later and reverse transcription was carried out to produce cDNA. Real-time qPCR was carried out probing for NF-κB target genes IL-8 and PTEN, using RPL13A as a reference gene. Results were normalised using the Δ ΔCt

method, and graphs were plotted and statistically tested using GraphPad Prism.

Data presented in figure 36 demonstrates that changing media on plates to fresh media affects NF-κB target gene expression. Following exposure to fresh media, expression of IL-8 significantly increased over ten-fold ($p = 0.0353$), while PTEN expression decreased on average although not to significance. This shows that in the absence of any other stimulus, simply changing the media on plates is enough to activate NF-κB as measured by real-time qPCR.

The effects of fresh serum on NF-κB pathway activation could be masking any effects that occur after hypoxia and rapid reoxygenation so an alternative method of inducing rapid changes in gas levels should be used. One option would be to use gas-equilibrated serum-free media for transitions between oxygen conditions, however this starvation of cells would introduce other confounding factors into experiments; it would be impossible to determine the extent to which oxygen state and starvation is contributing to observations. An alternative option is to use spent media for these transitions; in this protocol identical plates would be set up in parallel purely for harvesting of spent media to be used for rapidly transitioning cells to or from hypoxia. This was the preferred option as it removed as many potential variables from the experiment as possible. All experiments from here on, unless stated otherwise, were carried out using this novel spent media protocol for rapid oxygen state transition.

As discussed in the introduction, the canonical NF-κB pathway is closely linked with other signalling pathways to coordinate specific and controlled cellular responses. To determine which of these pathways are affected by hypoxia and rapid reoxygenation, a western blot was performed on several proteins of interest; phospho-signal transducer and activator of transcription 3 (STAT3), phospho-Chk1, total HIF1α and phospho-Akt. The results showed that the state of the media, whether fresh, CO_2 equilibrated or fresh, had no effect on signalling through any of these proteins (data not shown).

This finding brings into question whether observations from previous experiments that have involved fresh media changes to induce hypoxia should be reassessed. For example Culver et al. [118] showed that exposure to hypoxia leads to an increase in IL-8 expression and a decrease in PTEN expression. Data presented here (Fig: 36) suggest that their findings could in fact be due to the fresh media change that is used to induce hypoxia rather than the exposure to a hypoxic environment itself. Further experiments need to be carried out to confirm this. It should be noted however that in many cases, such as during hypoxia and rapid reoxygenation time courses, media changes to fresh media are the current standard protocol. The change to fresh media is therefore not commonly considered in experimental design and is therefore not typically controlled for.

Due to the findings presented in this section experiments carried out in the rest of this thesis used spent rather than fresh media to carry out time courses. This was with the aim of removing any uncertainties regarding the causes of any observable effects.

4.5 ROS Production Following Hypoxia and Rapid Reoxygenation when a Spent Media Protocol is Used

To determine whether hypoxia and rapid reoxygenation lead to the production of ROS when spent media is used for rapid gas transition, the ENZO total ROS/superoxide detection kit was used again (ENZO; #51010), taking into consideration the caveat presented earlier that oxygen levels impact on the reactivity of the probes used (Fig. 30). As before, a microplate reader was used to detect fluorescence of the cell permeable 'oxidative stress' probe showing general ROS levels (hydrogen peroxide (H_2O_2), peroxynitrite ($ONOO^-$), hydroxyl radicals (HO), nitric oxide (NO) and peroxy radical (ROO)). Detection of the superoxide probe (measuring superoxide (O_2^-) levels only) was carried out in parallel. Data presented in figure 37 is therefore a direct repeat of the experiment described previously (Fig. 29) except using spent rather than fresh media.

After 1 hour of hypoxia a significant decrease in ROS as detected by the 'oxidative stress' probe was observed (Fig. 37A). This returned towards levels seen in normoxic samples following 24 hours of hypoxia and no further significant changes in ROS levels were observed following reoxygenation. Addition of NAC had no significant effect on ROS production following hypoxia however a significant increase was observed following reoxygenation. Superoxide levels remained unchanged throughout this experiment, however treatment with NAC lead to a significant decrease in levels across all time points (Fig. 37B).

The effects of NAC treatment on the production of ROS or superoxide remains constant between this experiment and the earlier fresh media experiment. This suggests that NAC is predominately a superoxide scavenger as the opposite effect is observed in the levels of ROS as detected by the 'oxidative stress' probe. The increase in ROS levels could be explained by the chemistry of these species, as they react to form one another in closely linked chemical pathways. A decrease in superoxide in one part of the pathway could have a knock-on effect elsewhere, leading to an increase in levels of other ROS measured in this experiment. The use of alternative anti-oxidants or ROS scavengers either separately or in combination would further our understanding of ROS production following hypoxia and rapid reoxygenation.

Some clear differences were observed between the ROS levels detected when a spent media protocol was used to carry out hypoxia and reoxygenation time courses compared with a fresh media protocol. Here the data carried out from both sets of ROS detection (fresh or spent media) experiments have been plotted together to allow direct comparisons to be made (Fig.38). Focussing on the oxidative stress species data first, the normalised data presented shows that there is no signifcant difference in 'oxidative stress' species levels following treatment with fresh or spent media after 1 hour of hypoxia or reoxygenation.

After 1 hour of hypoxia however, a 4-fold decrease in superoxide levels is observed after spent media is used to achieve changes in oxygen levels compared with fresh media ($p = 0.0052$). No significant differences are observed in superoxide levels when comparing

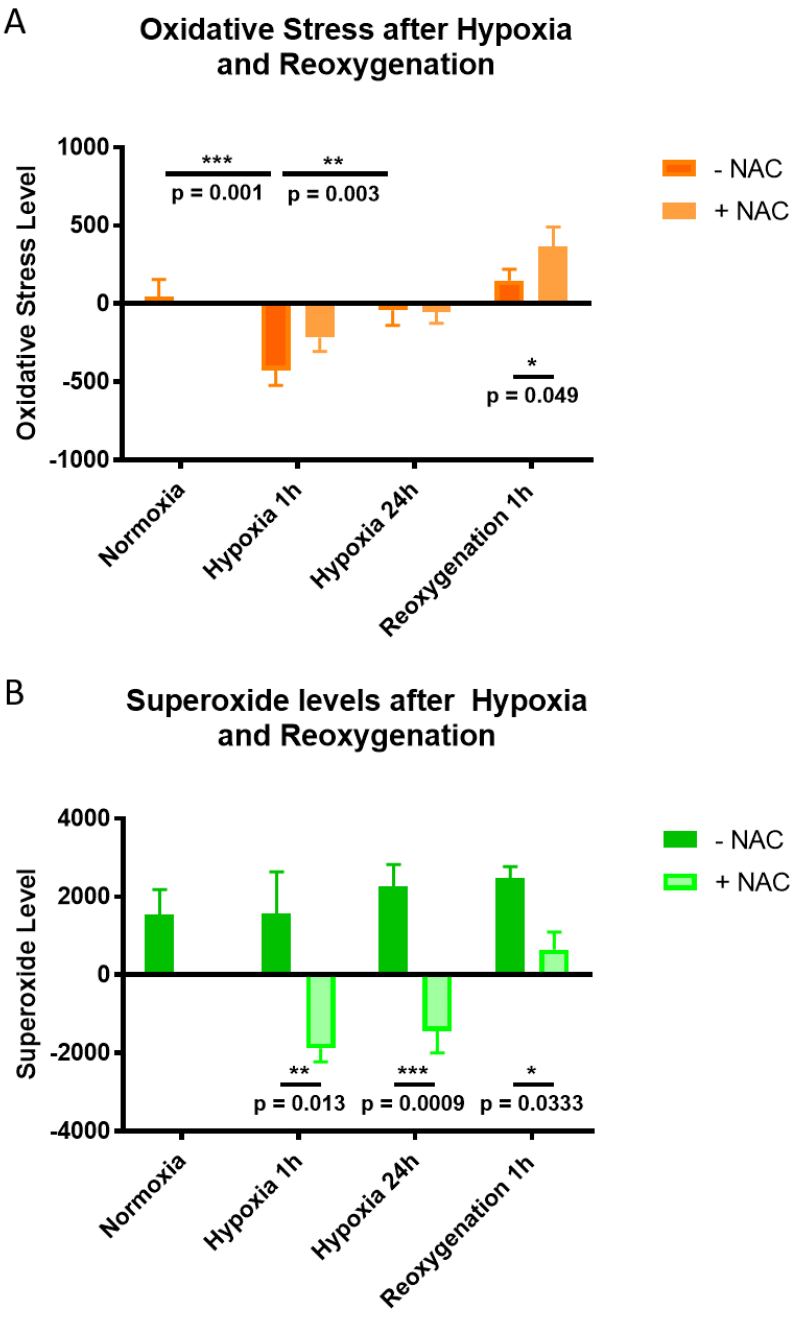

Figure 37. ROS Production in U-2 OS Cells After Hypoxia and Rapid Reoxygenation using Spent Media. U-2 OS cells were exposed to 1% O_2 for 1 hour, or were reoxygenated (21% O_2) for 1 hour after exposure to hypoxia for 24 hours. Cells underwent transition between these oxygen states using spent media with or without NAC treatment. A - Oxidative stress (OS) and B - superoxide (SO) levels were detected using a microplate reader following the manufacturer's protocol (ENZO Total ROS Detection Kit). Data shows that there is a decrease in ROS levels after 1 hour of hypoxia exposure compared to normoxia levels. NAC treatment leads to a decrease in superoxide levels compared to NAC-free samples across all treatments.

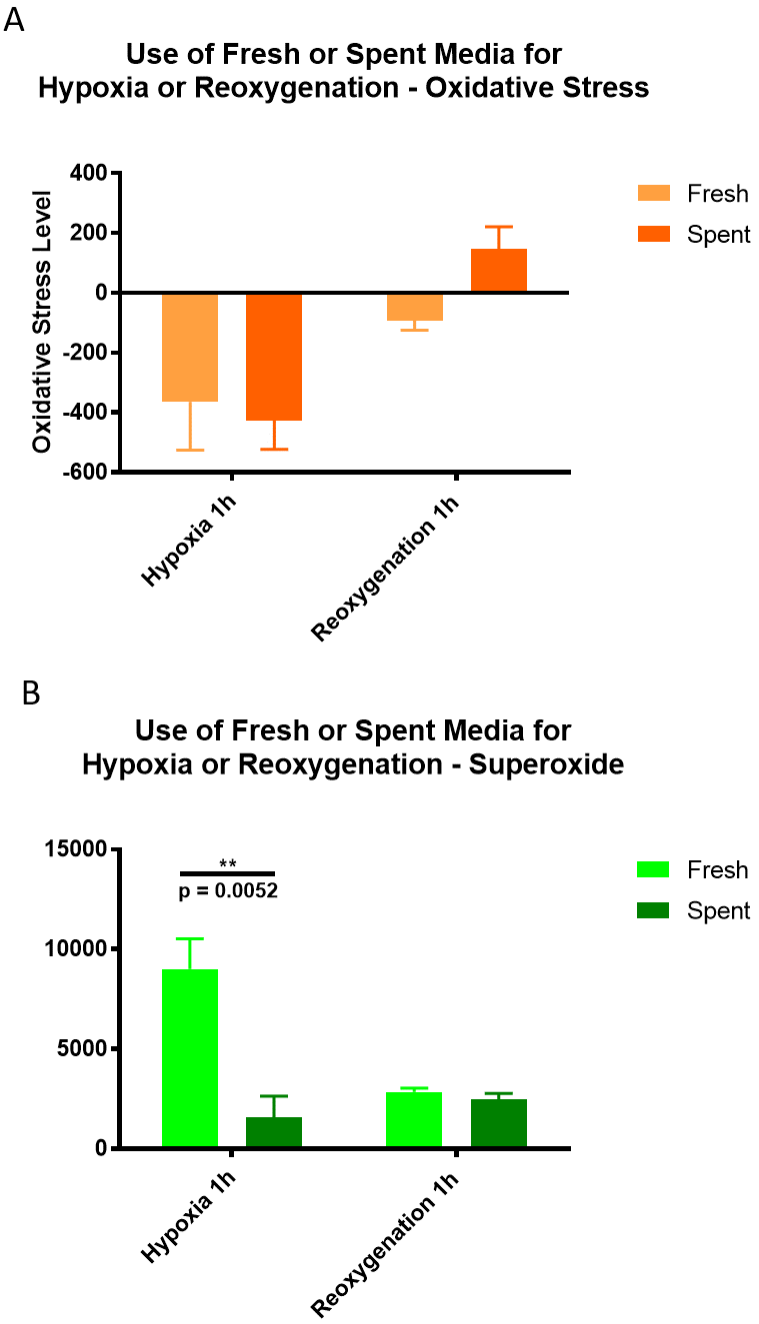

Figure 38. ROS Production in U-2 OS Cells Changes Depending on Whether Fresh or Spent Media is used during Oxygen State Transition. U-2 OS cells were exposed to hypoxia (1% O_2) for 1 hour, or were reoxygenated (21% O_2) for 1 hour after exposure to 24 hours of hypoxia. Cells underwent transition between these oxygen states using either fresh or spend media and; A - oxidative stress, and B - superoxide levels were detected using a microplate reader following the manufacturer's protocol (ENZO Total ROS Detection Kit). These results show that the use of fresh or spent media can have an effect on superoxide production following 1 hour of hypoxia ($p = 0.0052$). Data was analysed and presented as graphs using GraphPad Prism. Two-way Anova tests were performed and p-values were corrected for multiple comparisons using Sidak's test.

fresh and spent media usage following 1 hour of reoxygenation. This indicates that the freshness of the serum in the media used in hypoxia and reoxygenation experiments has an effect on oxidative stress and superoxide levels after hypoxia in U-2 OS cells. Once again though, it is important to consider the effects of hypoxia on the effectiveness of this ROS/superoxide detection kit. As discussed previously hypoxia exposure seems to affect the blank/background fluorescence readings, in the absence of cells (Fig. 30).

Once again this data does not clarify the effects that hypoxia and rapid reoxygenation have on ROS production and only adds to the body of conflicting reports on the effects of hypoxia and reoxygenation on the production of ROS [288][290][289][326]. As discussed earlier, a repeat of this experiment following a series of time points would give insight as to whether earlier bursts of ROS production have been missed, indeed constant monitoring of ROS would be a preferable approach to this experiments as shown in previously published work [288][290][289]. In addition, alternative methods to detect ROS could be implemented due to the complication encountered using the ENZO ROS detection kit in that the probes were influenced by the level of oxygen available.

4.6 NF-κB is Activated by Hypoxia and Rapid Reoxygenation when Spent Media is used

Following the observation that the presence of fresh serum in the media was able to activate the canonical NF-κB pathway, independently of other stimuli, experiments were carried out to determine whether the use of a novel, modified protocol to carry out hypoxia and rapid reoxygenation still triggered activation of the canonical NF-κB pathway (Fig. 39). Phosphorylation of STAT3 was analysed as an additional marker of hypoxia alongside HIF1α, as STAT3 is also known to be activated in response to hypoxia. It has also been shown to interact with RelA [327][328][329].

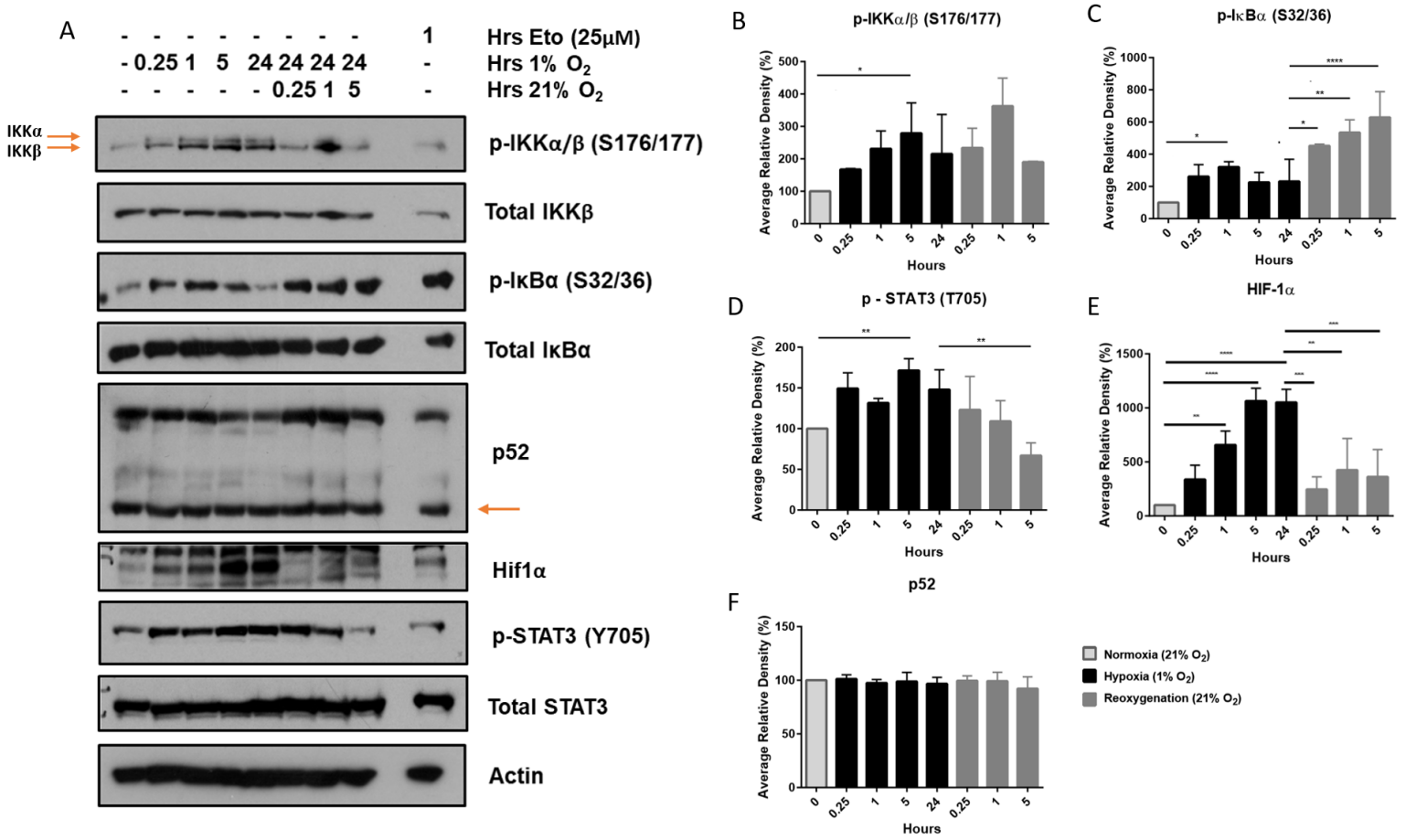

Figure 39. The Effects of Hypoxia and Reoxygenation on NF-κB Activation. U-2 OS cells were exposed to 1% O_2 for the indicated times. Reoxygenated samples were exposed to 1% O_2 for 24 hours prior to rapid reoxygenation. Etoposide was used as a positive control for canonical NF-κB activation. Proteins were extracted using urea lysis buffer with added protease inhibitors and western blots were performed probing for markers of canonical and non-canonical NF-κB activation as well as markers of hypoxia. A - Representative blot of 3 independent experiments. B-F - Relative density of 3 independent western blots, significance was determined using two-way ANOVA using Sidak's test for multiple comparisons.

The hypoxia controls of total HIF1α and STAT3 phosphorylation significantly increased as expected upon exposure of cells to 1% oxygen, confirming that a hypoxic state has been induced (Fig. 39A, D and E). Upon examining read-outs of canonical NF-κB activation, it was observed that exposure to hypoxia leads to the significant phosphorylation of both IKKα and IKKβ, whereas after reoxygenation phosphorylation of IKKα was more prominent although not to a significant level (Fig. 39A). A significant increase in phosphorylation of IκBα at serines 32 and 36 also occurs following both hypoxia and rapid reoxygenation, (Fig. 39A, B and C). Phosphorylation of these signalling factors is a well-established indicator of canonical NF-κB pathway activation although it is interesting to note that IKKα activation is more commonly associated with activation of the non-canonical NF-κB pathway. However, the non-canonical pathway response of p100 to p52 cleavage was not observed upon hypoxia and reoxygenation (Fig. 39A and F), thus providing further evidence for the involvement of the canonical pathway.

Once again, no change in total IκBα levels are observed. As discussed earlier phosphorylation of IκBα at the residues analysed here is commonly associated with degradation of IκBα [78][126][127][128]. More recent studies have indicated that sumoylation of IκBα can prevent its ubiquitin-mediated degradation [129][130]. It would be interesting to investigate whether this sumolyation is occurring following hypoxia and rapid reoxygenation. Further experiments should be carried out to explore the effects of sumoylation further.

Collectively these results demonstrate that hypoxia and reoxygenation lead to canonical NF-κB pathway activation via the canonical pathway, under conditions involving the use of spent media. Thus, the activation of the canonical NF-κB pathway following hypoxia and rapid reoxygenation, observed in earlier experiments (Fig. 32), is not soley due to the addition of fresh serum at the point of oxygen state transfer.

In addition to phosphorylation, understanding ubiquitination of proteins is essential in understanding cell signalling pathways as ubiquitination is required for targeting proteins for degradation by the proteosome. The same lysates run on the western blot presented in figure 39 were re-analysed by SDS-PAGE and western blot and probed for K48 and K63-linked ubiquitination events to determine whether ubiquitination was occurring under hypoxia and rapid reoxygenation (Fig. 40).

The western blot shown in figure 40 shows changes in ubiquitin levels after hypoxia and reoxygenation; the smears show increases in global ubiquitination of various proteins. In the blots presented, K48-linked ubiquitination reduces following 24 hours of hypoxia exposure. After rapid reoxygenation an increase in K48-linked ubiquitination is observed. No changes in K63-linked ubiquitination occur throughout the time course.

This experiment should be repeated before any firm conclusions can be drawn, however, if statistically significant differences in K48-linked ubiquitination were detected this could indicate that the unfolded protein response is being activated following reoxygenation. Certain stresses such as oxidation can cause proteins to misfold during folding

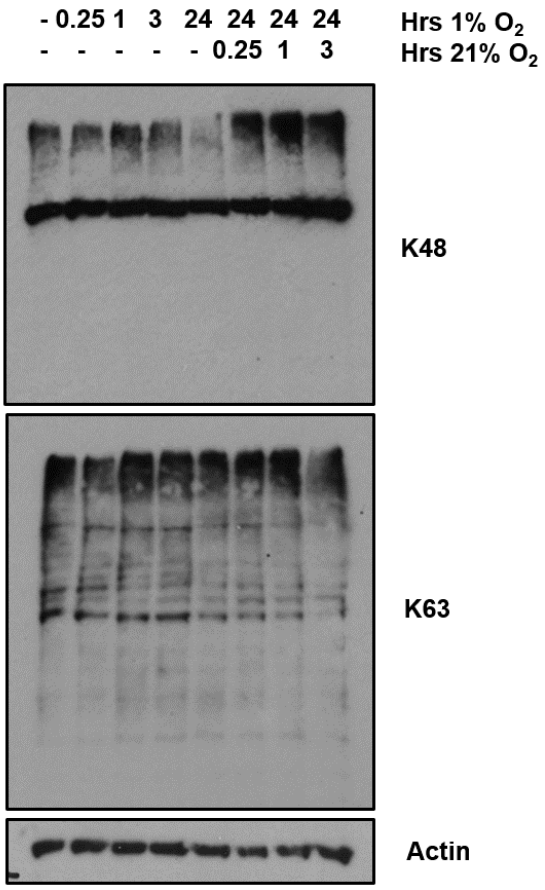

Figure 40. Hypoxia and Rapid Reoxygenation leads to Changes in Ubiquitination Events in U-2 OS Cells. U-2 OS cells were exposed to 1% O_2 for the indicated times. Reoxygenated samples were exposed to 1% O_2 for 24 hours prior to rapid reoxygenation. Cells were lysed with urea lysis buffer with added protease inhibitors and western blots were performed probing for K48- and K63-linked ubiquitination events.

and oligomerisation in the endoplsmic reticulum [330]. This production of possible non-functional proteins may be detrimental to the health and function of the endoplasmic reticulum and the cell. In these circumstances the misfolded proteins are chaperoned into the cytosol, and targeted for degradation by the proteosome through K48-linked ubiquitination; this process is known as ER-associated degradation [331]. The preliminary data presented here could indicate that reoxygenation is triggering oxidation and misfolding of proteins that must subsequently be degraded.

After confirming that hypoxia and rapid reoxygenation lead to canonical NF-κB activation in U-2 OS cells (Fig. 39) it was important to establish whether this occurs in other cell lines. A primary cell line of human foreskin fibroblasts was selected to confirm the U-2 OS cell findings. As primary cells, they are genetically, biologically and molecularly more similar to cells in a living organism. Experiments were carried out as described previously (Fig. 39), however spent media was not used in these experiments. The serum used to

culture primary cells is synthetically produced rather than from a biological source as used in immortalised cell lines. The serum was therefore not expected to have as much of an effect on cell signalling pathway activation. Further tests should be carried out to confirm this.

The results presented in figure 41A are similar to those shown in figure 39; exposure to hypoxia and rapid reoxygenation leads to the activation of the canonical NF-κB pathway as measured by IKKα/β and IκBα phosphorylation. Further analysis of the kinetics of this activation through quantification of band density (n = 3) reveals that these changes in phosphorylation are mostly not statistically significant, again this is most likely due to experimental variation in band density. The only significant change in phosphorylation levels observed in this experiment is that of IκBα phosphorylation following reoxygenation. Thus, this data indicates that reoxygenation leads to the activation of the canonical NF-κB pathway through IκBα (Fig. 39C), again in the absence of IκBα degradation. It is possible that the use of fresh media to carry out these experiments could be contributing to the activation of the canonical NF-κB pathway in this instance, further experiments should be carried out to determine whether this is the case.

So far this section has predominantly focussed on canonical NF-κB pathway activation, although other NF-κB pathway-linked pathways of interest have been explored such as HIF1α and STAT3. Another series of pathways that are known to crosstalk with NF-κB activation are the MAPK pathways. The next experiment aimed to determine how hypoxia and rapid reoxygenation affect MAPK signalling following the same experimental design described earlier (Fig. 39). Western blot analysis was performed to look at total levels and phosphorylation of all three MAPK proteins, ERK, p38 and JNK [332].

Following exposure to hypoxia there are no changes in the phosphorylation and subsequent activation of ERK1/2, p38 or JNK (Fig. 42). Following rapid reoxygenation no significant change in p38 or JNK phosphorylation occurs as determined by statistical analysis of relative band density (Fig. 42C and D), however a significant increase in phosphorylation and activation of ERK1/2 is observed (Fig. 42B). This increase in MAPK signalling through ERK suggests that reoxygenation is able to trigger proliferation and differentiation of cells.

The data presented in figure 42 demonstrates that exposure to hypoxia followed by rapid reoxygenation causes changes in MAPK signalling. This could indicate cross-talk is occurring between the canonical NF-κB pathway and the MAPK pathways, however since TAK1 as an upstream kinase of the JNK and p38 mitogen-activated protein kinase (p38) pathways and not ERK, it could be activated entirely independently of canonical NF-κB signalling [333]. Regardless of the kinetics of its activation, detection of MAPK pathway activation gives insight into the overall responses of U 2-OS to sudden exposure to hypoxia and rapid reoxygenation. The elevation in signalling through the ERK cascade indicates a potential increase in cell proliferation following rapid reoxygenation. This data infers that reoxygenation allows a reversal of reduction of proliferation that occurs during

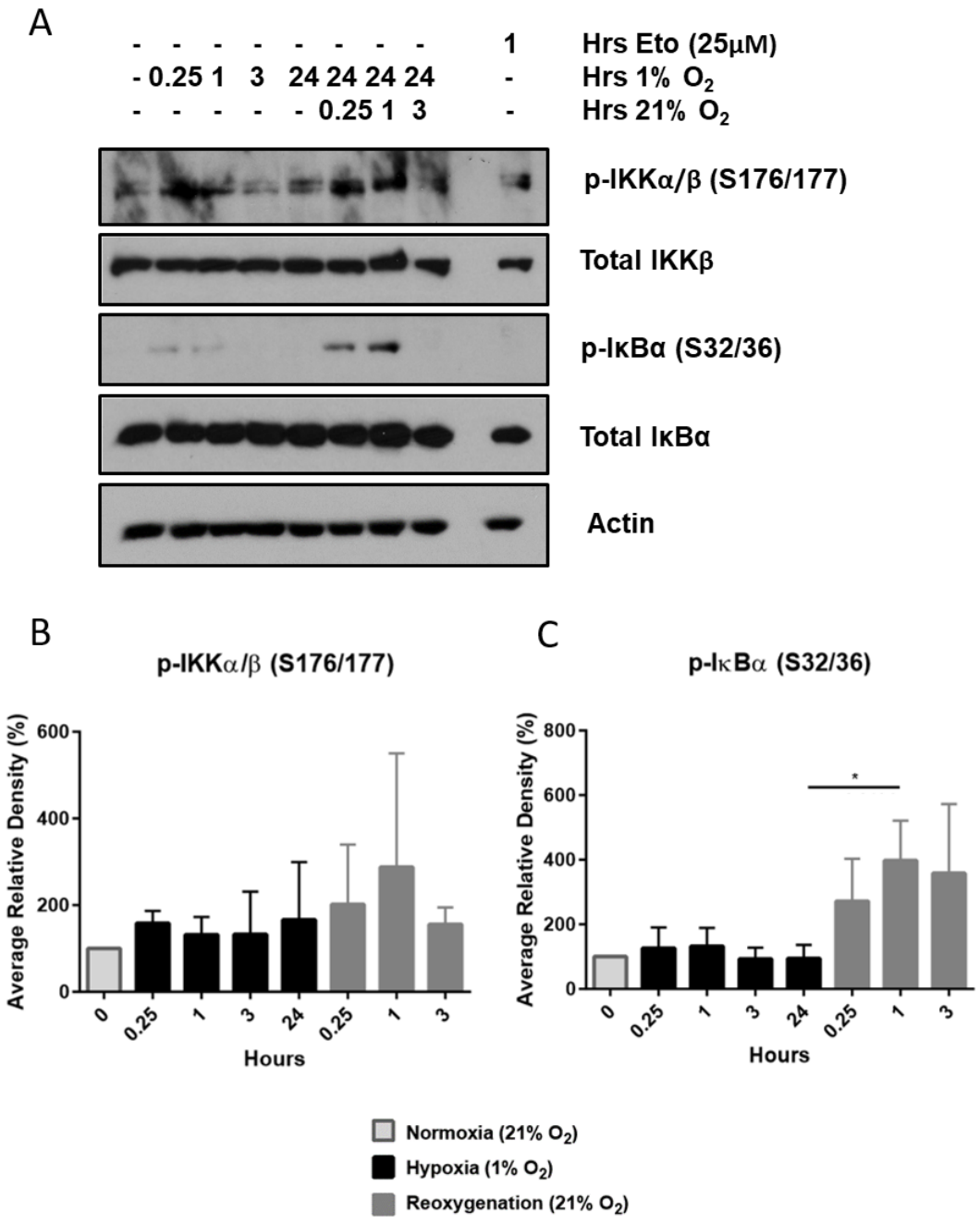

Figure 41. Hypoxia and Rapid Reoxygenation leads to NFκB Activation in HFF cells. HFF-1 cells were exposed to 1% O_2 for the indicated times. Reoxygenated samples were exposed to 1% O_2 for 24 hours prior to rapid reoxygenation. Cells were lysed with urea lysis buffer with added protease inhibitors and western blots were performed probing for markers of canonical NF-κB activation. A - Representative blot of 3 independent experiments. B and C - Mean relative density of 3 independent experiments. Statistical analyses were performed using two-way ANOVA with Sidak's test for multiple comparisons.

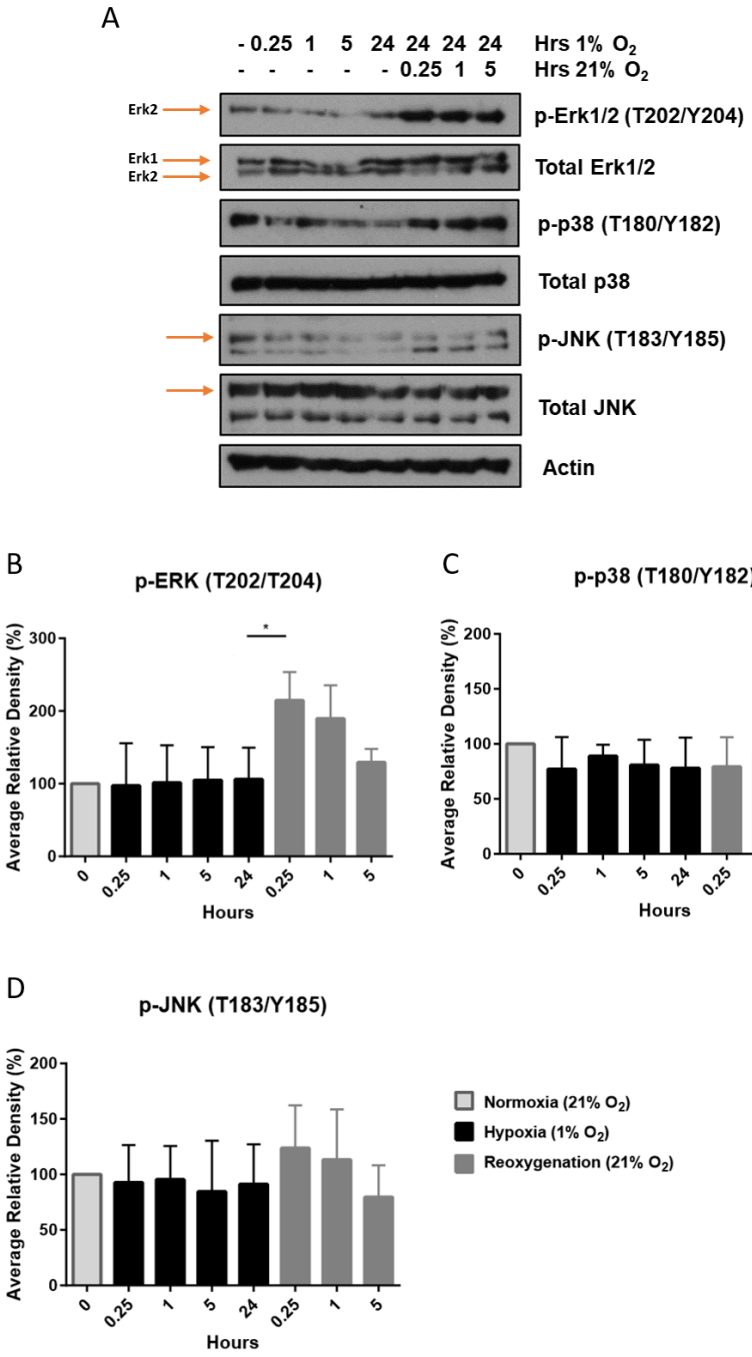

Figure 42. Hypoxia and Rapid Reoxygenation leads to Changes in MAPK Signalling in U-2 OS Cells. U-2 OS cells were exposed to 1% O_2 for the indicated times. Reoxygenated samples were exposed to 1% O_2 for 24 hours prior to rapid reoxygenation. Cells were lysed with urea lysis buffer with added protease inhibitors and western blots were performed probing for MAPK signalling pathway activation. A - Representative western blot of 3 independent experiments. B-D - Mean relative density of 3 western blots, statistical analyses were carried out using two-way ANOVA and Sidak's test for multiple comparisons.

hypoxia. Indeed previous work has indicated that in the majority of cell lines, a decrease in proliferation is observed following exposure to hypoxia [272], and is associated with reduced metabolic activity. An increase in proliferation has also been observed following reoxygenation, albeit following different hypoxia and reoxygenation protocols (4 hours of hypoxia only). Sung et al., demonstrated that the PI3K/protein kinase B (PKB) and ERK signalling pathways were involved in this response in neuronal cells [274].

4.7 Hypoxia and Rapid Reoxygenation Leads to Changes in the Expression of NF-κB Target Genes

Data presented so far in this thesis has demonstrated that the upstream canonical NF-κB pathway is activated after both hypoxia and rapid reoxygenation. It was therefore important to investigate whether this NF-κB activation induces transcription of target genes, and which genes were transcribed. Real-time quantitative PCR experiments were carried out after 6 hours of hypoxia or reoxygenation to determine this. The time point of 6 hours was selected due to personal communication with other laboratory members, as well as through observations that no changes of note occur at earlier time points (2 hours).

As discussed in section 1.4, the genes selected for analysis here are commonly associated with NF-κB activation or oxidative stress. While some of them have been previously implicated in the response to hypoxia or reoxygenation, the cell lines, oxygen levels and time points reported in these publications differ to those used here. Additionally the novel spent media method for gas exchange was most likely not utilised in previous work, therefore carrying out the following real-time qPCR experiments presented here is of great value when trying to understand the cellular response to hypoxia and reoxygenation.

For all real-time qPCR experiments U-2 O S cells were exposed to 1% O_2 for 6 hours to induce hypoxia. Reoxygenated samples were exposed to 1% O_2 for 24 hours followed by reoxygenation (21% O_2) for 6 hours (Fig. 44). The spent media method of inducing hypoxia or reoxygenation was used in all experiments. Total RNA was extracted, analysed and reverse transcription was carried out to produce cDNA. Real-time quantitative PCR was performed on the aforementioned target genes alongside the reference gene RPL13A. Data was analysed by the $\Delta\ \Delta$ Ct method, hypoxia samples were normalised to normoxia/untreated samples and reoxygenated samples were normalised to 24 hour hypoxia samples. Some genes have more repeats than others as they were investigated further in later sections of the thesis due to interesting preliminary data.

To ensure that the hypoxia chamber was working as expected, real-time qPCR was performed to amplify genes known to be induced by hypoxia; VEGF and CA9. VEGF is transcribed in response to low oxygen levels by HIF1α and HIF1β to promote vasculogenesis and angiogenesis to restore oxygen to cells [334][335]. CA9 is a zinc metalloenzyme

that catalyses the hydration of carbon dioxide in hypoxic conditions [336][337]. Expression of hypoxia inducible genes, VEGF and CA9, increase after exposure to hypoxia, thus confirming that the anaerobic chamber was working correctly (Fig. 43). Some samples do not appear to have increased levels of VEGF or CA9, however inspection of the raw data reveals that these points do not come from the same sample. These differences are therefore more likely to be a result of technical issues rather than a problem with the hypoxic incubator, as such, these data sets were not discarded from analysis.

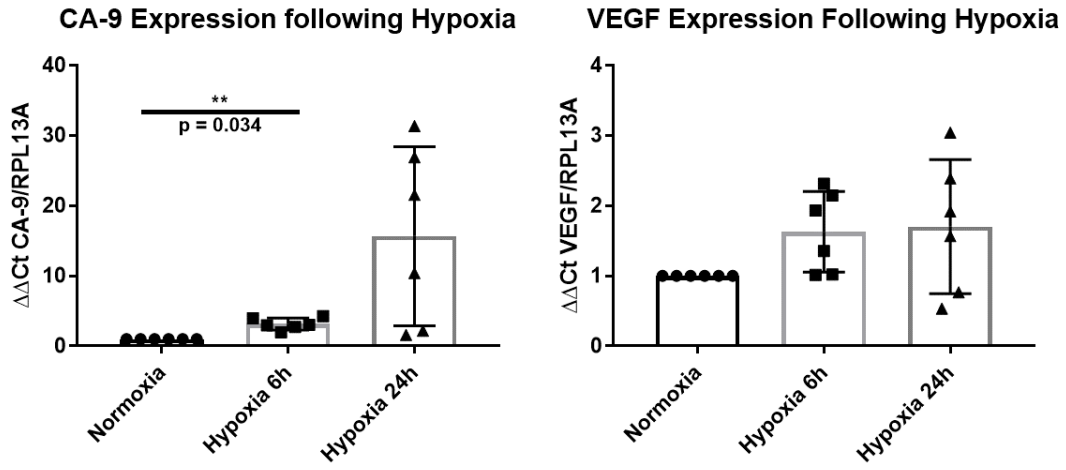

Figure 43. The Effects of Hypoxia on Levels of Hypoxia Control Genes. U-2 OS cells were exposed to 1% O_2 for 6 or 24 hours. Total RNA was extracted, reverse transcription was performed and cDNA was analysed by qPCR focussing on CA9 (A) and VEGF (B) expression using RPL13A as a reference gene. The Δ Δ Ct method of analysis was used, normalising to 24 hour hypoxia samples. Statistical analyses was carried out using one-way anovas using Tukey's test for multiple comparisons.

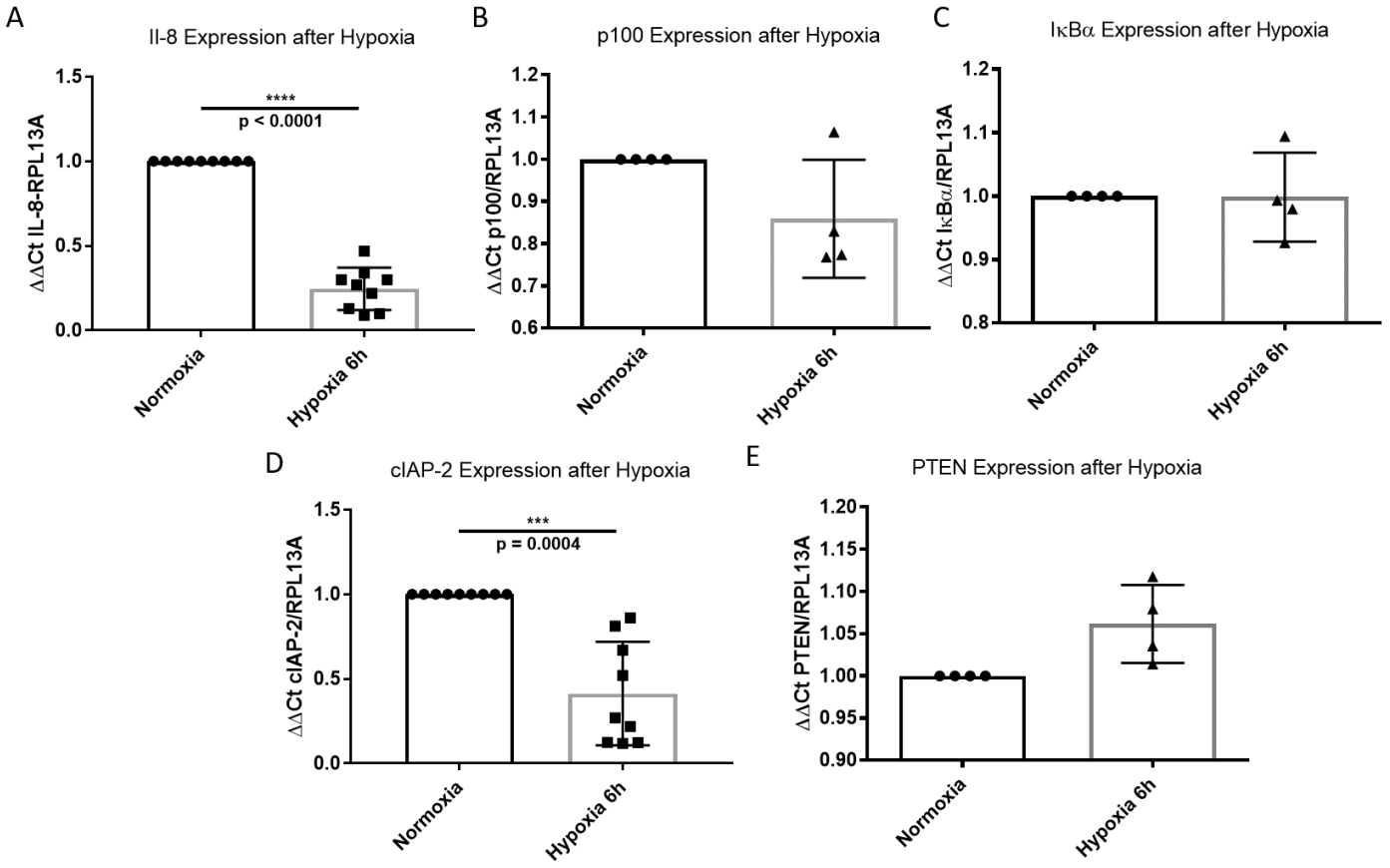

Figure 44. The Effects of Hypoxia on Levels of Genes of Interest. U-2 OS cells were exposed to 1% O_2 for the indicated times. Total RNA was extracted, reverse transcription was performed and cDNA was analysed by qPCR using RPL13A as a reference gene (A = IL-8, B = p100, C = IκBα, D = cIAP-2, E = PTEN). The Δ Δ Ct method of analysis was used, normalising to normoxia/untreated samples. Statistical analyses was carried out using two-tailed paired t-tests.

The first set of target genes to be analysed were genes commonly associated with NF-κB activation across a wide range of stimuli. Following 6 hours of hypoxia, expression of IL-8 and cIAP-2 decreased significantly (Fig. 44A and D) ($p < 0.0001$ and $p = 0.0004$ respectively). No significant change is observed in p100, IκBα or PTEN expression following exposure to hypoxia for 6 hours (Fig. 44B, C and E). Since the preliminary data from these genes did not show any major changes in expression following hypoxia, these genes were not selected for further analysis.

An interesting observation presented in figure 44 is the decrease in IL-8 expression following 6 hours of hypoxia. As discussed in section 1.4, multiple studies have observed a significant increase in IL-8 mRNA levels following exposure to hypoxia [295][296][298][299][118]. However many of the experiments presented in these publications were carried out following different methods from those shown here, as well as from each other regarding the cell lines used and the experimental design itself. Time of exposure varied from as low as 1 hour up to 48 hours, and some researchers opted to use serum-free methods of gas exchange while others did not. It is possible the use of spent rather than fresh media used here, as established earlier, has contributed to the difference in results presented in this thesis (Fig. 36). One could argue that the use of spent media is the most stringent method for inducing hypoxia; removing serum or adding fresh media adds potential additional stresses into the experiment, while using spent media does not. Indeed, this could also account for the contrasting data from the other genes, for example a decrease in cIAP-2 expression was observed here (Fig. 44), while Wang et al. observed a significant increase in cIAP-2 expression. [303].

The data presented in figure 44 indicate that activation of NF-κB could lead to the active repression of expression of target genes. This has been discussed previously in the context of other stimuli [119], and highlights the diverse nature of the NF-κB pathway. Different stimuli lead to slight variations in the activation mechanisms of NF-κB and the subsequent expression or repression of different genes. In the case of hypoxia, IL-8 and cIAP-2 expression is repressed; both of which play important roles in the inflammatory and immune response. The change in IL-8 expression is unexpected due to its role as a promoter of angiogenesis, one would expect an increase in new vasculature growth following hypoxia and therefore an increase in IL-8 expression. The decrease in cIAP-2 expression indicates that an increase in apoptosis may be occurring.

Investigations into the expression of genes associated with oxidative stress were also carried out with the aim of determining the kind of oxidative stress induced by exposure to 1% O_2 (Fig. 45). Expression of ferritin mRNA varied between biological repeats after exposure to hypoxia (Fig. 45A), as such after 6 hours of hypoxia no significant change in the levels of ferritin mRNA is observed. This indicates that production of hydrogen peroxide is not occurring after hypoxia as ferritin prevents the formation of harmful hydroxyl radicals through reacting with hydrogen peroxide [243]. The kinetics of antioxidant gene expression may of course differ from that of the the other NF-κB target genes studied

here, depending on the timings and type of ROS produced. As demonstrated in figure 23, production of ROS could include a plethora of different species that react with one another in a dynamic, ongoing manner. Thus the requirement for increased expression of antioxidant genes may change over time as the kinetics of ROS production alters following exposure to a stimuli.

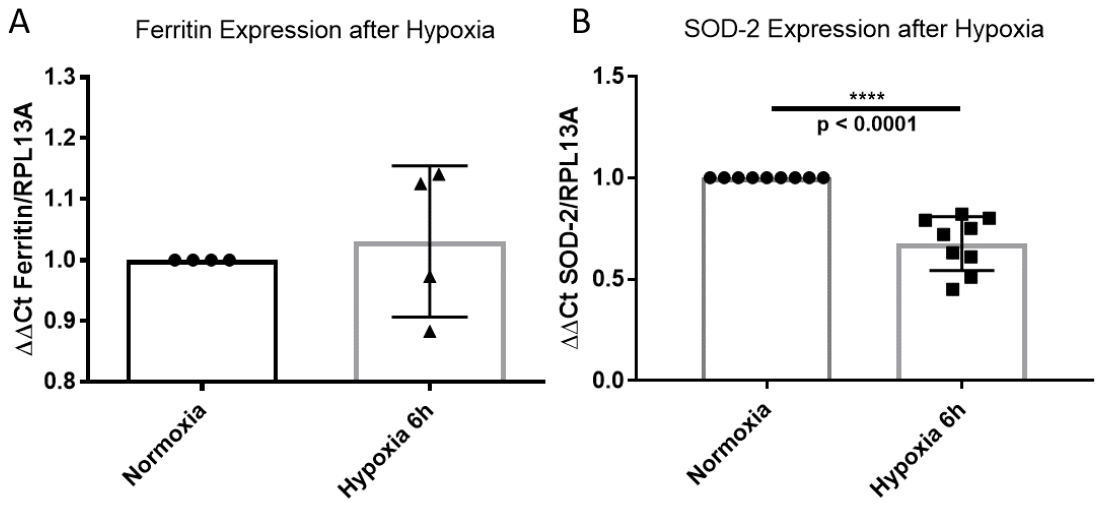

Figure 45. The Effects of Hypoxia on Levels of Genes of Interest Associated with Oxidative Stress. U-2 OS cells were exposed to 1% O_2 for the indicated times. Total RNA was extracted, reverse transcription was performed and cDNA was analysed by qPCR using RPL13A as a reference gene (A = Ferritin, B = SOD-2). The Δ Δ Ct method of analysis was used, normalising to normoxia/untreated samples. Statistical analyses was carried out using two-tailed paired t-tests. Data shows a significant decrease in SOD-2 expression following hypoxia expression ($p < 0.0001$).

In contrast, after 6 hours of hypoxia a significant decrease in SOD-2 expression is observed ($p < 0.0001$) (Fig. 45B). This indicates that following hypoxia exposure there is a reduction in the requirement for SOD-2 in the mitochondria, suggesting that there is a drop in superoxide produced due to a decrease in aerobic respiration. Ferritin was not examined further following this preliminary analysis as no large changes in expression were observed.

Figure 46 shows the effects of reoxygenation on the expression of genes commonly associated with NF-κB signalling activation. Rapid reoxygenation leads to a significant increase in the expression of IL-8 and cIAP-2 after 6 hours of treatment ($p = 0.0315$ and $p = 0.0095$ respectively) (Fig. 46A and D). This is the opposite response to that seen following exposure to hypoxia, highlighting the differences between the two stimuli. This could indeed be a return to basal expression levels following return to a normoxic state. Expression of p100, IκBα and PTEN does not change following reoxygenation.

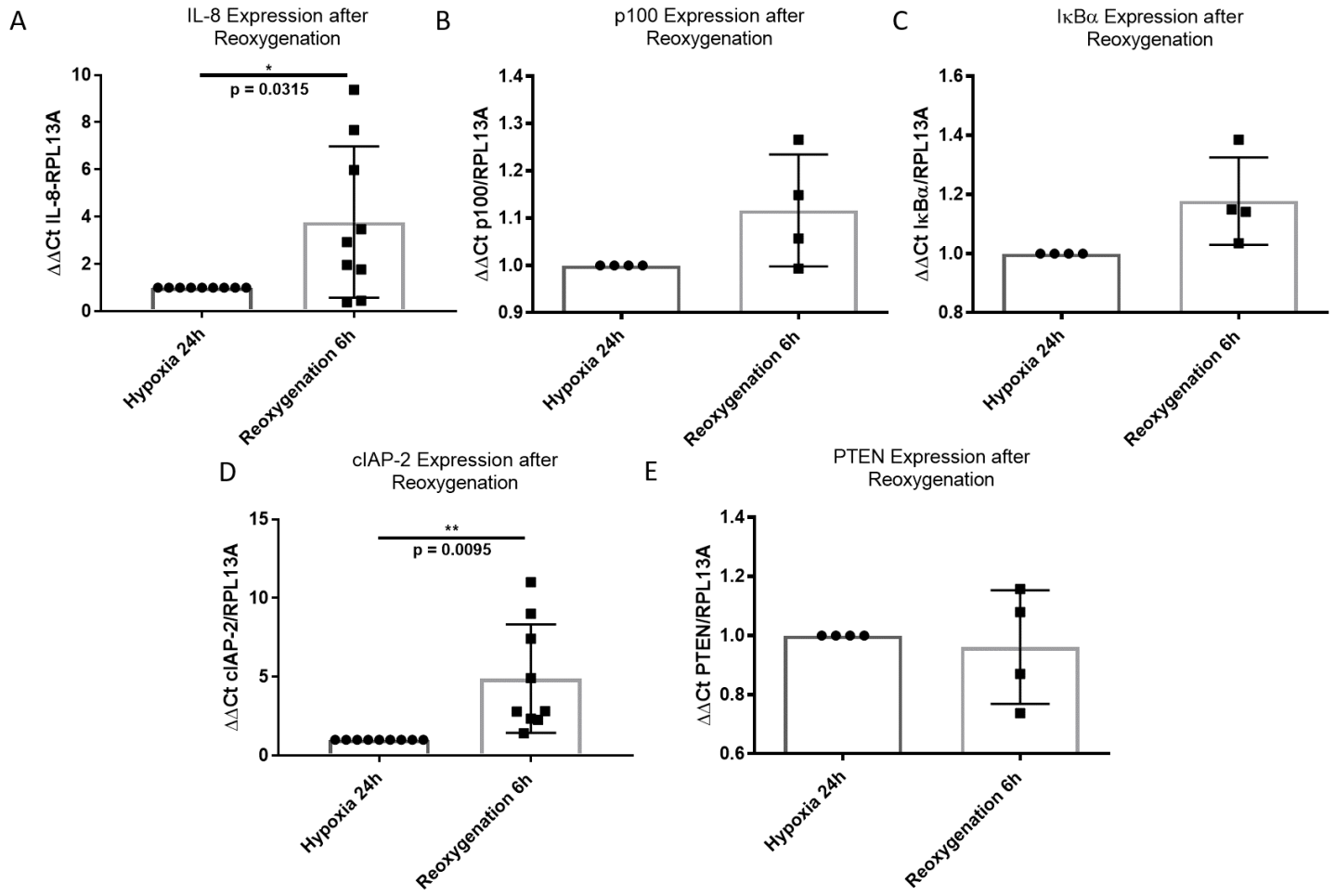

Figure 46. The Effects of Rapid Reoxygenation on Levels of Genes of Interest. U-2 OS cells were exposed to 1% O_2 for 24 hours followed by reoxygenation for the indicated times. Total RNA was extracted, reverse transcription was performed and cDNA was analysed by qPCR using RPL13A as a reference gene (A = IL-8, B = p100, C = IκBα, D = cIAP-2, E = PTEN). The Δ Δ Ct method of analysis was used, normalising to 24 hour hypoxia samples. Statistical analyses was carried out using two-tailed paired t-tests.

Expression of the NF-κB-transcribed oxidative stress-linked genes ferritin and SOD-2 was also investigated following rapid reoxygenation (Fig. 47). Changes in the expression of ferritin varied between biological replicates resulting in inconclusive data (Fig. 47A). SOD-2 expression does however change following rapid reoxygenation. After 6 hours of reoxygenation SOD-2 mRNA levels increase significantly ($p = 0.0428$). This increase in expression of SOD-2 following rapid reoxygenation indicates that there is an increased need for SOD-2 protein in the mitochondria. Since SOD-2 is required to catalyse the breakdown of superoxide after aerobic respiration this suggests that reoxygenation leads to an increase in superoxide production or an increase in respiration [338]. The latter is consistent with data presented earlier that shows an increase in ERK1/2 phosphorylation following reoxygenation (Fig. 42), indicating an increase in proliferation; an energy requiring process.

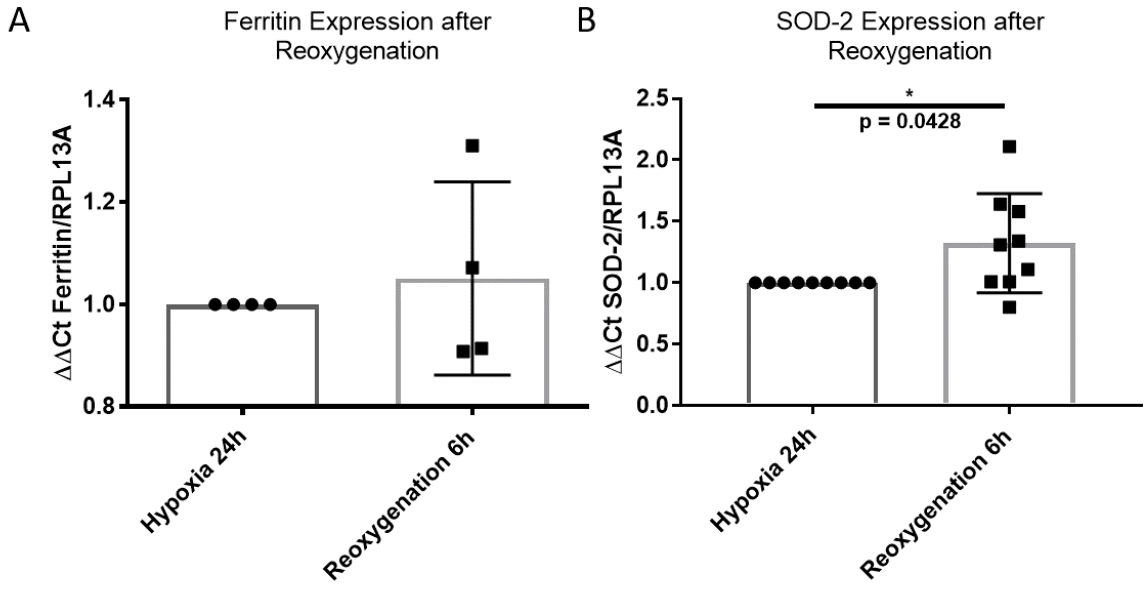

Figure 47. The Effects of Rapid Reoxygenation on Levels of Genes of Interest Associated with Oxidative Stress. U-2 OS cells were exposed to 1% O_2 for 24 hours followed by reoxygenation for the indicated times. Total RNA was extracted, reverse transcription was performed and cDNA was analysed by qPCR focussing on ferritin (A) and SOD-2 (B) expression using RPL13A as a reference gene. The Δ Δ Ct method of analysis was used, normalising to 24 hour hypoxia samples. Statistical analyses was carried out using two-tailed paired t-tests.

Interestingly many target genes selected for observation presented in figures 44, 45, 46 and 47 show very little changes in expression after exposure to 1% O_2 and rapid reoxygenation. This was unexpected and as discussed previously could be due to the use of spent media method of inducing rapid gas changes in cells.

This section has demonstrated that both hypoxia and rapid reoxygenation lead to changes

in the expression of NF-κB target genes. Hypoxia leads to a decrease in the expression of IL-8, cIAP2 and SOD-2, while the opposite is seen following reoxygenation. This suggests that active repression of gene expression occurs following hypoxia and that this is reversed following reoxygenation. Again this highlights the differences and similarities between the two stimuli.

4.8 Hypoxia and Rapid Reoxygenation have effects on Proliferation and Cell Survival

NF-κB activation has previously been linked with changes in proliferation and cell survival [42]. This can occur through regulation of NF-κB target gene transcription as well as through cross-talk with closely linked molecular signalling pathways. Previous work in this chapter has demonstrated that NF-κB is activated in response to hypoxia and rapid reoxygenation, alongside the ERK1/2 MAPK signalling pathway, suggesting that cell proliferation may be affected by exposure to these stimuli. In addition to this the change in expression of cIAP-2 following hypoxia and reoxygenation indicates that changes in oxygen levels may activate or repress apoptosis.

Proliferation was assessed using PrestoBlue assays. This measures viability through the reducing abilities, or mitochondrial activity of cells under the assumption that more cells correlates to greater mitochondrial activity. The blue resazurin is reduced to produce a red dye product by the cells and change can be measured by a spectrophotometer to determine viability. The initial experiment carried out here was to assess the growth of the cells over time. U-2 OS cells were plated out at 2,500 cells per well on a 96-well plate on day 0 and incubated in normoxic conditions. Plates were measured using PrestoBlue assays every 24 hours for 4 days. The results show a steady increase in proliferation over time, with a doubling rate of just over 24 hours (Fig. 48). Data was is presented as a percentage of the total cells on day 4.

Following analysis of the proliferation and growth of U-2 OS cells in normoxia over time, an experiment was performed to determine the effects of hypoxia and rapid reoxygenation on proliferation (Fig. 49). Cells were again plated out at 2,500 cells per well on 96-well plates on day 0 and left in a normoxic incubator for at least 24 hours. Five different time courses were carried out simultaneously, normoxia only, hypoxia for 24 hours, hypoxia for 48 hours, reoxygenation for 24 hours and reoxygenation for 48 hours. For the hypoxia time courses plates were exposed to 1% O_2 on day 2 or day 3, for 48 and 24 hours respectively before analysis. Reoxygenated samples were exposed to hypoxia for 24 hours before their return to 21% O_2. They were exposed to 1% O_2 on day 1 and day 2, followed by reoxygenation on day 2 and day 3 for 48 and 24 hours respectively. All plates were read 4 days after plating out so had the same amount of time to grow although in different conditions. Data is presented as a percentage of total proliferation in control plates.

U-2 OS cells show a decrease in overall proliferation after exposure to hypoxia. The effect

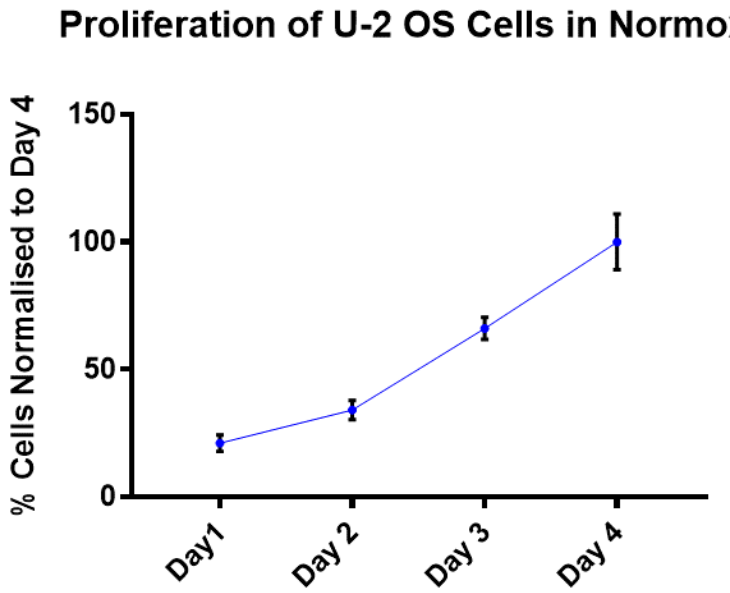

Figure 48. Proliferation of U-2 OS Cells in Normoxia. U-2 OS cells were plated out at 2,500 cells per well in 96-well plates on day zero and incubated in normoxic conditions. Cell proliferation was assessed using PrestoBlue assays every 24 hours for 4 days.

is statistically significant after 24 hours ($p = 0.0239$), and as the level of proliferation drops further after 48 hours of hypoxia the significance increases ($p = 0.0018$) (Fig. 50A). 24 hour hypoxia samples were moved into the hypoxia chamber after 3 days of normoxic growth and the percentage of proliferating cells is comparable to those observed on day 3 of growth assay (Fig. 48). This could suggest that rather than slowing proliferation, exposure to hypoxia stops proliferation, however without carrying out further experiments it is impossible to say for certain whether proliferation stops completely once cells enter hypoxia.

Cells were exposed to hypoxia for 24 hours prior to reoxygenation, therefore the results for the proliferation after rapid reoxygenation were compared directly to the results for proliferation after 24 hours of hypoxia (Fig. 50B). 24 hours post-reoxygenation an increase in proliferation is observed compared with those only exposed to hypoxia ($p = 0.0305$). Interestingly after 48 hours of reoxygenation levels of proliferation decrease again compared with those that were reoxygenated for 24 hours ($p = 0.0056$). This data suggests that the shorter term effects of rapid reoxygenation differ from the longer term effects. An immediate increase in proliferation could suggest a reversal of cell cycle arrest, however the decrease in proliferation that follows could be a result of further chronic damage to cells, perhaps due to DNA damage and induction of apoptosis.

The data presented here again highlights the profound differences between hypoxia and

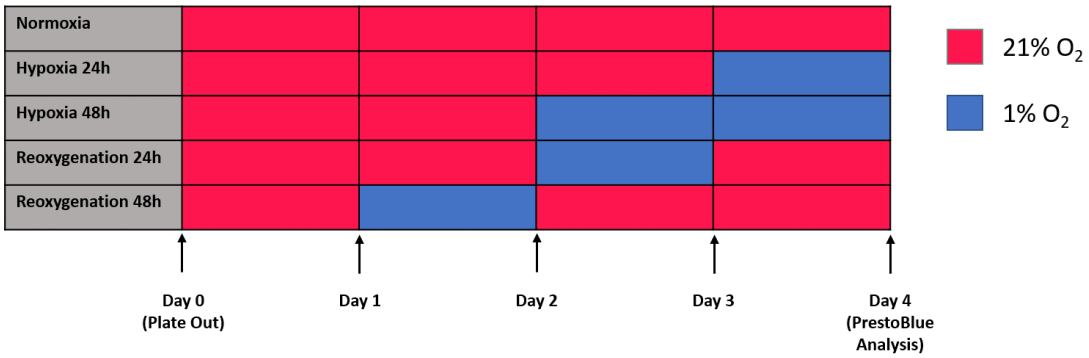

Figure 49. Schematic of Hypoxia and Rapid Reoxygenation Time Course for Proliferation Assays. U-2 OS cells were plated out at 2,500 cells per well in 96-well plates on day zero and incubated in normoxic conditions for at least 24 hours. Plates were then moved to and from the anaerobic chamber as the schematic demonstrates over the course of 4 days. For example the 24 hour reoxygenation plates were moved into 1% O_2 on day 2, 48 hours after plating out, and returned to 21% O_2 after 24 hours for a further 24 hours before reading proliferation by PrestoBlue.

rapid reoxygenation, and indicates that although rapid reoxygenation has an immediate positive effect on cell proliferation and health, the longer term implications may be different. To determine the chronic effects of reoxygenation on U-2 OS cells colony formation assays were performed over the course of 2 weeks. Here, cells were exposed to hypoxia for 24 hours, followed by rapid reoxygenation for 3 hours. Cells were then seeded sparsely onto 10cm plates. After 2 weeks surviving colonies were fixed, stained and imaged. Images were then blinded and colonies counted both computationally and manually and compared to control plates that contained normoxia only exposed colonies. Data presented is the percentage of manually counted colonies formed compared with total cells seeded. Results were plotted using GraphPad Prism and significance was calculated through two-tailed paired t-tests.

The results of the clonogenic assay show that reoxygenation has a significant effect on the ability of U-2 OS cells to form colonies ($p = 0.0055$) (Fig. 51). This result demonstrates that reoxygenation following 24 hours of hypoxia has long-term effects on the health and survival of U-2 OS cells. This indicates that although cells respond positively to reoxygenation in the short-term, long-term damage could be occurring within cells. The decrease in colonies formed following reoxygenation shows loss of cell survival and suggests that apoptosis or even necrosis could be occurring, possibly as a result of DNA damage. This will be explored in section 7.1.

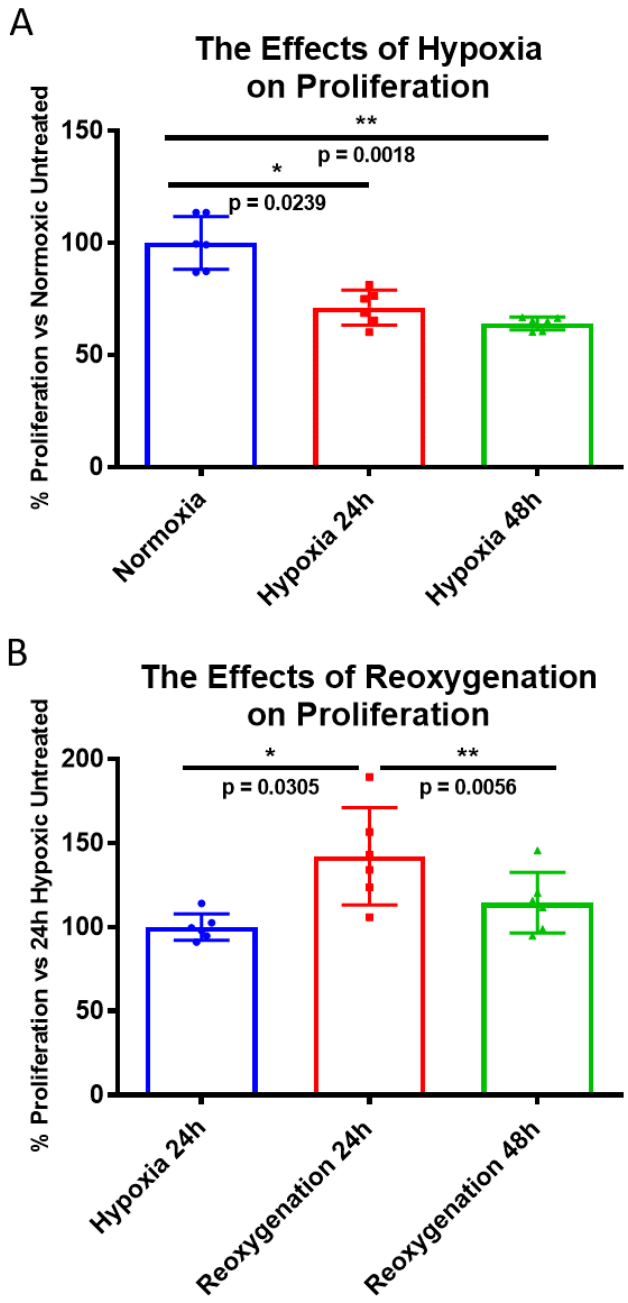

Figure 50. The Effects of Hypoxia and Rapid Reoxygenation on Proliferation of U-2 OS Cells. U-2 OS cells were treated as described in figure 49. Proliferation was analysed using PrestoBlue after 1 hour. Mean values of 3 independent experiments were plotted using GraphPad prism to determine the effect of hypoxia (A) and reoxygenation (B) on proliferation. P values were calculated using one-way ANOVA and correcting for multiple comparisons using Tukey's test.

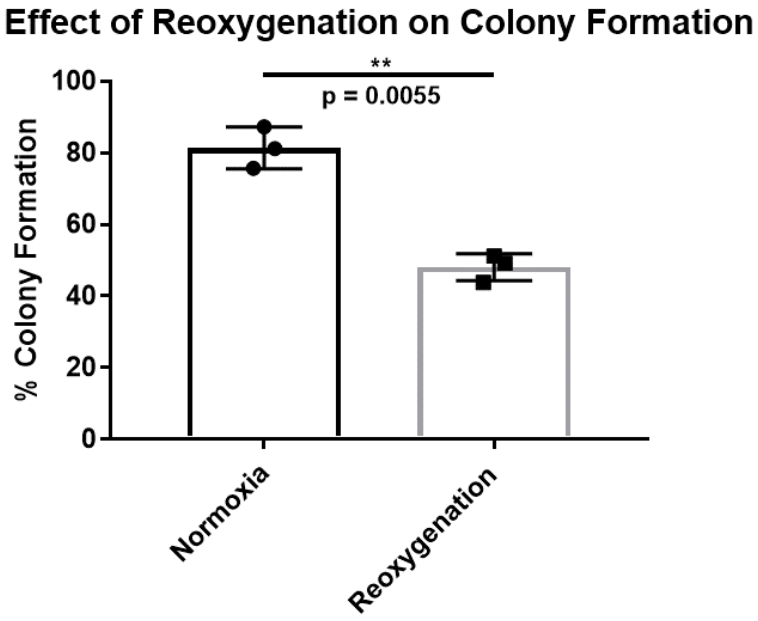

Figure 51. Reoxygenation Following 24 Hours of Hypoxia Affects Colony Formation and Cell Survival. U-2 OS cells were exposed to 1% O_2 for 24 hours prior to rapid reoxygenation. Following 3 hours of rapid reoxygenation, cells were trypsinised, counted and re-plated in a range of concentrations in twelve 10cm plates. Normoxia only control plates were plated out in parallel. Plates were left in 21% O_2 for 2 weeks to allow for colony formation. Colonies were fixed and stained using crystal violet before being blinded and counting both computationally and manually (manually counted data presented). Data presented is the percentage of colonies formed compared with total cells seeded. Means of three independent experiments were plotted using GraphPad Prism and significance was calculated through two-tailed paired t-tests.

4.9 Summary and Brief Discussion of Chapter 4

The data presented in this section have demonstrated that exposure to both hypoxia and rapid reoxygenation leads to the activation of the canonical NF-κB pathway. The data has also highlighted some key differences between the cellular responses to hypoxia and reoxygenation, particularly with regard to changes in gene expression and proliferation.

The initial experiments described in this chapter revealed that the use of fresh media (specifically fresh serum) to carry out the current protocol for the induction of hypoxia and rapid reoxygenation leads to activation of the canonical NF-κB pathway independently of these stimuli. Further investigations showed that the presence of fresh serum affects the formation of ROS as well as the transcription of NF-κB target genes. This in itself is an interesting discovery, and highlights that the effects of media changes should be considered when studying NF-κB even in the contexts of other stimuli. Spent media was therefore used to carry out subsequent hypoxia and reoxygenation protocols, as data is presented showing that this does not affect the activation of NF-κB independently of hypoxia or reoxygenation stimuli. Thus the data presented using this revised protocol is unique; all previously published studies regarding hypoxia and reoxygenation-induced activation of NF-κB have employed fresh media when altering O_2 levels [105][125][320][118].

This modified protocol has allowed us to demonstrate with certainty that hypoxia and rapid reoxygenation trigger activation of the canonical NF-κB pathway. This activation appears to be similar to that of hydrogen peroxide treatment, where upstream signals are transduced through IKKβ to activate RelA. Previous studies have demonstrated that in the response to hydrogen peroxide treatment, IκBα is phosphorylated on tyrosine 42 and does not undergo degradation as it does in response to other stimuli such as TNF [164]. Activation of NF-κB in response to hypoxia and reoxygenation is similar to this, however following hypoxia both IKKα and IKKβ are phosphorylated (Fig. 39), as opposed to just IKKβ or IKKα following hydrogen peroxide or reoxygenation treatment respectively (Fig. 27 and 39). Aside from this difference the downstream kinetics of canonical NF-κB signalling appear similar between hypoxia and reoxygenation, as observed in previous hydrogen peroxide studies, although IκBα is phosphorylated it is not degraded [164].

As discussed in section 4.3, the serine 32/36 phosphorylation of IκBα observed here is commonly associated with K48-linked ubiquitination and degradation of IκBα by the proteosome [78][126][127][128]. There have been reports that sumoylation of this residue prevents its ubiquitination, leading to the stabilisation of the protein [129][130]. Indeed this could be an explanation for the lack of IκBα degradation observed in this project. Activation of RelA is still possible in the absence of IκBα degradation as reported previously [164][129][130]. Culver et al. described this mechanism in the context of hypoxia, hypothesising that sumoylation alone on this critical lysine residue is sufficient to allow dissociation of IκBα from RelA. As long as RelA is no longer bound by IκBα it is able to translocate into the nucleus to control gene expression. Post-translational modifications

on RelA would then allow further control of transcription through regulation of RelA's binding to the promoters of target genes [42]. As discussed in section 4.4, Culver et al. used a different protocol for inducing gas exchange, as such the findings presented here (Fig. 36) contradict their reported findings [118]. Future experiments should therefore investigate whether this sumoylation is occurring following hypoxia and rapid reoxygenation to further uncover the process behind the activation of NF-κB observed here.

As discussed earlier, some of the genes selected for real-time qPCR analysis have been studied following exposure to hypoxia and reoxygenation previously, however there was some conflicting reports regarding these changes. This could be due to the cell lines, oxygen levels and time points used, there was therefore still value in analysing these genes. Changes in gene expression have not previously been examined using this modified protocol, here we observed a significant decrease in IL-8, cIAP-2 and SOD-2 following hypoxia, which is reversed upon reoxygenation. Again this further contradicts earlier reports, for example IL-8 expression is thought to increase following hypoxia [118][295][296][297][298][299], while SOD-2 expression is reported to decrease on reoxygenation [308]. This highlights the effects that scientific method can have on the outcome of an experiment, and reinforces the need for clear reporting on protocols used.

The results of real-time qPCR have indicated that active repression of several key genes could potentially be occurring following exposure to hypoxia, as observed by the decrease in expression of several genes of interest. This repression is reversed after reoxygenation of cells. Previous reports on the mechanism of NF-κB-regulated active repression have predominantly focussed on the response to DNA damage-induced NF-κB activation [119]. Here the active repression of anti-apoptotic genes such as Bcl-XL occurs in a RelA-dependent manner to promote apoptosis in the response to stress [119]. This could implicate genotoxic stress as a factor in hypoxia.

To investigate whether this decrease in gene expression under hypoxic conditions is due to NF-κB-dependent active repression, rescue experiments should be carried out. For example if active repression is occurring here, cells treated with siRNA to induce knockdown of RelA would show no change in gene expression following hypoxia, while those treated with off target, scrambled siRNA would still show the decrease [119]. The changes in expression of target genes presented here confirms the activation of the NF-κB pathway in response to stress but also implicates apoptosis in the response to these stresses due to the changes in cIAP-2 expression. In addition to this, changes in SOD-2 expression implicates superoxide as one of the ROS involved in this response. Alternatively, due to its role in the electron transport chain, a decrease in ROS indicates that a decrease in aerobic respiration, metabolism and proliferation is occurring in the cell following hypoxia, which is reversed following reoxygenation.

Although previous studies have aimed to characterise the species of ROS produced following hypoxia and reoxygenation, these reports have had conflicting findings. As discussed in section 1.4 the method used for detection [290] as well as the samples tested [289] can

affect the results of the experiment. This highlights the difficulty in defining the species of ROS produced within a cell or tissue. In this project characterisation of the ROS produced following hypoxia and reoxygenation has proven challenging due to the effects of hypoxia on the probes in the absence of cells (Fig. 30). Details of the exact probes used and the mechanism by which the redox sensitive dyes work is not available, as such one cannot be certain that the kit is accurately detecting oxidative stress or superoxide as it claims to. Future work should focus on more robust methods for determining oxidative stress such as detection of PRDX-3 oxidation.

A final aim was to explore the downstream effects of hypoxia and rapid reoxygenation in mammalian cells, as this would give insight into other pathways and proteins implicated in the cellular responses to these stimuli. These investigations were important in the creation of hypotheses to test in the coming chapters. Previous publications have described that in the majority of cell lines hypoxia leads to a reduction in proliferation as an oxygen starved cell struggles to carry out respiration and thus reduces its metabolic activity [272]. However it is also noted that many cancer cells proliferate at the same or an increased rate following exposure to hypoxia [272] due to mutations in key regulators of replication stress, the cell cycle and DNA damage response. This is particularly true of cell lines derived from osteosarcoma cancers [275][276]. Investigations in to the effects of reoxygenation have demonstrated that reoxygenation leads to an increase in proliferation, metastasis and invasion [273][274]. The effects of hypoxia and reoxygenation on U-2 OS cells had not previously been investigated.

Proliferation and cell survival was analysed using both PrestoBlue and colony formation assays, demonstrating that hypoxia leads to a decrease in proliferation but that reoxygenation causes proliferation to increase over 24 hours, but decrease again after 48 hours. Indeed, the results of the colony formation assays show that following reoxygenation there is a 50% decrease in survival compared with normoxic only cells. This highlights the potential differences between short and long term effects of rapid reoxygenation, indicating that apoptosis or necrosis is occurring, perhaps due to irreparable DNA damage. This will be explored in a later chapter.

Chapter 5: The Role of the IKK Complex and TAK1 in NF-κB Activation after Hypoxia and Rapid Reoxygenation

Data presented in chapter 4 demonstrated that the canonical NF-κB pathway is activated in response to hypoxia and rapid reoxygenation. It is clear that IκBα is involved in this activation, as highlighted by the significant increase in its phosphorylation following both hypoxia and rapid reoxygenation (Fig. 39). Although phosphorylated in response to these stresses, the role of the IKK complex in this activation however remains elusive.

The main member of the IKK complex that is associated with the activation of the canonical NF-κB pathway is IKKβ. IKKβ knockout mice have a similar phenotype to RelA knockout mice, highlighting the importance of this subunit in the activation of the canonical NF-κB pathway [339]. In addition, studies of IKKβ deficient embryonic fibroblasts have shown a marked reduction in canonical NF-κB activation following TNFα or interleukin 1-α treatment [340][341][342]. A previous study has concluded that IKKβ is required for the activation of the canonical NF-κB pathway following exposure to hypoxia, hypothesising that this occurs through loss of hydroxylation of IKKβ and subsequent phosphorylation and activation [343].

Aside from the scaffolding subunit, NEMO/IKKγ, the other main component of the canonical IKK complex is IKKα. IKKα homodimers are associated with the non-canonical NF-κB activation pathway more than the canonical pathway [339]. Some studies have shown that IKKα is dispensable in response to cytokine treatment, with canonical NF-κB activation occurring independently of the presence of this subunit [344] however other more recent studies have disputed this [345][346][347]. The role of IKKα in the activation of the canonical NF-κB pathway is therefore debated, with different stimuli, cell lines and groups presenting alternate conclusions regarding whether IKKα is involved in canonical NF-κB activation and to what extent. Interestingly, a previous study has implicated both IKKα and IKKβ as being critical in the response to hypoxia, as measured by stabilisation of HIF1α. Here they show that silencing of one subunit has little effect on HIF1α stabilisation, while loss of both completely blocks it [147]. As the HIF1α gene is transcribed by NF-κB this highlights a possible role for both subunits in the response to hypoxia.

The data presented in results chapter 1 has implicated IKKα in the response to hypoxia and rapid reoxygenation; phosphorylation of IKKα is observable by western blotting following exposure to these stresses. However, due to variation between experimental replicates only the increase in phosphorylation of IKKα/β following hypoxia, and not reoxygenation, was significant (Fig. 39). In addition data from primary cells was not significant with regard to IKKα/β phosphorylation (Fig. 41).

This section aimed to determine the role of IKKα and IKKβ in the transduction of

upstream signals to IκBα and RelA. In this chapter targeted inhibition of these kinases was carried out using small molecule inhibitors to determine the importance of each subunit in the transduction of the signal downstream. Upstream kinases of each of these proteins were also investigated in the same manner; TAK1 and NIK act upstream of IKKβ and IKKα respectively. The effects of these proteins on canonical NF-κB activation was determined by western blot analysis.

Another aim of this section was to investigate the cellular location of proteins of interest following hypoxia and rapid reoxygenation. Work presented in this section therefore explored whether different proteins such as the members of the IKK complex and RelA move into the nucleus following hypoxia and rapid reoxygenation. This would give insight into the roles of these proteins in response to these stimuli; for example localisation of a protein into the nucleus could suggest a role in transcription. This was carried out using immunofluorescence microscopy, and cytoplasmic and nuclear fraction analysis by western blot.

Finally, investigations into the downstream effects of canonical pathway activation were performed, focussing on gene expression, proliferation and survival. Real-time qPCR was employed for the gene expression analysis, and proliferation and cell survival were assayed using Presto Blue and colony forming assays, respectively, as in Chapter 4.8.

5.1 IKKα has a Potential Role in the Activation of the Canonical NF-κB Pathway After Rapid Reoxygenation

Data presented in chapter 4 demonstrated that key proteins in the canonical NF-κB pathway are activated following hypoxia and rapid reoxygenation. The experiments in this section aimed to determine whether the IKKα subunit is critical in the activation of the canonical NF-κB pathway in response to reoxygenation. These experiments utilised a small inhibitor of IKKα to competitively inhibit its activity during reoxygenation. The small molecule inhibitor was kindly provided by Prof. Simon Mackay of Strathclyde University. A recent publication demonstrated that these inhibitors are specific to IKKα by showing that canonical NF-κB pathway activation by TNF is not affected by this inhibition [348], while non-canonical signalling is. The specificity and half life of this inhibitor is unpublished, however the doses and timings used in this project followed advice given by the Mackay laboratory.

U-2 OS cells were exposed to hypoxia and rapid reoxygenation for the times indicated (Fig. 52), alongside control plates of normoxia only and hypoxia only treated cells. Plates targeted for IKKα inhibiton were exposed to 3μM of IKKα inhibitor for 30 minutes prior to reoxygenation, and spent media used for rapid reoxygenation was pre-treated with the inhibitor before use. Cells were harvested for whole cell extracts using urea lysis buffer and analysed by western blot as before probing for phosphorylation events associated with canonical NF-κB activation.

The phosphorylation of IKKβ does not change following rapid reoxygenation compared with normoxia and hypoxia only treatments as shown in this western blot (Fig. 52A and B). The only band visible on these western blots is the higher band of the larger IKKβ subunit, therefore the consequences of this inhibitor treatment on the phosphorylation of IKKα are unknown.

The effects of the IKKα inhibitor can be observed further down this signalling transduction pathway; activation of both IκBα and RelA following reoxygenation is significantly reduced in cells pretreated with the IKKα inhibitor (Fig. 52A, C and D). The results here indicate that IKKα plays an essential role in the activation of IκBα in the response to rapid reoxygenation.

To assess whether the effects of IKKα inhibition during rapid reoxygenation differ from IKKα inhibition following other stimuli, experiments were carried out using etoposide and TNF time courses (Fig. 53). U-2 OS cells were treated with 25μM of etoposide (Fig. 53A) or 10ng/ml of TNF (Fig. 53B) for the times indicated. Again, prior to this stimulation, cells undergoing IKKα inhibition were pretreated with 3μM of IKKα inhibitor. Cells were harvested for whole protein extracts and canonical NF-κB pathway activation was analysed as before. As this was not the main focus of this project, this experiment was not repeated sufficient times to allow for statistical analysis. Thus, this needs to be taken into consideration when discussing the results.

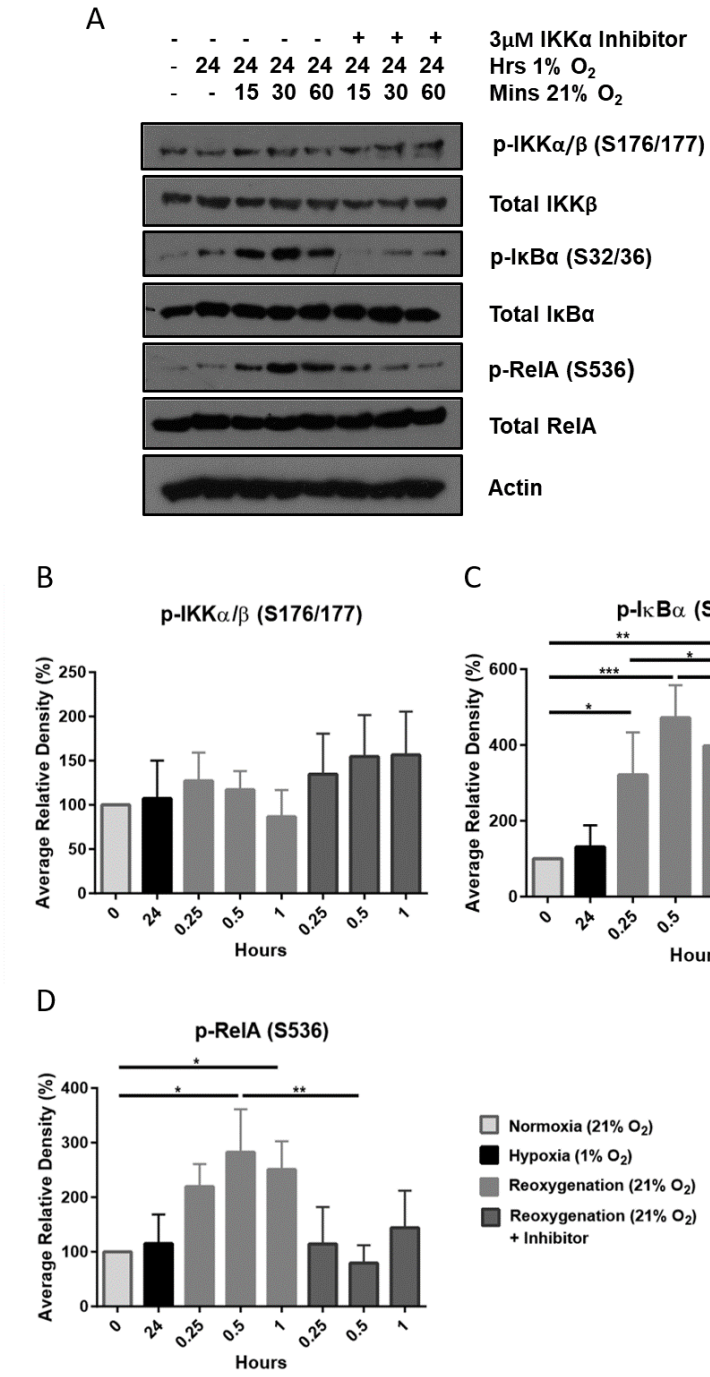

Figure 52. IKKα Inhibition blocks Canonical NF-κB Activation following Rapid Reoxygenation in U-2 OS Cells. U-2 OS cells were exposed to 1% O_2 for 24 hours prior to rapid reoxygenation for the times indicated, with or without treatment with a small molecule inhibitor of IKKα inhibitor (Strathclyde University). Whole cell extracts were harvested using urea lysis buffer with added protease inhibitors and western blots were performed probing for proteins and phosphorylation events associated with canonical NF-κB activation (A). Relative density of bands taken from 3 independent experiments was calculated and analysed using one-way ANOVA (Sidak's test) (B-D).

The pattern of activation presented in figure 53 differs from those seen after exposure to reoxygenation (Fig. 52). This highlights the fact that although the canonical NF-κB pathway is activated in response to both stimuli, the mechanism behind this can vary in response to different stresses.

As expected both etoposide and TNF treatments lead to the activation of the canonical NF-κB pathway as measured by phosphorylation of key proteins of interest (Fig. 53A and B). In addition to these markers of activation, degradation of Total IκBα is observed following TNF treatment. The timings of these responses appear to vary between the treatments, with phosphorylation events, as well as the subsequent dephosphorylation events, occurring earlier following TNF treatment.

Surprisingly, inhibition of IKKα appears to attenuate signalling through the canonical NF-κB pathway following treatment with etoposide or TNF (Fig. 53A and B). The effects are slight in the etoposide treated samples, however a decrease in IκBα phosphorylation is clearly observable. Inhibition of IKKα prior to TNF treatment does not block activation fully, rather it seems to delay the activation of the canonical NF-κB signalling pathway. Phosphorylation of IκBα and RelA still occurs in the presence of the inhibitor, but at a later time point than when the inhibitor is absent. These experiments should be repeated to validate the findings from this preliminary data.

Phosphorylation of both IKKα and IKKβ occurs following treatment with etoposide or TNF (Fig. 53), and an increase in signal from both the phospho-IKKα/β blot and the total IKKβ blot is observed following treatment with the inhibitor. Further analysis of the kinetics of this activation is required to determine whether an increase in IKKα/β phosphorylation occurs or the increase in signal is purely due to an increase in total IKK levels. The exact reason for this observation can only be hypothesised at this stage, it appears as though treatment with this inhibitor causes increase in total/phosphorylated protein through a feedback mechanism, perhaps with the aim of overcoming the effects of the inhibitor.

The western blots presented in this section indicate that IKKα could have a surprising role in the canonical NF-κB pathway response to both DNA damage (etoposide) and cytokine treatment (TNF). The results of the TNF experiment are particularly surprising, as this is a direct replicate of the experiment carried out by the Mackay laboratory which found that the IKKalpha inhibitor did not block TNF triggered NFkB activation based in IκBα phosphorylation [348]. The contrasting results between the work presented here and that shown in Anthony et al. indicates that the particular batch of inhibitors used in this project were not as effective as those presented in the paper. This brings into question the specificity of the inhibitor used here and highlights the importance of carrying out parallel experiments using alternative methods of protein inhibition such as siRNA treatment. Thus, further experiments should be carried out to investigate the role of IKKα in the response to reoxgenation.

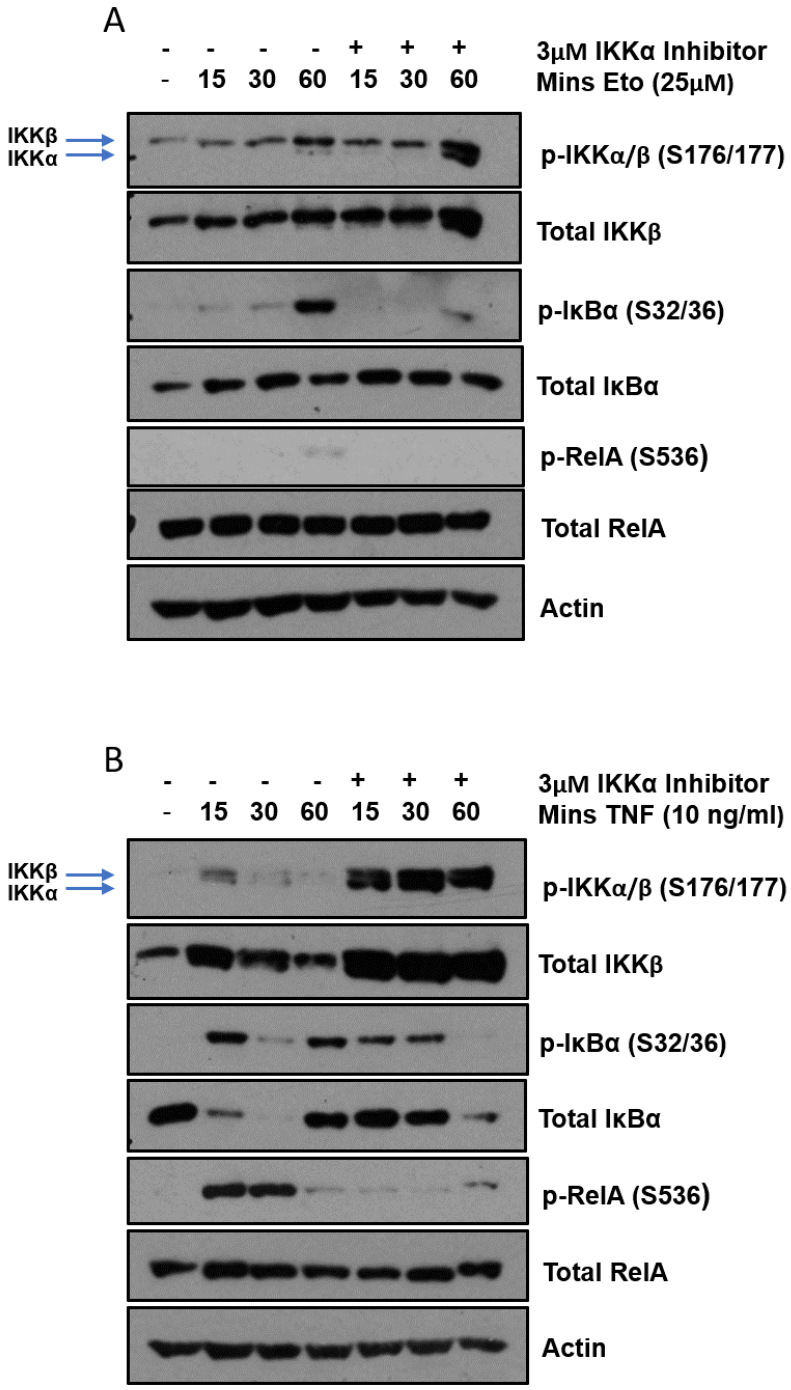

Figure 53. IKKα Inhibition Blocks Canonical NF-κB Activation following Etoposide and TNF Treatments in U-2 OS Cells. U-2 OS cells were treated with 25μM of etoposide (A) or 10ng/ml of TNF (B) for the times indicated, with or without treatment with an IKKα inhibitor (Strathclyde University). Whole cell extracts were harvested using urea lysis buffer supplemented with protease inhibitors and western blots were performed probing for phosphorylation events associated with canonical NF-κB activation.

5.2 A Role for TAK1 in the Activation of NF-κB after Hypoxia and Rapid Reoxygenation

The data presented so far has demonstrated that rapid reoxygenation leads to canonical NF-κB activation, however key upstream kinases involved in this activation have yet to be identified. To investigate this further, the effects of inhibition of the NIK and TAK1 kinases that regulate IKKα and IKKβ respectively, was examined through the use of small molecule inhibitors (Fig. 12).

To determine the role of NIK in the cellular response to rapid reoxygenation, a small molecular inhibitor of NIK was used (NIK SMI1) [349][350]. The data sheet states that aside from NIK1, this inhibitor has off-target effects on 3 out of 222 other kinases tested, and only at doses much higher than those used here. It has a predicted half life of 3.5 days [351]. The experiment was carried out as before (Fig. 52), however cells were treated with 150nM of the NIK inhibitor rather than the IKKα inhibitor.

In the western blot presented here, there is no significant difference in the phosphorylation of the markers of canonical NF-κB pathway activation following reoxygenation, when comparing samples treated with or without the NIK inhibitor (Fig. 54). The results from this experiment therefore indicate that NIK is not involved upstream of the canonical NF-κB signalling pathway in the response to rapid reoxygenation.

Next, the role of the TAK1 kinase was investigated. One consideration to be made when studying the role of TAK1 is that in addition to phosphorylating and activating IKKβ as part of the canonical NF-κB pathway, TAK1 is also an upstream kinase for the JNK pathway [113][115][352][353]. However earlier experiments presented in this thesis have shown that activation of the JNK pathway is not significant following hypoxia and rapid reoxygenation (Fig. 42).

Cells were pretreated with 10μM of 5z-7-oxozeanol for 30 minutes prior to rapid reoxygenation (dosage selected based on personal communication). This inhibitor is an ATP-competitive irreversible inhibitor, which has been used extensively in previous studies [354][355]. Since the cysteine in its ATP target site is also present in ERK2, MKK7 and MEK1 it also targets these proteins [356], however since the major point of crosstalk between these two pathways is through TAK1 itself, this shouldn't affect signalling through the canonical NF-κB pathway more than an inhibitor that specifically targets TAK1 would [332]. The Dundee Kinase Screen does not highlight any other potential off-targets of this inhibitor [357]. The predicted half life of this compound is 2.77 days, far longer than the time points used in this experiment [351]. Analysis of markers of canonical NF-κB activation was carried out as before.

As with previous experiments, the effects of reoxygenation on IKKα/β phosphorylation is not significant regardless of inhibition of upstream kinases. In contrast, phosphorylation of IκBα is significantly reduced following treatment with the TAK1 inhibitor during

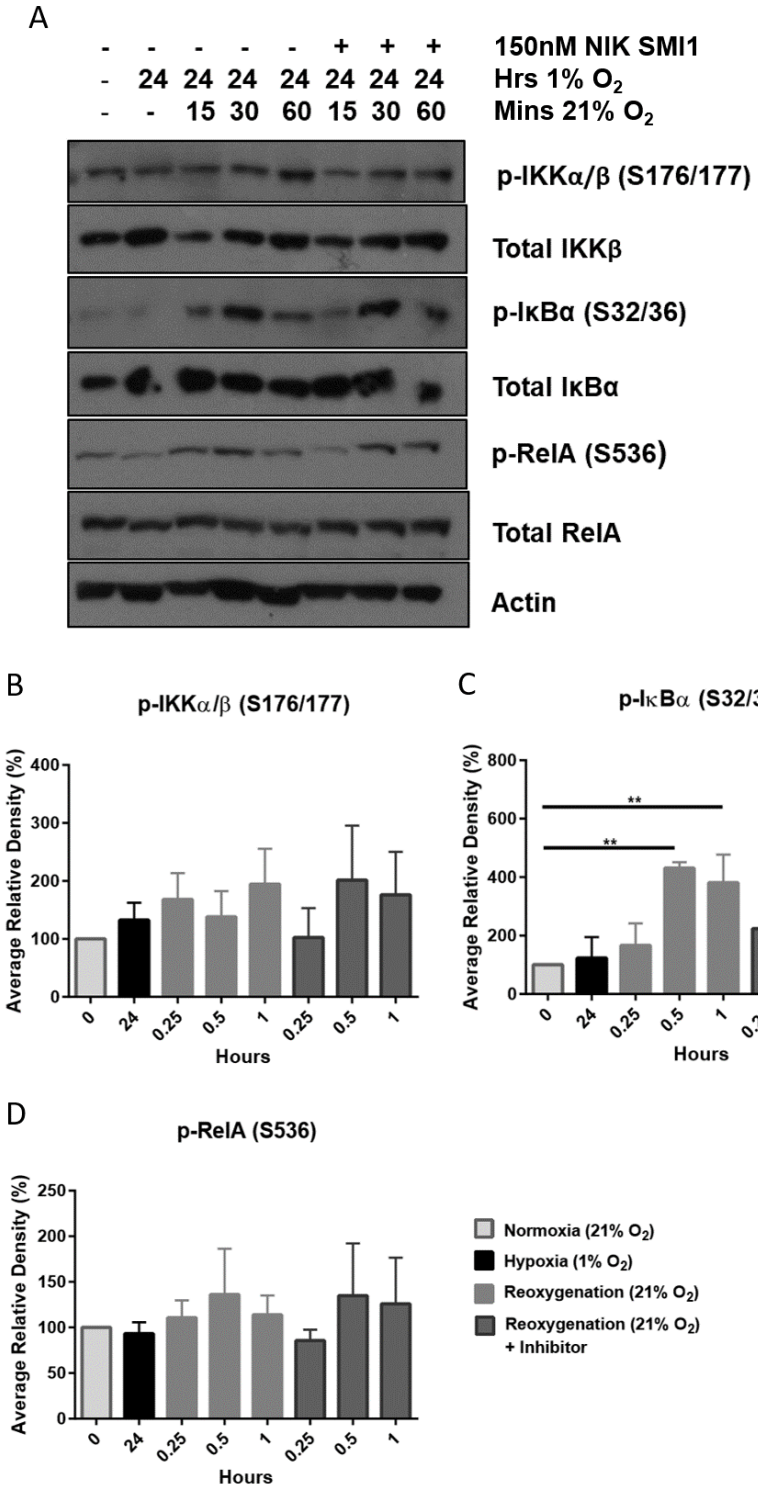

Figure 54. NIK Inhibition has no effect on Canonical NF-κB Activation following Rapid Reoxygenation in U-2 OS Cells. U-2 OS cells were exposed to 1% O_2 for 24 hours prior to rapid reoxygenation for the times indicated, with or without treatment with 150nM NIK SMI1. Whole cell extracts were harvested using urea lysis buffer with added protease inhibitors and western blots were performed probing for proteins and phosphorylation events associated with canonical NF-κB activation (A). Quantification of relative density was carried out across 3 independent experiments and analysed by one-way ANOVA (Sidak's test) (B-D).

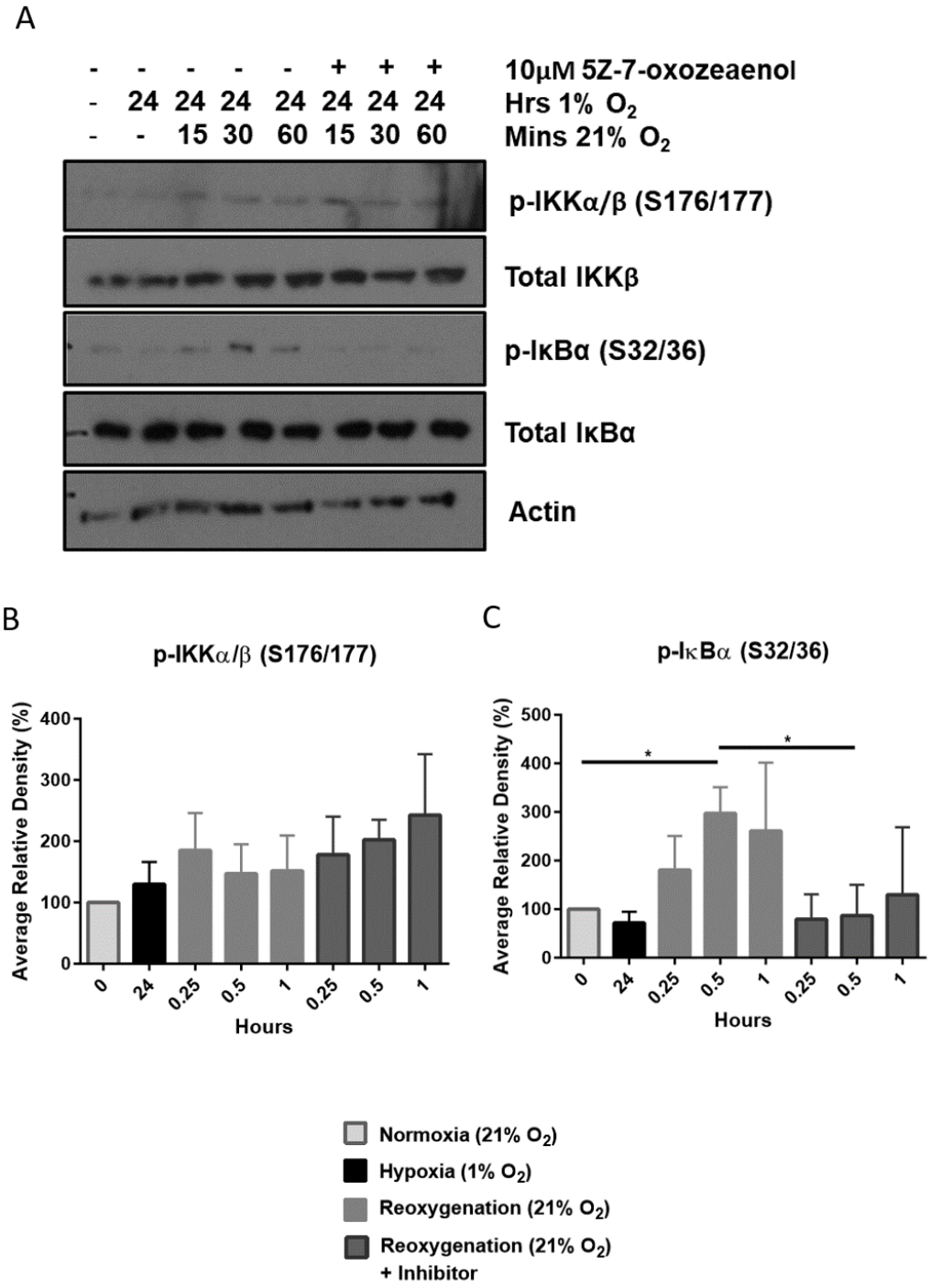

Figure 55. TAK1 Inhibition Blocks Canonical NF-κB Activation following Rapid Reoxygenation in U-2 OS Cells. U-2 OS cells were exposed to 1% O_2 for 24 hours prior to rapid reoxygenation for the times indicated, with or without treatment with 10μM of the small molecule inhibitor of TAK1; 5z-7-oxozeaenol. Whole cell extracts were harvested using urea lysis buffer with added protease inhibitors and western blots were performed probing for proteins and phosphorylation events associated with canonical NF-κB activation (A). Relative density was carried out across 3 independent experiments and statistics were carried out by one-way ANOVA (Sidak's test) (B and C).

reoxygenation. This indicates that TAK1 is involved in the transduction of signalling through the canonical NF-κB pathway.

5.3 Hypoxia and Rapid Reoxygenation Leads to Changes in Sub-Cellular Localisation of Key Proteins Involved in Canonical NF-κB Activation

As discussed in the introduction, following activation RelA and other NF-κB subunits translocate into the nucleus to control the expression of target genes. Data presented in previous sections of this thesis have demonstrated that the canonical NF-κB pathway is activated following both hypoxia and reoxygenation, with a reduction in activation following 24 hours of hypoxia. One would therefore expect to observe movement of RelA into the nucleus following shorter hypoxia time points, movement out of the nucleus following 24 hours of hypoxia, then movement into the nucleus again following reoxygenation.

It has also been reported that members of the IKK complex are able to move in and out of the nucleus in a complex with other proteins of interest. For example, following DNA damage ATM is thought to phosphorylate NEMO or IKKγ in the nucleus, NEMO has also been shown to couple with ATM to drive nuclear export of ATM [358]. In addition to this, IKKα has been demonstrated as having a nuclear role through phosphorylation of histone H3 in response to cytokine treatment [359]. Investigations into the location and phosphorylation of these proteins of interest would therefore give great insight into the roles that these proteins play in response to hypoxia and rapid reoxygenation.

To determine the cellular localisation of key proteins of interest involved in the activation of the canonical NF-κB pathway, U-2 OS cells were exposed to hypoxia and reoxygenation as before (Fig. 39). This time, cells were lysed for nuclear and cytoplasmic extracts before western blot analysis of proteins associated with canonical NF-κB activation (Fig. 56). In all repeats of this experiment (n = 5) apart from the one presented here, PARP and beta-tubulin were used as nuclear and cytoplasmic controls. Unfortunately they were not carried out for the blot presented, however all other extracts produced by this method during this project that were probed for these control proteins had no cross-contamination between nuclear and cytoplasmic extracts. This particular blot was selected for presentation as it is representative of all the other blots and is the only set of extracts that a complete, clean blot was available for all proteins of interest.

The most striking finding presented in figure 56 is the movement of all three members of the canonical IKK complex into the nucleus following hypoxia. Statistical analyses of relative density of these blots confirm that this movement is significant, although variations in the timings and levels of significance does occur (Fig. 56A, C, D and E). Following reoxygenation, although all members of this complex appear to leave the nucleus to some extent, this is only significant in the case of IKKα. These results indicate that a small

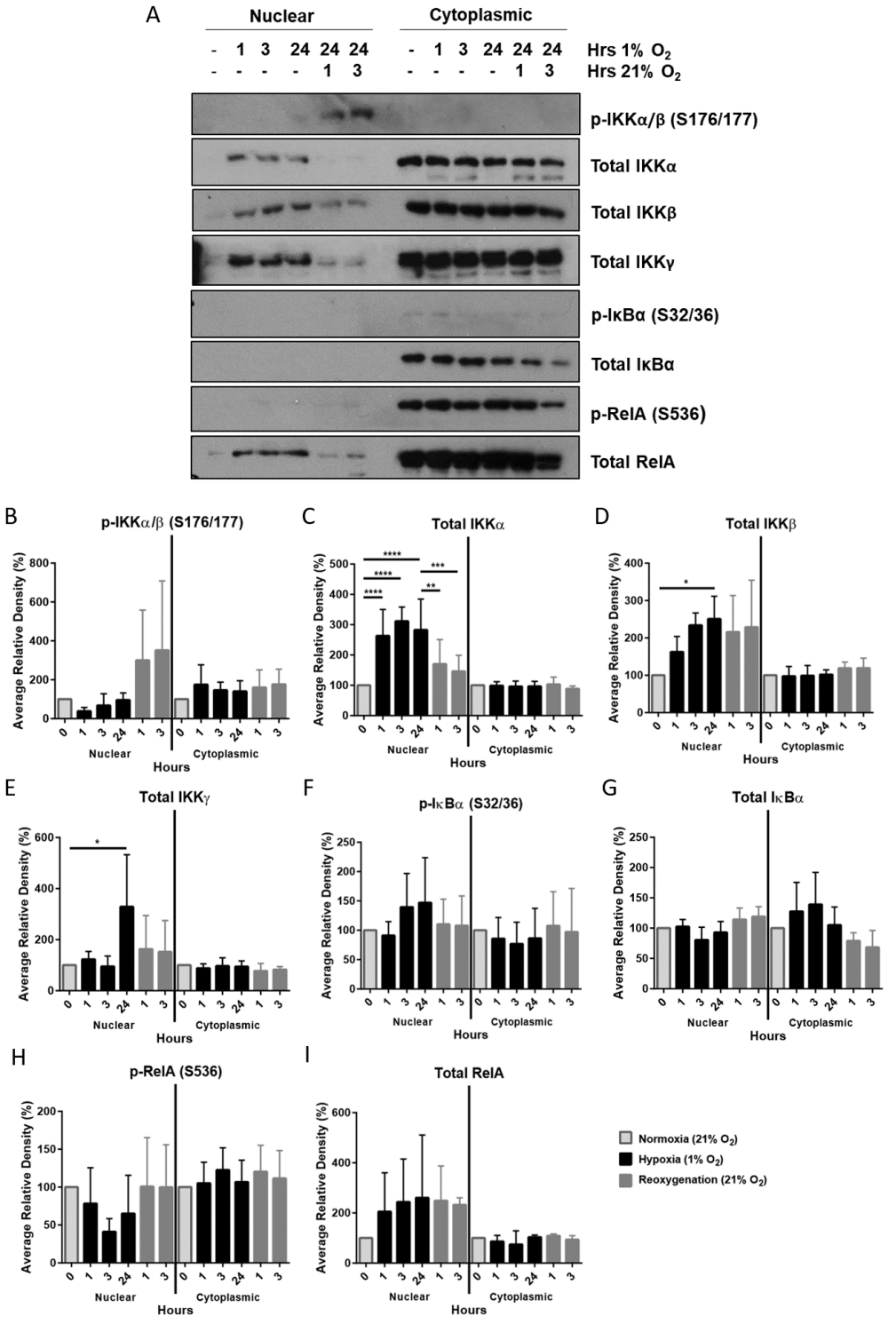

Figure 56. Hypoxia and Rapid Reoxygenation leads to Changes in Protein Localisation Events in U-2 OS Cells. U-2 OS cells were exposed to 1% O_2 for the indicated times. Reoxygenated samples were exposed to 1% O_2 for 24 hours prior to rapid reoxygenation. Nuclear and cytoplasmic proteins were carefully extracted and analysed by western blot probing for key proteins involved in canonical NF-κB activation (A). Relative density of blots from 5 independent experiments was analysed and statistically analysed (one-way ANOVA, Sidak's test) (B-I).

proportion of IKK proteins move into the nucleus following hypoxia where they are sequestered in preparation for the return of oxygen. From western blotting, it is impossible to tell whether the three proteins move as the canonical IKK complex, as part of a larger complex with other proteins, or independently of each other. Additional experimentation, for example through the use of co-immunoprecipitation, would give further insight into the mechanics and role of this response.

Analysis of phosphorylation events is more difficult after nuclear/cytoplasmic extraction as it does not preserve phosphorylation events as effectively, even in the presence of phosphatase inhibitors. Although some variation can be observed, no significant changes in phosphorylation of IKKα/β, IκBα or RelA occur here (Fig. 56A, B, F and H). This could be due to variation in the preservation of phosphorylation events between independent experiments, as well as the variability in effectiveness of these phospho-antibodies.

Following hypoxia and reoxygenation a surprisingly small increase in nuclear accumulation of RelA occurs. As such, this change in band density is not statistically significant following both stimuli (Fig. 56A and I). As we have observed previously, RelA is bound to chromatin following reoxygenation (Fig. 33), therefore this result is surprising. Personal communication with Perkins laboratory members, Dr. Yemm and Dr. Schlossmacher, reveals that RelA does not show strong nuclear accumulation in U-2 OS cells, even following stimulation with the potent RelA activator TNF.

The use of a second technique, immunofluorescence microscopy, to determine the location of IKKβ and NEMO was used to confirm whether translocation of the IKK complex does occur following hypoxia and rapid reoxygenation. IKKβ was selected for analysis as it is the main kinase associated with canonical NF-κB pathway activation and its apparent ability to translocate into the nucleus is a novel finding. In contrast, NEMO was selected as its translocation has been previously linked to genotoxic stress, confirmation of this movement could indicate that DNA damage is occurring following hypoxia and rapid-reoxygenation.

U-2 OS cells were plated out on 8-wells slides at 8,000 cells/well on day 0 and were left for 72 hours to grow prior to the start of the time course. Cells were exposed to hypoxia for 2 or 24 hours, or reoxygenated for 2 hours, and the cellular location of IKKβ and NEMO was determined by immunofluorescence using a Zeiss Axiolmager at 10x zoom. Images were analysed using ImageJ to automatically determine relative nuclear and whole cell signal intensity. From this the relative movement of protein in and out of the nucleus could be determined.

Data presented in figure 57 shows different results from that obtained by cell fractionation and western blotting (Fig. 56) with regard to the movement of IKKβ following hypoxia and reoxygenation. Microscopy data shows movement of IKKβ out of the nucleus following 2 hours of hypoxia ($p = 0.0186$), which continues up to 24 hours of hypoxia ($p = 0.0032$). Following rapid reoxygenation levels of nuclear IKKβ return to basal levels. This would

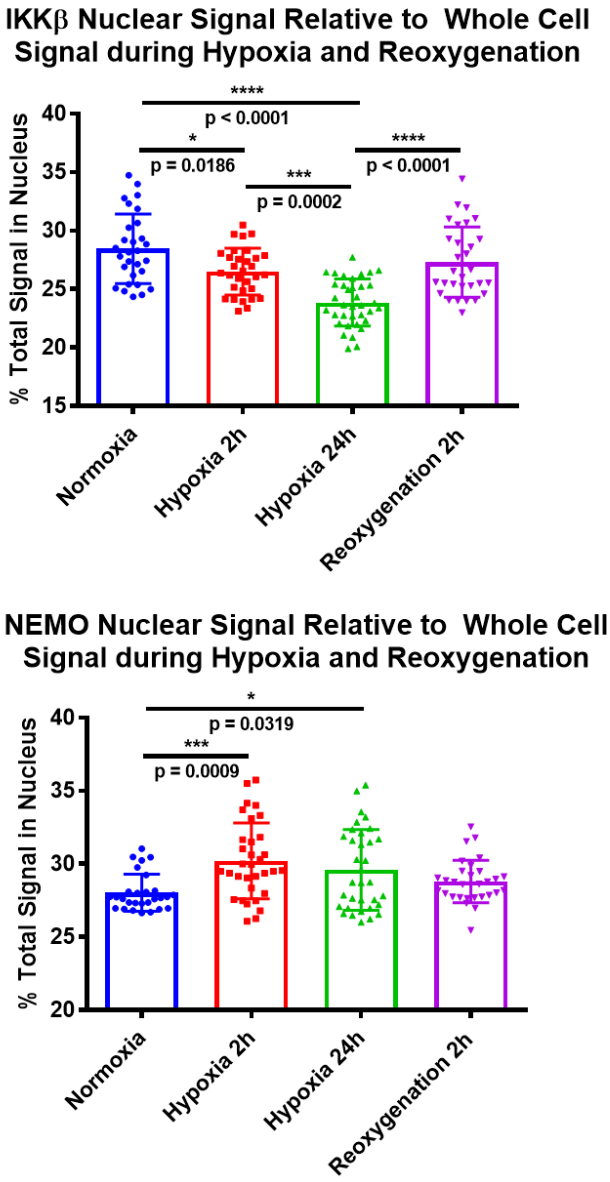

Figure 57. Hypoxia and Rapid Reoxygenation leads to Changes in Cellular Location of IKK Complex Subunits in U-2 OS Cells. U-2 OS cells were plated out on microscope growth slides and left to grow for 72 hours. U-2 OS cells were exposed to 1% O_2 for 2 hours or 24 hours. Reoxygenated samples were exposed to 1% O_2 for 24 hours prior to rapid reoxygenation for 2 hours. Cells were fixed and immunostained for proteins of interest. Images were taken at 10x zoom using a Zeiss Axiolmager without apotome and Zeiss' Zen software. Images were analysed using ImageJ software, to quantify the difference in nuclear signal compared with signal coming from the cell on its own. Points presented from 4 separate slides were statistically tested using one way anova tests using Sidak's test for multiple comparisons.

indicate a cytoplasmic role of IKKβ in the response to hypoxia. The opposing results obtained from the fractionation and microscopy approaches makes it difficult to formulate any conclusions; potential reasons for such discrepancies are expanded on in the discussion. The results from the NEMO microscopy experiment showed the same trend as those from the nuclear/cytoplasmic fractionation experiments (Fig. 57). Following 2 hours of hypoxia NEMO translocated into the nucleus ($p = 0.0009$) and remained there up to 24 hours of hypoxia. Following 2 hours of rapid reoxygenation NEMO translocated back out of the nucleus into the cytoplasm. This is consistent with the findings observed in figure 56 and suggest a nuclear role for NEMO in the response to hypoxia. These findings could indicate a role for ATM or DNA damage during hypoxia, as NEMO and ATM have previously been shown to interact following DNA damage [358].

5.4 Further Analysis of IKK Complex Movement during Hypoxia and Rapid Reoxygenation

This section aimed to further evaluate the role of IKKβ and its upstream kinase, TAK1, in the response to hypoxia and rapid reoxygenation, with particular focus on translocation of the IKK complex. This was carried out using the cellular fractionation protocol used in figure 56, but utilised small molecule inhibitors of TAK1 and IKKβ to determine whether they have a role in the control of translocation of the IKK complex in and out of the nucleus following hypoxia and reoxygenation.

The small molecular inhibitor of IKKβ, TPCA, was used in parallel to hypoxia and reoxygenation treatments to block IKKβ function [360][361]. Cells undergoing IKKβ inhibition were pretreated with 10μM of TPCA for 30 minutes prior to exposure to hypoxia or reoxygenation, doses and timings were determined by personal communications with members of the Perkins laboratory, who frequently use this compound on U-2 OS cells. The data sheet describes TPCA as a potent selective inhibitor of IKKβ, and has an IC50 to IKKβ that is over 20-fold lower than to the nearest off-target IKKα [362]. It also has a predicted half life of 6.11 days [351], longer than any time course used here.

The western blot presented here was selected as it shows the complete set of proteins of interest that were analysed and is representative of the effects observed across other blots (Fig. 58). Unfortunately, there are loading issues with the 24 hour hypoxia sample in this particular blot, however the graphs depict the impact of this treatment on the cellular localisation of proteins of interest.

Movement of IKKα, IKKβ and NEMO in and out of the nucleus following hypoxia and reoxygenation respectively, is consistent with data presented in figure 56. Analysis of the kinetics of translocation and the significance of these translocations as determined by quantification of band density differs however (Fig. 58). Again this is most likely due to variability between repeats when using this method of determining cellular localisation of proteins. Treatment with TPCA has no significant effect on the movement of the IKK

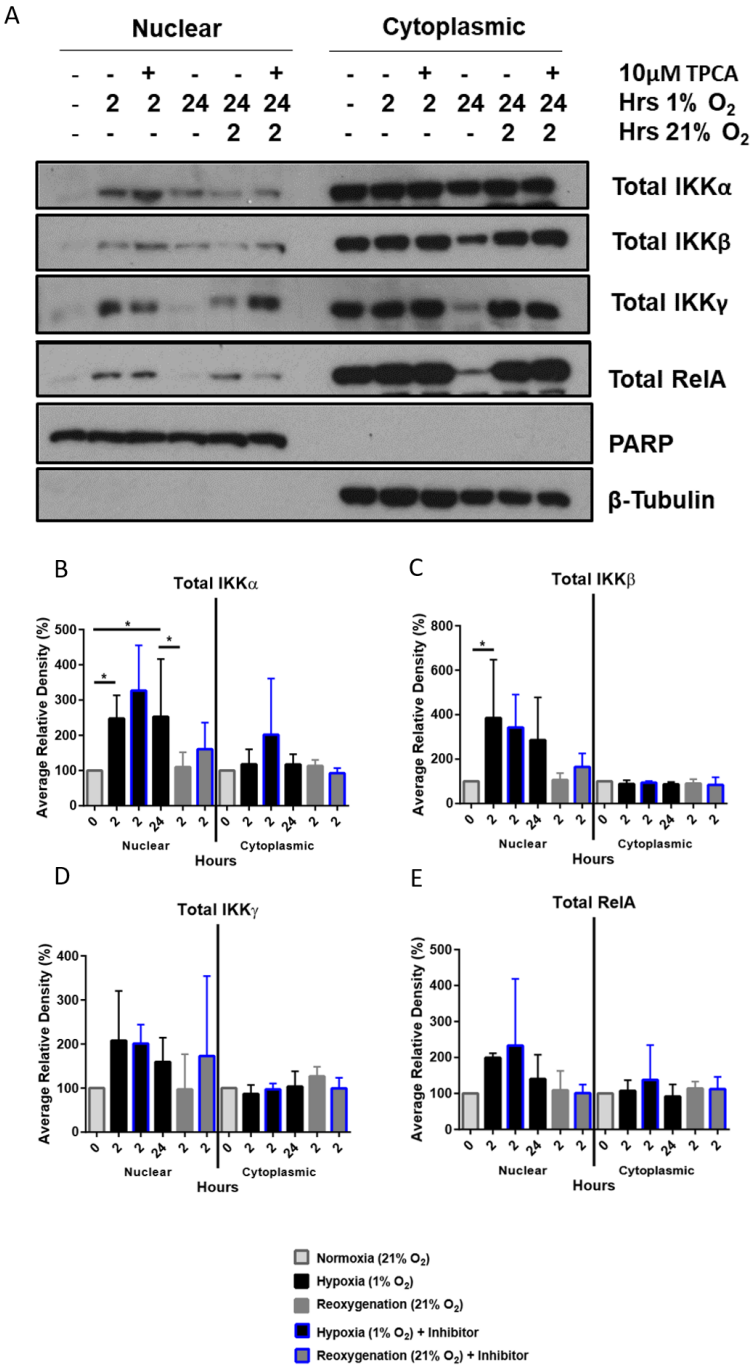

Figure 58. Effects of IKKβ Inhibition on Nuclear-Cytoplasmic Translocation following Hypoxia and Rapid Reoxygenation in U-2 OS Cells. U-2 OS cells were exposed to 1% O_2 for the indicated times. Reoxygenated samples were exposed to 1% O_2 for 24 hours prior to rapid reoxygenation. Cells undergoing IKKβ inhibition were treated with 10μM of TPCA for 30 minutes prior to exposure to hypoxia and rapid reoxygenation. Nuclear and cytoplasmic proteins were carefully extracted and analysed by western blot probing for key proteins involved in canonical NF-κB activation. A - Representative blot of 6 independent experiments, B-E - Relative density of bands statistically analysed by one-way ANOVA (Sidak's test).

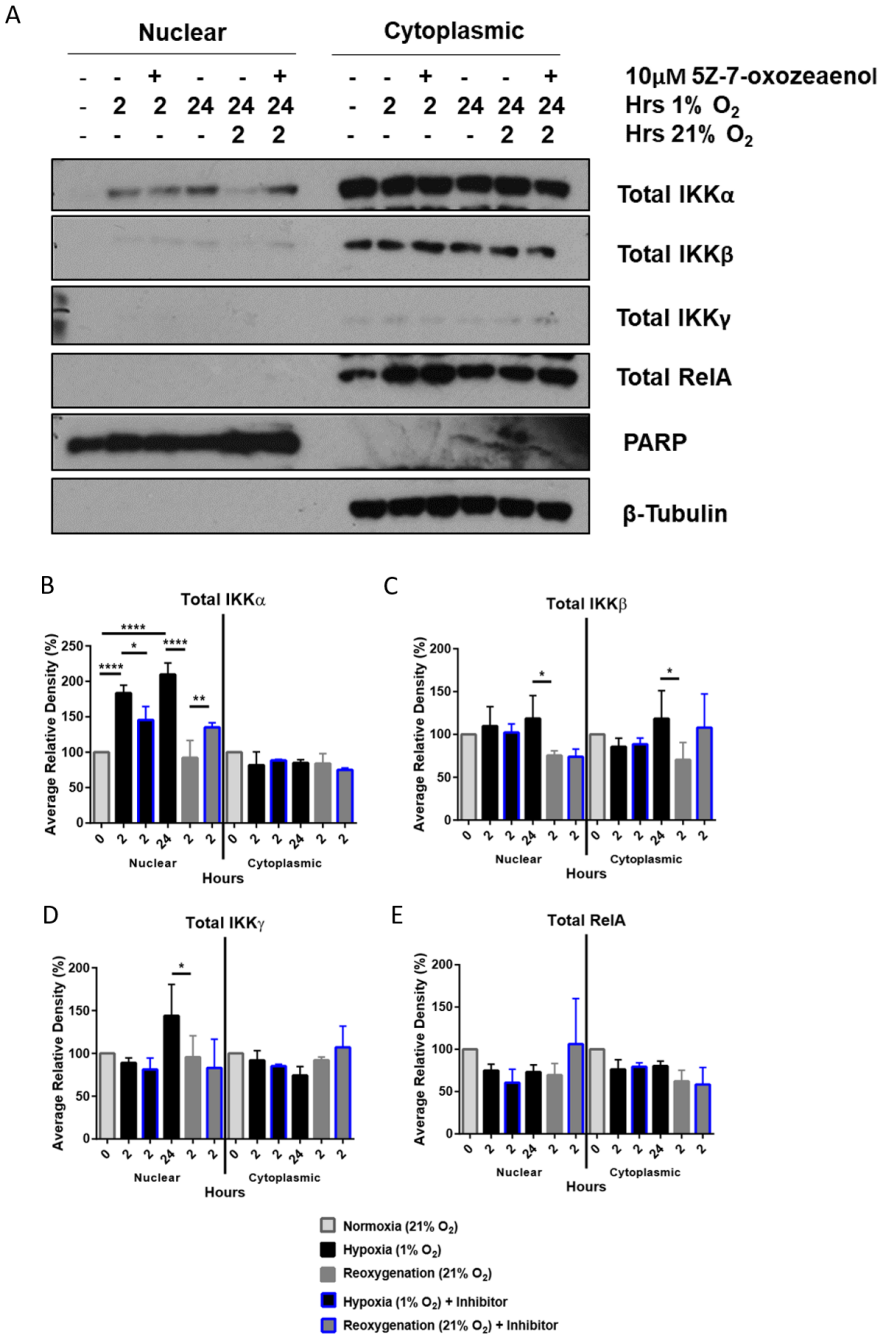

Figure 59. Effects of TAK1 Inhibition on Nuclear-Cytoplasmic Translocation following Hypoxia and Rapid Reoxygenation in U-2 OS Cells. U-2 OS cells were exposed to 1% O_2 for the indicated times. Reoxygenated samples were exposed to 1% O_2 for 24 hours prior to rapid reoxygenation. Cells undergoing TAK1 inhibition were treated with 10μM of 5Z-7-oxozeaenol for 30 minutes prior to exposure to hypoxia and rapid reoxygenation. Nuclear and cytoplasmic proteins were carefully extracted and analysed by western blot probing for key proteins involved in canonical NF-κB activation. A - Representative blot of 4 independent experiments, B-E - Relative density of bands statistically analysed by one-way ANOVA (Sidak's test).

subunits, indicating the IKKβ is not responsible for the translocation events observed here.

A second set of experiments was carried out to determine whether the upstream kinase of IKKβ, TAK1, is implicated in the translocation of the canonical IKK complex following hypoxia and reoxygenation. The experiment presented in figure 58 was therefore repeated with the addition of 10μM of the TAK1 inhibitor 5Z-7-oxozeaenol rather than TPCA.

Once again statistical significance of relative density of proteins of interest varies between this experiment (Fig. 59) and those carried out previously using this technique (Fig. 56 and 58). This highlights the need for these hypotheses to be tested using an alternative method that gives more consistent results. It is likely that the difference in findings and statistical significance from each set of repeated experiments is due to the magnitude of change in band density, this is particularly observable in the IKKβ and IKKγ blots presented here (Fig. 59A). The lack of consistent experimental repeats therefore makes it impossible to determine the impact of the TAK1 inhibitor on nuclear localisation of IKKβ and NEMO.

Although there have been inconsistencies in findings from most of the proteins analysed by nuclear and cytoplasmic fractionation, the movement of IKKα has remained consistent. Again, significant increases in nuclear IKKα is observed following hypoxia, which decreases following reoxygenation. Data presented in figure 59 demonstrates that inhibition of TAK1 significantly reduces the levels of nuclear IKKα following hypoxia, and significantly increases nuclear IKKα levels following reoxygenation. This suggests that TAK1 has a role in the control of IKKα localisation following hypoxia and reoxygenation, most likely through coordination of nuclear and cytoplasmic movement or control of stability of the protein to prevent or induce degradation by the proteosome.

5.5 The Role of IKKβ in Gene Transcription by NF-κB in Response to Hypoxia and Rapid Reoxygenation

Data presented in results chapter 1 showed that changes in the expression of IL-8, cIAP-2 and SOD-2 occurs following exposure to hypoxia and rapid reoxygenation. This section aims to investigate how the main canonical IKK complex subunit, IKKβ, affects gene expression following hypoxia and rapid reoxygenation. Experiments were carried out to assess the levels of IL-8, cIAP-2 and SOD-2 mRNA present in cells following hypoxia and rapid reoxygenation with and without inhibition of IKKβ.

Real-time qPCR experiments were carried out as before (Fig. 44) however in these experiments, cells undergoing IKKβ inhibition were treated with 5μM of BMS-345541 alongside exposure to hypoxia or rapid reoxygenation (dosage selected based on personal communication with colleagues who frequently use BMS-345541 on U-2 OS cells). BMS-345541 is an allosteric inhibitor of IKKβ, with a reported 10-fold greater specificity for IKKβ than

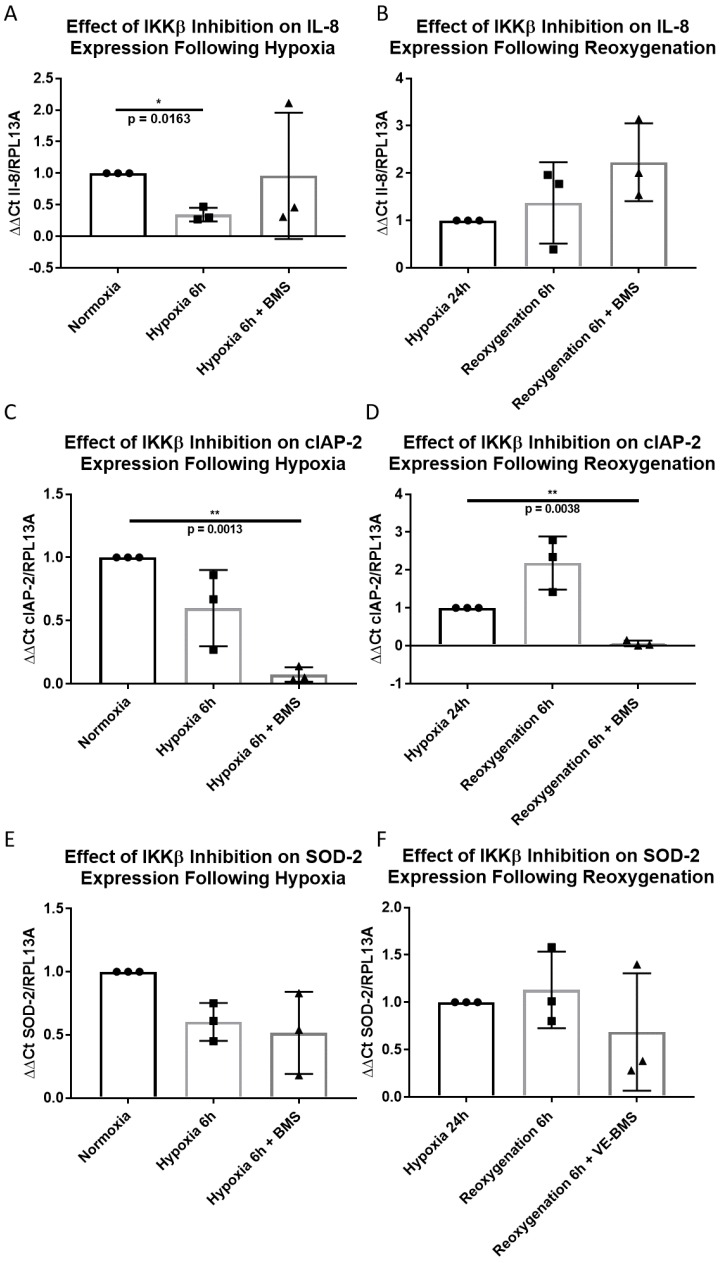

Figure 60. Treatment of U-2 OS cells with the IKKβ Inhibitor BMS-345541 affects Gene Expression following Hypoxia and Rapid Reoxygenation. U-2 OS cells were exposed to 1% O_2 for 6 hours. Reoxygenated samples were exposed to 1% O_2 for 24 hours prior to rapid reoxygenation. Total RNA was extracted, reverse transcription was performed and cDNA was analysed (A B = IL-8, C D = cIAP-2, E F = SOD-2) by qPCR using RPL13A as a reference gene. The Δ Δ Ct method of analysis was used, normalising hypoxia samples to normoxia samples and reoxygenated samples to 24 hour hypoxia samples. Mean values from 3 independent experiments is presented and statistical analysis was carried out using one-way ANOVAs using Tukey's test for multiple comparisons.

IKKα [363]. It has been shown to inhibit canonical NF-κB pathway activation in previous publications [364][365], and specificity tests revealed it to have no off-target effects on 15 other key kinases, even at doses of 100μM [363], and it has a predicted half-life of 3.35 days [351].

It should be noted that in some instances the data presented here that was significant in section 4.7, is not significant here (Fig. 60A). This is most likely due to the number of repeats; in some cases one of the 3 runs of each experiment appears to be an outlier, however with only 3 replicates it is difficult to determine with absolute confidence which one could be classed as an outlier. Closer inspection of the raw data has revealed that an outlier for one gene is not necessarily an outlier for the other genes; it is therefore not possible to confidently discard any specific data sets on the basis of a poor sample. Further repeats should be carried out to ensure that these outliers do not affect interpretation of the data.

As before, IL-8 expression decreases significantly after 6 hours of hypoxia exposure ($p = 0.0163$) (Fig. 60A). The results presented here make it unclear whether IKKβ inhibition has an effect on this as one out of three repeats shows an up-regulation in IL-8 expression while the others show no change. Again, in 2 out of 3 samples reoxygenation leads to an increase in IL-8 expression (Fig. 60B). Based on previous experiments we know that the repeat that does not show increased expression is an outlier (Fig. 46). Inhibition of IKKβ during reoxygenation leads to a small increase in IL-8 expression however this is not significant.

Again expression of cIAP-2 decreases following hypoxia, however this is not significant, most likely due to the low number of repeats (Fig. 60C). Following inhibition of IKKβ however, the expression of cIAP-2 decreases drastically compared to normoxia ($p = 0.0013$) and hypoxia untreated samples. This indicates an important role for IKKβ in the control of cIAP-2 expression in the response to hypoxia. Following reoxygenation expression of cIAP-2 increases once again; this is not significant in this figure (Fig. 60D). Interestingly, transcription of cIAP-2 is completely blocked following IKKβ inhibition, highlighting the role of IKKβ in canonical NF-κB control of gene expression. The data here indicate that IKKβ is important for cIAP-2 expression under all conditions tested, even in circumstances where cIAP-2 expression is repressed.

Expression of SOD-2 again decreases following exposure to hypoxia however this is not significant here (Fig. 60E). Inhibition of IKKβ does not have an effect on SOD-2 expression following hypoxia. Following reoxygenation SOD-2 expression remains unchanged in these samples, however earlier work has demonstrated that SOD-2 expression increases following reoxygenation (Fig. 60F). The data presented here shows that IKKβ inhibition leads to a slight decrease in SOD-2 expression following reoxygenation. Again, this data is not significant. Together these findings indicate that IKKβ may play a role in the NF-κB response to hypoxia and reoxygenation, however the exact nature of this is unclear as yet.

This ties in with the role of IKKβ as an upstream target in the activation of the canonical NF-κB pathway, as it controls cIAP-2 expression downstream.

The data presented in this section indicate that inhibition of IKKβ following hypoxia and reoxygenation can have different effects on the expression of NF-κB target genes. This highlights the specificity of gene expression in response to stress and demonstrates the complexity of the cellular response to this stress.

5.6 The Role of the IKK Complex in Cell Proliferation after Hypoxia and Rapid Reoxygenation

Data presented in chapter 4 showed that both hypoxia and rapid reoxygenation have significant effects on the proliferation of U-2 OS cells. Exposure to hypoxia caused a decrease in the proliferation of cells as measured by PrestoBlue, whilst rapid reoxygenation lead to an increase in proliferation over the first 24 hours followed by decrease following 48 hours. This section aims to determine how inhibition of IKKα and IKKβ affects proliferation of cells following hypoxia and rapid reoxygenation through the use of small molecule inhibitors.

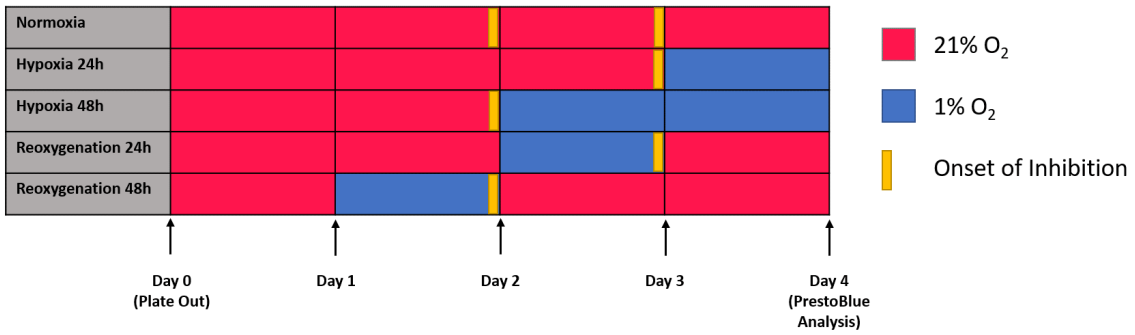

Figure 61. Schematic of Hypoxia and Rapid Reoxygenation Time Course for Proliferation Assays. U-2 OS cells were plated out at 2,500 cells per well in 96-well plates on day zero and incubated in normoxic conditions for at least 24 hours. Plates were then moved to and from the anaerobic chamber as the schematic demonstrates over the course of 4 days. For example the 24 hour reoxygenation plates were moved into 1% O_2 on day 2, 48 hours after plating out, and returned to 21% O_2 after 24 hours for a further 24 hours before reading proliferation by PrestoBlue. Inhibition of proteins in selected wells was carried out, these were treated either 24 hours or 48 hours prior to harvesting and throughout the remainder of the experiment. For example a selection of the normoxia only cells were treated for 24 hours prior to analysis, while another set were treated for 48 hours prior to analysis.

In this series of experiments the time course carried out was very similar to the one described in the previous chapter (Fig. 50), however small molecule inhibitors were used

alongside to inhibit members of the canonical IKK complex. To determine the effect of IKKβ inhibition on cell proliferation, a subset of plates from each separate time course were treated with 5μM of the small molecule inhibitor of IKKβ, BMS-345541, prior to and throughout exposure to hypoxia or rapid reoxygenation.

In separate experiments normoxia only cells were treated with BMS-345541 for 24 or 48 hours to assess the effects of IKKβ inhibition in the absence of other stimuli. This allows us to interpret the hypoxia and reoxygenation data with the knowledge of how the inhibitor affects proliferation in otherwise unstimulated cells. We were therefore able to correct for the inhibition of proliferation following normoxia when examining the role of the inhibitor in proliferation following hypoxia and reoxygenation.

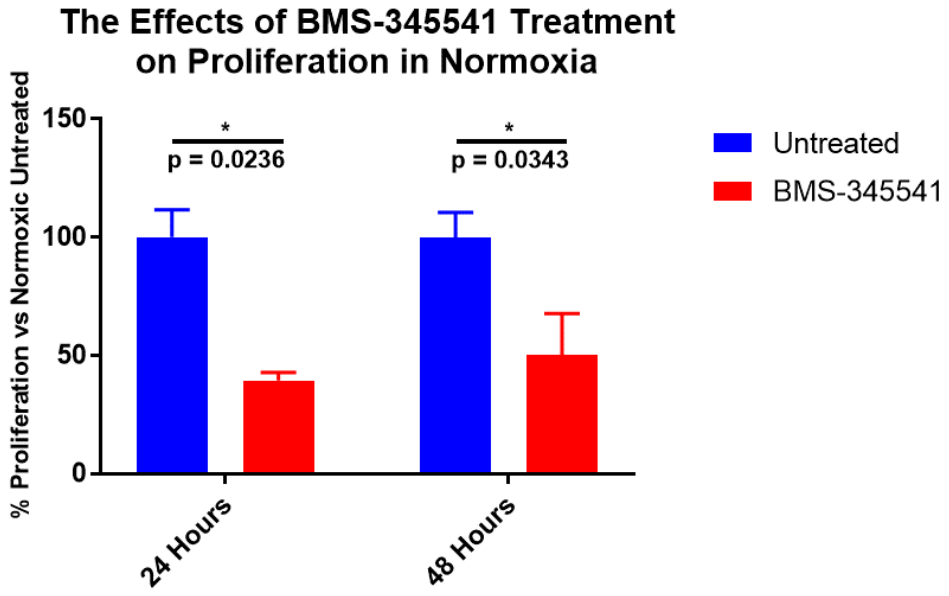

Figure 62. The Effects BMS-345541 Treatment on Proliferation of U-2 OS Cells. U-2 OS cells were treated a with 5μM of a small molecular inhibitor to IKKβ, BMS-345541, in normoxic conditions for 24 or 48 hours to assess the effects of this inhibitor on proliferation in the absence of other stimuli. Proliferation was analysed using PrestoBlue. Graphs were plotted using GraphPad prism and two-way ANOVA analyses were carried out using Tukey's test to account for multiple comparisons. Data is presented as a percentage of total proliferation in control plates.

Treatment of normoxia only cells with the IKKβ inhibitor BMS-345541 leads to around a 50% decrease in proliferation of U-2 OS cells following 24 and 48 hours of treatment (24h; p = 0.0236, 48h; p = 0.0343) (Fig. 62). This data demonstrates that inhibition of IKKβ, without any additional stress, leads to a a significant reduction in proliferation, highlighting the importance of functional IKKβ in normal cell function.

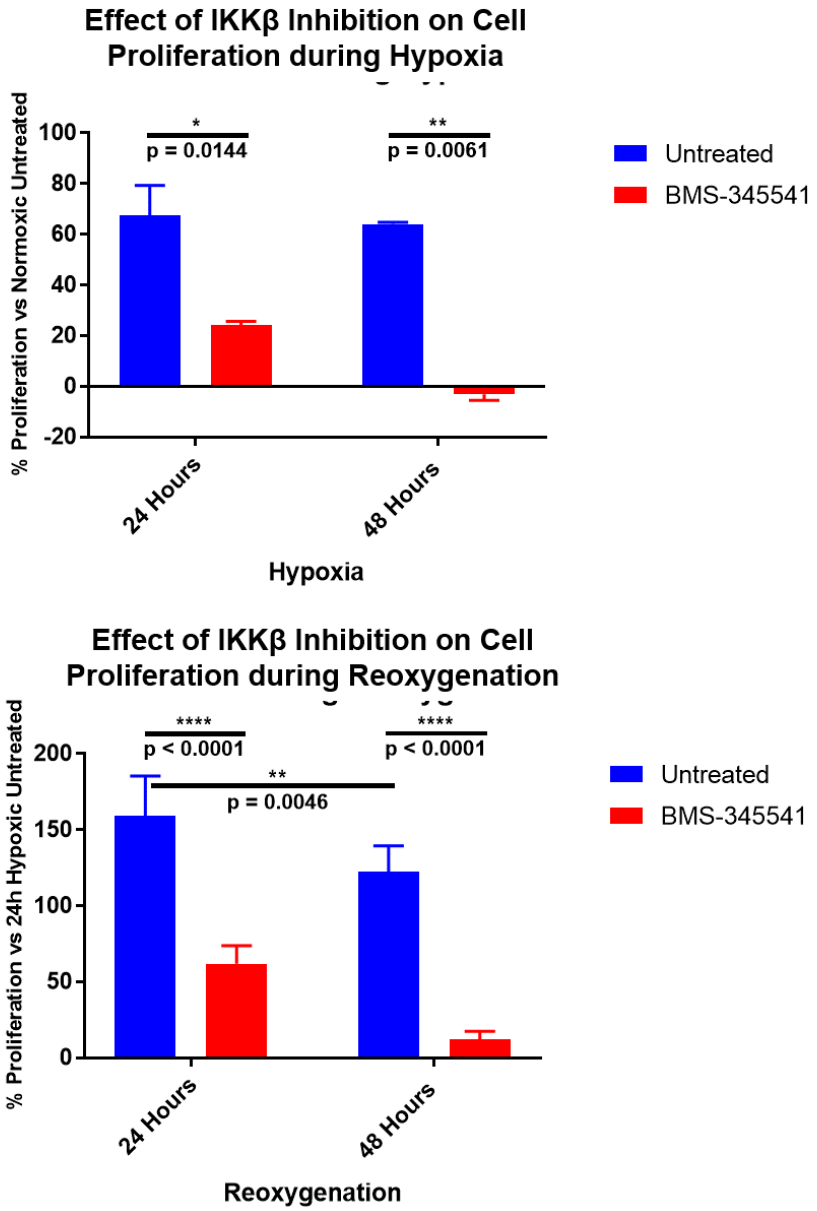

Figure 63. The Effects of Hypoxia and Rapid Reoxygenation on Proliferation of U-2 OS Cells Following IKKβ Inhibition. U-2 OS cells were treated as described in figure 61, however a subset of cells were treated with 5μM of a small molecular inhibitor to IKKβ, BMS-345541, prior to final exposure to hypoxia and rapid reoxygenation and for the remainder of the time course. Proliferation was analysed using PrestoBlue. Graphs were plotted using GraphPad prism to determine the effect of hypoxia exposure on cells compared with normoxia only cells, and to compare the effects of reoxygenation on cells compared with cells exposed to hypoxia for 24 hours. Two-way ANOVA analyses were carried out using Tukey's test to account for multiple comparisons.

As established previously exposure of U-2 OS cells to 1% O_2 leads to a decrease in proliferation (Fig. 63). Inhibition of IKKβ in combination with a 24 hour exposure to hypoxic conditions leads to a 60% decrease in the proliferation of cells. This change in proliferation after addition of the IKKβ inhibitor is greater in 24 hour hypoxia samples ($p = 0.0144$). This indicates that IKKβ is required in the response of cells to hypoxia. Although proliferation after 48 hours of hypoxia in the absence of the inhibitor remains fairly constant, the addition of the IKKβ inhibitor prevents proliferation ($p = 0.0061$). Moreover, as no cells are detected this suggests inhibition of IKKβ signalling during extended hypoxia triggers cell death due to apoptosis or necrosis. This is an additive effect of hypoxia exposure and treatment with the IKKβ inhibitor. This result demonstrates that IKKβ is absolutely critical in the cellular response to hypoxia, particularly following 48 hours of treatment, and indicates a potential anti-apoptotic role for NF-κB in the response to hypoxia-induced stress.

Reoxygenation again leads to an initial increase in proliferation of U-2 OS cells compared with levels seen in 24 hour hypoxia cells, followed by a decrease after 48 hours (Fig. 63). Treatment with the IKKβ inhibitor, BMS-345541, prevents any increase in proliferation after 24 hours ($p < 0.0001$) and 48 hours ($p < 0.0001$). This demonstrates that although inhibition of IKKβ affects proliferation of otherwise untreated cells, the combined effects of inhibition and reoxygenation have additive effects on proliferation. This clearly demonstrates that IKKβ is critical for the ability of cells to respond to rapid reoxygenation, and indicates a potential anti-apoptotic role for the canonical NF-κB pathway in the response to rapid reoxygenation induced stress.

As described in the first results chapter, rapid reoxygenation leads to an initial boost in proliferation, however following 48 hours this proliferation decreases and following 2 weeks colony formation is reduced (Fig. 51). The underlying reason for this is unclear, however could be linked to a sudden restoration of energy as aerobic respiration continues in the presence of oxygen. As shown in figure 63, IKKβ plays a key role in the response of U-2 OS cells to rapid reoxygenation 48 hours post-reoxygenation. To investigate how inhibition affects colony formation and cell survival following 2 weeks of rapid reoxygenation clonogenic assays were carried out looking at the effects of IKKβ inhibition on the number of colonies formed following rapid reoxygenation.

Colony formation experiments were carried out as before (Fig. 51). In parallel with the investigations presented earlier, a subset of normoxic and reoxygenation plates were treated with 10μM of the small molecule inhibitor of IKKβ, TPCA. This inhibitor was selected over BMS-345541 as it has a higher specificity for IKKβ over IKKα [363][362]. Both sets of plates were treated for a total of 3 hours and 30 minutes, however the first 30 minutes of TPCA treatment was carried out in hypoxia for the reoxygenated plates. Cells were then seeded onto 10cm plates and analysed after 2 weeks of growth. Data presented is the percentage of colonies formed compared with total cells seeded (manual counts). The graph presented in figure 64 contains some of the same data as was presented in

figure 51, the p-value presented differs slightly as multiple comparisons have been made during the statistical analysis of this data.

As demonstrated in results chapter 1, reoxygenation leads to a significant decrease in the ability of cells to form colonies compared to those kept in normoxic conditions (Fig. 51). Inhibition of IKKβ leads to a decrease in colony formation in normoxic cells that are otherwise untreated due to the toxicity of the inhibitor used (mean 67% with inhibitor vs. 81% without) (Fig. 64). Following inhibition of IKKβ there is no significant decrease in colony formation following reoxygenation compared to normoxic cells. This contradicts data from the proliferation assay (Fig. 63), which indicated that massive cell death occurs following prolonged IKKβ inhibition. These differences could be due the experimental design, in the previous experiment cells were exposed to the IKKβ inhibitor for an extended period of time, while in the colony formation experiment this inhibitor was removed after 3h 30m. Data from the clonogenic data therefore indicates that short-term IKKβ inhibition during reoxygenation has no impact on overall cell survival, while data from the proliferation assay indicates that long term inhibition of IKKβ during reoxygenation can have catastrophic consequences for the cell.

Previous work in this section has implicated IKKα in the canonical NF-κB response to hypoxia and rapid reoxygenation, although there are potential issues with the specificity of this inhibitor (Fig. 52). The first part of this experiment aimed to establish the effects of the IKKα inhibitor on proliferation of U-2 OS cells, that are not exposed to any other stimulus such as hypoxia or rapid reoxygenation (Fig. 66). Here, normoxia only cells were treated with 3μM of IKKα inhibitor (Strathclyde University) for 24 or 48 hours. The results show that following treatment for 24 hours there is around a 50% reduction in proliferating cells ($p = 0.0037$). After 48 hours of treatment with IKKα inhibitor proliferation decreases further ($p = 0.0030$). This data indicates that the IKKα inhibitor used for these experiments affects the general functionality of the cell regardless of other stimuli, and a longer treatment has a greater effect on the cells overall health.

One again proliferation of U-2 OS cells decreases following 24 hours of hypoxia and remains stable up to 48 hours (Fig. 66). Following treatment with the IKKα inhibitor, proliferation of cells decreases further following 24 hours of exposure to hypoxia, with around a 50% reduction in proliferation of 24 hour hypoxia samples following inhibition of IKKα ($p = 0.0018$). This is the same as the decrease observed when normoxic cells are treated with the inhibitor, indicating that this change is not due to hypoxia. After 48 hours of exposure to hypoxia, inhibition of IKKα leads to a large decrease in proliferation ($p = 0.0050$). This decrease is greater than those seen in normoxic cells that are treated with the IKKα inhibitor and the 48 hour hypoxia treated cells combined. This result indicates that these combined treatments are additive in their effects, and highlights the potential importance of IKKα in the cellular response to hypoxia-induced stress.

As shown in previous experiments, proliferation of cells increases following 24 hours of reoxygenation compared to cells exposed to hypoxia for 24 hours before decreasing again

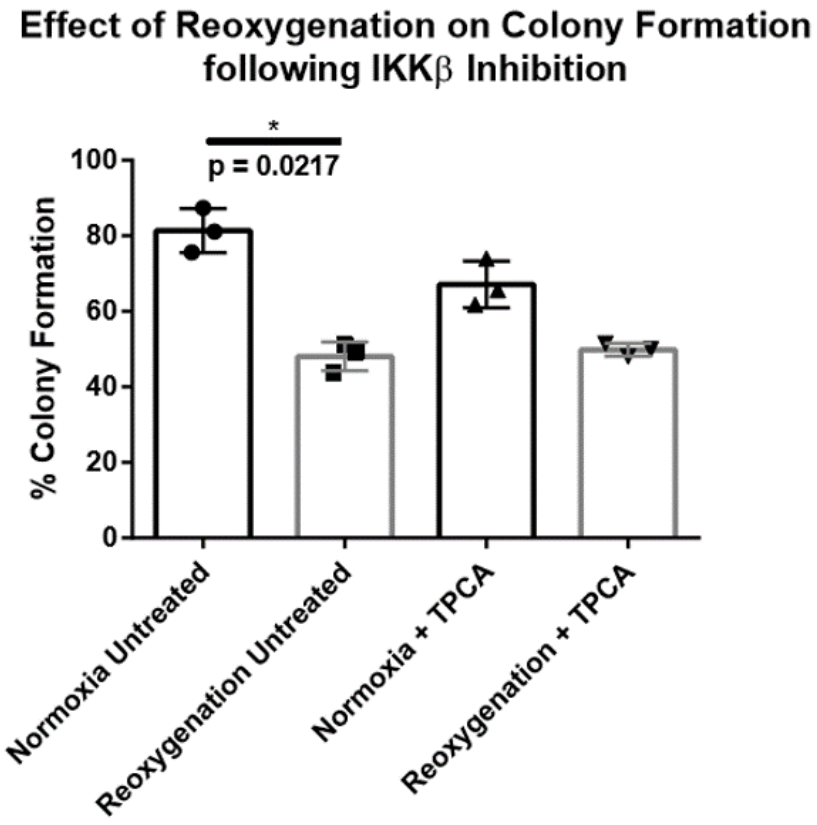

Figure 64. The Effects of IKKβ Inhibition During Reoxygenation on Colony Formation and Cell Survival. U-2 OS cells were exposed to 1% O_2 for 24 hours. A subset of plates were treated with 10 μM of the small molecule inhibitor of IKKβ, TPCA, prior to rapid reoxygenation or in parallel in normoxia. Following 3 hours of rapid reoxygenation, cells were trypsinised, counted and re-plated in a range of concentrations over 12 10cm plates. Normoxia only control plates were plated out in parallel. Plates were left in 21% O_2 for 2 weeks to allow for colony formation. Colonies were fixed and stained using crystal violet before being blinded and counting both computationally and manually. Data presented is the percentage of colonies formed compared with total cells seeded (manual counts). Results were plotted using GraphPad Prism and significance was calculated through two-way ANOVA, using Sidak's test for multiple comparisons.

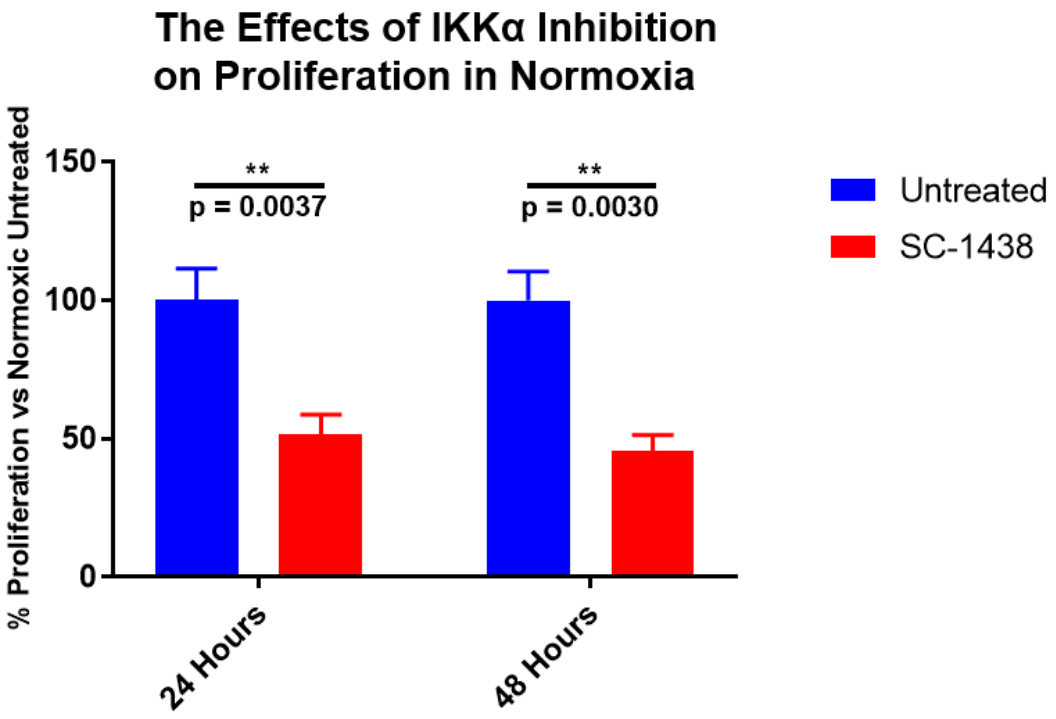

Figure 65. The Effects of IKKα inhibitor Treatment on Proliferation of U-2 OS Cells. U-2 OS cells were treated with 3μM of IKKα inhibitor in normoxic conditions for 24 or 48 hours to assess the effects of this inhibitor on proliferation in the absence of other stimuli. Proliferation was analysed using PrestoBlue. Graphs were plotted using GraphPad prism and two-way anova analyses were carried out using Tukey's test to account for multiple comparisons. Proliferation is presented as a percentage of proliferating cells compared to untreated controls.

after 48 hours (Fig. 66). Treatment with IKKα inhibitor in combination with 24 hours of reoxygenation leads to a decrease in proliferation ($p = 0.0016$), however again this change in proliferation of cells following inhibition of IKKα is around the same as that observed in IKKα inhibited normoxic cells. This indicates that following 24 hours of reoxygnenation, the decrease in proliferation is predominantly due to the addition of the inhibitor and not as a combination of IKKα inhibition and reoxygenation. After 48 hours of reoxygenation however the proportion of proliferating cells decreases greatly following treatment with the inhibitor ($p = 0.0003$). This demonstrates that IKKα plays an important role in the proliferation of cells after 48 hours of reoxygenation. This change is drastic although does not show as great a decrease in proliferation as that observed following treatment with the IKKβ inhibitor, BMS-345541.

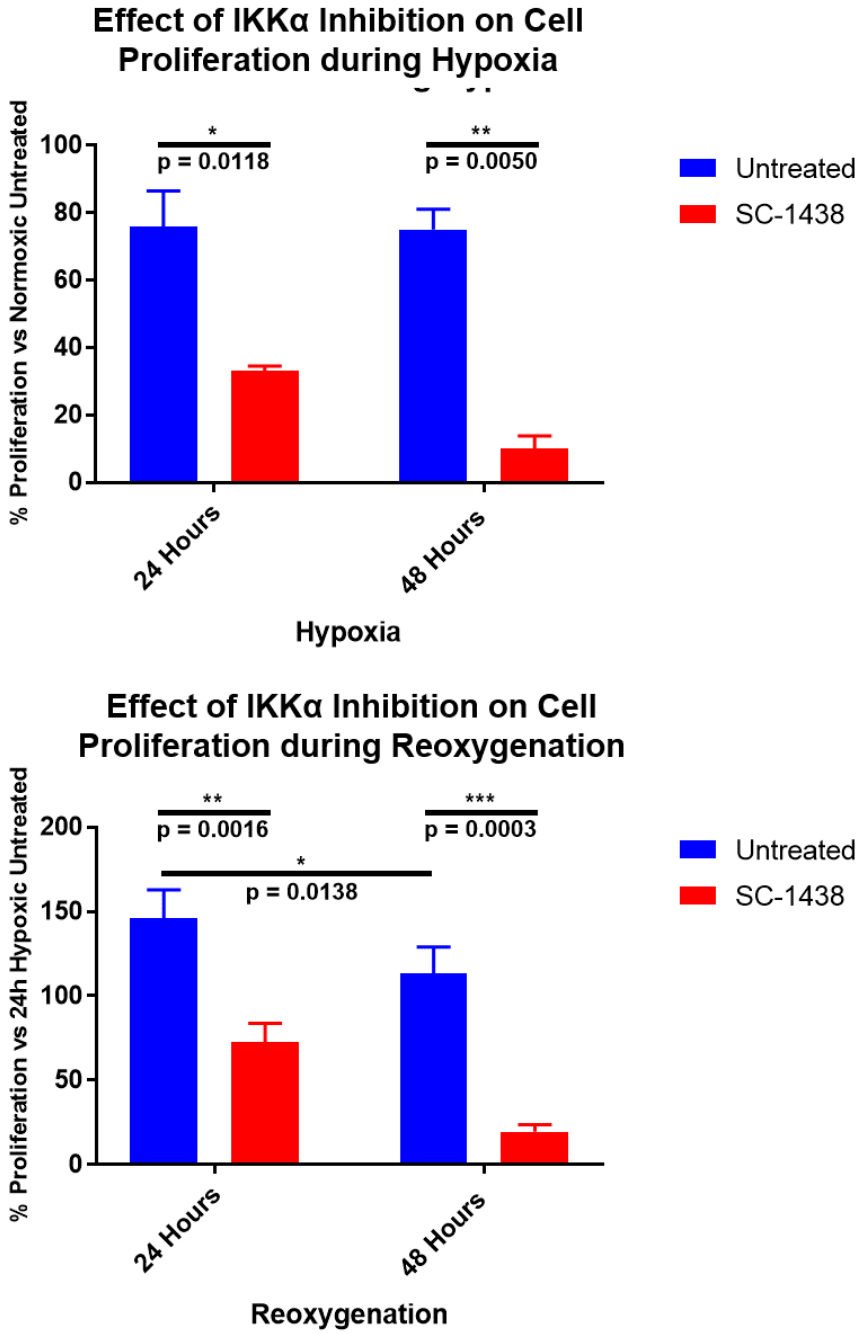

Figure 66. The Effects of Hypoxia and Rapid Reoxygenation on Proliferation of U-2 OS Cells Following IKKα Inhibition. U-2 OS cells were treated as described in figure 61, however a subset of cells were treated with 3μM of a small molecular inhibitor to IKKα prior to final exposure to hypoxia and rapid reoxygenation and for the remainder of the time course. Proliferation was analysed using PrestoBlue. Graphs were plotted using GraphPad prism to determine the effect of hypoxia exposure on cells compared with normoxia only cells, and to compare the effects of reoxygenation on cells compared with cells exposed to hypoxia for 24 hours. Two-way anova analyses were carried out using Tukey's test to account for multiple comparisons.

5.7 Brief Summary and Discussion of Chapter 5

This results section aimed to determine the roles of IKKα and IKKβ in the response to hypoxia and rapid reoxygenation. The data presented in this chapter predominantly supports a role for IKKβ over IKKα. Inhibition of IKKβ blocks gene expression of the NF-κB target cIAP-2 across all treatments (Fig. 60), and long term IKKβ inhibition prevents proliferation following both hypoxia and rapid reoxygenation to a level not observed in normoxic cells (Fig. 63). In addition to this, inhibition of the upstream kinase of IKKβ, TAK1, significantly reduces activation of the canonical NF-κB pathway through IκBα phosphorylation. Based on a thorough literature search, there is no evidence of the IKKβ inhibitors, TPCA or BMS-345541, ever being used in parallel with hypoxia and reoxygenation before this project.

Evidence to support the hypothesis that IKKα plays a role in the canonical NF-κB pathway response to hypoxia and rapid reoxgenation is dependent on the specificity of the IKKα inhibitor provided by Prof. Simon Mackay. Figure 52 shows that treatment with this IKKα inhibitor significantly reduces signalling through the canonical NF-κB pathway, however further experiment demonstrated that this blocking of canonical pathway signalling was not specific to the response to reoxygenation. Treatment of cells with this small molecule inhibitor prevented canonical NF-κB pathway activation following etoposide or TNF exposure (Fig. 53), which is broadly considered to be primarily mediated by IKKβ. In a recent publication by Prof. Mackay's group, inhibitors were tested for specificity by demonstrating that canonical NF-κB signalling following TNF stimulation was unaffected after high dosing with the inhibitor [348]. This indicates that the batch of inhibitor used in this project was having off target effects, potentially targeting IKKβ. Additional evidence that refutes a role for IKKα in the response to reoxygenation is that inhibition of its upstream kinase, NIK, has no effect on canonical NF-κB signalling (Fig. 55).

This contradicts previous work that has implicated both IKKα and IKKβ in the response to hypoxia [147]. Firstly they demonstrated that canonical NF-κB signalling is required for basal and TNF stimulated HIF1α expression, confirming the link between canonical NF-κB signalling and HIF1α levels. They then demonstrated that both IKK kinase subunits are involved in this signalling mechanism through siRNA knockdown of IKKα or IKKβ, and by exposing IKKα-/-, IKKβ-/- or IKKα/β-/- mouse embryonic fibroblasts to hypoxia (1% O_2) for 2 - 24 hours. The results show no reduction in HIF1α levels following hypoxia when only one of the kinases is knocked out, however following knockout of both subunits HIF1α levels are reduced completely [147]. This project has not focussed on HIF1α expression as a readout and many of the experiments have predominantly focussed on reoxygenation; this could explain some of the differences observed here. In addition due to the questions raised regarding the specificity of the IKKα inhibitor used in this project, one can not draw firm conclusions on what the effects of IKKα inhibition has on

the response to hypoxia and rapid reoxygenation.

Another study demonstrated that IKKβ plays a critical role in the response to hypoxia through triggering phosphorylation and degradation of IκBα [343], this degradation was not observed in data presented in this thesis. In this publication, Cummins et al. demonstrate that hypoxia leads to an increase in the pool and activity of IKKβ, increasing the canonical NF-κB pathway's sensitivity to other stimuli such as TNF. They propose that hydroxylation and degradation of a fraction of IKKβ occurs during normoxia. Inhibition of hydroxylation (such as through hypoxia) leads to stabilisation, which leads to this activation. Cummins et al. used DMOG, a hydroxylase inhibitor, to carry out the hydroxylation experiments, therefore experiments need to be repeated using hypoxia rather than DMOG to determine whether this is occurring in hypoxia or reoxygenation. Although DMOG treatment induces HIF stabilisation, it is not an effective substitute for hypoxia exposure, as such the observations presented by Cummins et al. could be artefactual.

One of the more surprising results from this section is the apparent translocation of the IKK complex subunits into the nucleus following hypoxia. This is reversed following rapid reoxygenation demonstrating again the differences between the two stimuli. Following quantification of relative band density across multiple independent blots, it was apparent that the statistical significance of this movement was variable between experiments as observed across figures 56, 58 and 59. This is most likely due to variability in signal strength between experiments; in some instances very low signal is observed, making it difficult to capture any quantifiable changes in relative band density. This lack of reproducibility highlights the need to carry out additional experiments using a difference technique to determine the cellular location of proteins of interest following hypoxia and rapid reoxygenation, for example through the use of immunofluorescence microscopy, which was utilised in some of the key localisation experiments.

Immunofluorescence microscopy was used to validate the findings of the nuclear-cytoplasmic fractionation experiments, unfortunately due to antibody availability this was only carried out on IKKβ and NEMO. In the future this experiment could be repeated with IKKα as a target protein. This microscopy data confirms the movement of NEMO in and out of the nucleus but shows the opposite pattern of movement of IKKβ. In this instance the use of a second technique only raised further questions regarding the effects of hypoxia and rapid reoxygenation on nuclear translocation of members of the IKK complex.

There are many possible reasons for the differences in results between the two techniques, particularly since NEMO showed consistent results across both techniques while IKKβ showed opposing results. On such reason could be due to the antibodies used. The IKKβ antibody used for the western blot was not suitable for use in microscopy and vice versa, therefore the differences in epitope binding could be affecting the ability of the antibody to bind to the protein. In contrast, the NEMO antibody was suitable for use across both techniques so was used for both methods.

Another caveat is the fact that both of these techniques have to have a significant amount of sample processing carried out in the anaerobic chamber. It is possible that the lower oxygen or higher temperature of harvesting samples in this environment, for both cell fractionation and cell fixing, could affect the data. Indeed the global brightness of the slides prepared in hypoxia was diminished compared with the slides prepared in normoxia. It was for this reason that data was analysed automatically and quantitatively, using a method designed to eradicate any effects of this variation in sample brightness.

The reason for this potential movement of IKK complex members is unknown, however the pattern of movement of NEMO is consistent with Miyamoto's papers describing the serine 85-dependent movement of NEMO into the nucleus following DNA damage where it interacts with ATM [358][366]. A series of publications have characterised this movement, with the current model describing sumoylation and ubiquitination events on NEMO that coordinate its sub-cellular localisation [367][368]. The cross-talk between the DNA damage response pathway and the canonical NF-κB pathway is coordinated by a cytoplasmic form of ATM, which is exported from the nucleus in a calcium-dependent manner in response to genotoxic stress [339]. Once in the cytoplasm it coordinates the activation of NEMO through phosphorylation on serine 85, which leads to its ubiquitination and activation. The nuclear localisation of NEMO observed in this study following hypoxia may indicate a role for ATM in the cellular response to hypoxic stress.

It is notable in this regard that TAK1 has been implicated in the activation of NEMO by ATM [127][369], and here our fractionation studies link TAK1 with a further IKK complex member, IKKα (Fig. 59). Although IKKα was not implicated in the ATM-dependent activation of NEMO in response to genotoxic stress, IKKα has previously been demonstrated as having a nuclear role as it phosphorylates histone H3 in response to cytokines [359]. It is possible that hypoxia could be triggering a similar response in these proteins.

The effects of IKKβ inhibition on gene transcription was also investigated in this section. Due to lack of reproducibility very little statistically significant data was obtained in these experiments, therefore further replicates are required before any meaningful conclusions can be formulated. In addition, alternative approaches could be employed to detect changes in gene expression such as using luciferase reporter assays. One notable result was obtained however, treatment with the small molecule inhibitor BMS-345541 drastically reduced levels of cIAP-2 mRNA following both hypoxia and rapid reoxygenation. This highlights the differences in the control of expression of different genes in response to a given stimuli as not all genes have behaved the same way. It should be noted however that the effects of the inhibitor in the absence of any other stimuli was not tested, therefore it is possible that this result is due to exposure to BMS-345541 alone.

Also covered in this section is the role of IKKα and IKKβ in cell proliferation and survival following hypoxia and rapid reoxygenation. The results presented here show that IKKβ is involved in the response to hypoxia; proliferation of cells decreases following hypoxia.

Inhibition of IKKα and IKKβ leads to a further decrease in proliferation following hypoxia, however due to the questions raised regarding the specificity of the IKKα inhibitor, we can only confidently say that IKKβ is involved in the continued proliferation of cells following hypoxia. After reoxygenation for 24 hours an increase in proliferation is seen compared with hypoxia only treated cells. IKKβ inhibition does not seem to affect proliferation at this time point, however inhibition alongside a 48 hour reoxygenation exposure leads to a significant decrease in proliferation highlighting a delayed and anti-apoptotic role for IKKβ following reoxygenation. Interestingly at longer time points of 2 weeks, colony formation and survival following reoxygenation is not significantly affected by inhibition of IKKβ. This could highlight the potential differences between the acute and chronic effects of reoxygenation on the cell or indeed the different consequences depending on the length of time that IKKβ is inhibited. It is likely however that the shorter IKKβ inhibitor exposure utilised in the colony forming assay compared with the proliferation assay could explain these differences in proliferation and survival. Again, confidence in these findings is entirely dependent on the specificity of the inhibitors used, as such experiments should be repeated using alternative means of protein inhibition.

Many of the experiments carried out in this section used small molecule inhibitors to selectively inhibit proteins of interest. Some benefits of using these over other methods of inhibition is that it is one of the simplest and cheapest methods of inhibiting a protein. In addition, many of the small molecule inhibitors available are being tested for, or are currently in use in patients, as treatments for conditions such as cancer [370]. Specificity of these kinases inhibitors can be an issue though, as off target effects on other kinases can be common. Indeed concerns have already been raised in this thesis regarding the specificity and potential off target effects of the IKKα inhibitor used here (Fig. 52) [348]. The inhibitors used in this thesis were checked for off target effects using the Dundee Kinase Screen database [371], as well as the information provided in the data sheets when inhibitors were purchased. Another potential problem associated with small molecule inhibitors is the half-lives, however the Opera database confirms that the half-lives of inhibitors used here were far longer than the times that they were used for treatment, the shortest being 3.14 days [351]. To increase confidence in the efficacy of these inhibitors, internal validation experiments could be performed in the future, for example dose response treatments could be performed measuring the effects on the target protein and other closely related proteins.

In spite of these precautions that were taken when selecting these small molecule inhibitors, it is necessary to repeat the experiments presented here using an alternative technique for protein inhibition. siRNA knockdown could be used to temporarily inhibit proteins of interest, although off target effects are possible, it is easy to test that the protein has been knocked down through western blotting for the target protein. Due to time constraints it was not possible to carry out siRNA treatments as part of this particular project, therefore future work should focus on this approach. For longer experiments,

alternative methods for knocking down a protein should be utilised such as shRNA or CRISPR as these produce more permanent knockdowns. These are far more time consuming and technically challenging however, and do not guarantee effective knockdown or deletion [372], and in the case of shRNA proteins can be re-expressed over weeks of passage [373]. As discussed earlier, previous studies have used mouse embryonic fibroblasts that are null for IKKα, IKKβ or both [147]. These could be utilised in future experiments to further investigate the role of IKKα and IKKβ, unfortunately these cell lines were not available to use during this project.

Chapter 6: The Role of ATR/ATM in NF-κB Activation after Hypoxia and Rapid Reoxygenation

Data presented so far has demonstrated that hypoxia and reoxygenation lead to activation of the canonical NF-κB pathway and that IKKβ is required for this activation. The upstream pathways responsible for this activation of the canonical NF-κB pathway are currently unknown. This final results chapter therefore aimed to determine the upstream kinases responsible for detecting and activating the signalling pathways discussed.

Previous work on hypoxia and reoxygenation has implicated the PIKK family members ATR and ATM in the response to hypoxia and reoxygenation respectively, although not in the context of NF-κB signalling [374]. The link between ATM and NF-κB pathway has however been investigated in response to other stresses, previous studies have also demonstrated that ATM can be activated in response to oxidative stress, but not genotoxic stress, in primary human fibroblasts [225]. While unpublished work in the Kenneth laboratory has implicated ATM in the canonical NF-κB response to hydrogen peroxide treatment. ATM and ATR could therefore be involved in the canonical NF-κB response to hypoxia and rapid reoxygenation.

As discussed in the introduction, ATM and ATR are critical responders to genotoxic and replication stresses respectively, and have key roles in the control of cell cycle progression. As such, the first part of this chapter aimed to determine whether double strand breaks or changes in cell cycle dynamics occur during hypoxia and reoxygenation. Indeed, both hypoxia and reoxygenation have been linked to the DNA damage response and cell cycle arrest previously [270][271]. These were investigated through flow cytometry analysis of cells probed for γH2AX and BrDU respectively.

Once the effects of hypoxia and rapid reoxygenation on DNA damage and cell cycle progression had been investigated, the role of ATM and ATR in the response to hypoxia and rapid reoxygenation was analysed. This involved a series of experiments using small molecule inhibitors targeted to proteins of interest followed by analysis of activation of their downstream targets as well as the canonical NF-κB pathway. These experiments used western blot analysis on whole protein extracts as well as nuclear and cytoplasmic extracts to determine the location of proteins of interest in the cell.

After establishing proteins that work upstream of the canonical NF-κB pathway in the response to hypoxia and rapid reoxygenation, the third and final aim for this chapter was to determine how ATM and ATR inhibition affects downstream cellular processes such as the regulation of gene transcription and cell proliferation. Again, small molecule inhibitors to were used to target ATM and ATR and cells were analysed for changes in expression of IL-8, cIAP-2 and SOD-2 through real-time qPCR. The effects of ATM and ATR inhibition on proliferation following hypoxia and reoxygenation was determined by PrestoBlue assays.

6.1 DNA Damage Analysis after Hypoxia and Rapid Reoxygenation

As discussed in section 1.4, oxidative stress is characterised by an imbalance of ROS, which are able to cause damage to proteins, lipids and DNA [235][236][237]. Data in the previous section (Fig. 56 and 57) has shown patterns of NF-κB activation following reoxygenation that are similar to those seen following genotoxic stress [117][358], particularly regarding the nuclear and cytoplasmic movement of NEMO [367][368] and the rapid activation of NF-κB through the canonical pathway in the absence of IκBα degradation [164]. It is widely known that DNA damage can lead to the activation of the canonical NF-κB pathway [92][93][94][42]. Determining whether DNA damage occurs following hypoxia and rapid reoxygenation was therefore critical for understanding the NF-κB response to hypoxia and rapid reoxygenation-induced oxidative stress.

To determine the effects of hypoxia and rapid reoxygenation on DNA damage, γH2AX levels were detected using flow cytometry. U-2 OS cells were exposed to hypoxia and reoxygenation for the times indicated (Fig. 67). Cells were fixed and stained for γH2AX to assess the presence of DNA double strand breaks. A negative control of IgG stain was carried out in parallel as well as an etoposide positive control (data not shown). Levels of γH2AX are similar between the etoposide controls and the 2 and 6 hour hypoxia samples. Levels of γH2AX signal was measured using flow cytometry and analysed using GraphPad Prism.

A significant increase in the percentage of cells that stain positive for γH2AX is observed following 6 hours of exposure to hypoxia (Fig. 67). Interestingly, following 24 hours of hypoxia the percentage of cells positive for γH2AX staining is the same as in normoxia only cells. This result indicates that DNA damage occurs in the form of double strand breaks following hypoxia, however cells are able to repair this damage while still in hypoxic conditions.

In contrast to the effects seen following exposure to hypoxia, rapid reoxygenation has no effect on the percentage of cells staining positive for γH2AX (Fig. 67). This indicates that no further DNA double strand breaks occur following reoxygenation, however it does not rule out the presence of other forms of DNA damage such as single strand breaks.

The results presented in this section indicate a potential role for DNA damage signalling in the cellular response to hypoxia. The increase in the proportion of cells staining positive for γH2AX indicates that double strand DNA breaks are occurring. This could implicate the PIKK family of proteins in this response, particularly ATM. However other family members such as ATR and DNA-PK could be implicated as they are also known to phosphorylate H2AX at the site analysed here in response to replication stress or double strand breaks respectively [195][271]. Reoxygenation does not seem to cause any increase in double strand breaks however this does not rule out other forms of DNA damage.

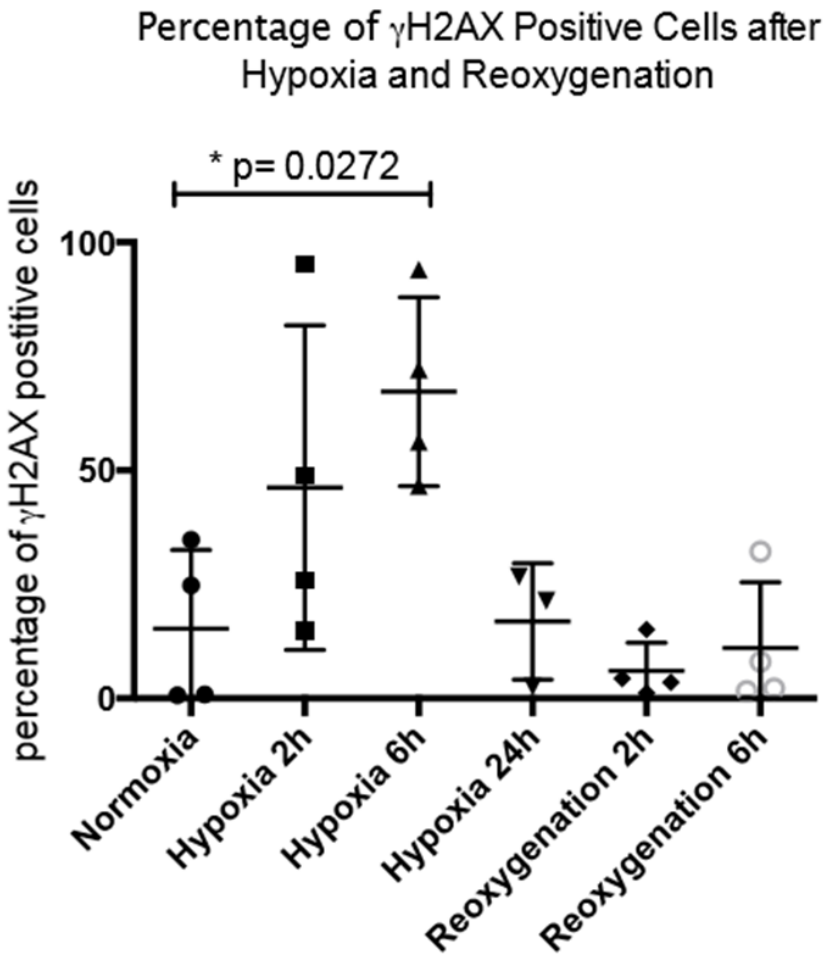

Figure 67. The Effects of Hypoxia and Rapid Reoxygenation on DNA Damage in U-2 OS Cells. U-2 OS cells were exposed to 1% O_2 for 2 hours, 6 hours or 24 hours. Reoxygenation was carried out for 2 hours or 6 hours following 24 hours of hypoxia exposure. Cells were harvested, fixed and stained for γH2AX and data was plotted and analysed using GraphPad Prism. Negative IgG stain controls and a positive etoposide treated controls were carried out in parallel (data not shown). Data was analysed using one way anova accounting for multiple comparisons using Tukey's test.

6.2 The Effects of Hypoxia and Rapid Reoxygenation on Cell Cycle Dynamics

The DNA damage sensing kinases ATM, ATR and DNA-PK play critical roles in the cell cycle, signalling to downstream targets to prevent progression through the cycle while DNA is repaired [202][203][204][211]. As such cell cycle dynamics are an indicator of overall cell health and gives insight into the nature of cell damage. In this section the effect of hypoxia and rapid reoxygenation on the cell cycle of U-2 OS cells was investigated.

U-2 OS cells were exposed to hypoxia or reoxygenated for the times indicated (Fig. 68). Cells were trypsinised, fixed and stained for BrDU to assess progression through the cell

cycle using flow cytometry. The percentage of cells in each phase of the cell cycle was determined and mean results from 4 independent experiments were plotted (Fig. 68).

No significant changes in cell cycle dynamics was observed during hypoxia, however small trends can be seen across all phases of the cell cycle (Fig. 68). Following rapid reoxygenation the percentage of cells in G1 phase significantly decreased towards levels seen in untreated/normoxia cells (Fig. 68), effectively reversing the effects observed following 24 hours of hypoxia exposure ($p = 0.0109$). These data suggest that reoxygenation of the cells has reversed a potential G1/S phase checkpoint block that occurred during hypoxia in a small proportion of cells. It is clear from the results presented in figure 68 that hypoxia and rapid reoxygenation have some effects on cell cycle dynamics, however these are marginal, and in the case of most of the data here, insignificant.

Another method for analysing cell cycle dynamics, proliferation and cell division levels is though determining the mitotic index of populations of cells. To do this cells were exposed to hypoxia and reoxygenation for the times (Fig. 69). Cells were fixed and stained with DAPI to visualise chromatin in the cell under fluorescence microscopy. Multiple images were taken across different slides and total cell number and mitotic index was determined using ImageJ. Mitotic index is the percentage of cells undergoing mitosis per image.

The results of the mitotic index analysis show that there are some small changes in the mean proportion of cells undergoing mitosis during hypoxia and rapid reoxygenation (Fig. 69). Following hypoxia, the percentage of cells undergoing mitosis increases up to 24 hours of hypoxia however this data is not significant. Following reoxygenation the levels of cells undergoing mitosis decrease significantly ($p = 0.0176$). This suggests that a G2/M phase block could be occurring during reoxygenation as fewer cells enter mitosis.

Changes in cell cycle dynamics following reoxygenation could be due to a number of factors. A decrease in G1 phase cells could indicate that more cells are entering S-phase, in the context of reoxygenation this could be due to the sudden increase in aerobic respiration allowing cells to produce components required for S-phase.

6.3 A Role for ATM in the Canonical NF-κB Pathway Response to Hypoxia and Rapid Reoxygenation

Work presented earlier in this section has demonstrated that hypoxia leads to a significant increase in γH2AX levels, indicating that hypoxia causes double strand DNA breaks, implicating ATM in the cellular response to hypoxia [375]. Other studies have shown that ATM activation in response to genotoxic stress leads to the repression of NF-κB target genes [374]. This is similar to what is observed in the response to hypoxia in experiments presented in this project; 6 hours of hypoxia exposure leads to the repression of transcription of IL-8, cIAP-2 and SOD-2. In addition to these findings, unpublished work in the Kenneth laboratory has implicated ATM in the canonical NF-κB response to

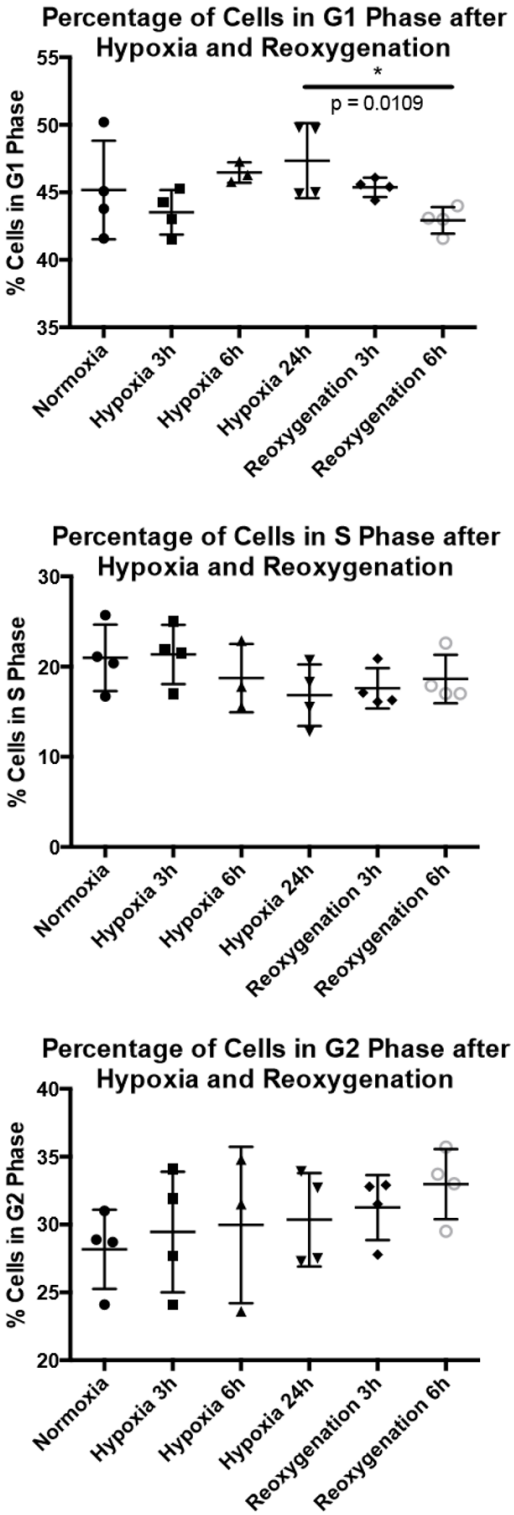

Figure 68. The Effects of Hypoxia and Rapid Reoxygenation on The Cell Cycle. U-2 OS cells were exposed to 1% O_2 for the times indicated. Reoxygenated samples were exposed to 1% O_2 for 24 hours before reoxygenation using spent media for 3 hours or 6 hours. Cells were trypsinised, fixed and stained for BrDU before analysis by flow cytometry. Results show that hypoxia and rapid reoxygenation have effects on cell cycle progression. Data was analysed using one-way ANOVA accounting for multiple comparisons using Tukey's test.

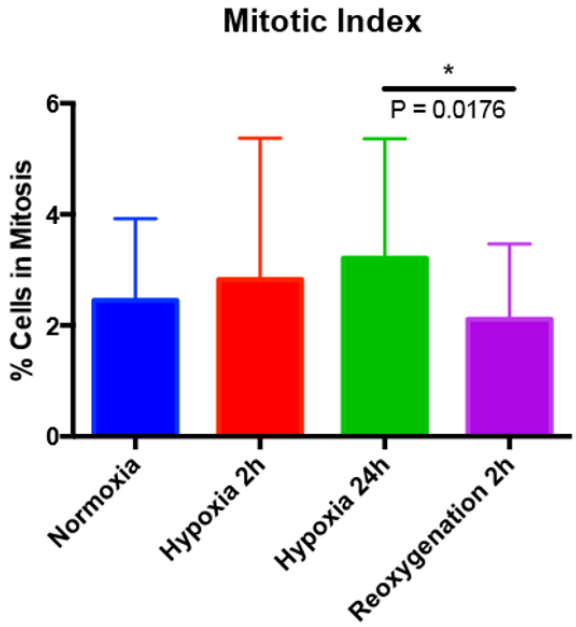

Figure 69. The Effects of Hypoxia and Rapid Reoxygenation on Mitotic Index. U-2 OS cells were exposed to 1% O_2 for the times indicated. Reoxygenated samples were exposed to 1% O_2 for 24 hours before reoxygenation using spent media for 3 hours or 6 hours. Cells were fixed and stained with DAPI before analysis using immunofluorescence microscopy. 10x zoom images were taken across 3 wells per treatment. One-way ANOVA statistical tests were performed using Tukey's test for multiple comparisons (n = 3).

hydrogen peroxide treatment. It is therefore plausible that ATM is involved in the NF-κB response to hypoxia and rapid reoxygenation.

Figure 27 (section 4.1) demonstrated that hydrogen peroxide treatment leads to canonical NF-κB activation, this experiment was also carried out in the presence of the ATM inhibitor, KU-55399 [376] (Fig. 70). KU-55933 is a selective and competitive ATM inhibitor, it has over 160-fold greater specificity to ATM than its nearest off target kinase, DNA-PK [377] and has been used successfully in multiple publications [378][379]. KU-55933 has a predicted half life of 4.41 days [351], it is therefore a suitable inhibitor for use in this project. Cells were treated with 20μM of hydrogen peroxide for the times indicated with or without a 30 minute pretreatment with 5μM of KU-55399. This dose was again selected based on personal communication with colleagues who have used this inhibitor on this cell line previously. Whole cell lysates were extracted and analysed as described in figure 27.

Data presented in figure 70 demonstrates that the activation of the canonical NF-κB pathway is unchanged following inhibition of ATM using the small molecule inhibitor KU-55399 (Fig. 70). This result is surprising as unpublished data (Kenneth lab) has implicated ATM as the upstream kinase responsible for the activation of the NF-κB

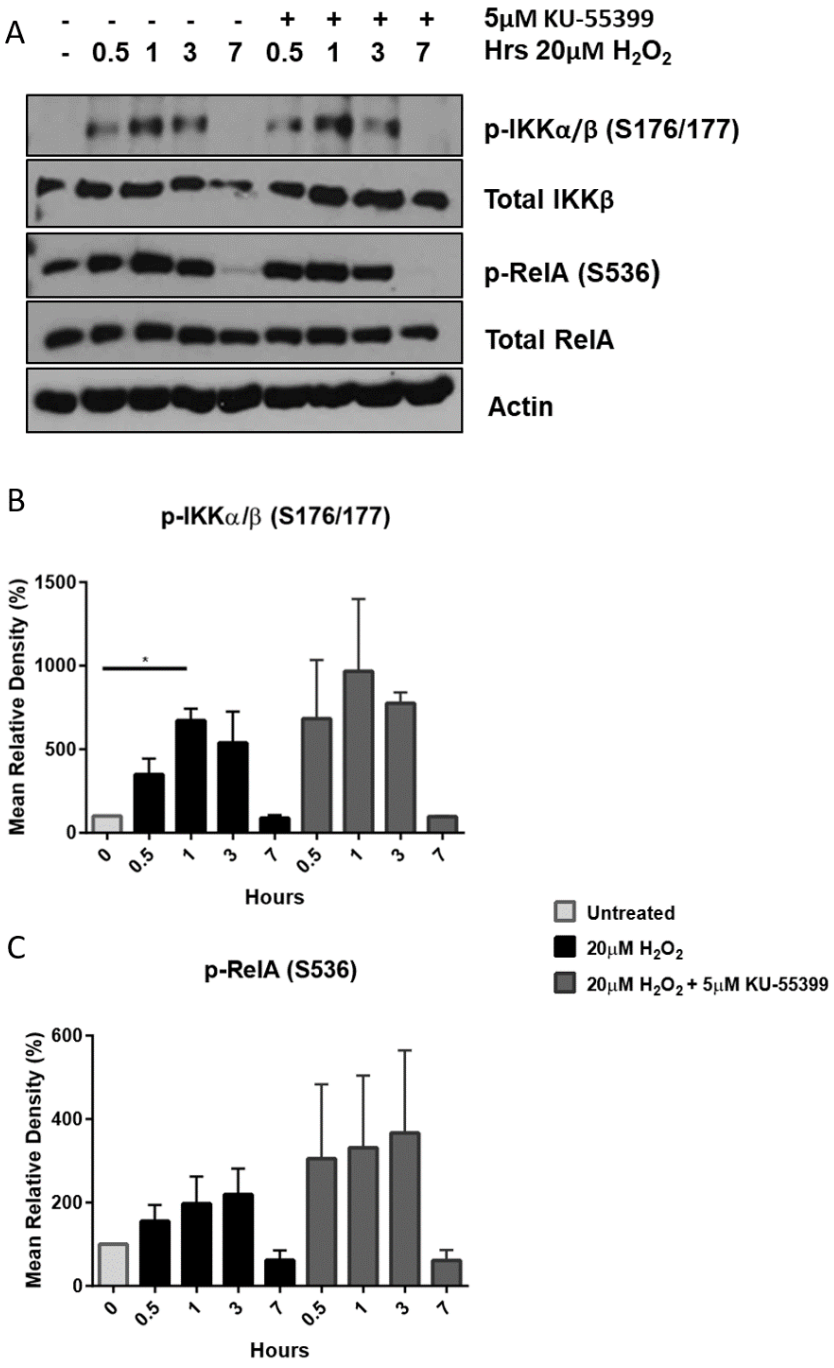

Figure 70. Hydrogen Peroxide Treatment leads to Canonical NF-κB Activation in U-2 OS Cells Independently of ATM. Cells were treated with 20μM of H_2O_2 for between 30 minutes and 7 hours, with or without pretreatment with the ATM inhibitor KU-55399. Whole cell lysates were extracted using 8M urea lysis buffer and western blots were performed looking at phosphorylation events associated with canonical NF-κB activation. A - Representative blot across 3 independent experiments. B-C - Mean relative density, analysed by one-way ANOVA using Sidak's test for multiple comparisons.

pathway in response to hydrogen peroxide in HEK293 cells. The small molecule inhibitor was again tested on etoposide treated cells and was shown to be working as expected (data not shown), therefore the results presented here demonstrate clearly that ATM is not involved in the canonical NF-κB pathway response to hydrogen peroxide treatment in U-2 OS cells. It was therefore important to determine whether ATM is activated in response to hydrogen peroxide treatment in this cell line. To test for this, extracts used in figure 70 were re-run and probed for markers of ATM and ATR activation.

A significant increase in Kap1, ATR and Chk1 is observed following hydrogen peroxide treatment (Fig. 71). The increase in Kap1 and Chk2 phosphorylation is indicative of ATM activation in response to double strand breaks, where ATM is phosphorylated and in turn phosphorylates Kap1 and Chk2. The increase in phosphorylation of ATR and its downstream target Chk1 suggests that the DNA damage that is occurring that cannot be solely resolved by ATM activation alone, possibly due to the presence of other forms of DNA damage such as single strand breaks. Previous studies have shown that ATR is responsible for phosphorylation of H2AX in the response to oxidative stress induced by hydrogen peroxide treatment [193]. This could be one of the cell signalling mechanisms that is occurring here. These data indicate that both genotoxic and oxidative stress is occurring following treatment with hydrogen peroxide, and both ATR and ATM appear to be activated in this response.

Focussing next on the effect of inhibition of ATM; KU-55399 treatment has no significant effect on Kap1, ATR or Chk1 activation following hydrogen peroxide treatment (Fig. 71). However Chk2 phosphorylation is significantly reduced following this inhibition of ATM, thus indicating that the inhibitor is effective. As Kap1 is a downstream target of ATM it was expected that inhibition of ATM would also prevent phosphorylation at this site. It is possible however that phosphorylation of Kap1 in this context is dependent on another kinase, indeed previous studies have suggested that ATR and DNA-PK are also able to phosphorylate Kap1 at this site [380]. Chk2 is responsible for the coordination of cell cycle arrest in response to genotoxic stress sensed by ATM; ATM therefore appears to control cell cycle arrest in response to hydrogen peroxide treatment.

Experiments that have focussed on the effects of hydrogen peroxide treatment on NF-κB and PIKK signalling have demonstrated that ATM coordinates downstream signalling to Chk2 (Fig. 71). To determine whether ATM is implicated in the cellular response to hypoxia and rapid reoxygenation, U-2 OS cells were exposed to hypoxia and rapid reoxygenation for the times indicated (Fig. 72). Total protein lysates were extracted and analysed as before (Fig. 71), probing for phosphorylation events associated with ATM activation.

Following exposure to hypoxia no significant changes in phosphorylation are observed across all proteins analysed (Fig. 72), indicating that ATM is not activated in the response to hypoxia. Following reoxygenation an increase in phosphorylation of Chk2 and ATM occurs, however quantification of these blots shows that the only significant increase that

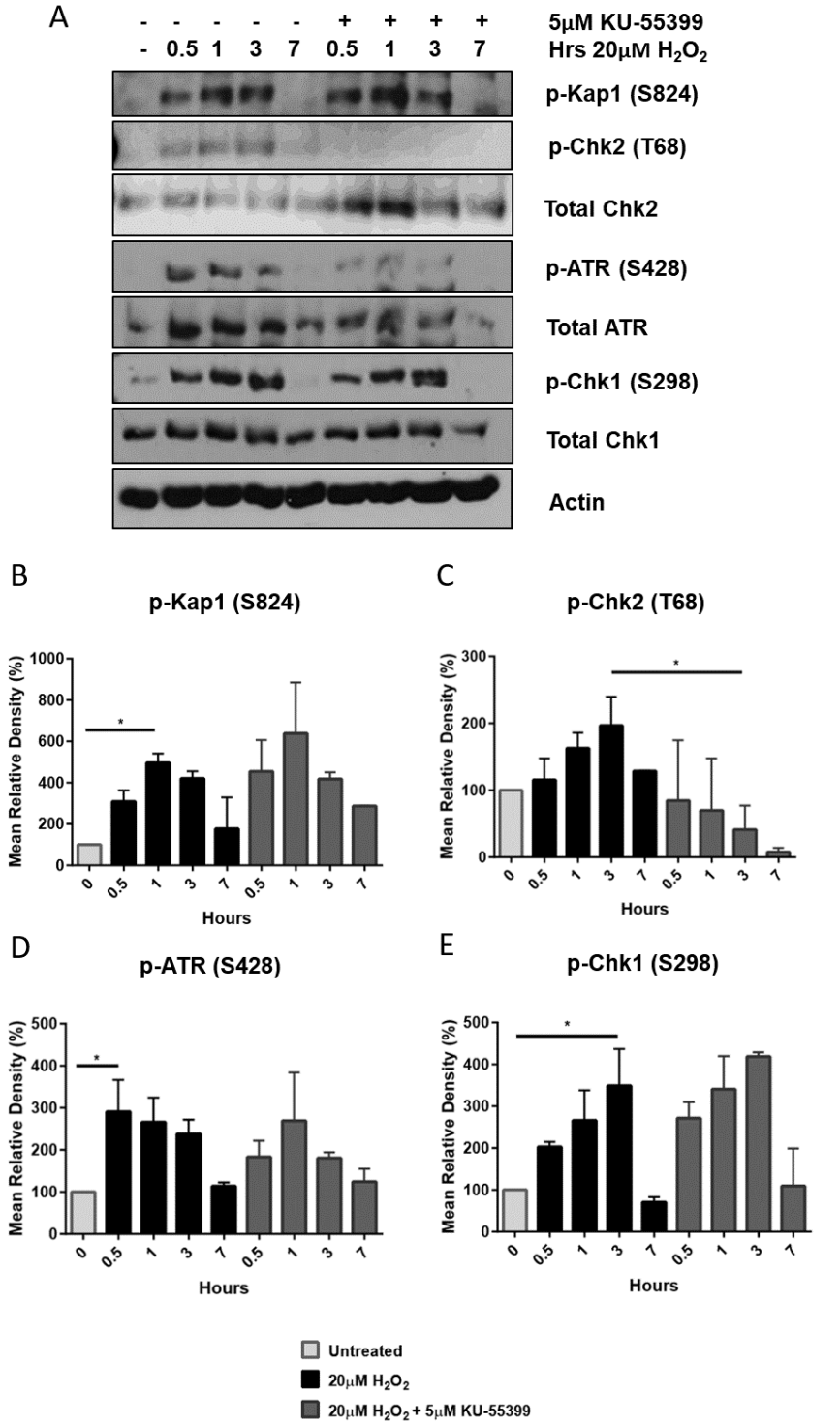

Figure 71. Hydrogen Peroxide Treatment leads to the Activation of PIKK Family Members in U-2 OS Cells. Cells were treated with 20μM of H_2O_2 for between 30 minutes and 3 hours. Whole cell lysates were extracted using 8M urea lysis buffer and western blots were performed looking at phosphorylation events associated with DNA damage responses. A - Representative blot across 3 independent experiments. B-E - Mean relative density, analysed by one-way ANOVA using Sidak's test for multiple comparisons.

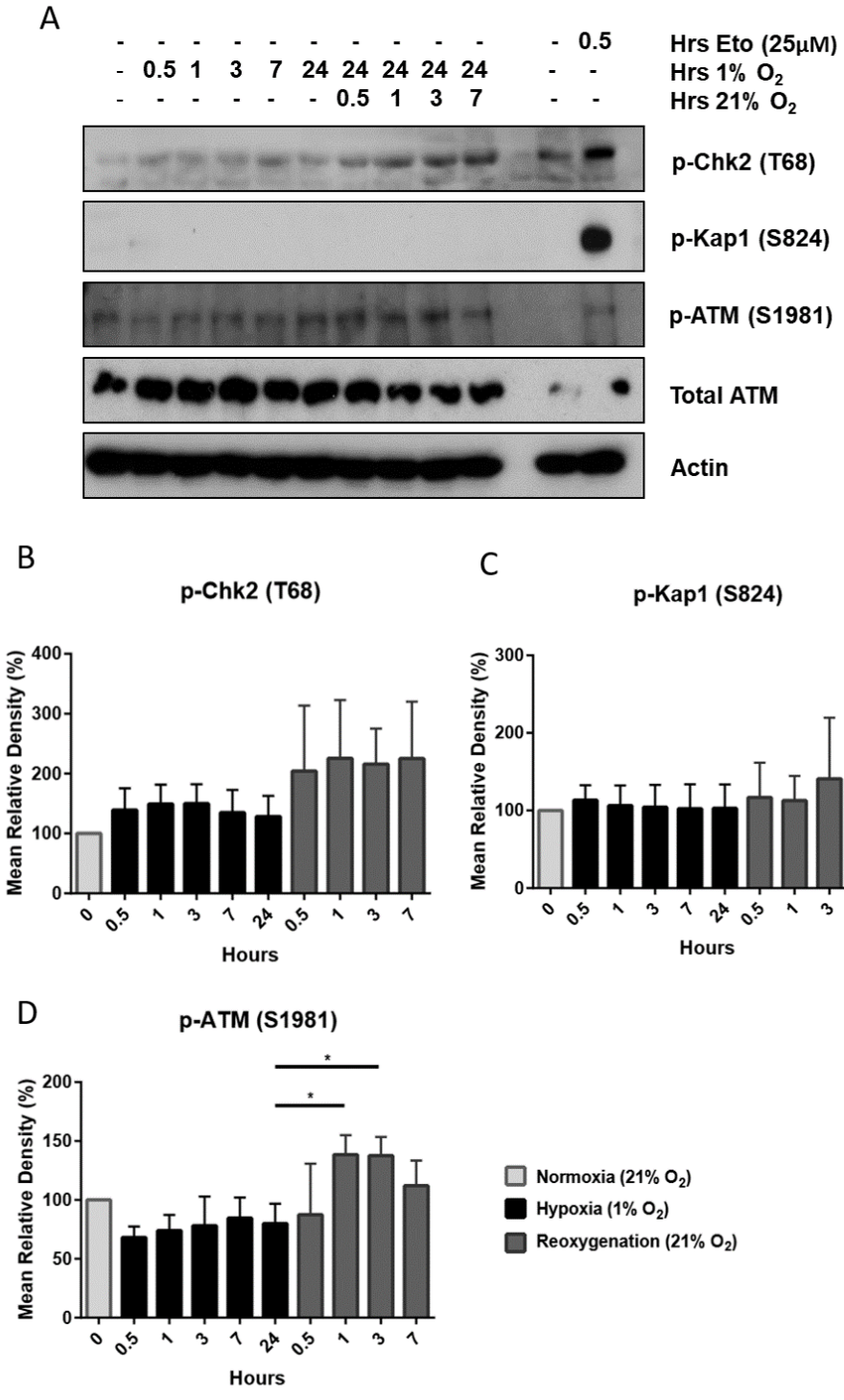

Figure 72. Rapid Reoxygenation leads to ATM Phosphorylation in U-2 OS Cells. Cells were exposed to hypoxia (1% O_2) for between 30 minutes and 24 hours, or reoxygenated (21% O_2) after 24 hours in hypoxia for between 30 minutes and 7 hours. Western blots were carried out probing for phsophorylation of ATM and its downstream targets Kap1 and Chk2. A 30 minute 25μM etoposide treatment was run as well as a positive control. A - Representative blot of 3 independent experiments. B-D - Relative band density (n = 3) presented as mean, statistical analyses were carried out using one-way ANOVA (Sidak's test).

occurs concerns ATM phosphorylation. These data implicates ATM in the response of cells to reoxygenation but not hypoxia.

In contrast to the previous blot that showed the response of these proteins to hydrogen peroxide treatment (Fig. 71), no genotoxic stress is induced in the response to hypoxia and reoxygenation as measured by phosphorylation of Kap1. Here we observe activation of ATM in the absence of genotoxic stress, indicating that oxidative stress alone is causing this response [225]. Together with the γH2AX data (Fig. 67) this indicates that DNA damage does not occur following reoxygenation, and suggests that the activation of H2AX during hypoxia as shown in figure 67 is a result of ATR responding to single strand breaks as described previously [193].

To determine whether ATM acts as an upstream kinase in the NF-κB response to rapid reoxygenation, experiments were carried out using the small molecule inhibitor of ATM; KU-55933 [376] (Fig. 73). This is a direct repeat of the experiment presented earlier (Fig. 52), albeit using a different inhibitor that targets ATM rather than IKKα.

Following rapid reoxygenation phosphorylation of all protein markers of canonical NF-κB pathway activation occurs, however in this set of experiments this is only significant with regard to IκBα phosphorylation (Fig. 73). Treatment with the small molecule inhibitor of ATM, KU-55933, has no significant effect on the levels of phosphorylation of the proteins analysed here. This demonstrates that activation of the canonical NF-κB pathway following reoxygenation is not dependent on ATM based on the assumption that this inhibitor is working as anticipated.

Earlier studies have implicated ATM in the response to reoxygenation [226], therefore the results observed in figure 73 were unexpected. Of course, one explanation for this discrepancy is that the data presented in this thesis was carried out using a modified reoxygenation protocol. Regardless, to confirm that the results presented here are not due to an ineffective inhibitor, experiments were designed to confirm that KU-55933 was functioning as expected. It is well established that ATM is involved in the response to etoposide-induced genotoxic stress through DNA damage response signalling and through the canonical NF-κB pathway. An etoposide treatment time course was therefore carried out with and without inhibition of ATM using KU-55933. Western blots were carried out on whole cell lysates, probing for markers of canonical NF-κB activation or the ATM-controlled DNA damage response.

The results of this experiment shows that etoposide treatment leads to significant phosphorylation of all members of the canonical NF-κB members analysed here (Fig. 74), demonstrating clearly that this pathway is activated in response to etoposide. Inhibition of ATM using KU-55933 significantly attenuates this activation in the case of IKKα/β and RelA phosphorylation. An insignificant decrease in IκBα phosphorylation is also observed. Treatment with the ATM inhibitor blocks signalling through the canonical NF-κB pathway in response to etoposide treatment.

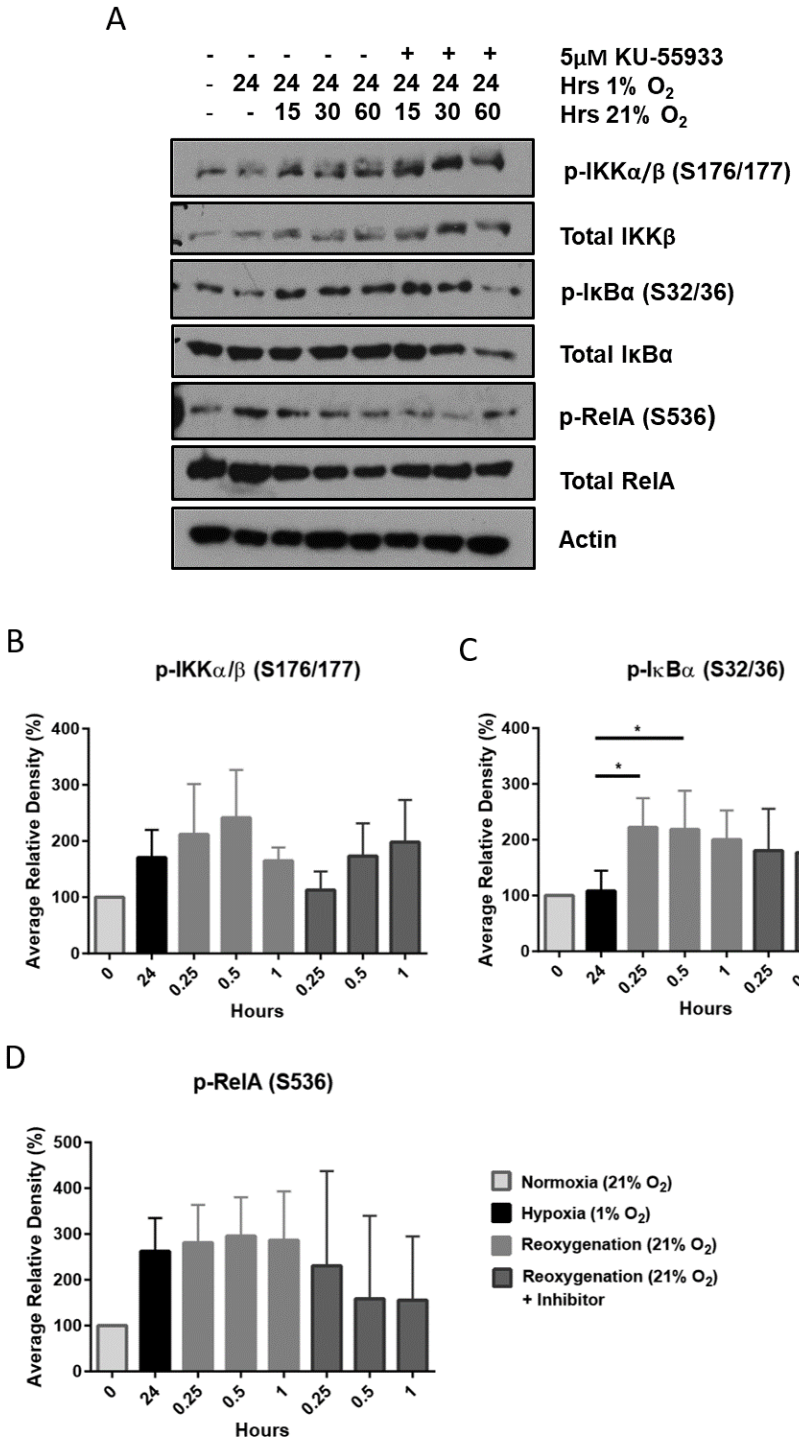

Figure 73. ATM Inhibition does not affect Canonical NF-κB Activation following Rapid Reoxygenation in U-2 OS Cells. U-2 OS cells were exposed to 1% O_2 for 24 hours prior to rapid reoxygenation for the times indicated, with or without treatment with 5μM of the inhibitor of ATM, KU-55933. Whole cell extracts were harvested using urea lysis buffer with added protease inhibitors and western blots were performed probing for proteins and phosphorylation events associated with canonical NF-κB activation. A - Representative blot of 3 independent experiments. B-D - Relative band density (n = 3) presented as mean, statistical analyses were carried out using one-way ANOVA (Sidak's test).

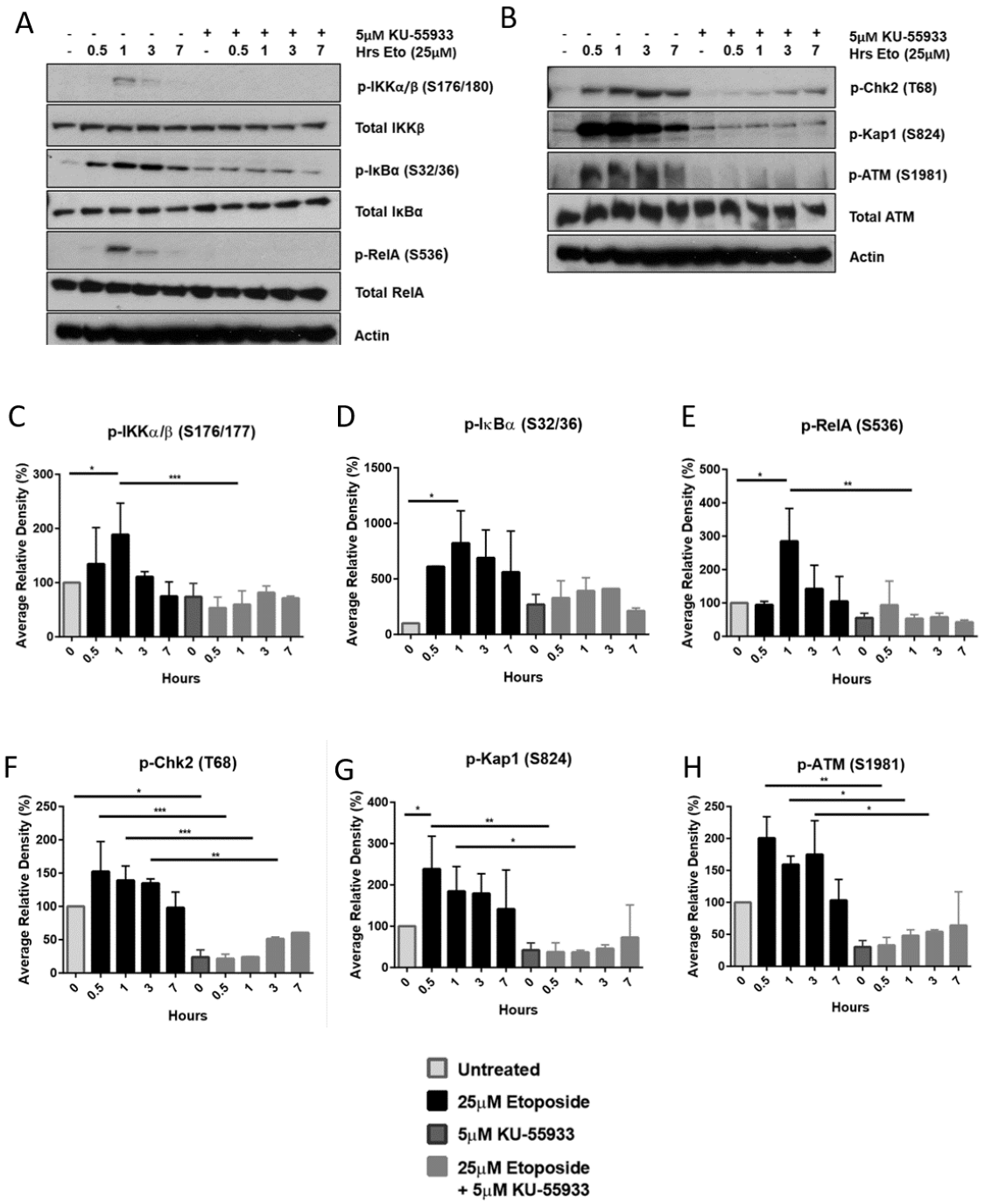

Figure 74. ATM Inhibition blocks Canonical NF-κB Activation and the DNA Damage Response following Etoposide Treatment in U-2 OS Cells. U-2 OS cells were treated with 25μM etoposide for the times indicated, with or without treatment with 5μM KU-55933. Whole cell extracts were harvested using urea lysis buffer with added protease inhibitors and western blots were performed probing for phosphorylation events associated with canonical NF-κB activation (A) or ATM activation (B). A-B - Representative blot of 3 independent experiments. C-H - Relative band density (n = 3) presented as mean, statistical analyses were carried out using one-way ANOVA (Sidak's test).

A significant increase in phosphorylation of all markers of ATM activation also occurs following treatment with etoposide (Fig. 74), demonstrating that etoposide treatment is causing genotoxic stress as expected. In addition to this, inhibition of ATM using KU-55933 significantly blocks this activation of ATM and its downstream targets. Together the data presented in figure 74 demonstrate that the ATM inhibitor is functioning correctly as it blocks signalling through these two well-established signalling pathways.

6.4 A Role for ATR in the Canonical NF-κB Pathway Response to Hypoxia and Rapid Reoxygenation

Another PIKK family member, ATR, has also been implicated in the response to hypoxia and reoxygenation [226][381]. These studies demonstrated that ATR is able to phosphorylate H2AX in the response to hypoxia-induced DNA damage [226], while others have demonstrated that this process can occur following hydrogen peroxide treatment in the absence of double-strand breaks [193]. Data presented in the previous section has shown that ATR is phosphorylated in response to hydrogen peroxide treatment. The results of the γH2AX stain indicate that no double strand breaks occur following reoxygenation, however ATR responds to single strand breaks and is able to phosphorylate H2AX in response to these [193].

This section therefore aimed to determine whether ATR could have a role in the NF-κB response to hypoxia and rapid reoxygenation. The following experiment was carried out as described earlier (Fig. 39), however blots were probed for phosphorylation events associated with ATR activation; the auto-phosphorylation sites on both ATR and its downstream kinase Chk1.

No significant increase in activation is observed following hypoxia, however significant auto-phosphorylation of both ATR and Chk1 occurs following reoxygenation (Fig. 75). This demonstrates that ATR is activated in the response to reoxygenation, it then most likely phosphorylates and activates Chk1, potentially to control progression through the cell cycle. Of course the increase in Chk1 activation could be due to phosphorylation from a second upstream kinase. The phosphorylation site analysed here is an auto-phosphorylation site that Chk1 auto-phosphorylates following a seperate phosphorylation from an upstream kinase at independent sites. Chk1 is phosphorylated by the active ATR on serines 317 and 345 prior to coordinating its autophosphorylation of serine 298 [382].

The results presented in figure 75 implicate ATR as an important protein in the cellular response to rapid reoxygenation-induced oxidative stress. To determine whether this activation of ATR is linked to the activation of the canonical NF-κB pathway experiments were carried out using the widely-used small molecular inhibitor of ATR, VE-821 [383][384]. VE-821 is a potent ATP-competitive inhibitor of ATR and has a half life of 3.17 days [351]. According to the data sheet provided, it has minimal off-target effects on other closely related PIKKs and against other kinases tested [385].

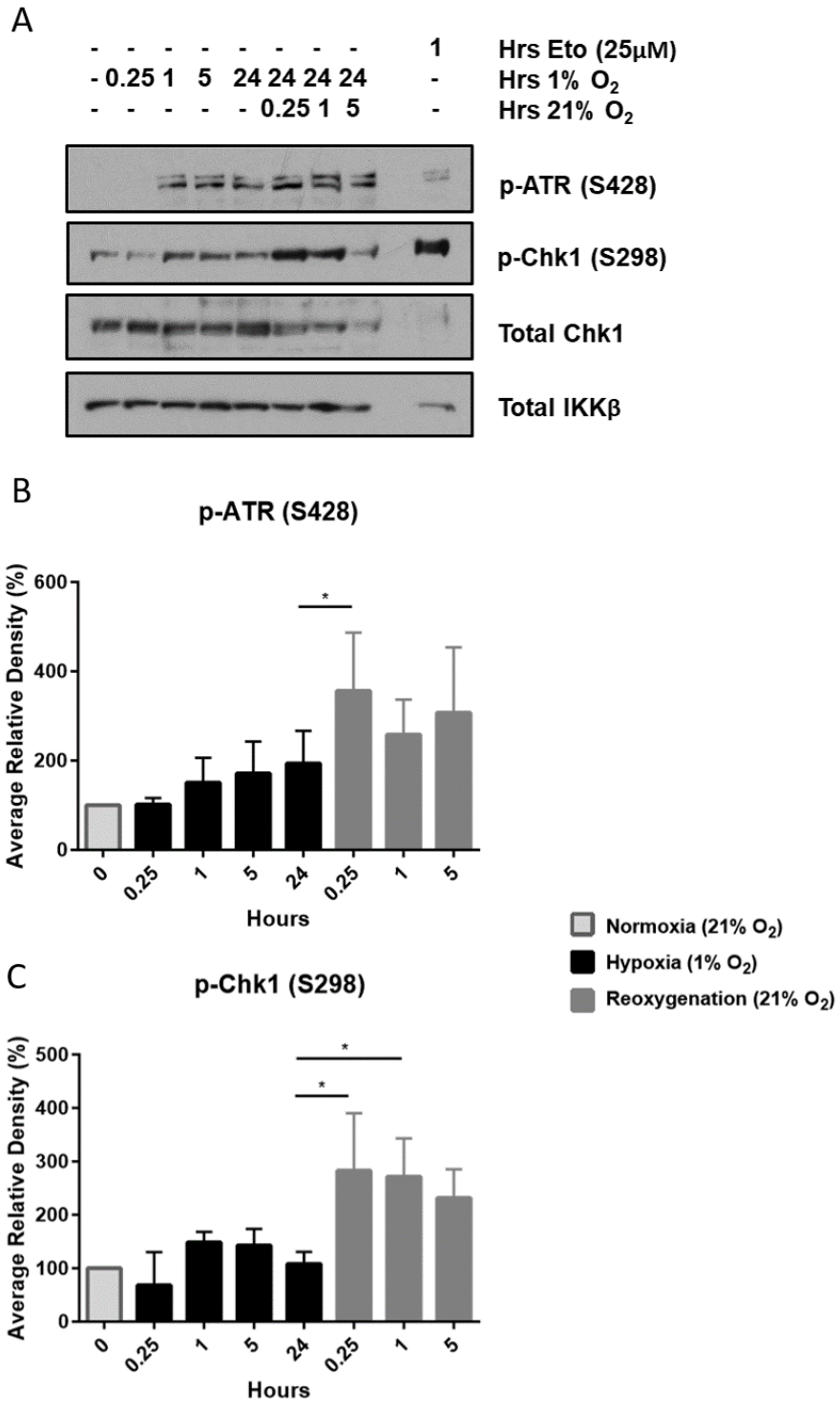

Figure 75. ATR and Chk1 are Activated following Rapid Reoxygenation in U-2 OS Cells. U-2 OS cells were exposed to 1% O_2 for the times indicated. Reoxygenated samples were exposed to hypoxia for 24 hours prior to rapid reoxygenation. Cells were lysed using urea lysis buffer with added protease inhibitors and western blots were performed probing for activation of ATR and Chk1. 1 hour of etoposide treatment was used as a positive control. A - Representative blot of 3 independent experiments. B-C - Relative band density (n = 3) presented as mean, statistical analyses were carried out using one-way ANOVA (Sidak's test).

This is a direct repeat of the experiments presented earlier (Fig. 52 and 73), however cells were targeted for ATR inhibition using 10μM of the competitive inhibitor VE-821 [386]. Timings and doses were again determined through personal communication with colleagues that commonly use this inhibitor on U-2 OS cells.

As determined previously, rapid reoxygenation leads to the activation of the canonical NF-κB pathway as measured by phosphorylation of IκBα and RelA; in this set of experiments this is only statistically significant in the case of IκBα (Fig. 76). Treatment with the ATR inhibitor reduces this activation across all time points measured for both proteins, however relative band density analysis has revealed that this difference is significant with regard to IκBα but not RelA. As perhaps the most reliable read-out of canonical NF-κB activation presented in this thesis, this significant decrease in phospho-IκBα levels suggests that ATR is involved in the canonical NF-κB response to reoxygenation.

Since ATR has been shown to have a role upstream of the canonical NF-κB pathway in response to reoxygenation the role of its downstream target Chk1 was investigated. Data presented in this thesis has already demonstrated that Chk1 is activated in the response to reoxygenation (Fig. 75), however whether this has a direct role in the activation of the canonical NF-κB pathway is unknown. To investigate the role of Chk1 in the response to rapid reoxygenation the previous experiments (Fig. 52, 73 and 76) were repeated for the 15 minutes and 1 hour time points using a Chk1 inhibitor; CCT245737 [387]. This inhibitor has over 1,000-fold selectivity over Chk2 and CDK1 [388], the predicted half life of this inhibitor is 2.86 hours [387], although shorter than the other inhibitors used, this is still longer than the time points used in this experiment.

Cells targeted for Chk1 inhibition were pretreated with 5μM of the ATP-competitive Chk1 inhibitor for 30 minutes prior to rapid reoxygenation (dosing and timings determined by personal communication). Since the upstream kinases, ATR and ATM, have been implicated in this response, they were targeted with small molecule inhibitors (10μM of VE-821 and 5μM KU-55399 respectively), allowing for direct comparisons of effects. Western blots were probed for markers of PIKK pathway activation and markers of canonical NF-κB pathway activation.

Although earlier figures showed a significant increase in ATM, ATR and Chk1 phosphorylation following reoxygenation (Fig. 72 and 75), only Chk1 phosphorylation shows a significant increase in phosphorylation in figure 77. These discrepancies are most likely due to variability in the quality of the western blots, either due to problems associated with the antibodies or due to technical issues.

The effects of inhibition of either Chk1, ATR or ATM are predominantly insignificant regarding the activation of the PIKK pathway members. The exception to this is observed in figure 77E, where treatment with the Chk1 inhibitor significantly reduces autophosphorylation and activation of Chk1.

As established previously, activation of the canonical NF-κB pathway occurs following

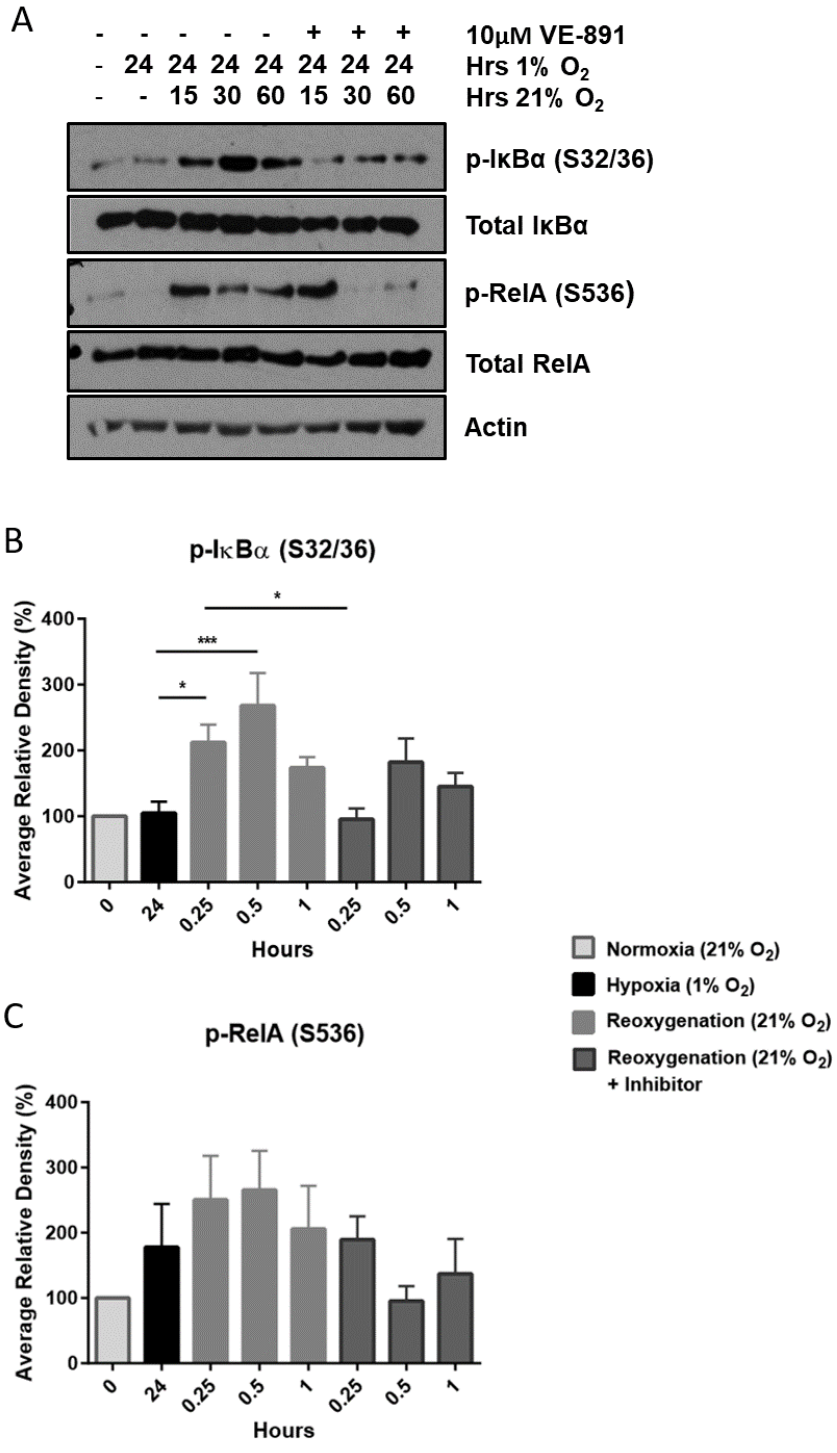

Figure 76. The Effect of ATR Inhibition on Canonical NF-κB Activation following Rapid Reoxygenation in U-2 OS Cells. U-2 OS cells were exposed to 1% O_2 for 24 hours prior to rapid reoxygenation for the times indicated, with or without treatment with 10μM of the small molecule inhibitor of ATR, VE-821. Whole cell extracts were harvested using urea lysis buffer with added protease inhibitors and western blots were performed probing for proteins and phosphorylation events associated with canonical NF-κB activation. A - Representative blot of 3 independent experiments. B-C - Mean relative band density (n = 3), statistical analyses were carried out using one-way ANOVA (Sidak's test).

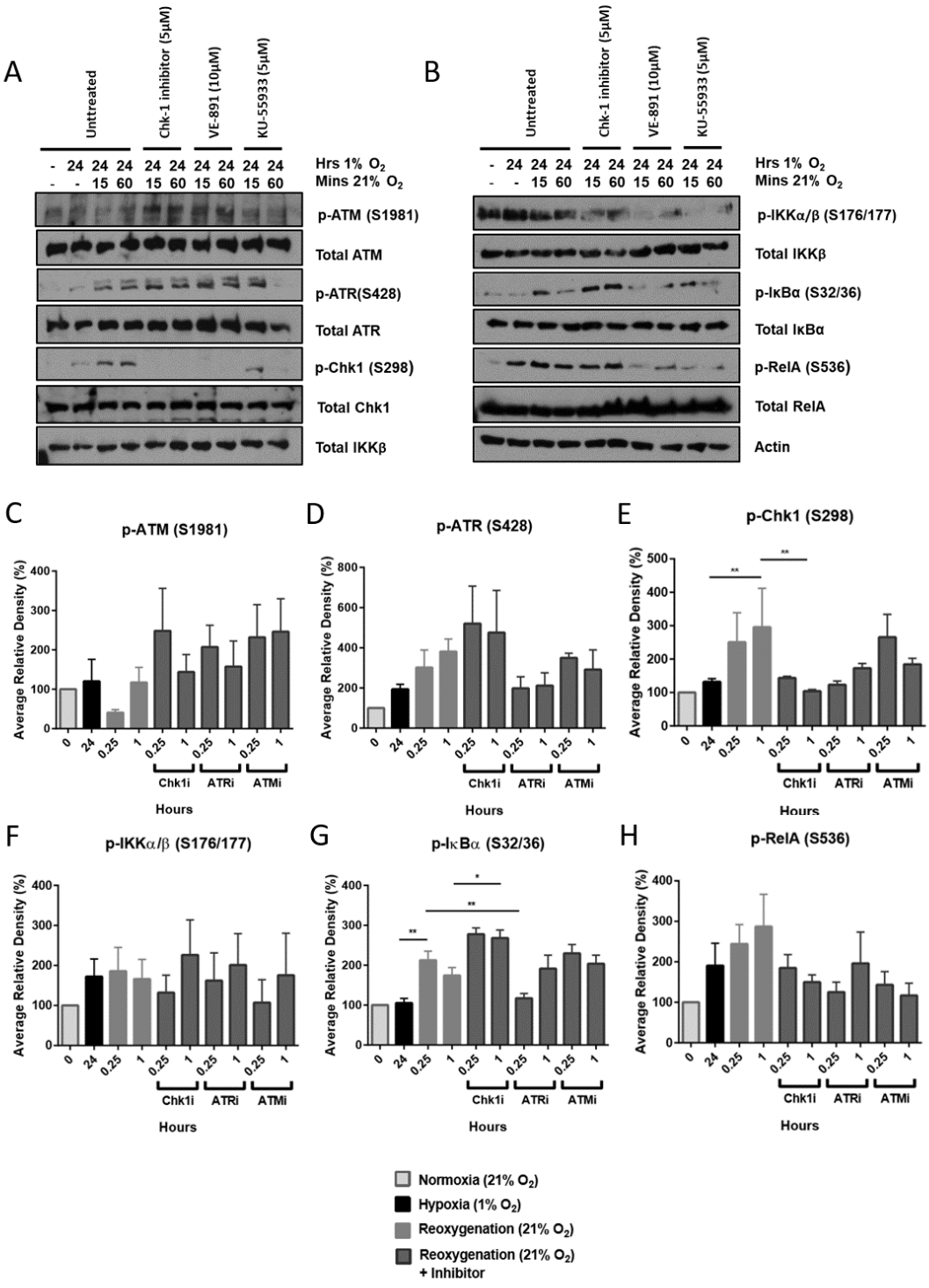

Figure 77. The Effects of Inhibition of Chk1, ATR and ATM on PIKK Signalling and NF-κB Activation following Rapid Reoxygenation in U-2 OS Cells. U-2 OS cells were exposed to hypoxia for 24 hours prior to rapid reoxygenation, with or without treatment with inhibitors of Chk1 (5μM), ATR (10μM) or ATM (5μM). Whole cell extracts were harvested using urea lysis buffer with added protease inhibitors and western blots were performed probing for phosphorylation events associated with PIKK or canonical NF-κB activation. A-B - Representative blot of 3 independent experiments. C-H - Relative density (n = 3), statistical analyses were carried out using one-way ANOVA (Sidak's test).

reoxygenation, as observed by a significant increase in IκBα phosphorylation (Fig. 77G). No significant change in IKKα/β or RelA phosphorylation is observed, in spite of the increase in the mean relative density of the latter. As shown previously, treatment with the ATM inhibitor has no effect on canonical NF-κB signalling, while treatment with the ATR inhibitor causes a significant decrease in activation as measured by IκBα phosphorylation (Fig. 77G). This confirms earlier findings that ATR, and not ATM, acts upstream of the canonical NF-κB pathway in response to reoxygenation.

Interestingly, treatment with the Chk1 inhibitor leads to a significant increase in IκBα phosphorylation following reoxygenation (Fig. 77G). This is indicative of a feedback loop where the cell tries to compensate for the loss of active Chk1. Perhaps in this case a cell cycle response fails, triggering further activation of ATR and a stronger canonical NF-κB pathway response. Further investigations should be carried out to investigate this hypothesis.

6.5 Localisation of ATM and ATR following Hypoxia and Reoxygenation

To assess the cellular location of ATR and ATM following hypoxia and rapid reoxygenation, the experiment presented in figure 56 was repeated. This time however membranes were probed for total ATR and total ATM. The data presented in figure 78 shows no significant changes in cellular localisation of ATR or ATM, or phosphorylation of ATR based on sub-cellular location.

Although not significant, an increase in cytoplasmic ATR and ATM is observed reoxygenation. Further experiments should be carried out using alternative techniques to determine whether this is truly occurring. As discussed earlier this method of determining sub-cellular location of proteins of interest has a high degree of variability between repeats, and therefore future work should be carried out to supplement these experiments.

6.6 NF-κB Controlled Gene Transcription After Hypoxia and Rapid Reoxygenation is Affected by Inhibition of Upstream Components

The previous section has explored the roles of ATM and ATR as upstream kinases in the NF-κB response to rapid reoxygenation, highlighting ATR as the main kinase responsible for the transduction of signal downstream through the canonical NF-κB pathway. The effects of ATM or ATR inhibition on gene transcription following hypoxia or reoxygenation is currently unknown. However, data presented in sections 6.3 and 6.4 suggest that ATM inhibition will have no effect, while ATR inhibition will.

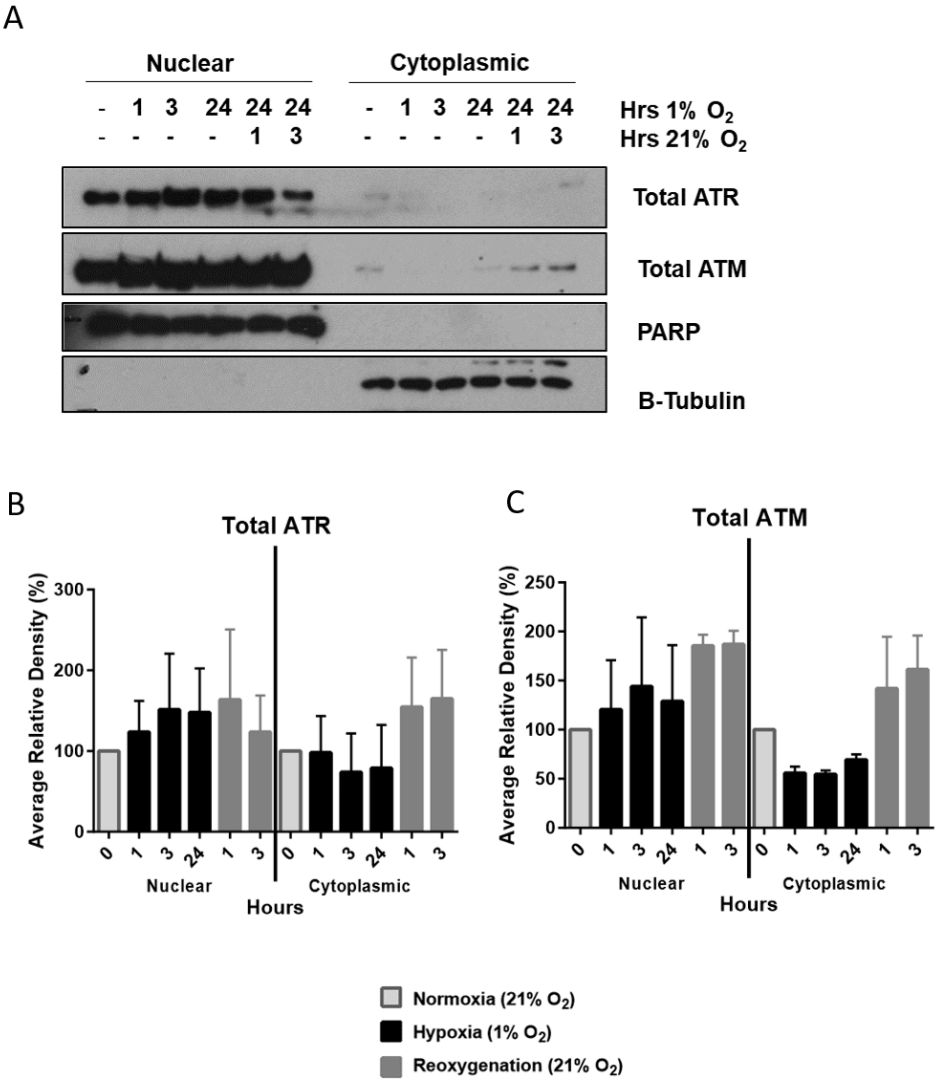

Figure 78. The Effects of Hypoxia and Rapid Reoxygenation on Sub-cellular Location of ATR and ATM. U-2 OS cells were exposed to 1% O_2 for the indicated times. Reoxygenated samples were exposed to 1% O_2 for 24 hours prior to rapid reoxygenation. Nuclear and cytoplasmic proteins were extracted and analysed by western blot probing for ATR and ATM. A - Representative blot of 3 independent experiments. B-D - Relative density (n = 3), statistical analyses were carried out using one-way ANOVA (Sidak's test).

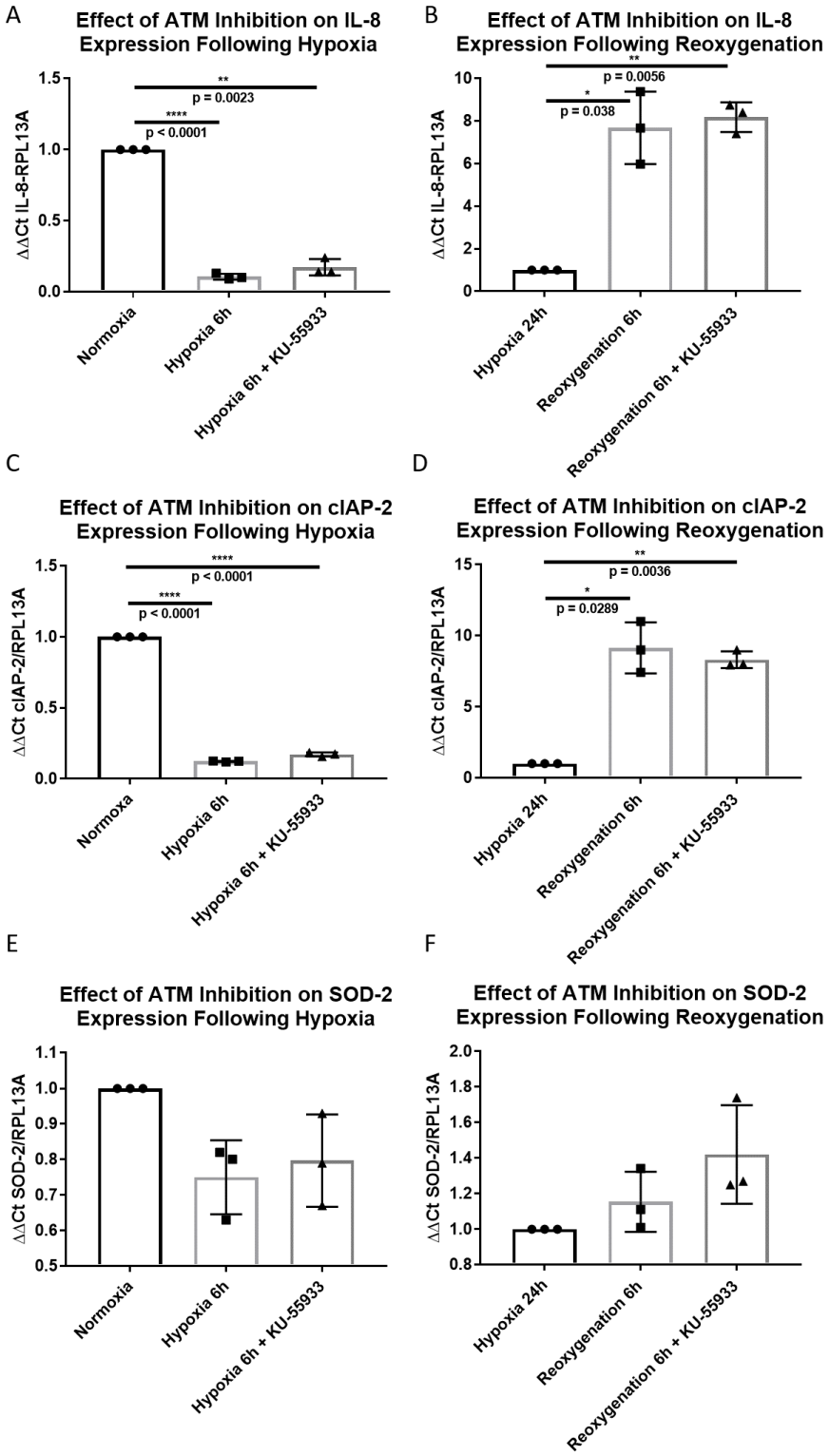

Figure 79. Treatment of U-2 OS cells with the ATM Inhibitor KU-55399 Does Not Affect Gene Expression following Hypoxia and Rapid Reoxygenation. U-2 OS cells were exposed to 1% O_2 for 6 hours. Reoxygenated samples were exposed to 1% O_2 for 24 hours prior to rapid reoxygenation. Total RNA was extracted, reverse transcription was performed and cDNA was analysed (A B = IL-8, C D = cIAP-2, E F = SOD-2) by qPCR using RPL13A as a reference gene. The Δ Δ Ct method of analysis was used, normalising hypoxia samples to normoxia samples and reoxygenated samples to 24 hour hypoxia samples. Statistical analysis was carried out using one-way ANOVA (Tukey's test).

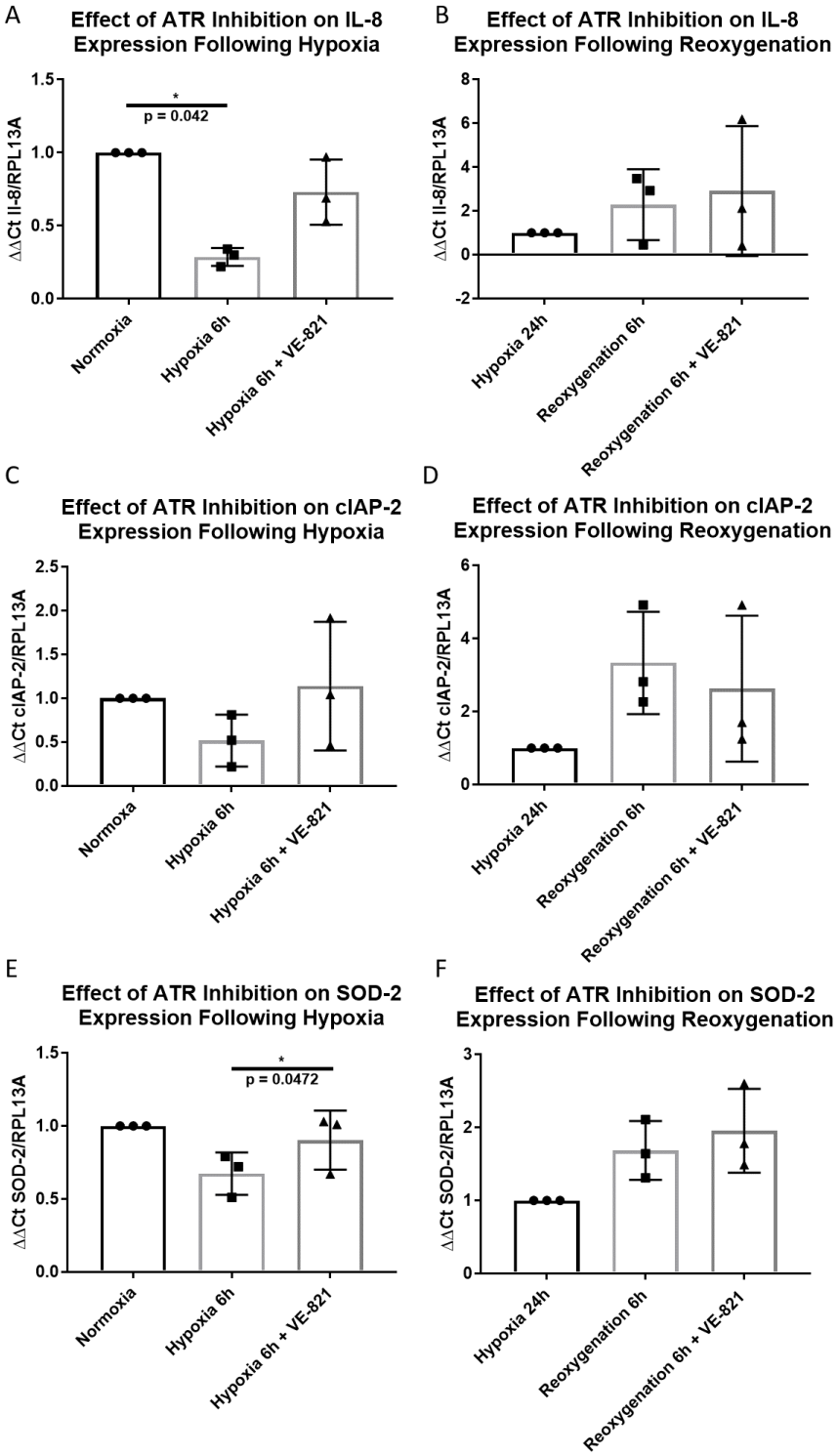

Figure 80. Treatment of U-2 OS cells with the ATR Inhibitor VE-821 affects Gene Expression following Hypoxia and Rapid Reoxygenation. U-2 OS cells were exposed to 1% O_2 for 6 hours. Reoxygenated samples were exposed to 1% O_2 for 24 hours prior to rapid reoxygenation. Total RNA was extracted, reverse transcription was performed and cDNA was analysed by qPCR using RPL13A as a reference gene. The Δ Δ Ct method of analysis was used, normalising hypoxia samples to normoxia samples and reoxygenated samples to 24 hour hypoxia samples. Statistical analysis was carried out using one-way ANOVA using Tukey's test for multiple comparisons.

The following experiments aimed to determine whether treatment of cells with small molecule inhibitors of ATM or ATR affects transcription of NF-κB target genes, IL-8, c-IAP-2 or SOD-2, following both hypoxia and rapid reoxygenation. Experiments were carried out as described earlier (Fig. 60), using 5μM of KU-55399 to inhibit ATM.

As seen previously, expression of IL-8 and cIAP-2 significantly decreases following exposure to hypoxia for 6 hours ($p < 0.0001$) and increases following reoxygenation (Fig. 79). Changes in SOD-2 expression are also observed as before but the 3 experiments presented here do not give significant results. As expected, inhibition of ATM using KU-55399 has no significant effect on the expression of any of these genes. Indicating that ATM is not directly involved in the activation of the canonical NF-κB pathway following hypoxia and rapid reoxygenation.

To assess the role of ATR in the response to hypoxia and reoxygenation cells were pretreated with 10μM of VE-821 as described in previous experiments (Fig. 76). In this set of experiments, expression of IL-8, cIAP-2 and SOD-2 decreases following hypoxia and increases following reoxygenation (Fig. 80) as observed in experiments presented in section 4.7. In this set of experiments however, the only significant changes in gene expression concern IL-8 following hypoxia. Indeed, inhibition of ATR has no significant effect on the expression of any of these target genes, however during hypoxia time points it appears to consistently prevent repression of these genes. Further repeats of the experiment would increase the experimental power and perhaps increase confidence in the data set.

The results presented in this section have demonstrated that ATR could play a role in the control of NF-κB gene expression following exposure to hypoxia, however further repeats should be carried out before any firm conclusions can be made. As expected, inhibition of ATM has no effect on the expression of IL-8, cIAP-2 and SOD-2. This is concordant with previous work that indicates that although is is activated in response to reoxygenation, it does not appear to play a role in the activation of the canonical NF-κB pathway.

6.7 The Role for ATM and ATR in Cell Proliferation after Hypoxia and Rapid Reoxygenation

Data presented in chapters 1 and 2 demonstrated that both hypoxia and rapid reoxygenation lead to significant changes in proliferation of U-2 OS cells, and that both IKKα and IKKβ are involved in this response. Exposure to hypoxia leads to a decrease in proliferation, while reoxygenation leads to an increase in proliferation after 24 hours but levels decrease again following 48 hours. Inhibition of IKKα or IKKβ has shown to decrease proliferation further following hypoxia and following 48 hours of reoxygenation.

This section aimed to further analyse the changes in proliferation following hypoxia and reoxygenation through inhibition of other proteins investigated in this project; ATM and ATR. As demonstrated earlier in this thesis, these upstream kinases have been implicated

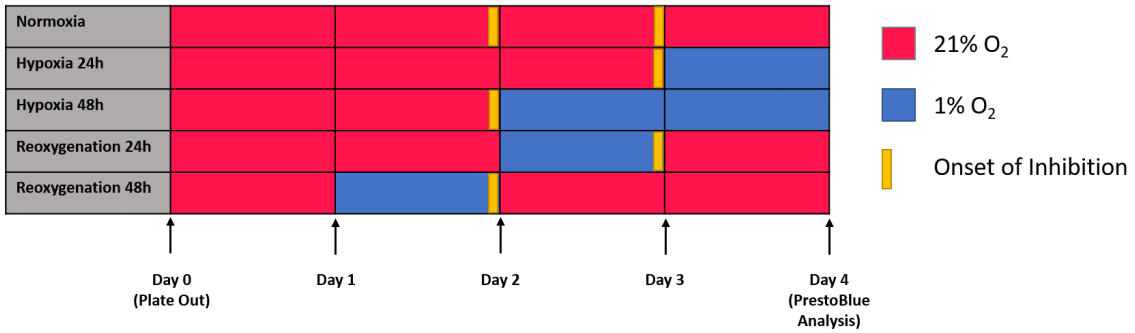

Figure 81. Schematic of Hypoxia and Rapid Reoxygenation Time Course for Proliferation Assays. U-2 OS cells were plated out at 2,500 cells per well in 96-well plates on day zero and incubated in normoxic conditions for at least 24 hours. Plates were then moved to and from the anaerobic chamber as the schematic demonstrates over the course of 4 days. For example the 24 hour reoxygenation plates were moved into 1% O_2 on day 2, 48 hours after plating out, and returned to 21% O_2 after 24 hours for a further 24 hours before reading proliferation by PrestoBlue. Inhibition of proteins in selected wells was carried out, these were treated either 24 hours or 48 hours prior to harvesting and throughout the remainder of the experiment. For example a selection of the normoxia only cells were treated for 24 hours prior to analysis, while another set were treated for 48 hours prior to analysis.

in the response to hypoxia and rapid reoxygenation, but only the latter appears to be involved in the canonical NF-κB pathway response to these stresses.

The time courses carried out in this section followed the same treatment times and exposure to changes in gas levels as described in chapter 5, except this time cells were treated with ATM or ATR inhibitors (Fig. 81). As before, to determine the effects of these inhibitors on otherwise untreated cells, normoxia only cells were dosed with inhibitors for 24 or 48 hours. Treatment of normoxia only cells with 5μM of the ATM inhibitor KU-55399 alone does not affect proliferation of U-2 OS cells to a significant level (Fig. 82).

As observed in previous experiments, hypoxia exposure leads to a decrease in proliferation of U-2 OS cells (Fig. 83). Treatment of cells with the ATM inhibitor KU-55399 caused a significant decrease in proliferation following 24 hours hypoxia. Since no significant effect is observed in inhibitor only treated cells (Fig. 82) we can conclude that this is due to the additive effects of hypoxia exposure and the presence of the inhibitor. No significant difference in proliferation is observed following ATM inhibition following 48 hours of hypoxia exposure. This indicates that ATM could be involved in the response to hypoxia in the first 24 hours of exposure.

Previous experiments presented here have shown that rapid reoxygenation has a significant effect on proliferation (Fig. 83). The data presented in figure 83 however show no significant changes in proliferation following reoxygenation. In addition, ATM inhibition

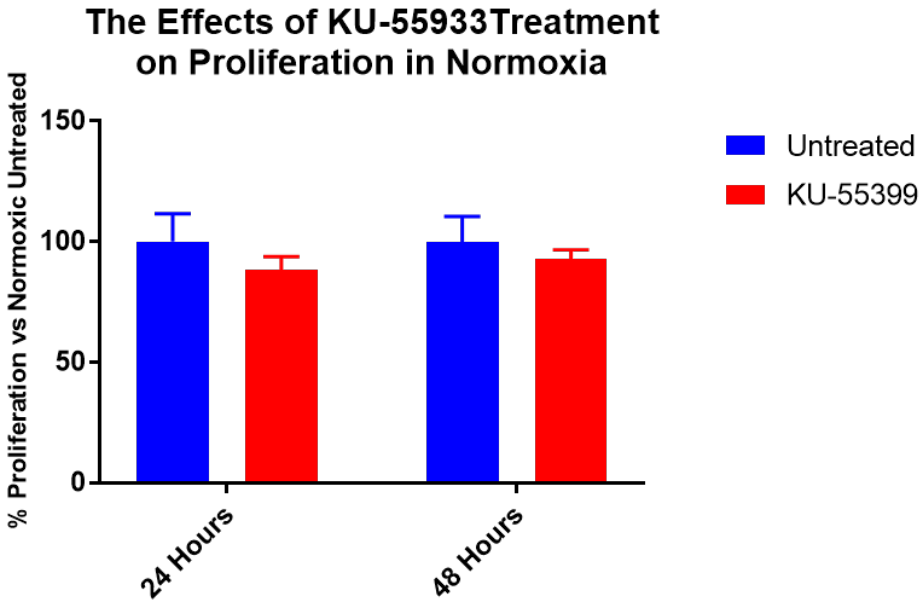

Figure 82. The Effects of KU-55933 Treatment on Proliferation of U-2 OS Cells. U-2 OS cells were treated with 5μM of a small molecular inhibitor to ATM, KU-55933, in normoxic conditions for 24 or 48 hours to assess the effects of this inhibitor on proliferation in the absence of other stimuli. Proliferation was analysed using PrestoBlue. Graphs were plotted using GraphPad prism and two-way ANOVA analyses were carried out using Tukey's test to account for multiple comparisons.

has no significant effect on proliferation following reoxygenation (Fig. 83). Overall the data presented in figure 83 indicate a role for ATM in the control of proliferation in the first 24 hours of hypoxia exposure but not during reoxygenation.

Since ATR has been shown to be involved upstream of the canonical NF-κB in response to reoxygenation (Fig. 76), its role in control of proliferation was analysed in the same manner. Previous work has shown that ATR's downstream target Chk1 is activated in the response to rapid reoxygenation, presumably to control cell cycle progression.

Again, initial experiments aimed to determine the effects of the inhibitor of ATR, VE-821, on proliferation of cells in the absence of other stimuli. Here, normoxia only cells were treated with 10μM of the ATR inhibitor VE-821 for 24 or 48 hours (Fig. 84). A significant reduction in proliferation is observed following 24 hours (25%) and 48 hours (50%) of VE-821 treatment. These results demonstrate that even in the absence of other stimuli, dosing of cells with the ATR inhibitor leads to a reduction in proliferation. It is important to note that this effect of ATR inhibition in the absence of other stimuli could be having an effect on proliferation due to mild oxidative and replicative stress induced as the cells grow at 21% O_2. This level of oxygen is far higher than levels observed *in vivo* therefore cells are more likely to obtain oxidative damage even in the absence of other stimuli.

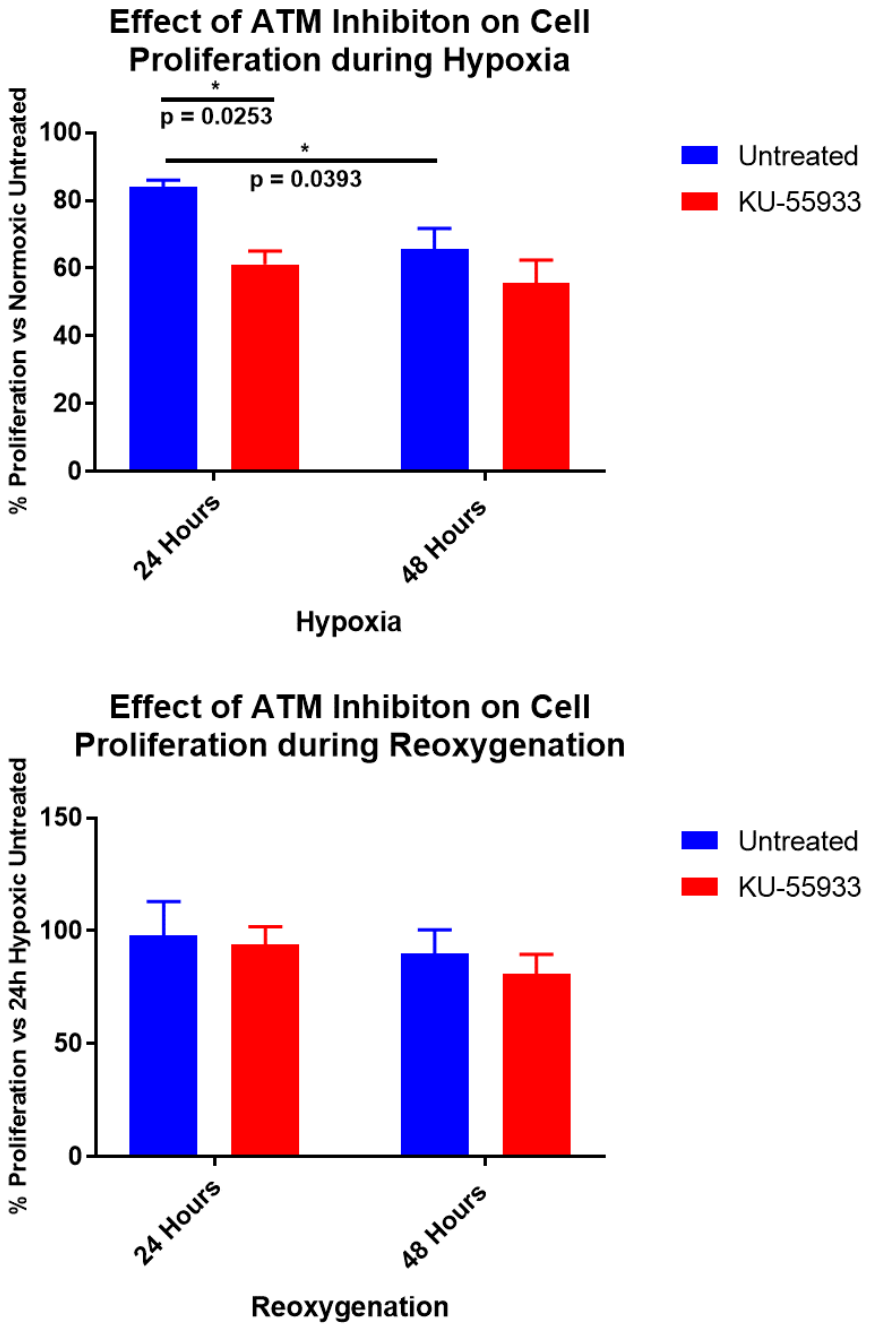

Figure 83. The Effects of Hypoxia and Rapid Reoxygenation on Proliferation of U-2 OS Cells Following ATM Inhibition. U-2 OS cells were treated as described in figure 61, however a subset of cells were treated with 5μM of a small molecular inhibitor to ATM, KU-55399, prior to final exposure to hypoxia and rapid reoxygenation and for the remainder of the time course. Proliferation was analysed using PrestoBlue after 1 hour. Graphs were plotted using GraphPad prism to determine the effect of hypoxia exposure on cells compared with normoxia only cells, and to compare the effects of reoxygenation on cells compared with cells exposed to hypoxia for 24 hours. Two-way ANOVA analyses were carried out using Tukey's test to account for multiple comparisons.

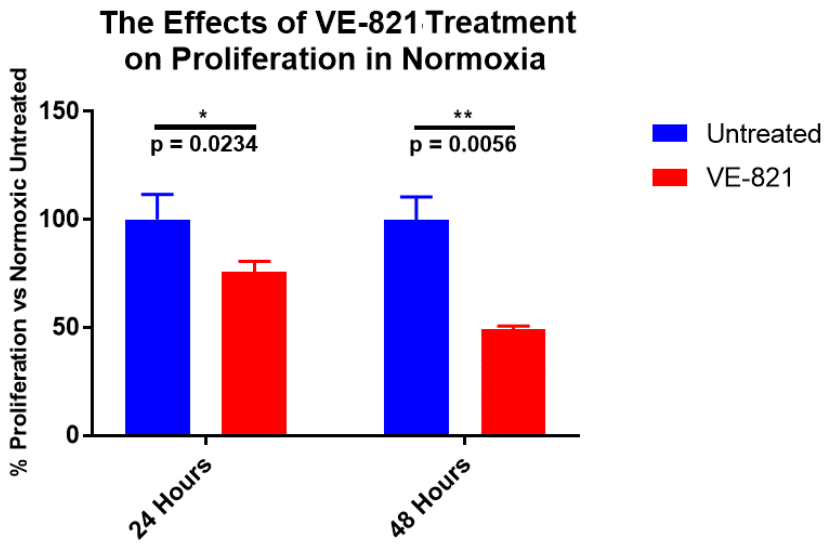

Figure 84. The Effects of VE-821 Treatment on Proliferation of U-2 OS Cells. U-2 OS cells were treated with 10μM of a small molecular inhibitor to ATR, VE-821, in normoxic conditions for 24 or 48 hours to assess the effects of this inhibitor on proliferation in the absence of other stimuli. Proliferation was analysed using PrestoBlue. Graphs were plotted using GraphPad prism and two-way ANOVA analyses were carried out using Tukey's test to account for multiple comparisons.

As seen before, following exposure to hypoxia proliferation of cells decreases (Fig. 85). Treatment with the small molecule inhibitor of ATR, VE-821, leads to a significant decrease in this proliferation. This could predominantly be due to the fact that inhibitor treatment in the absence of other stimuli leads to a decrease in proliferation, however the effect is larger in hypoxic conditions. This indicates that ATR plays a role in the control of proliferation of cells following hypoxia exposure.

Reoxygenation does not have as profound an effect as observed in other experiments (Fig. 50), however it is still possible to determine the effects of ATR inhibition on proliferation in these samples. Although data presented in figure 85 shows that treatment with VE-821 significantly decreases proliferation following reoxygenation, this decrease in proliferation following treatment is very similar to that observed when normoxia only cells are treated with the inhibitor. It is therefore impossible to say with confidence that ATR plays a role in proliferation of cells following reoxygenation.

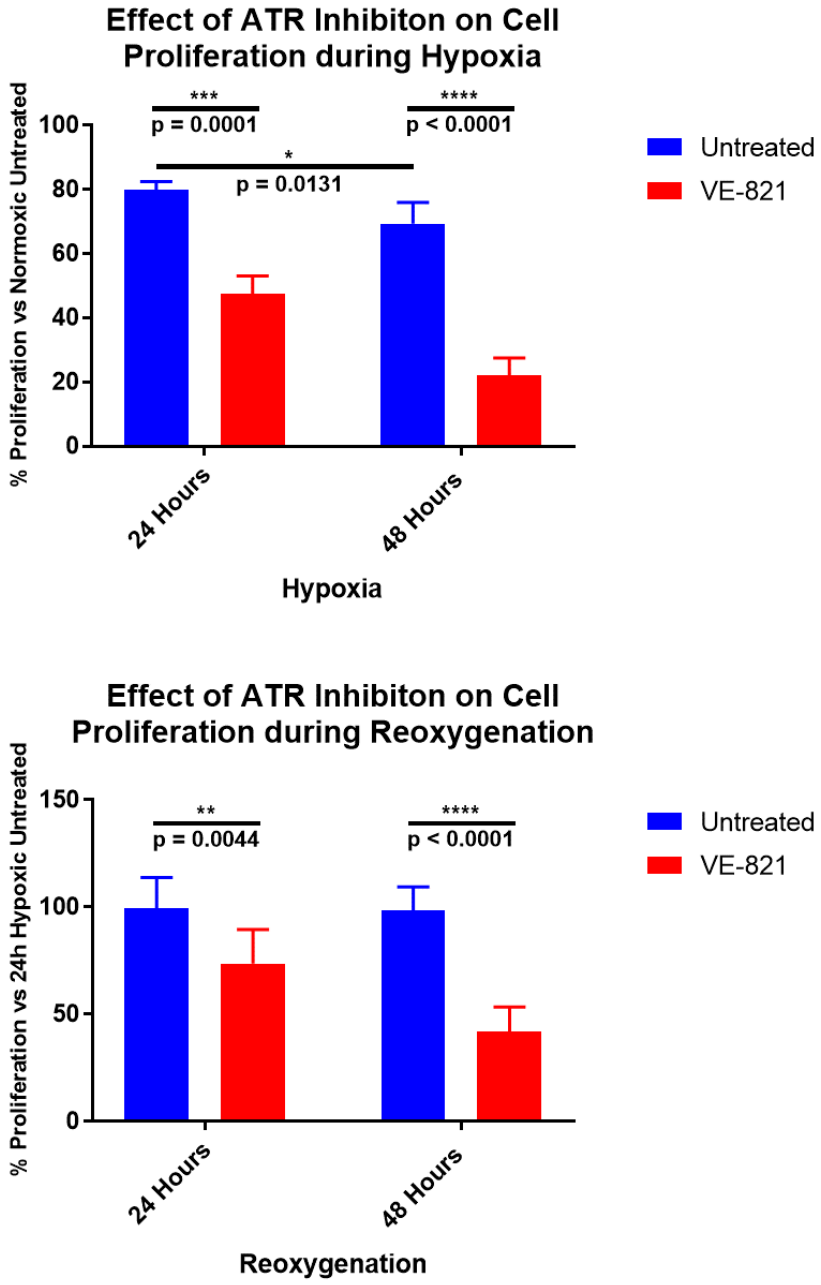

Figure 85. The Effects of Hypoxia and Rapid Reoxygenation on Proliferation of U-2 OS Cells Following ATR Inhibition. U-2 OS cells were treated as described in figure 61, however a subset of cells were treated with 10μM of a small molecular inhibitor to ATR, VE-821, prior to final exposure to hypoxia and rapid reoxygenation and for the remainder of the time course. Proliferation was analysed using PrestoBlue after 1 hour. Graphs were plotted using GraphPad prism to determine the effect of hypoxia exposure on cells compared with normoxia only cells, and to compare the effects of reoxygenation on cells compared with cells exposed to hypoxia for 24 hours. Two-way ANOVA analyses were carried out using Tukey's test to account for multiple comparisons.

6.8 Summary and Brief Discussion of Chapter 6

The results presented in this chapter demonstrate that both ATM and ATR are activated in the response to reoxygenation-induced stress, however this data only highlights a role for ATR in the canonical NF-κB response to this stress. The exact mechanism behind this activation and the complex upstream signalling pathway that links ATR activation to IKKβ activation remains unclear. Future research could aim to establish the precise kinetics behind this response.

The data presented in the first part of this chapter indicates that double strand breaks occur after exposure to hypoxia based on increased γH2AX levels. This damage appears to be repaired during hypoxia and is not present in reoxygenated samples. This implicates ATM in the response to hypoxia as ATM is one of the main sensors of double strand DNA breaks and coordinates the repair of this damage, usually through homologus recombination [159]. However studies have also shown that ATR [193] is able to phosphorylate H2AX at this serine 139 in response to single strand breaks, indicating that replication stress could be the reason for H2AX phosphorylation after hypoxia. This also could explain how the cell is able to overcome this damage so rapidly and within a hypoxic environment. The data presented here contradict previous findings that suggest that reoxygenation, not hypoxia leads to DNA damage [389][270], however 0.01-0.02% O_2 was used in their studies. This data is however concurrent with the findings of Pires et al., who suggest that replication stress and stalled replication forks during hypoxia is caused by depletion in nucleotide levels [271].

The technique used here to detect γH2AX only indicates the proportion of cells that stain positive for γH2AX, it does not show the number of foci therefore we cannot determine the quantity of double strand breaks that have occurred (Fig. 67) [390]. To analyse this immunofluorescence microscopy could be carried out, however due to the low fluorescence signal that results from fixing cells in hypoxia would have made quantification and reproducibility difficult. Foci were markedly less visible in hypoxia samples therefore the results would not be valid as any foci present would be harder to detect both manually and automatically. This observation of a decreased signal from hypoxia-fixed samples could be due to low oxygen levels affecting how formaldehyde works as a fixative.

The data generated in this chapter indicate that hypoxia and reoxygenation do not significantly affect cell cycle progression with the exception of reoxygenation, which leads to a decrease in G1-phase cells as well as a decrease in mitotic cells. This indicates that some minor shifts in cell cycle dynamics occurs, indeed the overall trend of the data indicates that a G1-S arrest is reversed following reoxygenation in a small population of cells. Proliferation assays revealed that inhibition of ATR leads to a small decrease in proliferation following hypoxia and reoxygenation (Fig. 85), although some of this effect is due to the inhibitor alone (Fig. 84). Following on from this, ATR inhibition prevented the decrease in SOD2 expression seen following hypoxia (Fig, 80). Although speculative

at this stage, together this data implicates ATR in the control of cell proliferation and metabolism following exposure to hypoxia.

This section has highlighted the difference in the kinetics of NF-κB pathway activation in response to hydrogen peroxide, reoxygenation and etoposide treatments. Phosphorylation of ATM is observed across all treatments, however phosphorylation of Kap1 reveals that DNA damage only occurs following hydrogen peroxide and etoposide treatments. Following inhibition of ATM, Kap1 phosphorylation is only blocked in the context of etoposide treatment. This perhaps highlights alternate roles for ATM across these three stimuli. Activated ATM only transduces signal through the canonical NF-κB pathway following etoposide treatment, indicating that although genotoxic stress occurs following both hydrogen peroxide and etoposide treatment, the former activates NF-κB through a different mechanism. This mechanism was not established as part of this project, however one hypothesis is that it follows a similar activation pathway to that of reoxygenation. In this context the activation of the canonical NF-κB pathway is dependent on ATR.

Again, the validity of these experiments that aimed to investigate the role of ATM and ATR in NF-κB activation following hypoxia and reoxygenation relies solely on the effectiveness of the small molecule inhibitors used to target proteins of interest. Although every effort has been made to ensure that these kinase inhibitors were specific to the target, had been used in previous publications and had an appropriate half life, further experiments should be carried out using different mechanisms of knockdown. As discussed in section 5.7, siRNA, shRNA or CRISPR could be utilised in the future. Unfortunately due to time restrictions this could not be carried out as part of the project presented here.

Discussion

The main aim of this project was to determine the molecular mechanism of NF-κB pathway activation following hypoxia and rapid reoxygenation. Although previous studies have aimed to establish the kinetics of activation in the response to hypoxia, the findings have been conflicting due to variations in hypoxic protocol and the cell lines used. Studies on the effects of reoxygenation on NF-κB activation have been minimal, with very little known about the mechanism behind this response. As discussed in chapter 4, all of the major findings in this report were carried out using an improved method of inducing rapid oxygen changes in cells. As such, the majority of data presented here is novel, as previous reports on hypoxia and reoxygenation have utilised a method of gas exchange that can stimulate NF-κB activation independently of other stresses. Indeed, this could explain some of the different results observed in this thesis compared to previous publications.

Data in this thesis has demonstrated that the mechanism of NF-κB activation following hypoxia is very similar to that following reoxygenation. Signal is transduced through the IKK complex to IκBα, which is then phosphorylated on serines 32 and 36. Activation of NF-κB occurs, as RelA translocates into the nucleus to control gene expression. The main observable difference between these two pathways is that although IKKβ is phosphorylated in response to both stimuli, IKKα phosphorylation is also observed during hypoxia. The importance of this difference is currently unknown as experiments that focussed on the role of IKKα relied on a potentially non-xpecific IKKα inhibitor [348]. Previous work has implicated phosphorylation of tyrosine 42 in the response to hypoxia, this particular post-translational modification has been associated with the activation of NF-κB in the absence of IκBα degradation [125]. The lack of IκBα degradation has also been linked to sumoylation of critical residues that are normally ubiquitinated to target IκBα for proteasomal degradation [118]. In this project degradation of IκBα was not observed following hypoxia and reoxygenation, indicating that this mechanism could be activated here. Further work should aim to determine whether this is the case.

A large part of this project utilised small molecule inhibitors to inhibit activation of proteins of interest. A major proportion of the data presented in this thesis is therefore reliant on the effectiveness and specificity of these inhibitors. As such every effort was made to determine that they would not have off target effects, had an appropriate half-life for the experiments being carried out and had been used in peer-reviewed publications where possible. The use of the IKKα inhibitor in particular highlighted some of the problems with using these as a method of inhibition. Even though IKKα has not been previously associated with the response to TNF or etoposide, treatment with this inhibitor completely blocked signalling through the canonical NF-κB pathway. More alarmingly, in a recent publication these inhibitors were tested using the exact same protocol presented in this thesis and showed that treatment with the inhibitor had no effect on canonical NF-κB signalling. As such, it is very probable that the IKKα inhibitor used in this thesis

was not behaving as expected, and was having off-target effects, perhaps to IKKβ. Due to this finding it is impossible to draw any firm conclusions on the role of IKKα in the response to reoxygenation.

To reduce any concerns regarding the effectiveness of the inhibitors, additional work should be carried out using alternative methods for either knocking down or inhibiting a protein of interest. Preliminary tests using siRNA targeted to IKKα, IKKβ, ATR and ATM were carried out during this project (data not shown), all of which showed effective total protein knockdown. Unfortunately due to time restrictions further experimentation was not possible. Future work should focus on repeating any inhibitor experiments using siRNA to confirm findings; the resulting increased confidence in the data would improve the chances of publication of this data in a peer-reviewed journal. Additional methods for carrying out genetic knockdowns could include shRNA and CRISPR, these methods are more time consuming and as such were not carried out as part of this project.

Some of the experiments presented in this thesis studied the cellular translocation of proteins of interest following hypoxia and reoxygenation. Results obtained through western blotting of cytoplasmic and nuclear extracts indicated that IKKα, IKKβ, NEMO, ATR and ATM translocate into the nucleus following hypoxia, and return to the cytoplasm following reoxygenation. Unfortunately, although several repeats of each experiment was carried out, it was impossible to obtain consistently significant findings between experiments perhaps indicating that this is not a real observation. The only protein that showed consistent translocation in this manner was IKKα, perhaps indicating alternative roles of this protein in the response to hypoxia and reoxygenation. Indeed nuclear IKKα has been observed previously in response to proinflammatory cytokines, pathogens, and growth factors, here it is able to bind to DNA and coordinate NF-κB target gene expression [391]. This nuclear role of IKKα should be investigated further to gain more insight into the kinetics of canonical NF-κB signalling in response to oxidative stress. Confirmation of chromatin binding could be carried out using Ch-IP and protein-protein interactions could be investigated out by co-IP. Although an interesting observation as it stands, carrying out these additional experiments would increase the confidence in the data set and would contribute to a publishable mechanism of the IKKα response to hypoxia.

The trends observed in the western blots studying the translocation of other proteins of interest were not consistently statistically significant. This was most likely due to the technique used to determine cellular location of proteins of interest. Immunofluorescence microscopy was utilised alongside nuclear and cytoplasmic fractionation experiments probing for IKKβ and NEMO. As discussed in chapter 5, in the case of NEMO translocation results were consistent across both techniques indicating a nuclear role for NEMO in response to hypoxia. In contrast, studies on IKKβ translocation showed opposite results, most likely due to the use of a different antibody. We cannot therefore make any conclusions regarding the movement of IKKβ following hypoxia and reoxygenation. The movement of NEMO however is consistent with reports of a nuclear activation of NF-κB

following genotoxic stress where it dimerises with ATM, is exported from the nucleus and activates the canonical NF-κB pathway [358]. Indeed, based on western blot analysis, ATM and ATR follow the same pattern of movement as the IKK complexes, indicating that this could be the case here. Although as discussed above, this movement needs to be confirmed by an alternative method such as immunofluorescence microscopy, and further research should be carried out using techniques such as co-IPs to determine whether protein-protein interactions are at play here. Although this data is not of publishable standard as it stands, it does provide some interesting preliminary data that could be used to direct a further project focussing on the kinetics of NF-κB pathway activation following exposure to hypoxia and reoxygenation.

As discussed on section 1.4, many of the genes analysed in this report had previously been studied in hypoxia, while only 2 genes had been studied in the context of reoxygenation. Due to differences in the hypoxia protocol and cell lines used, many previous publications had opposing findings regarding the direction of change in gene expression. Since an alternative method of hypoxia induction was used in this thesis, again there are some contradictory findings from those previously published in the literature. Previous work has shown that IL-8 and cIAP-2 gene expression increases following hypoxia, while data presented here shows a significant decrease. In addition, SOD-2 expression decreased significantly following hypoxia. Data identifying changes in NF-κB target genes in response to reoxygenation was scarce, results presented in this thesis shows the effects of reoxygenation on 7 genes of interest. An increase in expression was observed in IL-8, cIAP-2 and SOD-2, indicating that the effects of hypoxia exposure are reversed following reoxygenation. The change in expression of SOD-2 in particular could suggest that this is due to changes in metabolic activity of the cell as rates of aerobic respiration changes due to oxygen fluctuations. Further work could focus on other genes of interest and the effects of protein inhibition on gene expression should be re-evaluated using siRNA knockdown and with a larger number of experimental replicates. In addition, the potential role of active repression following hypoxia should be investigated as it would add to previous literature that has shown this unusual effect of NF-κB signalling. As discussed in section 4 this could be investigated using rescue experiments as described previously [119], alongside Ch-IP experiments.

In chapter 4 several experiments were carried out with the aim of determining the exact ROS produced following exposure to hypoxia and reoxygenation. Previous work had failed to elucidate the exact species of ROS responsible for the effects observed in cells following these stimuli. This is due to variations in the method of reading ROS, the time points studied and the cell or tissue type used. The results presented in this thesis failed to find an answer due to a number of factors; the time point used, the effects of hypoxia on the dye and the lack of detail on the exact probes used in the kit. PRDX-3 western blots did not help in this case due to the protein extraction method used, however analysing oxidation of proteins in future experiments is probably the best approach to show the

effects of ROS on cell signalling. Further work should therefore aim to characterise the oxidation state of PRDX-3 and members of the canonical NF-κB signalling pathway [240][241][239][256]. This could be carried out through western blot analysis on extracts that have been harvested under acid lysis conditions to prevent artefactual oxidation events during sample preparation.

In addition to characterising the effects of hypoxia and reoxygenation on gene expression and canonical NF-κB signalling, one of the aims of this project was to determine the effects of hypoxia and reoxygenation on cellular functions such as proliferation, cell cycle dynamics and DNA damage. Although previous work has focussed on some of these key cellular processes, the protocols followed differed and did not account for the effects of fresh media on the cell. The effects of hypoxia and reoxygenation were the same as reported in earlier publications, with a decrease and increase in proliferation observed respectively [272][273][274].

Again, treatment with the small molecule inhibitors should be repeated using an alternative method of knockdown before any firm conclusions can be made, however IKKβ inhibition appears to affect proliferation following both hypoxia and reoxygenation. Future work should aim to confirm this as well as explore some of the effects of inhibition of other proteins of interest. Although some longer clonogenicity experiments were carried out, the roles of proteins of interest in this response is currently unknown due to the short length of time that the cells were exposed to the inhibitor for. The used of shRNA knockdown would be a far better approach to tackling this question as proteins would be knocked down long term, throughout the course of the whole experiment.

The effects of hypoxia and reoxygenation on cell cycle progression indicated that some small changes in cell cycle progression occurs as oxygen levels are changed. This was only significant with regard to a decrease in G1-phase cells following reoxygenation. This result indicates that in a small, not significant, population of cells hypoxia prevents progression into S-phase; this is reversed following reoxygenation. The exact reason for these changes can only be speculated at this point, but could explain the decrease in proliferation observed following hypoxia. Perhaps the lack of oxygen blocks production of key components required for S-phase such as nucleotides due to a decrease in metabolic activity. The effect of hypoxia and reoxygenation on DNA damage indicates that this could be the case.

A previous study has indicated that DNA damage only occurs following reoxygenation [270], however data presented here is more concurrent with the findings of Pires et al, who observe replication stress during hypoxia [271]. DNA damage analysis showed that exposure to hypoxia leads to an increase in γH2AX levels, this returns to normal after 24 hours of hypoxia and does not re-occur following reoxygenation. Initially this implicated ATM in the response to hypoxia as it phosphorylates H2AX in the response to double strand breaks, however other PIKK family members, ATR and DNA-PK have been shown to phosphorylate H2AX at this residue [193][194][195]. Additional experiments could be

carried out to further characterise this effect, for example through the use of alternative methods of DNA damage detection such as though COMET assays or through DNA fibre assays. Pires et al. suggest that stalled replication forks could be causing this H2AX phosphorylation, implicating ATR in this response, this hypothesis could be tested through inhibition of ATR using siRNA knockdown [271]. If ATR is the kinase responsible for this effect then changes in γH2AX levels would be affected by its inhibition.

Indeed, ATR was identified as a potential upstream kinase responsible for activation of the canonical NF-κB pathway in response to reoxygenation in this project. Western blot analysis showed that although both ATM and ATR are activated in the response to reoxygenation, only inhibition of ATR affects signalling downstream to the canonical NF-κB pathway. These inhibition experiments were again only carried out though the use of small molecule inhibitors, as such they must be repeated to increase the quality of the data set to a publishable standard.

Notwithstanding the issues raised above, this study has determined the basic mechanism behind NF-κB activation following hypoxia and reoxygenation. This involves IKKβ (and IKKα during hypoxia), serine 32/36 phosphorylation of IκBα and activation of NF-κB in the absence of IκBα degradation. While carrying out this aim certain further experiments of interest have been highlighted, such as investigating the potential role of tyrosine 42 phosphorylation and sumoylation of IκBα, or the oxidation of proteins in the canonical NF-κB pathway. A potential upstream activator of the canonical NF-κB pathway in response to reoxygenation was also identified in the form of ATR. This is a novel finding and would be a publishable observation following further analysis. Future experiments should aim to confirm the results shown here, further characterise the kinetics of ATR activation and its interactions with other proteins downstream to activate NF-κB. This should be carried out using an alternative mechanism of ATR inhibition, through further investigations into other proteins such as TAK1 and the TAK1-binding protein (TAB) proteins and a series of co-IP and cellular localisation experiments. This data would build on some of the other findings of this project that focussed on the effects of hypoxia and reoxygenation on other cellular processes such as cell cycle progression, proliferation and DNA damage. Indeed, since ATR has been implicated in all of these responses previously or in this report, further investigations into the role of ATR in these cellular processes following hypoxia and reoxygenation would create an interesting and novel picture of the NF-κB response to these stimuli. Future projects should therefore build on the work presented here to answer the remaining questions that have been highlighted, together this would produce interesting and publishable data on the response of the NF-κB pathway to hypoxia and reoxygenation.

References

[1] Ole Haagen Nielsen, Mehmet Coskun, Casper Steenholdt, and Gerhard Rogler. The role and advances of immunomodulator therapy for inflammatory bowel disease. *Expert Review of Gastroenterology & Hepatology*, 9(2):177–189, feb 2015.

[2] Vinit Kumar, Stefano Palazzolo, Samer Bayda, Giuseppe Corona, Giuseppe Toffoli, and Flavio Rizzolio. DNA Nanotechnology for Cancer Therapy. *Theranostics*, 6(5):710–25, 2016.

[3] A. Jansen and K. J. Verstrepen. Nucleosome Positioning in Saccharomyces cerevisiae. *Microbiology and Molecular Biology Reviews*, 75(2):301–320, jun 2011.

[4] Alena Shmakova, Michael Batie, Jimena Druker, and Sonia Rocha. Chromatin and oxygen sensing in the context of JmjC histone demethylases. *Biochemical Journal*, 462(3):385–395, sep 2014.

[5] Mary C. Thomas and Cheng-Ming Chiang. The General Transcription Machinery and General Cofactors. *Critical Reviews in Biochemistry and Molecular Biology*, 41(3):105–178, jan 2006.

[6] B Lemon and R Tjian. Orchestrated response: a symphony of transcription factors for gene control. *Genes & development*, 14(20):2551–69, oct 2000.

[7] Y Li, P M Flanagan, H Tschochner, and R D Kornberg. RNA polymerase II initiation factor interactions and transcription start site selection. *Science (New York, N.Y.)*, 263(5148):805–7, feb 1994.

[8] D. A. Bushnell and R. D. Kornberg. Complete, 12-subunit RNA polymerase II at 4.1-A resolution: Implications for the initiation of transcription. *Proceedings of the National Academy of Sciences*, 100(12):6969–6973, jun 2003.

[9] Wensheng Deng and Stefan G. E. Roberts. TFIIB and the regulation of transcription by RNA polymerase II. *Chromosoma*, 116(5):417–429, sep 2007.

[10] O Flores, H Lu, M Killeen, J Greenblatt, Z F Burton, and D Reinberg. The small subunit of transcription factor IIF recruits RNA polymerase II into the preinitiation complex. *Proceedings of the National Academy of Sciences of the United States of America*, 88(22):9999–10003, nov 1991.

[11] G Orphanides, T Lagrange, and D Reinberg. The general transcription factors of RNA polymerase II. *Genes & development*, 10(21):2657–83, nov 1996.

[12] A. L. Gnatt, P Cramer, J Fu, D A Bushnell, and R D Kornberg. Structural Basis of Transcription: An RNA Polymerase II Elongation Complex at 3.3 A Resolution. *Science*, 292(5523):1876–1882, jun 2001.

[13] Steven Hahn. Structure and mechanism of the RNA polymerase II transcription machinery. *Nature Structural & Molecular Biology*, 11(5):394–403, may 2004.

[14] Mahadeb Pal, Alfred S. Ponticelli, and Donal S. Luse. The Role of the Transcription Bubble and TFIIB in Promoter Clearance by RNA Polymerase II. *Molecular Cell*, 19(1):101–110, jul 2005.

[15] Tong Ihn Lee and Richard A. Young. Transcription of Eukaryotic Protein-Coding Genes. *Annual Review of Genetics*, 34(1):77–137, dec 2000.

[16] Stephen Buratowski. Progression through the RNA Polymerase II CTD Cycle. *Molecular Cell*, 36(4):541–546, nov 2009.

[17] K. Glover-Cutter, S. Larochelle, B. Erickson, C. Zhang, K. Shokat, R. P. Fisher, and D. L. Bentley. TFIIH-Associated Cdk7 Kinase Functions in Phosphorylation of C-Terminal Domain Ser7 Residues, Promoter-Proximal Pausing, and Termination by RNA Polymerase II. *Molecular and Cellular Biology*, 29(20):5455–5464, oct 2009.

[18] Steven J. Kim and Harold G. Martinson. Poly(A)-dependent Transcription Termination. *Journal of Biological Chemistry*, 278(43):41691–41701, oct 2003.

[19] Ferenc Müller, Màté A Demény, and Làszlò Tora. New problems in RNA polymerase II transcription initiation: matching the diversity of core promoters with a variety of promoter recognition factors. *The Journal of biological chemistry*, 282(20):14685–9, may 2007.

[20] C. J. Fry and Craig L Peterson. TRANSCRIPTION: Unlocking the Gates to Gene Expression. *Science*, 295(5561):1847–1848, mar 2002.

[21] Mark Ptashne and Alexander Gann. Transcriptional activation by recruitment. *Nature*, 386(6625):569–577, apr 1997.

[22] Stewart MacArthur, Xiao-Yong Li, Jingyi Li, James B Brown, Hou Cheng Chu, Lucy Zeng, Brandi P Grondona, Aaron Hechmer, Lisa Simirenko, Soile VE Keränen, David W Knowles, Mark Stapleton, Peter Bickel, Mark D Biggin, and Michael B Eisen. Developmental roles of 21 Drosophila transcription factors are determined by quantitative differences in binding to an overlapping set of thousands of genomic regions. *Genome Biology*, 10(7):R80, 2009.

[23] Anders M. Näär, Bryan D. Lemon, and Robert Tjian. Transcriptional Coactivator Complexes. *Annual Review of Biochemistry*, 70(1):475–501, jun 2001.

[24] A. H. Brivanlou and James E Darnell. Signal Transduction and the Control of Gene Expression. *Science*, 295(5556):813–818, feb 2002.

[25] M Madan Babu, Nicholas M Luscombe 3ã, L Aravind, Mark Gerstein, and Sarah A Teichmann. Structure and evolution of transcriptional regulatory networks. *Current Opinion in Structural Biology*, 14:283–291, 2004.

[26] S Y Wu and C M Chiang. TATA-binding protein-associated factors enhance the recruitment of RNA polymerase II by transcriptional activators. *The Journal of biological chemistry*, 276(36):34235–43, sep 2001.

[27] Shwu-Yuan Wu, Tianyuan Zhou, and Cheng-Ming Chiang. Human mediator enhances activator-facilitated recruitment of RNA polymerase II and promoter recognition by TATA-binding protein (TBP) independently of TBP-associated factors. *Molecular and cellular biology*, 23(17):6229–42, sep 2003.

[28] Matthias Mann and Ole N. Jensen. Proteomic analysis of post-translational modifications. *Nature Biotechnology*, 21(3):255–261, mar 2003.

[29] George A. Khoury, Richard C. Baliban, and Christodoulos A. Floudas. Proteome-wide post-translational modification statistics: frequency analysis and curation of the swiss-prot database. *Scientific Reports*, 1(1):90, dec 2011.

[30] Mark Hochstrasser. Evolution and function of ubiquitin-like protein-conjugation systems. *Nature Cell Biology*, 2(8):E153–E157, aug 2000.

[31] M Hochstrasser. Biochemistry. All in the ubiquitin family. *Science (New York, N.Y.)*, 289(5479):563–4, jul 2000.

[32] Puck Knipscheer, Willem J van Dijk, Jesper V Olsen, Matthias Mann, and Titia K Sixma. Noncovalent interaction between Ubc9 and SUMO promotes SUMO chain formation. *The EMBO Journal*, 26(11):2797–2807, jun 2007.

[33] Suzanne Elsasser, Rayappa R. Gali, Martin Schwickart, Christopher N. Larsen, David S. Leggett, Britta Müller, Matthew T. Feng, Fabian Tübing, Gunnar A.G. Dittmar, and Daniel Finley. Proteasome subunit Rpn1 binds ubiquitin-like protein domains. *Nature Cell Biology*, 4(9):725–730, sep 2002.

[34] J. S. Thrower, L Hoffman, M Rechsteiner, and C M Pickart. Recognition of the polyubiquitin proteolytic signal. *The EMBO Journal*, 19(1):94–102, jan 2000.

[35] P Young, Q Deveraux, R E Beal, C M Pickart, and M Rechsteiner. Characterization of two polyubiquitin binding sites in the 26 S protease subunit 5a. *The Journal of biological chemistry*, 273(10):5461–7, mar 1998.

[36] Nei-Li Chan and Christopher P. Hill. Defining polyubiquitin chain topology. *Nature Structural Biology*, 8(8):650–652, aug 2001.

[37] Mark Hochstrasser. Origin and function of ubiquitin-like proteins. *Nature*, 458(7237):422–429, mar 2009.

[38] Kirby N Swatek and David Komander. Ubiquitin modifications. *Cell Research*, 26(4):399–422, apr 2016.

[39] Fumiyo Ikeda and Ivan Dikic. Atypical ubiquitin chains: new molecular signals. 'Protein Modifications: Beyond the Usual Suspects' Review Series. *EMBO reports*, 9(6):536–542, jun 2008.

[40] Ranjan Sen and David Baltimore. Multiple nuclear factors interact with the immunoglobulin enhancer sequences. *Cell*, 46(5):705–716, aug 1986.

[41] Kiyoshi Kawakami, Claus Scheidereit, and Robert G Roeder. Identification and purification of a human immunoglobulin- enhancer-binding protein (NF-KB) that activates transcription from a human immunodeficiency virus type 1 promoter in vitro (transcription factor/lymphoid-specific protein/UV crosslinking/DNase I &. *Biochemistry Communicated by James E. Darnell, Jr*, 85:4700–4704, 1988.

[42] Matthew S Hayden and Sankar Ghosh. NF-κB, the first quarter-century: remarkable progress and outstanding questions. *Genes & development*, 26(3):203–34, feb 2012.

[43] Thomas Gilmore. NF-kB Target Genes » NF-kB Transcription Factors — Boston University.

[44] Qian Zhang, Michael J. Lenardo, and David Baltimore. 30 Years of NF-κB: A Blossoming of Relevance to Human Pathobiology. *Cell*, 168(1-2):37–57, jan 2017.

[45] Jie Dong, Eijiro Jimi, Caroline Zeiss, Matthew S Hayden, and Sankar Ghosh. Constitutively active NF-kappaB triggers systemic TNFalpha-dependent inflammation and localized TNFalpha-independent inflammatory disease. *Genes & development*, 24(16):1709–17, aug 2010.

[46] Alberto Mantovani, Paola Allavena, Antonio Sica, and Frances Balkwill. Cancer-related inflammation. *Nature*, 454(7203):436–444, jul 2008.

[47] Peter Libby. Inflammation and cardiovascular disease mechanisms. *The American journal of clinical nutrition*, 83(2):456S–460S, feb 2006.

[48] A. Csiszar, M. Wang, E. G. Lakatta, and Z. Ungvari. Inflammation and endothelial dysfunction during aging: role of NF- B. *Journal of Applied Physiology*, 105(4):1333–1341, jul 2008.

[49] K.A. Collister and B.C. Albensi. Potential therapeutic targets in the NF-kappaB pathway for Alzheimer's disease. *Drug News & Perspectives*, 18(10):623, dec 2005.

[50] Makio Mogi, Tomoyoshi Kondo, Yoshikuni Mizuno, and Toshiharu Nagatsu. p53 protein, interferon-γ, and NF-κB levels are elevated in the parkinsonian brain. *Neuroscience Letters*, 414(1):94–97, feb 2007.

[51] Qian Yang, Gui-Qiu Zhao, Qian Li, and Xiang-Ping Liu. Expression of nuclear factor-kappaB in traumatic cataract. *Chinese journal of traumatology = Zhonghua chuang shang za zhi*, 9(2):86–90, apr 2006.

[52] H. Lang, Bradley A Schulte, Daohong Zhou, Nancy Smythe, Samuel S Spicer, and Richard A Schmiedt. Nuclear Factor B Deficiency Is Associated with Auditory Nerve Degeneration and Increased Noise-Induced Hearing Loss. *Journal of Neuroscience*, 26(13):3541–3550, mar 2006.

[53] Takashi Okamoto. NF-kappaB and rheumatic diseases. *Endocrine, metabolic & immune disorders drug targets*, 6(4):359–72, dec 2006.

[54] J W Christman, R T Sadikot, and T S Blackwell. The role of nuclear factor-kappa B in pulmonary diseases. *Chest*, 117(5):1482–7, may 2000.

[55] Lilly Madjdpour, Sita Kneller, Christa Booy, Thomas Pasch, Ralph C Schimmer, and Beatrice Beck-Schimmer. Acid-induced lung injury: role of nuclear factor-kappaB. *Anesthesiology*, 99(6):1323–32, dec 2003.

[56] Heike L Pahl. Activators and target genes of Rel/NF-kappaB transcription factors. *Oncogene*, 18(49):6853–6866, 1999.

[57] Irfan Rahman and Iain Kilty. Antioxidant therapeutic targets in COPD. *Current drug targets*, 7(6):707–20, jun 2006.

[58] Mathilde Rottner, Simon Tual-Chalot, H Ahmed Mostefai, Ramaroson Andriantsitohaina, Jean-Marie Freyssinet, and María Carmen Martínez. Increased oxidative stress induces apoptosis in human cystic fibrosis cells. *PloS one*, 6(9):e24880, 2011.

[59] G Valen, Z Q Yan, and G K Hansson. Nuclear factor kappa-B and the heart. *Journal of the American College of Cardiology*, 38(2):307–14, aug 2001.

[60] Hirofumi Sawada, Yoshihide Mitani, Junko Maruyama, Bao Hua Jiang, Yukiko Ikeyama, Francis A. Dida, Hatsumi Yamamoto, Kyoko Imanaka-Yoshida, Hideto Shimpo, Akira Mizoguchi, Kazuo Maruyama, and Yoshihiro Komada. A Nuclear Factor-κB Inhibitor Pyrrolidine Dithiocarbamate Ameliorates Pulmonary Hypertension in Rats. *Chest*, 132(4):1265–1274, oct 2007.

[61] K. Z. Gong, G. Song, J. P. Spiers, E. J. Kelso, and Z. G. Zhang. Activation of immune and inflammatory systems in chronic heart failure: novel therapeutic approaches. *International Journal of Clinical Practice*, 61(4):611–621, mar 2007.

[62] S H Wilson, N M Caplice, R D Simari, D R Holmes, P J Carlson, and A Lerman. Activated nuclear factor-kappaB is present in the coronary vasculature in experimental hypercholesterolemia. *Atherosclerosis*, 148(1):23–30, jan 2000.

[63] Jian-Jun Li and Run-Lin Gao. Should atherosclerosis be considered a cancer of the vascular wall? *Medical Hypotheses*, 64(4):694–698, jan 2005.

[64] T. J. Guzik and D. G. Harrison. Endothelial NF- B As a Mediator of Kidney Damage: The Missing Link Between Systemic Vascular and Renal Disease? *Circulation Research*, 101(3):227–229, aug 2007.

[65] Tomás Zima and Marta Kalousová. Oxidative stress and signal transduction pathways in alcoholic liver disease. *Alcoholism, clinical and experimental research*, 29(11 Suppl):110S–115S, nov 2005.

[66] Keith D. Gray, Misho O. Simovic, Timothy S. Blackwell, John W. Christman, Addison K. May, Kelly S. Parman, William C. Chapman, and Steven C. Stain. Activation of Nuclear Factor kappa B and Severe Hepatic Necrosis May Mediate Systemic Inflammation in Choline-deficient/Ethionine-supplemented Diet-induced Pancreatitis. *Pancreas*, 33(3):260–267, oct 2006.

[67] C W Yang, M S Wu, and M J Pan. Leptospirosis renal disease. *Nephrology, dialysis, transplantation : official publication of the European Dialysis and Transplant Association - European Renal Association*, 16 Suppl 5:73–7, 2001.

[68] A S Peña and M Peñate. Genetic susceptibility and regulation of inflammation in Crohn's disease. Relationship with the innate immune system. *Revista espanola de enfermedades digestivas : organo oficial de la Sociedad Espanola de Patologia Digestiva*, 94(6):351–60, jun 2002.

[69] Ken Chen, You-Ming Long, Hui Wang, Lei Lan, and Zhen-He Lin. Activation of nuclear factor-kappa B and effects of pyrrolidine dithiocarbamate on TNBS-induced rat colitis. *World journal of gastroenterology*, 11(10):1508–14, mar 2005.

[70] M F Neurath, C Becker, and K Barbulescu. Role of NF-kappaB in immune and inflammatory responses in the gut. *Gut*, 43(6):856–60, dec 1998.

[71] Cormac T. Taylor and Sean P. Colgan. Regulation of immunity and inflammation by hypoxia in immunological niches. *Nature Reviews Immunology*, 17(12):774–785, oct 2017.

[72] Holger K. Eltzschig and Peter Carmeliet. Hypoxia and Inflammation. *New England Journal of Medicine*, 364(7):656–665, feb 2011.

[73] G. Melillo. Hypoxia: jump-starting inflammation. *Blood*, 117(9):2561–2562, mar 2011.

[74] Mi Hee Park and Jin Tae Hong. Roles of NF-κB in Cancer and Inflammatory Diseases and Their Therapeutic Approaches. *Cells*, 5(2), mar 2016.

[75] D. E. Nelson, A E C Ihekwaba, M Elliott, J R Johnson, C A Gibney, B E Foreman, G Nelson, V See, C A Horton, D G Spiller, S W Edwards, H P McDowell, J F Unitt, E Sullivan, R Grimley, N Benson, D Broomhead, D B Kell, and M R H White. Oscillations in NF- B Signaling Control the Dynamics of Gene Expression. *Science*, 306(5696):704–708, oct 2004.

[76] Sahdeo Prasad, Jayaraj Ravindran, and Bharat B. Aggarwal. NF-κB and cancer: how intimate is this relationship. *Molecular and Cellular Biochemistry*, 336(1-2):25–37, mar 2010.

[77] D C Guttridge, C Albanese, J Y Reuther, R G Pestell, and A S Baldwin. NF-kappaB controls cell growth and differentiation through transcriptional regulation of cyclin D1. *Molecular and cellular biology*, 19(8):5785–99, aug 1999.

[78] A A Beg and D Baltimore. An essential role for NF-kappaB in preventing TNF-alpha-induced cell death. *Science (New York, N.Y.)*, 274(5288):782–4, nov 1996.

[79] D J Van Antwerp, S J Martin, T Kafri, D R Green, and I M Verma. Suppression of TNF-alpha-induced apoptosis by NF-kappaB. *Science (New York, N.Y.)*, 274(5288):787–9, nov 1996.

[80] Brian R Lane, Jianguo Liu, Paul J Bock, Dominique Schols, Michael J Coffey, Robert M Strieter, Peter J Polverini, and David M Markovitz. Interleukin-8 and growth-regulated oncogene alpha mediate angiogenesis in Kaposi's sarcoma. *Journal of virology*, 76(22):11570–83, nov 2002.

[81] Christopher Mark Overall and Carlos López-Otín. Strategies for mmp inhibition in cancer: innovations for the post-trial era. *Nature Reviews Cancer*, 2(9):657–672, sep 2002.

[82] Mary L. Disis. Immune Regulation of Cancer. *Journal of Clinical Oncology*, 28(29):4531–4538, oct 2010.

[83] Ranjan Sen and David Baltimore. Multiple nuclear factors interact with the immunoglobulin enhancer sequences. *Cell*, 46(5):705–716, aug 1986.

[84] L Shurman, R Sen, and Y Bergman. Adenovirus E1A products activate the Ig k-chain enhancer in fibroblasts. A possible involvement of the NF-kB binding site. *The Journal of Immunology*, 143(11), 1989.

[85] D W Ballard, E Böhnlein, J W Lowenthal, Y Wano, B R Franza, and W C Greene. HTLV-I tax induces cellular proteins that activate the kappa B element in the IL-2 receptor alpha gene. *Science (New York, N.Y.)*, 241(4873):1652–5, sep 1988.

[86] L C Sambucetti, J M Cherrington, G W Wilkinson, and E S Mocarski. NF-kappa B activation of the cytomegalovirus enhancer is mediated by a viral transactivator and by T cell stimulation. *The EMBO journal*, 8(13):4251–8, dec 1989.

[87] L Osborn, S Kunkel, and G J Nabel. Tumor necrosis factor alpha and interleukin 1 stimulate the human immunodeficiency virus enhancer by activation of the nuclear factor kappa B. *Proceedings of the National Academy of Sciences of the United States of America*, 86(7):2336–40, apr 1989.

[88] A Israël, O Le Bail, D Hatat, J Piette, M Kieran, F Logeat, D Wallach, M Fellous, and P Kourilsky. TNF stimulates expression of mouse MHC class I genes by inducing an NF kappa B-like enhancer binding activity which displaces constitutive factors. *The EMBO journal*, 8(12):3793–800, dec 1989.

[89] V Ivanov, B Stein, I Baumann, D A Dobbelaere, P Herrlich, and R O Williams. Infection with the intracellular protozoan parasite Theileria parva induces constitutively high levels of NF-kappa B in bovine T lymphocytes. *Molecular and cellular biology*, 9(11):4677–86, nov 1989.

[90] K Busam, C Gieringer, M Freudenberg, and H P Hohmann. Staphylococcus aureus and derived exotoxins induce nuclear factor kappa B-like activity in murine bone marrow macrophages. *Infection and immunity*, 60(5):2008–15, may 1992.

[91] J Garcia, B Lemercier, S Roman-Roman, and G Rawadi. A Mycoplasma fermentans-derived synthetic lipopeptide induces AP-1 and NF-kappaB activity and cytokine secretion in macrophages via the activation of mitogen-activated protein kinase pathways. *The Journal of biological chemistry*, 273(51):34391–8, dec 1998.

[92] Bernard Piret, Sonia Schoonbroodt, and Jacques Piette. The ATM protein is required for sustained activation of NF-kappaB following DNA damage. *Oncogene*, 18(13):2261–71, 1999.

[93] Zhongzhen Nie, Yun Mei, Mary Ford, Leonard Rybak, Adrianna Marcuzzi, Hongzu Ren, Gary L Stiles, and Vickram Ramkumar. Oxidative Stress Increases A 1 Adenosine Receptor Expression by Activating Nuclear Factor kB. *Mol. Pharmacol.*, 53(4):663–669, 1998.

[94] Rikimaru Bessho, Kousaku Matsubara, Masaru Kubota, Katsuji Kuwakado, Haruyo Hirota, Yoshihiro Wakazono, Ying Wei Lin, Akiro Okuda, Masahiko Kawai, Ryuta Nishikomori, and Toshio Heike. Pyrrolidine dithiocarbamate, a potent inhibitor of nuclear factor κB (NF-κB) activation, prevents apoptosis in human promyelocytic leukemia HL-60 cells and thymocytes. *Biochemical Pharmacology*, 48(10):1883–1889, nov 1994.

[95] I Berberich, G L Shu, and E A Clark. Cross-linking CD40 on B cells rapidly activates nuclear factor-kappa B. *Journal of immunology (Baltimore, Md. : 1950)*, 153(10):4357–66, nov 1994.

[96] K S Lee, M Buck, K Houglum, and M Chojkier. Activation of hepatic stellate cells by TGF alpha and collagen type I is mediated by oxidative stress through c-myb expression. *Journal of Clinical Investigation*, 96(5):2461–2468, nov 1995.

[97] Q Lan, K O Mercurius, and P F Davies. Stimulation of transcription factors NF kappa B and AP1 in endothelial cells subjected to shear stress. *Biochemical and biophysical research communications*, 201(2):950–6, jun 1994.

[98] B Stein, M Krämer, H J Rahmsdorf, H Ponta, and P Herrlich. UV-induced transcription from the human immunodeficiency virus type 1 (HIV-1) long terminal repeat and UV-induced secretion of an extracellular factor that induces HIV-1 transcription in nonirradiated cells. *Journal of virology*, 63(11):4540–4, nov 1989.

[99] Masanori Nishikawa, Nobumasa Kakemizu, Takaaki Ito, Makoto Kudo, Takeshi Kaneko, Motoyoshi Suzuki, Naoko Udaka, Hirotada Ikeda, and Takao Okubo. Superoxide Mediates Cigarette Smoke-Induced Infiltration of Neutrophils into the Airways through Nuclear Factor- κ B Activation and IL-8 mRNA Expression in Guinea Pigs In Vivo. *American Journal of Respiratory Cell and Molecular Biology*, 20(2):189–198, feb 1999.

[100] Govindarajan T. Ramesh, Sunil K. Manna, Bharat B. Aggarwal, and Arun L. Jadhav. Lead Activates Nuclear Transcription Factor -κB, Activator Protein-1, and Amino-Terminal c-Jun Kinase in Pheochromocytoma Cells. *Toxicology and Applied Pharmacology*, 155(3):280–286, mar 1999.

[101] M Goebeler, J Roth, E B Bröcker, C Sorg, and K Schulze-Osthoff. Activation of nuclear factor-kappa B and gene expression in human endothelial cells by the common haptens nickel and cobalt. *Journal of immunology (Baltimore, Md. : 1950)*, 155(5):2459–67, sep 1995.

[102] R Schreck, P Rieber, and P A Baeuerle. Reactive oxygen intermediates as apparently widely used messengers in the activation of the NF-kappa B transcription factor and HIV-1. *The EMBO journal*, 10(8):2247–58, aug 1991.

[103] L M Shea, C Beehler, M Schwartz, R Shenkar, R Tuder, and E Abraham. Hyperoxia activates NF-kappaB and increases TNF-alpha and IFN-gamma gene expression in mouse pulmonary lymphocytes. *Journal of immunology (Baltimore, Md. : 1950)*, 157(9):3902–8, nov 1996.

[104] Cecília Gabriel, Carles Justicia, Antoni Camins, and Anna M Planas. Activation of nuclear factor-κ-B in the rat brain after transient focal ischemia. *Molecular Brain Research*, 65(1):61–69, 1999.

[105] Rudolf A. Rupec and Patrick A. Baeuerle. The Genomic Response of Tumor Cells to Hypoxia and Reoxygenation. Differential Activation of Transcription Factors AP-1 and NF-kappaB. *European Journal of Biochemistry*, 234(2):632–640, dec 1995.

[106] Trine H Mogensen. Pathogen recognition and inflammatory signaling in innate immune defenses. *Clinical microbiology reviews*, 22(2):240–73, Table of Contents, apr 2009.

[107] Michael J Morgan and Zheng-gang Liu. Crosstalk of reactive oxygen species and NF-κB signaling. *Cell research*, 21(1):103–15, jan 2011.

[108] N. L. Reynaert, A. van der Vliet, A. S. Guala, T. McGovern, M. Hristova, C. Pantano, N. H. Heintz, J. Heim, Y.-S. Ho, D. E. Matthews, E. F. M. Wouters, and Y. M. W. Janssen-Heininger. Dynamic redox control of NF- B through glutaredoxin-regulated S-glutathionylation of inhibitory B kinase beta. *Proceedings of the National Academy of Sciences*, 103(35):13086–13091, aug 2006.

[109] Melanie Herscovitch, William Comb, Thomas Ennis, Kate Coleman, Sheila Yong, Brinda Armstead, Demetrios Kalaitzidis, Sushil Chandani, and Thomas D. Gilmore. Intermolecular disulfide bond formation in the NEMO dimer requires Cys54 and Cys347. *Biochemical and Biophysical Research Communications*, 367(1):103–108, feb 2008.

[110] Ilona Jaspers, Wenli Zhang, Alison Fraser, James M. Samet, and William Reed. Hydrogen Peroxide Has Opposing Effects on IKK Activity and I κ B α Breakdown in Airway Epithelial Cells. *American Journal of Respiratory Cell and Molecular Biology*, 24(6):769–777, jun 2001.

[111] Hideaki Kamata, Tomoyuki Manabe, Shin ichi Oka, Keiko Kamata, and Hajime Hirata. Hydrogen peroxide activates IkappaB kinases through phosphorylation of serine residues in the activation loops. *FEBS letters*, 519(1-3):231–7, may 2002.

[112] Hans Häcker and Michael Karin. Regulation and Function of IKK and IKK-Related Kinases. *Science Signaling*, 2006(357), 2006.

[113] Alain Israël. The IKK complex, a central regulator of NF-kappaB activation. *Cold Spring Harbor perspectives in biology*, 2(3):a000158, mar 2010.

[114] Daniel Krappmann and Claus Scheidereit. A pervasive role of ubiquitin conjugation in activation and termination of IkappaB kinase pathways. *EMBO reports*, 6(4):321–6, apr 2005.

[115] C Wang, L Deng, M Hong, G R Akkaraju, J Inoue, and Z J Chen. TAK1 is a ubiquitin-dependent kinase of MKK and IKK. *Nature*, 412(6844):346–51, jul 2001.

[116] Chenguang Fan, Qiang Li, Dan Ross, and John F Engelhardt. Tyrosine Phosphorylation of IκBα Activates NFκB Through a Redox-Regulated and c-Src-Dependent Mechanism Following Hypoxia/Reoxygenation Molecular Biology Graduate Program. *JBC Papers in Press. Published on November*, 11, 2002.

[117] T T Huang, S M Wuerzberger-Davis, B J Seufzer, S D Shumway, T Kurama, D A Boothman, and S Miyamoto. NF-kappaB activation by camptothecin. A linkage between nuclear DNA damage and cytoplasmic signaling events. *The Journal of biological chemistry*, 275(13):9501–9, mar 2000.

[118] Carolyn Culver, Anders Sundqvist, Sharon Mudie, Andrew Melvin, Dimitris Xirodimas, and Sonia Rocha. Mechanism of hypoxia-induced NF-kappaB. *Molecular and cellular biology*, 30(20):4901–21, oct 2010.

[119] Kirsteen J Campbell, Sonia Rocha, and Neil D Perkins. Active repression of antiapoptotic gene expression by RelA(p65) NF-kappa B. *Molecular cell*, 13(6):853–65, mar 2004.

[120] Vinay Tergaonkar, Virginie Bottero, Masahito Ikawa, Qiutang Li, and Inder M Verma. IkappaB kinase-independent IkappaBalpha degradation pathway: functional NF-kappaB activity and implications for cancer therapy. *Molecular and cellular biology*, 23(22):8070–83, nov 2003.

[121] Tomohisa Kato, Mireille Delhase, Alexander Hoffmann, and Michael Karin. CK2 Is a C-Terminal IkappaB Kinase Responsible for NF-kappaB Activation during the UV Response. *Molecular cell*, 12(4):829–39, oct 2003.

[122] K Bender, M Göttlicher, S Whiteside, H J Rahmsdorf, and P Herrlich. Sequential DNA damage-independent and -dependent activation of NF-kappaB by UV. *The EMBO journal*, 17(17):5170–81, sep 1998.

[123] Tony T Huang, Shelby L Feinberg, Sainath Suryanarayanan, and Shigeki Miyamoto. The zinc finger domain of NEMO is selectively required for NF-kappa B activation by UV radiation and topoisomerase inhibitors. *Molecular and cellular biology*, 22(16):5813–25, aug 2002.

[124] Albert C Koong, Eunice Y Chen, Nahid F Mivechi, Nicholas C Denko, Peter Stambrook, and Amato J. Giaccia. Hypoxic Activation of Nuclear Factor-kB Is Mediated by a Ras and Raf Signaling Pathway and Does Not Involve MAP Kinase (ERK1 or ERK2). *Cancer Research*, 54(20):5273–5279, 1994.

[125] Véronique Imbert, Rudolf A Rupec, Antonia Livolsi, Heike L Pahl, E B Traenckner, Christoph Mueller-Dieckmann, Dariush Farahifar, Bernard Rossi, Patrick Auberger, Patrick A Baeuerle, and J F Peyron. Tyrosine phosphorylation of I kappa B-alpha activates NF-kappa B without proteolytic degradation of I kappa B-alpha. *Cell*, 86(5):787–798, 1996.

[126] S C Sun, P A Ganchi, D W Ballard, and W C Greene. NF-kappa B controls expression of inhibitor I kappa B alpha: evidence for an inducible autoregulatory pathway. *Science (New York, N.Y.)*, 259(5103):1912–5, mar 1993.

[127] Kenneth Wu, Jordan Kovacev, and Zhen-Qiang Pan. Priming and extending: a UbcH5/Cdc34 E2 handoff mechanism for polyubiquitination on a SCF substrate. *Molecular cell*, 37(6):784–96, mar 2010.

[128] N. Kanarek, N. London, O. Schueler-Furman, and Y. Ben-Neriah. Ubiquitination and Degradation of the Inhibitors of NF- B. *Cold Spring Harbor Perspectives in Biology*, 2(2):a000166–a000166, feb 2010.

[129] María Carmen Mulero, Dolors Ferres-Marco, Abul Islam, Pol Margalef, Matteo Pecoraro, Agustí Toll, Nils Drechsel, Cristina Charneco, Shelly Davis, Nicolás Bellora, Fernando Gallardo, Erika López-Arribillaga, Elena Asensio-Juan, Verónica Rodilla, Jessica González, Mar Iglesias, Vincent Shih, M. Mar Albà, Luciano Di Croce, Alexander Hoffmann, Shigeki Miyamoto, Jordi Villà-Freixa, Nuria López-Bigas, William M. Keyes, María Domínguez, Anna Bigas, and Lluís Espinosa. Chromatin-Bound IκBα Regulates a Subset of Polycomb Target Genes in Differentiation and Cancer. *Cancer Cell*, 24(2):151–166, aug 2013.

[130] Neil D Perkins. Previews Emerging from NF-kB's Shadow, SUMOylated IkBa Represses Transcription. 2013.

[131] Sang-Hyun Lee and Mark Hannink. Characterization of the nuclear import and export functions of Ikappa B(epsilon). *The Journal of biological chemistry*, 277(26):23358–66, jun 2002.

[132] W F Tam and R Sen. IkappaB family members function by different mechanisms. *The Journal of biological chemistry*, 276(11):7701–4, mar 2001.

[133] Martin L Scott, Takashi Fujita, Hsiou-Chi Liou, Garry P Nolan, and David Baltimore. The p65 subunit of NF-KB regulates IKB by two distinct mechanisms. *Genes & development*, 7:1266–1276, 1993.

[134] R M Ten, C V Paya, N Israël, O Le Bail, M G Mattei, J L Virelizier, P Kourilsky, and A Israël. The characterization of the promoter of the gene encoding the p50 subunit of NF-kappa B indicates that it participates in its own regulation. *The EMBO journal*, 11(1):195–203, jan 1992.

[135] L Lombardi, P Ciana, C Cappellini, D Trecca, L Guerrini, A Migliazza, A T Maiolo, and A Neri. Structural and functional characterization of the promoter regions of the NFKB2 gene. *Nucleic acids research*, 23(12):2328–36, jun 1995.

[136] M Hannink and H M Temin. Structure and autoregulation of the c-rel promoter. *Oncogene*, 5(12):1843–50, dec 1990.

[137] Gary D Bren, Nancie J Solan, Hiroko Miyoshi, Kevin N Pennington, Lori J Pobst, and Carlos V Paya. Transcription of the RelB gene is regulated by NF-κB. *Oncogene*, 20(53):7722–7733, nov 2001.

[138] C Kunsch and C A Rosen. NF-kappa B subunit-specific regulation of the interleukin-8 promoter. *Molecular and cellular biology*, 13(10):6137–46, oct 1993.

[139] Ho-Bum Kang, Young-Eun Kim, Hyung-Joo Kwon, Dai-Eun Sok, and Younghee Lee. Enhancement of NF- κ B Expression and Activity Upon Differentiation of Human Embryonic Stem Cell Line SNUhES3. *Stem Cells and Development*, 16(4):615–624, aug 2007.

[140] A N Shakhov, M A Collart, P Vassalli, S A Nedospasov, and C V Jongeneel. Kappa B-type enhancers are involved in lipopolysaccharide-mediated transcriptional activation of the tumor necrosis factor alpha gene in primary macrophages. *The Journal of experimental medicine*, 171(1):35–47, jan 1990.

[141] M A Collart, P Baeuerle, and P Vassalli. Regulation of tumor necrosis factor alpha transcription in macrophages: involvement of four kappa B-like motifs and of constitutive and inducible forms of NF-kappa B. *Molecular and cellular biology*, 10(4):1498–506, apr 1990.

[142] Christian Stehlik, Rainer de Martin, Bernd R. Binder, and Joachim Lipp. Cytokine Induced Expression of Porcine Inhibitor of Apoptosis Protein (iap) Family Member Is Regulated by NF-κB. *Biochemical and Biophysical Research Communications*, 243(3):827–832, feb 1998.

[143] Douglas J. Turner, Samuel M. Alaish, Tongtong Zou, Jaladanki N. Rao, Jian-Ying Wang, and Eric D. Strauch. Bile Salts Induce Resistance to Apoptosis Through NF-??B-mediated XIAP Expression. *Annals of Surgery*, 245(3):415–425, mar 2007.

[144] K. Toualbi-Abed, F. Daniel, M. C. Guller, A. Legrand, J.-L. Mauriz, A. Mauviel, and D. Bernuau. Jun D cooperates with p65 to activate the proximal B site of the cyclin D1 promoter: role of PI3K/PDK-1. *Carcinogenesis*, 29(3):536–543, oct 2007.

[145] M Hinz, D Krappmann, A Eichten, A Heder, C Scheidereit, and M Strauss. NF-kappaB function in growth control: regulation of cyclin D1 expression and G0/G1-to-S-phase transition. *Molecular and cellular biology*, 19(4):2690–8, apr 1999.

[146] Hakan H Kucuksayan and Sakir S Akgun. Medicinal chemistry Open Access Pl3K/Akt/NF-κB Signalling Pathway on NSCLC Invasion. *Med chem (Los Angeles)*, 6(4):234, 2016.

[147] Patrick van Uden, Niall S. Kenneth, and Sonia Rocha. Regulation of hypoxia-inducible factor-1α by NF-κB. *Biochemical Journal*, 412(3):477–484, jun 2008.

[148] Agnes Görlach and Steve Bonello. The cross-talk between NF-κB and HIF-1: further evidence for a significant liaison: Figure 1. *Biochemical Journal*, 412(3):e17–e19, jun 2008.

[149] Ana I Rojo, Marta Salinas, Daniel Martín, Rosario Perona, and Antonio Cuadrado. Regulation of Cu/Zn-superoxide dismutase expression via the phosphatidylinositol 3 kinase/Akt pathway and nuclear factor-kappaB. *The Journal of neuroscience : the official journal of the Society for Neuroscience*, 24(33):7324–7334, aug 2004.

[150] Kumuda C Das, Yvette Lewis-Molock, and Carl W White. Activation of NF-KB and elevation of MnSOD gene expression by thiol reducing agents in lung adenocarcinoma (A549) cells. *Am J Physiol*, 269(5):588–602, 1995.

[151] Kang Shen Yao and Peter J. O'Dwyer. Involvement of NF-??B in the induction of NAD(P)H: Quinone oxidoreductase (DT-diaphorase) by hypoxia, oltipraz and mitomycin C. *Biochemical Pharmacology*, 49(3):275–282, 1995.

[152] Dana Cahill, Brian Connor, and James P Carney. Mechanisms of eukaryotic DNA double strand break repair. *Frontiers in bioscience : a journal and virtual library*, 11:1958–76, may 2006.

[153] Claire Wyman and Roland Kanaar. DNA Double-Strand Break Repair: Alls Well that Ends Well. *Annual Review of Genetics*, 40(1):363–383, dec 2006.

[154] T HELLEDAY, J LO, D VANGENT, and B ENGELWARD. DNA double-strand break repair: From mechanistic understanding to cancer treatment. *DNA Repair*, 6(7):923–935, jul 2007.

[155] Eric Weterings and Dik C. van Gent. The mechanism of non-homologous end-joining: a synopsis of synapsis. *DNA Repair*, 3(11):1425–1435, nov 2004.

[156] Sandeep Burma, Benjamin P.C. Chen, and David J. Chen. Role of non-homologous end joining (NHEJ) in maintaining genomic integrity. *DNA Repair*, 5(9-10):1042–1048, sep 2006.

[157] D C van Gent and M van der Burg. Non-homologous end-joining, a sticky affair. *Oncogene*, 26(56):7731–7740, dec 2007.

[158] M de Jager, J van Noort, D C van Gent, C Dekker, R Kanaar, and C Wyman. Human Rad50/Mre11 is a flexible complex that can tether DNA ends. *Molecular cell*, 8(5):1129–35, nov 2001.

[159] Andrea L. Bredemeyer, Girdhar G. Sharma, Ching-Yu Huang, Beth A. Helmink, Laura M. Walker, Katrina C. Khor, Beth Nuskey, Kathleen E. Sullivan, Tej K. Pandita, Craig H. Bassing, and Barry P. Sleckman. ATM stabilizes DNA double-strand-break complexes during V(D)J recombination. *Nature*, 442(7101):466–470, jul 2006.

[160] Jacob Falck, Julia Coates, and Stephen P. Jackson. Conserved modes of recruitment of ATM, ATR and DNA-PKcs to sites of DNA damage. *Nature*, 434(7033):605–611, mar 2005.

[161] J.-H. Lee and Tanya T Paull. ATM Activation by DNA Double-Strand Breaks Through the Mre11-Rad50-Nbs1 Complex. *Science*, 308(5721):551–554, apr 2005.

[162] Oliver Limbo, Charly Chahwan, Yoshiki Yamada, Robertus A.M. de Bruin, Curt Wittenberg, and Paul Russell. Ctp1 Is a Cell-Cycle-Regulated Protein that Functions with Mre11 Complex to Control Double-Strand Break Repair by Homologous Recombination. *Molecular Cell*, 28(1):134–146, oct 2007.

[163] Alessandro A. Sartori, Claudia Lukas, Julia Coates, Martin Mistrik, Shuang Fu, Jiri Bartek, Richard Baer, Jiri Lukas, and Stephen P. Jackson. Human CtIP promotes DNA end resection. *Nature*, 450(7169):509–514, nov 2007.

[164] Shunichi Takeda, Kyoko Nakamura, Yoshihito Taniguchi, and Tanya T. Paull. Ctp1/CtIP and the MRN Complex Collaborate in the Initial Steps of Homologous Recombination. *Molecular Cell*, 28(3):351–352, nov 2007.

[165] Claire Wyman, Dejan Ristic, and Roland Kanaar. Homologous recombination-mediated double-strand break repair. *DNA Repair*, 3(8-9):827–833, aug 2004.

[166] Michael Lisby and Rodney Rothstein. Choreography of recombination proteins during the DNA damage response. *DNA Repair*, 8(9):1068–1076, sep 2009.

[167] Karen H. Almeida and Robert W. Sobol. A unified view of base excision repair: Lesion-dependent protein complexes regulated by post-translational modification. *DNA Repair*, 6(6):695–711, jun 2007.

[168] Muralidhar L Hegde, Tapas K Hazra, and Sankar Mitra. Early steps in the DNA base excision/single-strand interruption repair pathway in mammalian cells. *Cell Research*, 18(1):27–47, jan 2008.

[169] Sherif F. El-Khamisy, Sachin Katyal, Poorvi Patel, Limei Ju, Peter J. McKinnon, and Keith W. Caldecott. Synergistic decrease of DNA single-strand break repair

rates in mouse neural cells lacking both Tdp1 and aprataxin. *DNA Repair*, 8(6):760–766, jun 2009.

[170] Giuseppina Giglia-Mari, Angelika Zotter, and Wim Vermeulen. DNA Damage Response. *Cold Spring Harbor Perspectives in Biology*, 3(1), 2011.

[171] J H Hoeijmakers. Nucleotide excision repair. II: From yeast to mammals. *Trends in genetics : TIG*, 9(6):211–7, jun 1993.

[172] Ludovic C. J. Gillet and Orlando D. Schärer. Molecular Mechanisms of Mammalian Global Genome Nucleotide Excision Repair. *Chemical Reviews*, 106(2):253–276, feb 2006.

[173] V A Bohr, D S Okumoto, and P C Hanawalt. Survival of UV-irradiated mammalian cells correlates with efficient DNA repair in an essential gene. *Proceedings of the National Academy of Sciences of the United States of America*, 83(11):3830–3, jun 1986.

[174] P C Hanawalt. Transcription-coupled repair and human disease. *Science (New York, N.Y.)*, 266(5193):1957–8, dec 1994.

[175] C Masutani, K Sugasawa, J Yanagisawa, T Sonoyama, M Ui, T Enomoto, K Takio, K Tanaka, P J van der Spek, and D Bootsma. Purification and cloning of a nucleotide excision repair complex involving the xeroderma pigmentosum group C protein and a human homologue of yeast RAD23. *The EMBO journal*, 13(8):1831–43, apr 1994.

[176] Kaoru Sugasawa, Jun-ichi Akagi, Ryotaro Nishi, Shigenori Iwai, and Fumio Hanaoka. Two-Step Recognition of DNA Damage for Mammalian Nucleotide Excision Repair: Directional Binding of the XPC Complex and DNA Strand Scanning. *Molecular Cell*, 36(4):642–653, nov 2009.

[177] S Keeney, A P Eker, T Brody, W Vermeulen, D Bootsma, J H Hoeijmakers, and S Linn. Correction of the DNA repair defect in xeroderma pigmentosum group E by injection of a DNA damage-binding protein. *Proceedings of the National Academy of Sciences of the United States of America*, 91(9):4053–6, apr 1994.

[178] M Yokoi, C Masutani, T Maekawa, K Sugasawa, Y Ohkuma, and F Hanaoka. The xeroderma pigmentosum group C protein complex XPC-HR23B plays an important role in the recruitment of transcription factor IIH to damaged DNA. *The Journal of biological chemistry*, 275(13):9870–5, mar 2000.

[179] M Volker, M J Moné, P Karmakar, A van Hoffen, W Schul, W Vermeulen, J H Hoeijmakers, R van Driel, A A van Zeeland, and L H Mullenders. Sequential assembly of the nucleotide excision repair factors in vivo. *Molecular cell*, 8(1):213–24, jul 2001.

[180] W L de Laat, E Appeldoorn, K Sugasawa, E Weterings, N G Jaspers, and J H Hoeijmakers. DNA-binding polarity of human replication protein A positions nucleases in nucleotide excision repair. *Genes & development*, 12(16):2598–609, aug 1998.

[181] A M Sijbers, W L de Laat, R R Ariza, M Biggerstaff, Y F Wei, J G Moggs, K C Carter, B K Shell, E Evans, M C de Jong, S Rademakers, J de Rooij, N G Jaspers, J H Hoeijmakers, and R D Wood. Xeroderma pigmentosum group F caused by a defect in a structure-specific DNA repair endonuclease. *Cell*, 86(5):811–22, sep 1996.

[182] Tomoo Ogi, Siripan Limsirichaikul, René M. Overmeer, Marcel Volker, Katsuya Takenaka, Ross Cloney, Yuka Nakazawa, Atsuko Niimi, Yoshio Miki, Nicolaas G. Jaspers, Leon H.F. Mullenders, Shunichi Yamashita, Maria I. Fousteri, and Alan R. Lehmann. Three DNA Polymerases, Recruited by Different Mechanisms, Carry Out NER Repair Synthesis in Human Cells. *Molecular Cell*, 37(5):714–727, mar 2010.

[183] Jill Moser, Hanneke Kool, Ioannis Giakzidis, Keith Caldecott, Leon H.F. Mullenders, and Maria I. Fousteri. Sealing of Chromosomal DNA Nicks during Nucleotide Excision Repair Requires XRCC1 and DNA Ligase IIIα in a Cell-Cycle-Specific Manner. *Molecular Cell*, 27(2):311–323, jul 2007.

[184] Richard Fishel. Mismatch repair. *The Journal of biological chemistry*, 290(44):26395–403, oct 2015.

[185] George W Templeton and Greg B G Moorhead. The phosphoinositide-3-OH-kinase-related kinases of Arabidopsis thaliana. *EMBO reports*, 6(8):723–8, aug 2005.

[186] Natsuko Izumi, Akio Yamashita, and Shigeo Ohno. Integrated regulation of PIKK-mediated stress responses by AAA+ proteins RUVBL1 and RUVBL2. *Nucleus*, 3(1):29–43, jan 2012.

[187] Harri Lempiäinen and Thanos D Halazonetis. Emerging common themes in regulation of PIKKs and PI3Ks. *The EMBO Journal*, 28(20):3067–3073, oct 2009.

[188] Courtney A. Lovejoy and David Cortez. Common mechanisms of PIKK regulation. *DNA Repair*, 8(9):1004–1008, sep 2009.

[189] Fengxia Du, Minjie Zhang, Xiaohua Li, Caiyun Yang, Hao Meng, Dong Wang, Shuang Chang, Ye Xu, Brendan Price, and Yingli Sun. Dimer monomer transition and dimer re-formation play important role for ATM cellular function during DNA repair. *Biochemical and biophysical research communications*, 452(4):1034–9, oct 2014.

[190] Lana Bozulic, Banu Surucu, Debby Hynx, and Brian A. Hemmings. PKB??/Akt1 Acts Downstream of DNA-PK in the DNA Double-Strand Break Response and Promotes Survival. *Molecular Cell*, 30(2):203–213, 2008.

[191] A. Marechal and L. Zou. DNA Damage Sensing by the ATM and ATR Kinases. *Cold Spring Harbor Perspectives in Biology*, 5(9):a012716–a012716, sep 2013.

[192] Sergei V. Kozlov, Mark E. Graham, Burkhard Jakob, Frank Tobias, Amanda W. Kijas, Marcel Tanuji, Philip Chen, Phillip J. Robinson, Gisela Taucher-Scholz, Keiji Suzuki, Sairai So, David Chen, and Martin F. Lavin. Autophosphorylation and ATM Activation. *Journal of Biological Chemistry*, 286(11):9107–9119, mar 2011.

[193] T. Katsube, M. Mori, H. Tsuji, T. Shiomi, B. Wang, Q. Liu, M. Nenoi, and M. Onoda. Most hydrogen peroxide-induced histone H2AX phosphorylation is mediated by ATR and is not dependent on DNA double-strand breaks. *Journal of Biochemistry*, 156(2):85–95, aug 2014.

[194] Tom Stiff, Mark O'Driscoll, Nicole Rief, Kuniyoshi Iwabuchi, Markus Löbrich, and Penny A Jeggo. ATM and DNA-PK function redundantly to phosphorylate H2AX after exposure to ionizing radiation. *Cancer research*, 64(7):2390–6, apr 2004.

[195] Eun-Jung Park, Doug W Chan, Ji-Hye Park, Marjorie A Oettinger, and Jongbum Kwon. DNA-PK is activated by nucleosomes and phosphorylates H2AX within the nucleosomes in an acetylation-dependent manner. *Nucleic acids research*, 31(23):6819–27, dec 2003.

[196] N Rhind, B Furnari, and P Russell. Cdc2 tyrosine phosphorylation is required for the DNA damage checkpoint in fission yeast. - PubMed - NCBI. *Genes Dev*, 11(4):504–11, 1997.

[197] Bunsyo Shiotani and Lee Zou. Single-Stranded DNA Orchestrates an ATM-to-ATR Switch at DNA Breaks. *Molecular Cell*, 33(5):547–558, mar 2009.

[198] Christopher E. Helt, William A. Cliby, Peter C. Keng, Robert A. Bambara, and Michael A. O'Reilly. Ataxia Telangiectasia Mutated (ATM) and ATM and Rad3-related Protein Exhibit Selective Target Specificities in Response to Different Forms of DNA Damage. *Journal of Biological Chemistry*, 280(2):1186–1192, jan 2005.

[199] Edward A Nam, Runxiang Zhao, Gloria G Glick, Carol E Bansbach, David B Friedman, and David Cortez. Thr-1989 phosphorylation is a marker of active ataxia telangiectasia-mutated and Rad3-related (ATR) kinase. *The Journal of biological chemistry*, 286(33):28707–14, aug 2011.

[200] Shizhou Liu, Bunsyo Shiotani, Mayurika Lahiri, Alexandre Maréchal, Alice Tse, Charles Chung Yun Leung, J N Mark Glover, Xiaohong H Yang, and Lee Zou. ATR autophosphorylation as a molecular switch for checkpoint activation. *Molecular cell*, 43(2):192–202, jul 2011.

[201] Joanne Smith, Lye Mun Tho, Naihan Xu, and David A Gillespie. The ATM-Chk2 and ATR-Chk1 pathways in DNA damage signaling and cancer. *Advances in cancer research*, 108:73–112, jan 2010.

[202] Helfrid Hochegger, Shunichi Takeda, and Tim Hunt. Cyclin-dependent kinases and cell-cycle transitions: does one fit all? *Nature Reviews Molecular Cell Biology*, 9(11):910–916, nov 2008.

[203] David O. Morgan. CYCLIN-DEPENDENT KINASES: Engines, Clocks, and Microprocessors. *Annual Review of Cell and Developmental Biology*, 13(1):261–291, nov 1997.

[204] A Satyanarayana and P Kaldis. Mammalian cell-cycle regulation: several Cdks, numerous cyclins and diverse compensatory mechanisms. *Oncogene*, 28(33):2925–2939, aug 2009.

[205] Katrien Vermeulen, Zwi N. Berneman, and Dirk R. Van Bockstaele. Cell cycle and apoptosis. *Cell Proliferation*, 36(3):165–175, jun 2003.

[206] Michael B. Kastan and Jiri Bartek. Cell-cycle checkpoints and cancer. *Nature*, 432(7015):316–323, nov 2004.

[207] A Carnero and G J Hannon. The INK4 family of CDK inhibitors. *Current topics in microbiology and immunology*, 227:43–55, 1998.

[208] Dana Branzei and Marco Foiani. Regulation of DNA repair throughout the cell cycle. *Nature Reviews Molecular Cell Biology*, 9(4):297–308, apr 2008.

[209] Wynand P. Roos and Bernd Kaina. DNA damage-induced cell death by apoptosis. *Trends in Molecular Medicine*, 12(9):440–450, sep 2006.

[210] Karlene A. Cimprich and David Cortez. ATR: an essential regulator of genome integrity. *Nature Reviews Molecular Cell Biology*, 9(8):616–627, aug 2008.

[211] Martin F. Lavin and Sergei Kozlov. ATM Activation and DNA Damage Response. *Cell Cycle*, 6(8):931–942, apr 2007.

[212] Vassiliki Nikoletopoulou, Maria Markaki, Konstantinos Palikaras, and Nektarios Tavernarakis. Crosstalk between apoptosis, necrosis and autophagy. *Biochimica et Biophysica Acta (BBA) - Molecular Cell Research*, 1833(12):3448–3459, dec 2013.

[213] R M Locksley, N Killeen, and M J Lenardo. The TNF and TNF receptor superfamilies: integrating mammalian biology. *Cell*, 104(4):487–501, feb 2001.

[214] D. Wallach, E. E. Varfolomeev, N. L. Malinin, Yuri V. Goltsev, A. V. Kovalenko, and M. P. Boldin. TUMOR NECROSIS FACTOR RECEPTOR AND Fas SIGNALING MECHANISMS. *Annual Review of Immunology*, 17(1):331–367, apr 1999.

[215] R A LOCKSHIN and C M WILLIAMS. PROGRAMMED CELL DEATH–I. CYTOLOGY OF DEGENERATION IN THE INTERSEGMENTAL MUSCLES OF THE PERNYI SILKMOTH. *Journal of insect physiology*, 11:123–33, feb 1965.

[216] Brent E. Fitzwalter and Andrew Thorburn. Recent insights into cell death and autophagy. *FEBS Journal*, 282(22):4279–4288, nov 2015.

[217] Mohamed Hassan, Hidemichi Watari, Ali AbuAlmaaty, Yusuke Ohba, and Noriaki Sakuragi. Apoptosis and molecular targeting therapy in cancer. *BioMed research international*, 2014:150845, 2014.

[218] N A Thornberry and Y Lazebnik. Caspases: enemies within. *Science (New York, N.Y.)*, 281(5381):1312–6, aug 1998.

[219] Xavier Saelens, Nele Festjens, Lieselotte Vande Walle, Maria van Gurp, Geert van Loo, and Peter Vandenabeele. Toxic proteins released from mitochondria in cell death. *Oncogene*, 23(16):2861–2874, apr 2004.

[220] D. R. Green and Guido Kroemer. The Pathophysiology of Mitochondrial Cell Death. *Science*, 305(5684):626–629, jul 2004.

[221] S D Catz and J L Johnson. Transcriptional regulation of bcl-2 by nuclear factor kappa B and its significance in prostate cancer. *Oncogene*, 20(50):7342–51, nov 2001.

[222] Reinout Schauvliege, Jill Vanrobaeys, Peter Schotte, and Rudi Beyaert. Caspase-11 Gene Expression in Response to Lipopolysaccharide and Interferon-γ Requires Nuclear Factor-κB and Signal Transducer and Activator of Transcription (STAT) 1. *Journal of Biological Chemistry*, 277(44):41624–41630, nov 2002.

[223] V Cryns and J Yuan. Proteases to die for. *Genes & development*, 12(11):1551–70, jun 1998.

[224] Barbara Kaltschmidt, Christian Kaltschmidt, Thomas G. Hofmann, Steffen P. Hehner, Wulf Dröge, and M. Lienhard Schmitz. The pro- or anti-apoptotic function of NF-κB is determined by the nature of the apoptotic stimulus. *European Journal of Biochemistry*, 267(12):3828–3835, jun 2000.

[225] Zhi Guo, Sergei Kozlov, Martin F. Lavin, Maria D. Person, and Tanya T. Paull. ATM activation by oxidative stress. *Science (New York, N.Y.)*, 330(6003):517–521, 2010.

[226] Ester M Hammond, Mary Jo Dorie, and Amato J Giaccia. ATR/ATM targets are phosphorylated by ATR in response to hypoxia and ATM in response to reoxygenation. *The Journal of biological chemistry*, 278(14):12207–13, apr 2003.

[227] Joe M. McCord. The evolution of free radicals and oxidative stress, 2000.

[228] J M McCord and I Fridovich. Superoxide dismutase. An enzymic function for erythrocuprein (hemocuprein). *The Journal of biological chemistry*, 244(22):6049–55, nov 1969.

[229] Bernard M. Babior, Ruby S. Kipnes, and John T. Curnutte. Biological Defense Mechanisms. THE PRODUCTION BY LEUKOCYTES OF SUPEROXIDE, A POTENTIAL BACTERICIDAL AGENT. *Journal of Clinical Investigation*, 52(3):741–744, mar 1973.

[230] F Rossi, V Della Bianca, and P de Togni. Mechanisms and functions of the oxygen radicals producing respiration of phagocytes. *Comparative immunology, microbiology and infectious diseases*, 8(2):187–204, 1985.

[231] B E Britigan, M S Cohen, and G M Rosen. Detection of the production of oxygen-centered free radicals by human neutrophils using spin trapping techniques: a critical perspective. *Journal of leukocyte biology*, 41(4):349–62, apr 1987.

[232] R F Furchgott and P M Vanhoutte. Endothelium-derived relaxing and contracting factors. *FASEB journal : official publication of the Federation of American Societies for Experimental Biology*, 3(9):2007–18, jul 1989.

[233] R M Palmer, D D Rees, D S Ashton, and S Moncada. L-arginine is the physiological precursor for the formation of nitric oxide in endothelium-dependent relaxation. *Biochemical and biophysical research communications*, 153(3):1251–6, jun 1988.

[234] Jehad Shaikhali, Isabelle Heiber, Thorsten Seidel, Elke Ströher, Heiko Hiltscher, Stefan Birkmann, Karl-Josef Dietz, and Margarete Baier. The redox-sensitive transcription factor Rap2.4a controls nuclear expression of 2-Cys peroxiredoxin A and other chloroplast antioxidant enzymes. *BMC plant biology*, 8:48, apr 2008.

[235] Dunyaporn Trachootham, Weiqin Lu, Marcia A Ogasawara, Rivera-Del Valle Nilsa, and Peng Huang. Redox regulation of cell survival. *Antioxidants & redox signaling*, 10(8):1343–74, aug 2008.

[236] J M Downey. Free radicals and their involvement during long-term myocardial ischemia and reperfusion. *Annual review of physiology*, 52(1):487–504, oct 1990.

[237] D N Granger and R J Korthuis. Physiologic mechanisms of posteschemic tissue injury. *Annual Review of Physiology*, 57(1):311–332, oct 1995.

[238] J L Zweier, J T Flaherty, and M L Weisfeldt. Direct measurement of free radical generation following reperfusion of ischemic myocardium. *Proceedings of the National Academy of Sciences of the United States of America*, 84(5):1404–7, mar 1987.

[239] Jean-Yves Matroule, Cedric Volanti, and Jacques Piette. NF-κB in Photodynamic Therapy: Discrepancies of a Master Regulator. *Photochemistry and Photobiology*, 82(5):1241, 2006.

[240] S Schoonbroodt, S Legrand-Poels, M Best-Belpomme, and J Piette. Activation of the NF-kappaB transcription factor in a T-lymphocytic cell line by hypochlorous acid. *The Biochemical journal*, 321 (Pt 3(Pt 3):777–85, feb 1997.

[241] Sandra Levrand, Benoît Pesse, François Feihl, Bernard Waeber, Pal Pacher, Joëlle Rolli, Marie-Denise Schaller, and Lucas Liaudet. Peroxynitrite is a potent inhibitor of NF-{kappa}B activation triggered by inflammatory stimuli in cardiac and endothelial cell lines. *The Journal of biological chemistry*, 280(41):34878–87, oct 2005.

[242] Arjang Djamali. Oxidative stress as a common pathway to chronic tubulointerstitial injury in kidney allografts. *American journal of physiology. Renal physiology*, 293(2):F445–55, aug 2007.

[243] E. L. Kwak, D. A. Larochelle, C. Beaumont, S V Torti, and F. M. Torti. Role for NF-kappa B in the regulation of ferritin H by tumor necrosis factor-alpha. *The Journal of biological chemistry*, 270(25):15285–93, jun 1995.

[244] Jixiang Zhang, Xiaoli Wang, Vikash Vikash, Qing Ye, Dandan Wu, Yulan Liu, and Weiguo Dong. ROS and ROS-Mediated Cellular Signaling. *Oxidative Medicine and Cellular Longevity*, 2016:1–18, feb 2016.

[245] Krithika Lingappan. NF-κB in oxidative stress. *Current Opinion in Toxicology*, 7:81–86, feb 2018.

[246] Michael J. Morgan, You-Sun Kim, and Zhenggang Liu. Lipid Rafts and Oxidative Stress–Induced Cell Death. *Antioxidants & Redox Signaling*, 9(9):1471–1484, sep 2007.

[247] Florence Hazane-Puchi, Mathilde Bonnet, Kita Valenti, Sylvianne Schnebert, Robin Kurfurst, Alain Favier, and Sylvie Sauvaigo. Study of fibroblast gene expression in response to oxidative stress induced by hydrogen peroxide or UVA with skin aging. *Eur J Dermatol*, 20(3):308–320, 2010.

[248] Ji H ye Lee, D S un Lim, and W S an Joo im. Gene expression profiling of oxidative stress on atrial fibrillation in humans. Technical Report 5, 2003.

[249] John Isaac Murray, Michael L Whitfield, Nathan D Trinklein, Richard M Myers, Patrick O Brown, and David Botstein. Diverse and specific gene expression responses to stresses in cultured human cells. *Molecular biology of the cell*, 15(5):2361–74, may 2004.

[250] Maria Giulia Battelli, Letizia Polito, Massimo Bortolotti, and Andrea Bolognesi. Xanthine oxidoreductase in cancer: more than a differentiation marker. *Cancer Medicine*, 5(3):546–557, mar 2016.

[251] J W Lim, H Kim, and K H Kim. Nuclear factor-kappaB regulates cyclooxygenase-2 expression and cell proliferation in human gastric cancer cells. *Laboratory investigation; a journal of technical methods and pathology*, 81(3):349–60, mar 2001.

[252] Etsuro Hatano, Brydon L. Bennett, Anthony M. Manning, Ting Qian, John J. Lemasters, and David A. Brenner. NF-κB stimulates inducible nitric oxide synthase to protect mouse hepatocytes from TNF-α– and Fas-mediated apoptosis. *Gastroenterology*, 120(5):1251–1262, apr 2001.

[253] Manu Jatana, Shailendra Giri, Mubeen A Ansari, Chinnasamy Elango, Avtar K Singh, Inderjit Singh, and Mushfiquddin Khan. Inhibition of NF-kappaB activation by 5-lipoxygenase inhibitors protects brain against injury in a rat model of focal cerebral ischemia. *Journal of neuroinflammation*, 3:12, may 2006.

[254] Maral Jamshidi, Jirina Bartkova, Dario Greco, Johanna Tommiska, Rainer Fagerholm, Kristiina Aittomäki, Johanna Mattson, Kenneth Villman, Radek Vrtel, Jiri Lukas, Päivi Heikkilä, Carl Blomqvist, Jiri Bartek, and Heli Nevanlinna. NQO1 expression correlates inversely with NFκB activation in human breast cancer. *Breast Cancer Research and Treatment*, 132(3):955–968, apr 2012.

[255] Michael J Morgan and Zheng-gang Liu. Crosstalk of reactive oxygen species and NF-κB signaling. *Cell research*, 21(1):103–15, jan 2011.

[256] G Gloire, E Charlier, S Rahmouni, C Volanti, A Chariot, C Erneux, and J Piette. Restoration of SHIP-1 activity in human leukemic cells modifies NF-κB activation pathway and cellular survival upon oxidative stress. *Oncogene*, 25(40):5485–5494, sep 2006.

[257] Geoffrey Gloire, Sylvie Legrand-Poels, and Jacques Piette. NF-κB activation by reactive oxygen species: Fifteen years later. *Biochemical Pharmacology*, 72(11):1493–1505, nov 2006.

[258] Lokesh Gambhir, Rahul Checker, Deepak Sharma, M. Thoh, Anand Patil, M. Degani, Vikram Gota, and Santosh K. Sandur. Thiol dependent NF-κB suppression and inhibition of T-cell mediated adaptive immune responses by a naturally occurring steroidal lactone Withaferin A. *Toxicology and Applied Pharmacology*, 289(2):297–312, dec 2015.

[259] Solange H Korn, Emiel F M Wouters, Nanda Vos, and Yvonne M W Janssen-Heininger. Cytokine-induced Activation of Nuclear Factor-B Is Inhibited by Hydrogen Peroxide through Oxidative Inactivation of IB Kinase. 2001.

[260] Yuyeon Jung, Hojin Kim, Sun Hee Min, Sue Goo Rhee, and Woojin Jeong. Dynein Light Chain LC8 Negatively Regulates NF-κB through the Redox-dependent Interaction with IκBα. *Journal of Biological Chemistry*, 283(35):23863–23871, aug 2008.

[261] Eóin N. McNamee, Darlynn Korns Johnson, Dirk Homann, and Eric T. Clambey. Hypoxia and hypoxia-inducible factors as regulators of T cell development, differentiation, and function. *Immunologic Research*, 55(1-3):58–70, mar 2013.

[262] Leon Zheng, Caleb J. Kelly, and Sean P. Colgan. Physiologic hypoxia and oxygen homeostasis in the healthy intestine. A Review in the Theme: Cellular Responses to Hypoxia. *American Journal of Physiology-Cell Physiology*, 309(6):C350–C360, sep 2015.

[263] Matthew E Hardee, Mark W Dewhirst, Nikita Agarwal, and Brian S Sorg. Novel imaging provides new insights into mechanisms of oxygen transport in tumors. *Current molecular medicine*, 9(4):435–41, may 2009.

[264] M Navab, S Y Hama, B J Van Lenten, D C Drinkwater, H Laks, and A M Fogelman. A new antiinflammatory compound, leumedin, inhibits modification of low density lipoprotein and the resulting monocyte transmigration into the subendothelial space of cocultures of human aortic wall cells. *The Journal of clinical investigation*, 91(3):1225–30, mar 1993.

[265] Mohamad Navab, Alan M. Fogelman, Judith A. Berliner, Mary C. Territo, Linda L. Demer, Joy S. Frank, Andrew D. Watson, Peter A. Edwards, and Aidons J. Lusis. Pathogenesis of atherosclerosis. *The American Journal of Cardiology*, 76(9 SUPPL. 1):18C–23C, sep 1995.

[266] S. Grotti and T. Gori. Endothelium, ischemia and the good side of oxygen free radicals. *Clinical Hemorheology and Microcirculation*, 39(1-4):197–203, 2008.

[267] Stefan Zahler, Christian Kupatt, and Bernhard F Becker. Endothelial preconditioning by transient oxidative stress reduces inflammatory responses of cultured endothelial cells to TNF-alpha. *FASEB journal : official publication of the Federation of American Societies for Experimental Biology*, 14(3):555–64, 2000.

[268] Douglas Hanahan and Robert A. Weinberg. Hallmarks of cancer: The next generation, 2011.

[269] Douglas Hanahan and Robert A Weinberg. The hallmarks of cancer. *Cell*, 100(1):57–70, 2000.

[270] Rachel A Freiberg, Ester M Hammond, Mary Jo Dorie, Scott M Welford, and Amato J Giaccia. DNA damage during reoxygenation elicits a Chk2-dependent checkpoint response. *Molecular and cellular biology*, 26(5):1598–609, mar 2006.

[271] Isabel M Pires, Zuzana Bencokova, Chris McGurk, and Ester M Hammond. Exposure to acute hypoxia induces a transient DNA damage response which includes Chk1 and TLK1. *Cell cycle (Georgetown, Tex.)*, 9(13):2502–7, jul 2010.

[272] Maimon E. Hubbi and Gregg L. Semenza. Regulation of cell proliferation by hypoxia-inducible factors. *American Journal of Physiology-Cell Physiology*, 309(12):C775–C782, dec 2015.

[273] Yoshihiro Morifuji, Hideya Onishi, Hironori Iwasaki, Akira Imaizumi, Kenji Nakano, Masao Tanaka, and Mitsuo Katano. Reoxygenation from chronic hypoxia promotes metastatic processes in pancreatic cancer through the Hedgehog signaling. *Cancer science*, 105(3):324–33, mar 2014.

[274] Sang Min Sung, Dae Soo Jung, Chae Hwa Kwon, Ji Yeon Park, Soo Kyung Kang, and Yong Keun Kim. Hypoxia/Reoxygenation Stimulates Proliferation Through PKC-Dependent Activation of ERK and Akt in Mouse Neural Progenitor Cells. *Neurochemical Research*, 32(11):1932–1939, sep 2007.

[275] Bhuvana A. Setty, Yi Jin, Peter J. Houghton, Nicholas D. Yeager, Thomas G. Gross, and Leif D. Nelin. Hypoxic Proliferation of Osteosarcoma Cells Depends on Arginase II. *Cellular Physiology and Biochemistry*, 39(2):802–813, 2016.

[276] Kaifu Wang and Zhenggang Bi. Hypoxia promotes proliferation and invasion of osteosarcoma cell line SaOS-2 in vitro by activating Wnt/β-catenin signaling. Technical report.

[277] Gregg L. Semenza. Oxygen homeostasis. *Wiley Interdisciplinary Reviews: Systems Biology and Medicine*, 2(3):336–361, may 2010.

[278] Niall Steven Kenneth and Sonia Rocha. Regulation of gene expression by hypoxia. *Biochemical Journal*, 414(1):19–29, aug 2008.

[279] William G. Kaelin. PROLINE HYDROXYLATION AND GENE EXPRESSION. *Annual Review of Biochemistry*, 74(1):115–128, jun 2005.

[280] Patrick H. Maxwell, Michael S. Wiesener, Gin-Wen Chang, Steven C. Clifford, Emma C. Vaux, Matthew E. Cockman, Charles C. Wykoff, Christopher W. Pugh, Eamonn R. Maher, and Peter J. Ratcliffe. The tumour suppressor protein VHL targets hypoxia-inducible factors for oxygen-dependent proteolysis. *Nature*, 399(6733):271–275, may 1999.

[281] M. Ivan, K. Kondo, H. Yang, W. Kim, J. Valiando, M. Ohh, A. Salic, J. M. Asara, W. S. Lane, and W. G. Kaelin. HIFalpha Targeted for VHL-Mediated Destruction by Proline Hydroxylation: Implications for O2 Sensing. *Science*, 292(5516):464–468, apr 2001.

[282] Andrew Melvin and Sonia Rocha. Chromatin as an oxygen sensor and active player in the hypoxia response. *Cellular Signalling*, 24(1):35–43, jan 2012.

[283] Song Wang and Oliver Hankinson. Functional Involvement of the Brahma/SWI2-related Gene 1 Protein in Cytochrome P4501A1 Transcription Mediated by the Aryl Hydrocarbon Receptor Complex. *Journal of Biological Chemistry*, 277(14):11821–11827, apr 2002.

[284] Ina Kirmes, Aleksander Szczurek, Kirti Prakash, Iryna Charapitsa, Christina Heiser, Michael Musheev, Florian Schock, Karolina Fornalczyk, Dongyu Ma, Udo Birk, Christoph Cremer, and George Reid. A transient ischemic environment induces reversible compaction of chromatin. *Genome biology*, 16:246, nov 2015.

[285] Michael Batie, Luis Del Peso, and Sonia Rocha. Hypoxia and Chromatin: A Focus on Transcriptional Repression Mechanisms. *Biomedicines*, 6(2), apr 2018.

[286] Jun Yang, Ioanna Ledaki, Helen Turley, Kevin C. Gatter, Juan-Carlos Martinez Montero, Ji-Liang Li, and Adrian L. Harris. Role of Hypoxia-Inducible Factors in Epigenetic Regulation via Histone Demethylases. *Annals of the New York Academy of Sciences*, 1177(1):185–197, oct 2009.

[287] Ian P. Newton, Niall S. Kenneth, Paul L. Appleton, Inke Näthke, and Sonia Rocha. Adenomatous Polyposis Coli and Hypoxia-inducible Factor-1α Have an Antagonistic Connection. *Molecular Biology of the Cell*, 21(21):3630–3638, nov 2010.

[288] Robert D. Guzy, Beatrice Hoyos, Emmanuel Robin, Hong Chen, Liping Liu, Kyle D. Mansfield, M. Celeste Simon, Ulrich Hammerling, and Paul T. Schumacker. Mitochondrial complex III is required for hypoxia-induced ROS production and cellular oxygen sensing. *Cell Metabolism*, 1(6):401–408, jun 2005.

[289] Andre Bernardini, Ulf Brockmeier, Eric Metzen, Utta Berchner-Pfannschmidt, Eva Harde, Amparo Acker-Palmer, Dmitri Papkovsky, Helmut Acker, and Joachim Fandrey. Measurement of ROS Levels and Membrane Potential Dynamics in the Intact Carotid Body Ex Vivo. In *Advances in experimental medicine and biology*, volume 860, pages 55–59. 2015.

[290] Juha P. Näpänkangas, Erkki V. Liimatta, Päivi Joensuu, Ulrich Bergmann, Kari Ylitalo, and Ilmo E. Hassinen. Superoxide production during ischemia–reperfusion in the perfused rat heart: A comparison of two methods of measurement. *Journal of Molecular and Cellular Cardiology*, 53(6):906–915, dec 2012.

[291] Q. Liu, U. Berchner-Pfannschmidt, U. Moller, M. Brecht, C. Wotzlaw, H. Acker, K. Jungermann, and T. Kietzmann. A Fenton reaction at the endoplasmic reticulum is involved in the redox control of hypoxia-inducible gene expression. *Proceedings of the National Academy of Sciences*, 101(12):4302–4307, mar 2004.

[292] José López-Barneo, Ricardo Pardal, and Patricia Ortega-Sáenz. Cellular Mechanism of Oxygen Sensing. *Annual Review of Physiology*, 63(1):259–287, mar 2001.

[293] J J Zulueta, F S Yu, I A Hertig, V J Thannickal, and P M Hassoun. Release of hydrogen peroxide in response to hypoxia-reoxygenation: role of an NAD(P)H oxidase-like enzyme in endothelial cell plasma membrane. *American Journal of Respiratory Cell and Molecular Biology*, 12(1):41–49, jan 1995.

[294] E. P. Cummins, K. M. Oliver, C. R. Lenihan, S. F. Fitzpatrick, U. Bruning, C. C. Scholz, C. Slattery, M. O. Leonard, P. McLoughlin, and C. T. Taylor. NF- B Links CO2 Sensing to Innate Immunity and Inflammation in Mammalian Cells. *The Journal of Immunology*, 185(7):4439–4445, oct 2010.

[295] Marcin Wysoczynski, Dong-Myung Shin, Magda Kucia, Mariusz Z Ratajczak, and James Graham. Selective upregulation of interleukin-8 by human rhabdomyosarcomas in response to hypoxia: therapeutic implications. *Cancer Cell Biology Int. J. Cancer*, 126:371–381, 2010.

[296] Daniel Martin, Rebeca Galisteo, and J Silvio Gutkind. CXCL8/IL8 Stimulates Vascular Endothelial Growth Factor (VEGF) Expression and the Autocrine Activation of VEGFR2 in Endothelial Cells by Activating NFB through the CBM (Carma3/Bcl10/Malt1) Complex *. 2008.

[297] Alexander Kuett, Christina Rieger, Deborah Perathoner, Tobias Herold, Michaela Wagner, Silvia Sironi, Karl Sotlar, Hans-Peter Horny, Christian Deniffel, Heidrun Drolle, and Michael Fiegl. IL-8 as mediator in the microenvironment-leukaemia network in acute myeloid leukaemia. *Scientific Reports*, 5(1):18411, nov 2016.

[298] Nikhil Hirani, Frank Antonicelli, Robert M Strieter, Michael S Wiesener, Chris Haslett, and Seamas C Donnelly. The Regulation of Interleukin-8 by Hypoxia in Human Macrophages-A Potential Role in the Pathogenesis of the Acute Respiratory Distress Syndrome (ARDS). *Molecular Medicine*, 7(10):685–697, 2001.

[299] J. K. Ahn, E.-M. Koh, H.-S. Cha, Y. S. Lee, J. Kim, E.-K. Bae, and K.-S. Ahn. Role of hypoxia-inducible factor-1 in hypoxia-induced expressions of IL-8, MMP-1 and MMP-3 in rheumatoid fibroblast-like synoviocytes. *Rheumatology*, 47(6):834–839, mar 2008.

[300] M You, P T Ku, R Hrdlicková, and H R Bose. ch-IAP1, a member of the inhibitor-of-apoptosis protein family, is a mediator of the antiapoptotic activity of the v-Rel oncoprotein. *Molecular and cellular biology*, 17(12):7328–41, dec 1997.

[301] D. Xia, H. Srinivas, Y.-h. Ahn, G. Sethi, X. Sheng, W. K. A. Yung, Q. Xia, P. J. Chiao, H. Kim, P. H. Brown, I. I. Wistuba, B. B. Aggarwal, and J. M. Kurie. Mitogen-activated Protein Kinase Kinase-4 Promotes Cell Survival by Decreasing

PTEN Expression through an NF B-dependent Pathway. *Journal of Biological Chemistry*, 282(6):3507–3519, nov 2006.

[302] Sinead Walsh, Catherine Gill, Amanda O'Neill, John M. Fitzpatrick, and R. William G. Watson. Hypoxia increases normal prostate epithelial cell resistance to receptor-mediated apoptosis via AKT activation. *International Journal of Cancer*, 124(8):1871–1878, apr 2009.

[303] Xiaohui Wang, Tuanzhu Ha, Yuanping Hu, Chen Lu, Li Liu, Xia Zhang, Race Kao, John Kalbfleisch, David Williams, and Chuanfu Li. MicroRNA-214 protects against hypoxia/reoxygenation induced cell damage and myocardial ischemia/reperfusion injury via suppression of PTEN and Bim1 expression. *Oncotarget*, 7(52):86926–86936, dec 2016.

[304] Amit Agrawal, Sachin Gajghate, Harvey Smith, D. Greg Anderson, Todd J. Albert, Irving M. Shapiro, and Makarand V. Risbud. Cited2 modulates hypoxia-inducible factor-dependent expression of vascular endothelial growth factor in nucleus pulposus cells of the rat intervertebral disc. *Arthritis & Rheumatism*, 58(12):3798–3808, dec 2008.

[305] Yao-Hui Gao, Cai-Xia Li, Shao-Ming Shen, Hui Li, Guo-Qiang Chen, Qing Wei, and Li-Shun Wang. Hypoxia-inducible factor 1α mediates the down-regulation of superoxide dismutase 2 in von Hippel–Lindau deficient renal clear cell carcinoma. *Biochemical and Biophysical Research Communications*, 435(1):46–51, may 2013.

[306] Małgorzata Goralska, Lloyd N Fleisher, and M Christine McGahan. Hypoxia induced changes in expression of proteins involved in iron uptake and storage in cultured lens epithelial cells. *Experimental eye research*, 125:135–41, aug 2014.

[307] Guochao Sun, Ying Lu, Yingxia Li, Jun Mao, Jun Zhang, Yanling Jin, Yan Li, Yan Sun, Lei Liu, and Lianhong Li. miR-19a protects cardiomyocytes from hypoxia/reoxygenation-induced apoptosis via PTEN/PI3K/p-Akt pathway. *Bioscience Reports*, 37(6):BSR20170899, dec 2017.

[308] Dave Lanoix, Andrée-Anne Lacasse, Russel J. Reiter, and Cathy Vaillancourt. Melatonin: The watchdog of villous trophoblast homeostasis against hypoxia/reoxygenation-induced oxidative stress and apoptosis. *Molecular and Cellular Endocrinology*, 381(1-2):35–45, dec 2013.

[309] COSMIC. U-2-OS - bone - Mutations - Cell Line Synopsis.

[310] Chad Kerksick and Darryn Willoughby. The antioxidant role of glutathione and N-acetyl-cysteine supplements and exercise-induced oxidative stress. *Journal of the International Society of Sports Nutrition*, 2:38–44, jan 2005.

[311] J D Dignam, R M Lebovitz, and R G Roeder. Accurate transcription initiation by RNA polymerase II in a soluble extract from isolated mammalian nuclei. *Nucleic acids research*, 11(5):1475–89, mar 1983.

[312] Max Gassmann, Beat Grenacher, Bianca Rohde, and Johannes Vogel. Quantifying Western blots: Pitfalls of densitometry. *ELECTROPHORESIS*, 30(11):1845–1855, jun 2009.

[313] Han Yen Tan and Tuck Wah Ng. Accurate step wedge calibration for densitometry of electrophoresis gels. *Optics Communications*, 281(10):3013–3017, may 2008.

[314] Hervé Abdi. The Bonferonni and Šidák Corrections for Multiple Comparisons. Technical report.

[315] Zulfiqar Ali and S Bala Bhaskar. Basic statistical tools in research and data analysis. *Indian journal of anaesthesia*, 60(9):662–669, sep 2016.

[316] Niall S Kenneth, George E Hucks, Andrew J Kocab, Annie L McCollom, and Colin S Duckett. Copper is a potent inhibitor of both the canonical and non-canonical NFκB pathways. *Cell cycle (Georgetown, Tex.)*, 13(6):1006–14, jan 2014.

[317] Doug Wieczorek, Laurence Delauriere, and Trista Schagat. Methods of RNA Quality Assessment, 2012.

[318] ZEHUA BIAN, YANG YU, CHAO QUAN, RONGWEI GUAN, YAN JIN, JIE WU, LIDAN XU, FENG CHEN, JING BAI, WENJING SUN, and SONGBIN FU. RPL13A as a reference gene for normalizing mRNA transcription of ovarian cancer cells with paclitaxel and 10-hydroxycamptothecin treatments. *Molecular Medicine Reports*, 11(4):3188–3194, apr 2015.

[319] Quentin Geissmann. OpenCFU, a new free and open-source software to count cell colonies and other circular objects. *PloS one*, 8(2):e54072, jan 2013.

[320] Ulrich Sieben, Guido Franzoso, and Keith Brown. STRUCTURE, REGULATION AND FUNCTION OF NF-1d3. *Annu. Rev. Cell Bioi*, 10:405–55, 1994.

[321] M M Chaturvedi, B Sung, V R Yadav, R Kannappan, and B B Aggarwal. NF-κB addiction and its role in cancer: 'one size does not fit all'. *Oncogene*, 30(14):1615–1630, apr 2011.

[322] Brian Cunniff, Alexandra N. Wozniak, Patrick Sweeney, Kendra DeCosta, and Nicholas H. Heintz. Peroxiredoxin 3 levels regulate a mitochondrial redox setpoint in malignant mesothelioma cells. *Redox Biology*, 3:79–87, 2014.

[323] Genecards. Genecards PRDX-3, 2018.

[324] Narasimhaswamy S Belaguli, Mao Zhang, F Charles Brunicardi, and David H Berger. Forkhead box protein A2 (FOXA2) protein stability and activity are regulated by sumoylation. *PloS one*, 7(10):e48019, 2012.

[325] Petra Koudelkova, Victor Costina, Gerhard Weber, Steven Dooley, Peter Findeisen, Peter Winter, Rahul Agarwal, Karin Schlangen, and Wolfgang Mikulits. Transforming Growth Factor-β Drives the Transendothelial Migration of Hepatocellular Carcinoma Cells. *International journal of molecular sciences*, 18(10), oct 2017.

[326] Timothy P. Cash, Yi Pan, and M. Celeste Simon. Reactive oxygen species and cellular oxygen sensing. *Free Radical Biology and Medicine*, 43(9):1219–1225, nov 2007.

[327] Wei Gao, Jennifer McCormick, Mary Connolly, Emese Balogh, Douglas J Veale, and Ursula Fearon. Hypoxia and STAT3 signalling interactions regulate pro-inflammatory pathways in rheumatoid arthritis. *Annals of the Rheumatic Diseases*, 74(6):1275–1283, jun 2015.

[328] J E Darnell, I M Kerr, and G R Stark. Jak-STAT pathways and transcriptional activation in response to IFNs and other extracellular signaling proteins. *Science (New York, N.Y.)*, 264(5164):1415–21, jun 1994.

[329] James N. Ihle. Cytokine receptor signalling. *Nature*, 377(6550):591–594, oct 1995.

[330] Karin Römisch. ENDOPLASMIC RETICULUM–ASSOCIATED DEGRADATION. *Annual Review of Cell and Developmental Biology*, 21(1):435–456, nov 2005.

[331] Ren Ming Dai and Chou-Chi H. Li. Valosin-containing protein is a multi-ubiquitin chain-targeting factor required in ubiquitin—[ndash]—proteasome degradation. *Nature Cell Biology*, 3(8):740–744, aug 2001.

[332] Marie Cargnello and Philippe P Roux. Activation and function of the MAPKs and their substrates, the MAPK-activated protein kinases. *Microbiology and molecular biology reviews : MMBR*, 75(1):50–83, mar 2011.

[333] Mary E Choi, Yan Ding, and Sung Il Kim. TGF-β signaling via TAK1 pathway: role in kidney fibrosis. *Seminars in nephrology*, 32(3):244–52, may 2012.

[334] D H Kim, W Xu, S Kamel-Reid, X Liu, C W Jung, S Kim, and J H Lipton. Clinical relevance of vascular endothelial growth factor (VEGFA) and VEGF receptor (VEGFR2) gene polymorphism on the treatment outcome following imatinib therapy. *Annals of oncology : official journal of the European Society for Medical Oncology*, 21(6):1179–88, jun 2010.

[335] Toshiyuki Sakaeda, Motohiro Yamamori, Akiko Kuwahara, Satoko Hiroe, Tsutomu Nakamura, Katsuhiko Okumura, Tatsuya Okuno, Ikuya Miki, Naoko Chayahara,

Noboru Okamura, and Takao Tamura. VEGF G-1154A is predictive of severe acute toxicities during chemoradiotherapy for esophageal squamous cell carcinoma in Japanese patients. *Therapeutic drug monitoring*, 30(4):497–503, aug 2008.

[336] Hyo Song Kim, Won Seog Kim, Se Hoon Park, Chul Won Jung, Han Yong Choi, Hyun Moo Lee, Seong Soo Jeon, Hongil Ha, In Gyu Hwang, Seungkoo Lee, and Ho Yeong Lim. Molecular biomarkers for advanced renal cell carcinoma: implications for prognosis and therapy. *Urologic oncology*, 28(2):157–63.

[337] Michela de Martino, Tobias Klatte, David B Seligson, Jeffrey LaRochelle, Brian Shuch, Randy Caliliw, Zhenhua Li, Fairooz F Kabbinavar, Allan J Pantuck, and Arie S Belldegrun. CA9 gene: single nucleotide polymorphism predicts metastatic renal cell carcinoma prognosis. *The Journal of urology*, 182(2):728–34, aug 2009.

[338] Kimberly Cramer-Morales, Collin D Heer, Kranti A Mapuskar, and Frederick E Domann. SOD2 targeted gene editing by CRISPR/Cas9 yields Human cells devoid of MnSOD. *Free radical biology & medicine*, 89:379–86, dec 2015.

[339] Michael Hinz and Claus Scheidereit. The I??B kinase complex in NF-kB regulation and beyond, jan 2014.

[340] Q Li, D Van Antwerp, F Mercurio, K F Lee, and I M Verma. Severe liver degeneration in mice lacking the IkappaB kinase 2 gene. *Science (New York, N.Y.)*, 284(5412):321–5, apr 1999.

[341] Z W Li, W Chu, Y Hu, M Delhase, T Deerinck, M Ellisman, R Johnson, and M Karin. The IKKbeta subunit of IkappaB kinase (IKK) is essential for nuclear factor kappaB activation and prevention of apoptosis. *The Journal of experimental medicine*, 189(11):1839–45, jun 1999.

[342] M Tanaka, M E Fuentes, K Yamaguchi, M H Durnin, S A Dalrymple, K L Hardy, and D V Goeddel. Embryonic lethality, liver degeneration, and impaired NF-kappa B activation in IKK-beta-deficient mice. *Immunity*, 10(4):421–9, apr 1999.

[343] Eoin P Cummins, Edurne Berra, Katrina M Comerford, Amandine Ginouves, Kathleen T Fitzgerald, Fergal Seeballuck, Catherine Godson, Jens E Nielsen, Paul Moynagh, Jacques Pouyssegur, and Cormac T Taylor. Prolyl hydroxylase-1 negatively regulates IkappaB kinase-beta, giving insight into hypoxia-induced NFkappaB activity. *Proceedings of the National Academy of Sciences of the United States of America*, 103(48):18154–9, nov 2006.

[344] K Takeda, O Takeuchi, T Tsujimura, S Itami, O Adachi, T Kawai, H Sanjo, K Yoshikawa, N Terada, and S Akira. Limb and skin abnormalities in mice lacking IKKalpha. *Science (New York, N.Y.)*, 284(5412):313–6, apr 1999.

[345] Mazhar Adli, Evan Merkhofer, Patricia Cogswell, and Albert S. Baldwin. IKKα and IKKβ Each Function to Regulate NF-κB Activation in the TNF-Induced/Canonical Pathway. *PLoS ONE*, 5(2):e9428, feb 2010.

[346] Q Li, Q Lu, J Y Hwang, D Büscher, K F Lee, J C Izpisua-Belmonte, and I M Verma. IKK1-deficient mice exhibit abnormal development of skin and skeleton. *Genes & development*, 13(10):1322–8, may 1999.

[347] Y Hu, V Baud, M Delhase, P Zhang, T Deerinck, M Ellisman, R Johnson, and M Karin. Abnormal morphogenesis but intact IKK activation in mice lacking the IKKalpha subunit of IkappaB kinase. *Science (New York, N.Y.)*, 284(5412):316–20, apr 1999.

[348] Nahoum G Anthony, Jessica Baiget, Giacomo Berretta, Marie Boyd, David Breen, Joanne Edwards, Carly Gamble, Alexander I Gray, Alan L Harvey, Sophia Hatzieremia, Ka Ho Ho, Judith K Huggan, Stuart Lang, Sabin Llona-Minguez, Jia Lin Luo, Kathryn McIntosh, Andrew Paul, Robin J Plevin, Murray N Robertson, Rebecca Scott, Colin J Suckling, Oliver B Sutcliffe, Louise C Young, and Simon P Mackay. Inhibitory Kappa B Kinase α (IKKα) Inhibitors That Recapitulate Their Selectivity in Cells against Isoform-Related Biomarkers. *Journal of medicinal chemistry*, 60(16):7043–7066, aug 2017.

[349] ProbeChem. NIK SMI1 CAS:1660114-31-7 Probechem Biochemicals.

[350] Hans D. Brightbill, Eric Suto, Nicole Blaquiere, Nandhini Ramamoorthi, Swathi Sujatha-Bhaskar, Emily B. Gogol, Georgette M. Castanedo, Benjamin T. Jackson, Youngsu C. Kwon, Susan Haller, Justin Lesch, Karin Bents, Christine Everett, Pawan Bir Kohli, Sandra Linge, Laura Christian, Kathy Barrett, Allan Jaochico, Leonid M. Berezhkovskiy, Peter W. Fan, Zora Modrusan, Kelli Veliz, Michael J. Townsend, Jason DeVoss, Adam R. Johnson, Robert Godemann, Wyne P. Lee, Cary D. Austin, Brent S. McKenzie, Jason A. Hackney, James J. Crawford, Steven T. Staben, Moulay H. Alaoui Ismaili, Lawren C. Wu, and Nico Ghilardi. NF-kB inducing kinase is a therapeutic target for systemic lupus erythematosus. *Nature Communications*, 9(1):179, dec 2018.

[351] EPA Opera. Chemistry Dashboard Opera Half Life.

[352] S Vidal, R S Khush, F Leulier, P Tzou, M Nakamura, and B Lemaitre. Mutations in the Drosophila dTAK1 gene reveal a conserved function for MAPKKKs in the control of rel/NF-kappaB-dependent innate immune responses. *Genes & development*, 15(15):1900–12, aug 2001.

[353] Neal Silverman, Rui Zhou, Rachel L. Erlich, Mike Hunter, Erik Bernstein, David Schneider, and Tom Maniatis. Immune Activation of NF-κB and JNK Requires

Drosophila TAK1. *Journal of Biological Chemistry*, 278(49):48928–48934, dec 2003.

[354] Jun Ninomiya-Tsuji, Taisuke Kajino, Koichiro Ono, Toshihiko Ohtomo, Masahiko Matsumoto, Masashi Shiina, Masahiko Mihara, Masayuki Tsuchiya, and Kunihiro Matsumoto. A resorcylic acid lactone, 5Z-7-oxozeaenol, prevents inflammation by inhibiting the catalytic activity of TAK1 MAPK kinase kinase. *The Journal of biological chemistry*, 278(20):18485–90, may 2003.

[355] Mark Windheim, Christine Lang, Mark Peggie, Lorna A Plater, and Philip Cohen. Molecular mechanisms involved in the regulation of cytokine production by muramyl dipeptide. *The Biochemical journal*, 404(2):179–90, jun 2007.

[356] SigmaAldrich. 5Z-7-Oxozeaenol (HPLC) Sigma-Aldrich.

[357] University of Dundee, MRC PPU, and Protein Phosphorylation and Ubiquitylation Unit. Kinase Profiling Inhibitor Database — International Centre for Kinase Profiling, 2017.

[358] Shigeki Miyamoto. Nuclear initiated NF-κB signaling: NEMO and ATM take center stage. *Cell research*, 21(1):116–30, jan 2011.

[359] Yumi Yamamoto, Udit N. Verma, Shashi Prajapati, Youn-Tae Kwak, and Richard B. Gaynor. Histone H3 phosphorylation by IKK-α is critical for cytokine-induced gene expression. *Nature*, 423(6940):655–659, jun 2003.

[360] Jeremy S. Tilstra, Daniel F. Gaddy, Jing Zhao, Shaival H. Davé, Laura J. Niedernhofer, Scott E. Plevy, and Paul D. Robbins. Pharmacologic IKK/NF-kB inhibition causes antigen presenting cells to undergo TNFa dependent ROS-mediated programmed cell death. *Scientific Reports*, 4(1):3631, may 2015.

[361] J. Nan, Y. Du, X. Chen, Q. Bai, Y. Wang, X. Zhang, N. Zhu, J. Zhang, J. Hou, Q. Wang, and J. Yang. TPCA-1 Is a Direct Dual Inhibitor of STAT3 and NF-B and Regresses Mutant EGFR-Associated Human Non-Small Cell Lung Cancers. *Molecular Cancer Therapeutics*, 13(3):617–629, mar 2014.

[362] SigmaAldrich. TPCA-1 (HPLC) Sigma-Aldrich.

[363] Merck. United Kingdom.

[364] Kavitha Gowrishankar, Dilini Gunatilake, Stuart J. Gallagher, Jessamy Tiffen, Helen Rizos, and Peter Hersey. Inducible but Not Constitutive Expression of PD-L1 in Human Melanoma Cells Is Dependent on Activation of NF-kB. *PLOS ONE*, 10(4):e0123410, apr 2015.

[365] James R. Burke, Mark A. Pattoli, Kurt R. Gregor, Patrick J. Brassil, John F. MacMaster, Kim W. McIntyre, Xiaoxia Yang, Violetta S. Iotzova, Wendy Clarke, Joann Strnad, Yuping Qiu, and F. Christopher Zusi. BMS-345541 Is a Highly Selective Inhibitor of IkB Kinase That Binds at an Allosteric Site of the Enzyme and Blocks NF-kB-dependent Transcription in Mice. *Journal of Biological Chemistry*, 278(3):1450–1456, jan 2003.

[366] Tony T Huang, Shelly M Wuerzberger-Davis, Zhao-Hui Wu, and Shigeki Miyamoto. Sequential modification of NEMO/IKKgamma by SUMO-1 and ubiquitin mediates NF-kappaB activation by genotoxic stress. *Cell*, 115(5):565–76, nov 2003.

[367] D Wu, B Chen, K Parihar, L He, C Fan, J Zhang, L Liu, A Gillis, A Bruce, A Kapoor, and D Tang. ERK activity facilitates activation of the S-phase DNA damage checkpoint by modulating ATR function. *Oncogene*, 25(8):1153–1164, 2006.

[368] Kevin W McCool and Shigeki Miyamoto. DNA damage-dependent NF-κB activation: NEMO turns nuclear signaling inside out. *Immunological reviews*, 246(1):311–26, mar 2012.

[369] Yibin Yang, Fang Xia, Nicole Hermance, Angela Mabb, Sara Simonson, Sarah Morrissey, Pallavi Gandhi, Mary Munson, Shigeki Miyamoto, and Michelle A Kelliher. A cytosolic ATM/NEMO/RIP1 complex recruits TAK1 to mediate the NF-kappaB and p38 mitogen-activated protein kinase (MAPK)/MAPK-activated protein 2 responses to DNA damage. *Molecular and cellular biology*, 31(14):2774–86, jul 2011.

[370] Dana-Farber Cancer Institute Peter C. Enzinger, MD. Docetaxel, Cisplatin, Irinotecan and Bevacizumab (TPCA) in Metastatic Esophageal and Gastric Cancer - Full Text View - ClinicalTrials.gov.

[371] Dundee Kinase Screen. Kinase Profiling Inhibitor Database — International Centre for Kinase Profiling.

[372] Chris B Moore, Elizabeth H Guthrie, Max Tze-Han Huang, and Debra J Taxman. Short hairpin RNA (shRNA): design, delivery, and assessment of gene knockdown. *Methods in molecular biology (Clifton, N.J.)*, 629:141–58, 2010.

[373] Xingjie Ren, Zhihao Yang, Jiang Xu, Jin Sun, Decai Mao, Yanhui Hu, Su-Juan Yang, Huan-Huan Qiao, Xia Wang, Qun Hu, Patricia Deng, Lu-Ping Liu, Jun-Yuan Ji, Jin Billy Li, and Jian-Quan Ni. Enhanced Specificity and Efficiency of the CRISPR/Cas9 System with Optimized sgRNA Parameters in Drosophila. *Cell Reports*, 9(3):1151–1162, nov 2014.

[374] Hélène Sabatel, Emmanuel Di Valentin, Geoffrey Gloire, Franck Dequiedt, Jacques Piette, and Yvette Habraken. Phosphorylation of p65(RelA) on Ser547 by ATM

Represses NF-κB-Dependent Transcription of Specific Genes after Genotoxic Stress. *PLoS ONE*, 7(6):e38246, jun 2012.

[375] S Burma, B P Chen, M Murphy, A Kurimasa, and D J Chen. ATM phosphorylates histone H2AX in response to DNA double-strand breaks. *The Journal of biological chemistry*, 276(45):42462–7, nov 2001.

[376] Ian Hickson, Yan Zhao, Caroline J Richardson, Sharon J Green, Niall M B Martin, Alisdair I Orr, Philip M Reaper, Stephen P Jackson, Nicola J Curtin, and Graeme C M Smith. Identification and Characterization of a Novel and Specific Inhibitor of the Ataxia-Telangiectasia Mutated Kinase ATM Identification and Characterization of a Novel and Specific Inhibitor of the Ataxia-Telangiectasia Mutated Kinase ATM. *Cancer Research*, 64(24):9152–9159, 2004.

[377] Abcam. KU-55933 Abcam.

[378] Jakub Chwastek, Danuta Jantas, and Władysław Lasoń. The ATM kinase inhibitor KU-55933 provides neuroprotection against hydrogen peroxide-induced cell damage via a yH2AX/p-p53/caspase-3-independent mechanism: Inhibition of calpain and cathepsin D. *The International Journal of Biochemistry & Cell Biology*, 87:38–53, jun 2017.

[379] Y. Li and D.-Q. Yang. The ATM Inhibitor KU-55933 Suppresses Cell Proliferation and Induces Apoptosis by Blocking Akt In Cancer Cells with Overactivated Akt. *Molecular Cancer Therapeutics*, 9(1):113–125, jan 2010.

[380] J N Sarkaria, E C Busby, R S Tibbetts, P Roos, Y Taya, L M Karnitz, and R T Abraham. Inhibition of ATM and ATR kinase activities by the radiosensitizing agent, caffeine. *Cancer research*, 59(17):4375–82, sep 1999.

[381] Ester M Hammond, Mary Jo Dorie, and Amato J Giaccia. Inhibition of ATR leads to increased sensitivity to hypoxia/reoxygenation. *Cancer research*, 64(18):6556–62, sep 2004.

[382] Naoyuki Okita, Shota Minato, Eri Ohmi, Sei-ichi Tanuma, and Yoshikazu Higami. DNA damage-induced CHK1 autophosphorylation at Ser296 is regulated by an intramolecular mechanism. *FEBS letters*, 586(22):3974–9, nov 2012.

[383] Remko Prevo, Emmanouil Fokas, Philip M Reaper, Peter A Charlton, John R Pollard, W Gillies McKenna, Ruth J Muschel, and Thomas B Brunner. The novel ATR inhibitor VE-821 increases sensitivity of pancreatic cancer cells to radiation and chemotherapy. *Cancer biology & therapy*, 13(11):1072–81, sep 2012.

[384] Hiroshi Fujisawa, Nakako Izumi Nakajima, Shigeaki Sunada, Younghyun Lee, Hirokazu Hirakawa, Hirohiko Yajima, Akira Fujimori, Mitsuru Uesaka, and Ryuichi

Okayasu. VE-821, an ATR inhibitor, causes radiosensitization in human tumor cells irradiated with high LET radiation. *Radiation oncology (London, England)*, 10:175, aug 2015.

[385] SigmaAldrich. VE-821 (HPLC) Sigma-Aldrich.

[386] Remko Prevo, Emmanouil Fokas, Philip M Reaper, Peter A Charlton, John R Pollard, W Gillies McKenna, Ruth J Muschel, and Thomas B Brunner. The novel ATR inhibitor VE-821 increases sensitivity of pancreatic cancer cells to radiation and chemotherapy. *Cancer biology & therapy*, 13(11):1072–81, sep 2012.

[387] Mike I Walton, Paul D Eve, Angela Hayes, Alan T Henley, Melanie R Valenti, Alexis K De Haven Brandon, Gary Box, Kathy J Boxall, Matthew Tall, Karen Swales, Thomas P Matthews, Tatiana McHardy, Michael Lainchbury, James Osborne, Jill E Hunter, Neil D Perkins, G Wynne Aherne, John C Reader, Florence I Raynaud, Suzanne A Eccles, Ian Collins, and Michelle D Garrett. The clinical development candidate CCT245737 is an orally active CHK1 inhibitor with preclinical activity in RAS mutant NSCLC and Eu-MYC driven B-cell lymphoma. *Oncotarget*, 7(3):2329–42, jan 2016.

[388] SelleckChem. CCT245737 Chk inhibitor Read Reviews Product Use Citations.

[389] Z. Bencokova, M. R. Kaufmann, I. M. Pires, P. S. Lecane, A. J. Giaccia, and E. M. Hammond. ATM Activation and Signaling under Hypoxic Conditions. *Molecular and Cellular Biology*, 29(2):526–537, jan 2009.

[390] Linda J Kuo and Li-Xi Yang. Gamma-H2AX - a novel biomarker for DNA double-strand breaks. *In vivo (Athens, Greece)*, 22(3):305–9.

[391] Bo-Wen Huang, Masaki Miyazawa, and Yoshiaki Tsuji. Distinct regulatory mechanisms of the human ferritin gene by hypoxia and hypoxia mimetic cobalt chloride at the transcriptional and post-transcriptional levels. *Cellular signalling*, 26(12):2702–9, dec 2014.